
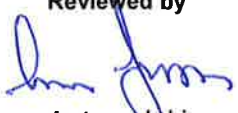



Design guide for additive manufacturing of metal components by SLM process

Authors: Petteri Kokkonen, Leevi Salonen, Jouko Virta, Björn Hemming, Pasi Laukkanen, Mikko Savolainen, Erin Komi, Jukka Junttila, Kimmo Ruusuvuori, Simo Varjus, Antti Vaajoki, Seija Kivi, Jouni Welling

Confidentiality: Public report

Report's title	
Design guide for additive manufacturing of metal components by SLM process	
Customer, contact person, address	Order reference
Tekes PL 69 00101 Helsinki	Tekes 40160/14; Dno 1852/31/2014
Project name	Project number/Short name
AM-Liito	101201/AM-Liito
Author(s)	Pages
Petteri Kokkonen, Leevi Salonen, Jouko Virta, Björn Hemming, Pasi Laukkanen, Mikko Savolainen, Erin Komi, Jukka Junntila, Kimmo Ruusuvoori, Simo Varjus, Antti Vaajoki, Seija Kivi, Jouni Welling	131 pages / 6 appendices
Keywords	Report identification code
Additive manufacturing, selective laser melting, design for AM, dimensional accuracy, 3D-printing	VTT-R-03160-16
Summary	
<p>The work presented in this paper is part of the TEKES funded research project AM-Liito. The objective of the work was to prepare design rules for load bearing structural components manufactured by the selective laser melting process (SLM).</p> <p>Design rules for metal components manufactured by the selective laser melting process were assessed based on evaluation of test prints and a mock-up test component. The test print series were designed to cover the most common geometrical features used in structural and machine components. After evaluating the printability of the geometrical features, a mock-up component was designed, with design intent to include the common geometrical features in a load bearing structural component. The component was finished by machining and sand blasting after 3D-printing and thermal treatment. The geometry of the component was measured after printing and after the thermal treatment.</p> <p>Design studies demonstrating the possibilities of additive manufacturing are presented.</p>	
Confidentiality	Public report
Espoo 8.9.2016	
Written by	Reviewed by
	
Petteri Kokkonen Senior scientist	Antero Jokinen Senior scientist
	Accepted by
	
	Pasi Puukko Research team leader
VTT's contact address	
VTT, Biologinkuja 5, Espoo, Finland	
Distribution (customer and VTT)	
Tekes and project group, pdf file VTT, original	
<p><i>The use of the name of the VTT Technical Research Centre of Finland (VTT) in advertising or publication in part of this report is only permissible with written authorisation from the VTT Technical Research Centre of Finland.</i></p>	

Contents

Contents	2
1. Introduction	4
1.1 Objectives	4
1.2 Limitations	4
1.3 The work group	4
1.4 Literature review	5
1.5 Additive manufacturing terminology	5
2. Selective laser melting process from design point of view	5
2.1 Overview of design utilising the selective laser melting process	5
2.2 Design freedom	7
2.3 Materials for selective laser melting process	8
2.4 Manufacturing constraints and the basic design rules for SLM	9
2.5 Basic design example	17
2.6 Support design	17
2.6.1 Supports for build jobs	18
2.6.2 Support design principles and support types	18
2.7 Thermal stresses and distortions	22
3. Test series of individual design features	24
3.1 Inclined plates with varying angles and arch like junctions	25
3.2 Overhangs and small details	26
3.3 Fillets and junctions with smooth transitions	26
3.4 Holes	27
3.5 Surface quality	29
3.6 Lattice structures	31
3.7 Tensile test specimen and tensile test results	33
3.8 Process settings used in the test series	34
3.9 Examples of the test prints	34
3.10 Evaluation of the test prints	37
3.10.1 Inclined plates	37
3.10.2 Holes and channels	38
3.10.3 Slots and grooves	41
3.10.4 Unsupported overhangs	51
3.10.5 Surface quality	52
3.10.6 Wall thickness	59
3.10.7 Small details	60
3.10.8 Lattice structure test prints	61
3.11 Logos, texts and markings	62
3.12 Patterns and textures	62
3.13 Test serie of various support types	62
3.14 Manufacturing defects	66
3.15 Porosity	67
3.16 Etched macro specimens	73
3.17 Lack of fusion type defects	77
3.18 Study of required amount of machining allowances	80

3.19 Study of effect of porosity on fatigue strength of SLM H13 steel.....	84
4. Test print of a mock-up component design.....	86
4.1 Basis of design of a structural test component.....	86
4.2 Support design of the test component.....	96
4.3 Assessment of heat concentration locations	98
4.4 Fatigue critical locations	100
4.5 Exporting the CAD model for printing	101
4.6 Thermal imaging of the component during printing	102
4.7 Trial prints of the test component	103
4.8 Printed test component	103
4.9 Removal of support structures.....	107
4.10 Machining	108
4.11 Alternative designs	112
4.12 Brief topology optimization study for the test component.....	114
5. Design studies	116
5.1 Topology optimized components.....	116
5.2 Light weight components utilising lattice structures.....	117
5.3 Patterns and textures	119
5.4 Design study of an ergonomic handle utilising re-engineering	120
5.5 Concept study of consolidation of functions into single AM part	122
6. Design and analysis workflows drafted for future research	124
6.1 Geometrically accurate SLM components.....	124
6.2 Defect tolerant design of fatigue critical SLM components.....	124
7. Discussion	127
7.1 Geometric accuracy of SLM components.....	127
7.2 Machining allowances	127
7.3 Surface quality of the SLM test prints.....	127
7.4 Fatigue strength estimates of the SLM test prints	128
8. Conclusions	129
References	130

Appendices

Appendix A – Summary of SLM design rules in one slide

Appendix B – Summary of SLM design principles in one slide

Appendix C – AM terminology

Appendix D – Sources of geometric inaccuracy in SLM

Appendix E – Manufacturing defects

Appendix F – Murakami-Endo analyses of example manufacturing defects

1. Introduction

The work presented in this paper is part of the TEKES funded research project AM-Liito. The objective of the work was to prepare design rules for load bearing structural components manufactured by the selective laser melting process (SLM).

Design rules for metal components manufactured by the selective laser melting process were assessed based on evaluation of test prints and a mock-up test component. The test print series were designed to cover the most common geometrical features used in structural and machine components. After evaluating the printability of the geometrical features, a mock-up component was designed, with design intent to include the common geometrical features in a load bearing structural component. The component was finished by machining and sand blasting after 3D-printing and thermal treatment. The geometry of the component was measured after printing and after the thermal treatment.

Design studies utilising topology optimization and the possibilities of additive manufacturing are presented.

1.1 Objectives

The objectives of the work are to:

1. Design, print and evaluate test series representing typical design features, to study best practises of using the Selective Laser Melting (SLM) process for component design.
2. Determine the manufacturing constraints of SLM process based on literature and the test prints.
3. Apply the geometrical features commonly used in mechanical engineering into a mock-up component design, and print and evaluate the component.
4. Study use of topology optimization with SLM for component design.
5. Practises utilising proven and cost effective approaches, such as minimising manual work and amount of machining are preferred.
6. Experiment with design studies to demonstrate the design possibilities of SLM.
7. Study effect of manufacturing defects on the design of fatigue critical components manufactured by SLM.
8. Summarise the findings as design rules for metal SLM component design.

1.2 Limitations

The main focus in the work was in design of load bearing structural components in metals using the Selective Laser Melting (SLM) process. This work is limited to small test pieces and a rather small test component, that are possible to be printed using the SLM 125 printer.

1.3 The work group

Heat input, metallurgy, heat transfer, thermal stresses and distortions, defects and their contribution to fatigue, machining, non-destructive testing (NDT), quality assurance, etc. are all well known in the fields of casting and welding. As SLM is basically building a component by multipass welding, the casting and welding design guidelines were reviewed briefly as basis for the SLM design guideline.

The topology optimization related topics were studied and developed by Erin Komi, and are reported separately in [18] with brief summary of the topology optimization and design of AM in this report by Erin Komi. Preparation of components for printing and support design in

Magics were done and work flows for these were developed by Mikko Savolainen. Printing was done by Kimmo Ruusuvoori, Petri Laakso and Simo Varjus. Post processing of the printed parts was done by Jouni Welling. Petri Laakso and Antero Jokinen were the project managers and Pasi Puukko the project owner at VTT.

3D printed metal prints were studied earlier at VTT by Jari Mäkelä, Reetta Riihiaho and Juha Halme by printing test prints using EOSINT M 270 printer at VTT Oulu, and studying the printed samples at VTT Expert Service Ltd., Espoo, by metallurgic analyses and material testing [17].

The SLM material and manufacturing topics and the various topics related to the work were developed and discussed, and the test components printed together with the AM-Liito project group at VTT. The material development and testing were led by Antero Jokinen and Petri Laakso, who were also project managers in this work. The machining related topics were studied and developed with Leevi Salonen from KTS-mekano Oy, Ilkka Palosuo, Pasi Laukkanen, Björn Hemming and Veli-Pekka Esala from Centre for Metrology and Accreditation, MIKES and Jouko Virta from VTT. Microscope analyses were done by Seija Kivi. The surface finish topics were studied by Antti Vaajoki and 3D laser scanning by Jukka Junntila, Mika Jokipii and Antti Vaajoki. MIKES is part of the VTT group.

1.4 Literature review

The documents related to SLM design [1], [3], [4], [5], [6], [7], [10] and [12] were studied as basis for this work. The systematic approaches in design and evaluation of test prints for example by Dr. Guido A.O. Adam and Dr. Daniel Thomas had a significant influence on this work at VTT.

1.5 Additive manufacturing terminology

The additive manufacturing terminology and the various abbreviations were listed while reading the literature and commented. The list is enclosed as Appendix C. The standard terminology for additive manufacturing is defined for example in [13].

2. Selective laser melting process from design point of view

2.1 Overview of design utilising the selective laser melting process

An overview of the field considered in engineering structural, load bearing components manufactured by the selective laser melting process (SLM). From design point of view, the additive manufacturing (AM) favours starting the design work with blanco paper. Even use of traditional CAD software should be questioned, as AM is better utilised by free form design tools. The free form design software are well suited for the work, and even the shapes resulting from technical analyses and optimisation can be rather readily used as basis of form giving with AM.

To best utilise the possibilities of AM designer should be familiar with the manufacturing process and its limits. The material properties of AM components differ typically significantly from the traditionally manufactured components. This is both a limitation and a possibility. The AM processes are prone to material defects and low ductility that the designer needs to be aware when the application is a load bearing component. Quality assurance and material testing is important in AM applications. On the other hand designs are not limited to traditional limits, and material properties can be tailored and high strength materials used. Material properties are improving as the manufacturing processes develop and process parameters are being optimised.

The build time versus material density is an important factor in AM. Even as defect free material may be possible to manufacture, it may be cost effective to specify the locations of component where the defect free material is really needed, based on stress level for example. There are

already software that allow the user to use computed stress distributions to map the material density. However, to apply this to real, load bearing applications, a systematic approach is needed for fatigue design when defects are allowed. This is often referred as the defect tolerant design concept.

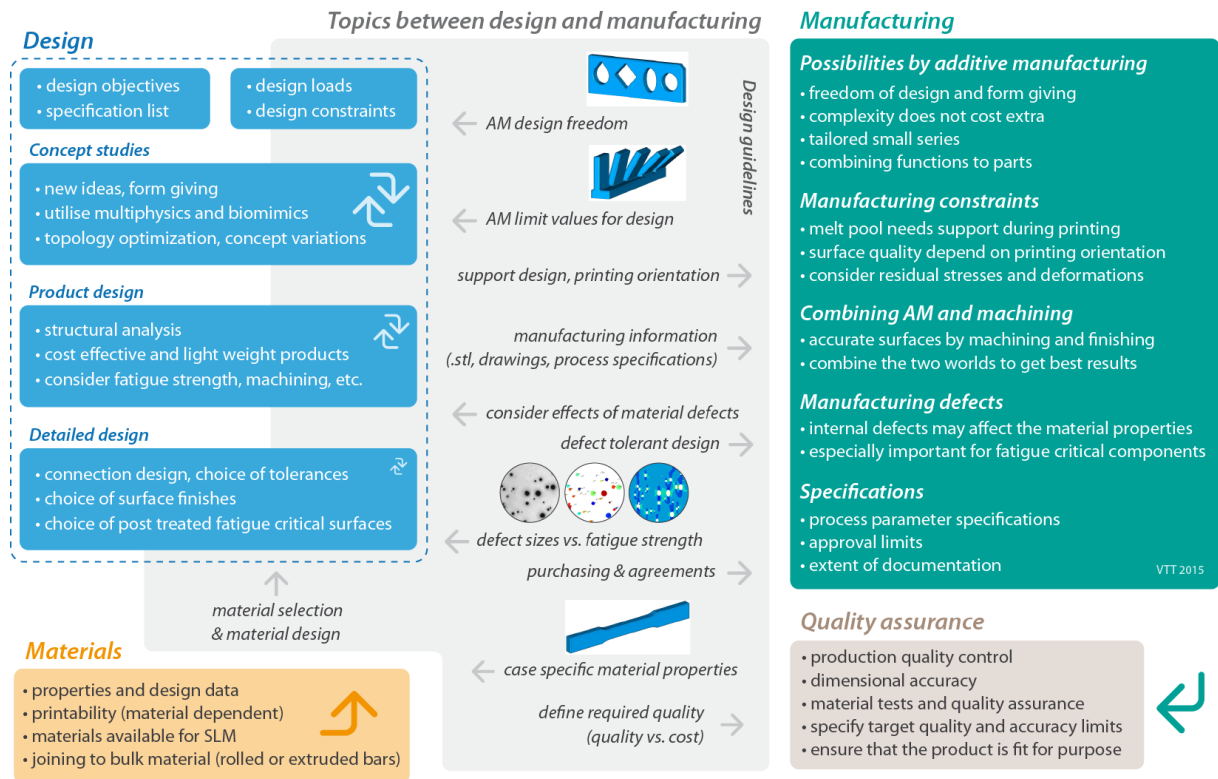


Figure 1. Overview of design utilising the selective laser melting process.

The things to consider in design utilising the selective laser melting process are drafted as lists in Figure 2. Ideation methods and systematic concepting are rising interest with AM, as the freedom of design enables completely new solutions.

	<i>Design</i>	<i>Materials</i>	<i>Printing</i>	<i>Machining and finishing</i>
<i>Functions and costs</i>	<ul style="list-style-type: none"> • design intent - specification list • design for AM - design freedom - manufacturing constraints - thermal input in SLM • concept design - combining functions - bionic design - topology optimization - design variations • defect tolerant design - manage defects vs. fatigue strength • manufacturing drawings - supports, printing orientation 	<ul style="list-style-type: none"> • limit angle in printing • elastic modulus, density • hardness • thermal properties • electrical properties • thermal treatments - hardness and strength - stress relief • typically - weldable materials - high alloyed - contain defects 	<ul style="list-style-type: none"> • printing orientation - minimize supports - minimize heat input • chamber size - maximum dimensions • support design - in CAD or before printing • removal of supports • surface quality - as-built vs. machined - material defects - esthetics • build time and cost - layer thickness 	<ul style="list-style-type: none"> • machining allowances • tools and accessibility • geometric tolerances • surface quality • surface treatments - abrasive - shot peening • non-traditional methods - abrasive flow machining - remelting of surfaces - laser shock peening • joining by - welding, bolts, adhesives
<i>Loads</i>	<ul style="list-style-type: none"> • alternating loads • ultimate loads • pressure loads - ductility requirements • electrical loads • thermal loads 	<ul style="list-style-type: none"> • fatigue strength - porosity, defects - surface quality - dross formation • ultimate strength • elongation / ductility 	<ul style="list-style-type: none"> • thermal stresses - torn supports - distortions - cracks • material and shape dependent 	<ul style="list-style-type: none"> • fixings for machining • relief of residual stresses - distortions
<i>Quality</i>	<ul style="list-style-type: none"> • specifications for QA • (lack of) standards for AM • purchasing & agreements • fit for purpose -assessment 	<ul style="list-style-type: none"> • SLM test series - printability assessment • tensile tests • fatigue tests • macro specimens - hardness, microstructure - defects • defects vs. required strength 	<ul style="list-style-type: none"> • powder QA • powder handling - oxygen, moisture • process parameters • process specifications 	<ul style="list-style-type: none"> • dimensional accuracy - EN-ISO GPS standards • surface quality • are approval limits fulfilled

Figure 2. The things to consider in design utilising the selective laser melting process.

2.2 Design freedom

The main benefits of AM in component design repeat a lot in literature. The most common benefits of AM are collected below.

- Ability to produce complex shapes is the main benefit of AM.
- AM is well suited for decreasing the amount of material and produce light weight structures.
- Internal cavities, undercuts and channels are possible with AM. However, the powder needs in general to be removed from the internal cavities.
- Conformal shapes such as conformal cooling channels and conformal lattice structures are possible with AM. Conformal shapes are internal shapes following smoothly the surface shapes of the component, therefore leading to constant wall thickness of cavities in parts with complex geometries.
- Parts traditionally assembled together can be combined (or consolidated) into a single component with AM. Functions can be combined to less parts. Leakage and heat resistances typical to mating surfaces in bolted connections can be avoided.
- Customization, tailoring and small serie production are also often listed as benefits of AM.

However, there are also manufacturing limitations. The current limitations of AM are for example:

- Need of support structures during printing and the effort of their removal.
- Variation of manufacturing quality and lack of control of process parameters.
- Lack of design rules and material data.
- Lack of fatigue test results and fatigue design curves.

- AM is currently more or less limited to small scale production (size of both components and series), although series up to 2000 pieces per year by SLM are being reported (in 2015).
- Lack of standards and quality assurance processes.
- Surfaces need in many cases to be post treated for suitable surface roughness.

The AM industry is currently developing fast, and solutions and practices are widely expected to emerge to pass the current limitations.

2.3 Materials for selective laser melting process

The materials available for SLM and the material properties are discussed in detail in [19] (in Finnish). The main points from the design point of view are:

- Anisotropic material properties
 - The mechanical properties of SLM materials are typically slightly different in x, y and z –directions, due to the layered manufacturing process.
 - The difference is recommended to be checked for the materials to be used from tensile test results.
 - In practise isotropic properties can be used in early design and the effect of anisotropic properties on the stresses etc. can be checked before final design.
 - If the anisotropic behaviour becomes critical, the printing orientation vs. stresses etc. shall be checked carefully.
- SLM materials are typically high alloyed materials, some with very high strength and hardness.
 - The high material and manufacturing cost can in many cases be compensated by using light weight structures and less material.
 - Note, that ductility (elongation until fracture) may be much less than of the similar grade in traditional rolled condition. Many real life applications are controlled by standards and regulations, where the minimum elongation until fracture is specified.
- Fatigue strength data is not yet widely available for SLM process, but the fatigue properties typically
 - depend on the manufacture specific process parameters and powder.
 - depend on the surface quality.
 - depend on the material defects. The effect of defects on fatigue strength can be estimated for example by the Murakami-Endo approach.
 - can be assessed by (case specific) fatigue test series.
- Heat treatments are specified for many of the SLM materials.
 - For stress relieving and obtaining the final material properties.
- SLM materials are typically weldable
 - This allows the SLM parts to be joined by welding.
 - Weldability assessment and welding tests are recommended to ensure appropriate quality.

2.4 Manufacturing constraints and the basic design rules for SLM

The layer by layer manufacturing approach used in SLM and in many AM processes sets the basis of many of the manufacturing constraints and design rules. As the topmost powder layer is melted, the stability of the melt pool depends on the support provided by the preceding layer. In addition, the thermal conditions of the melted region depend largely on the formerly built geometry. The SLM and other AM processes are discussed in depth in for example [2].

The SLM process is illustrated as an overview in the following figure.

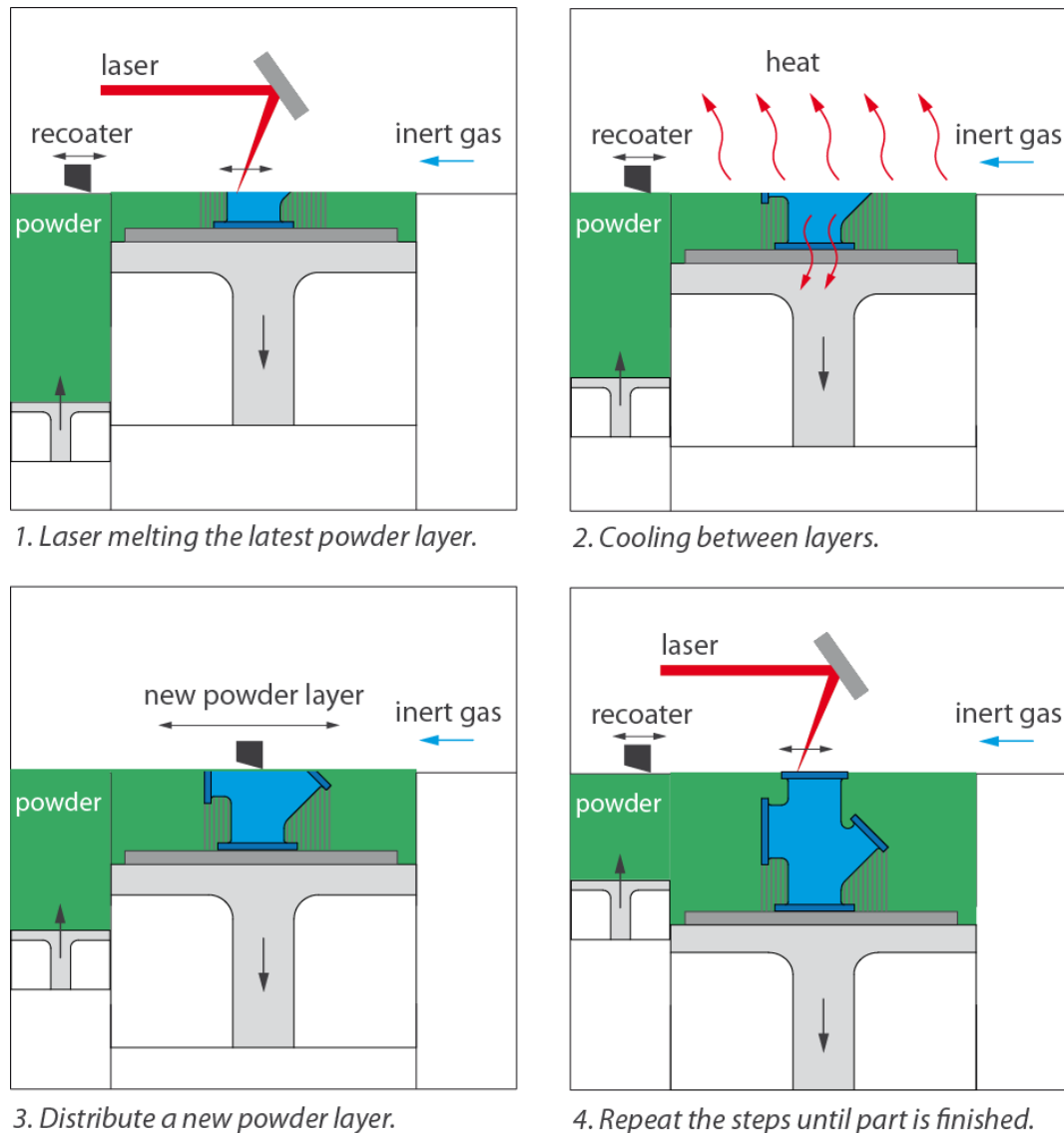


Figure 3. The SLM process in brief. The typical build times are from hours to a couple of days for a component that can be printed in the SLM 125 build chamber, of size 125x125x125 mm.

The basic instructions according to [1] for placing the components for printing to avoid collision between the coater and the component are presented in the following figure. The component is typically placed on the base plate slightly inclined respect to the recoater (wiper), in order to prevent the recoater from breaking. This requirement often limits the usable printing dimensions and the designer should consider the maximum printing dimensions in the early phase of the design task.

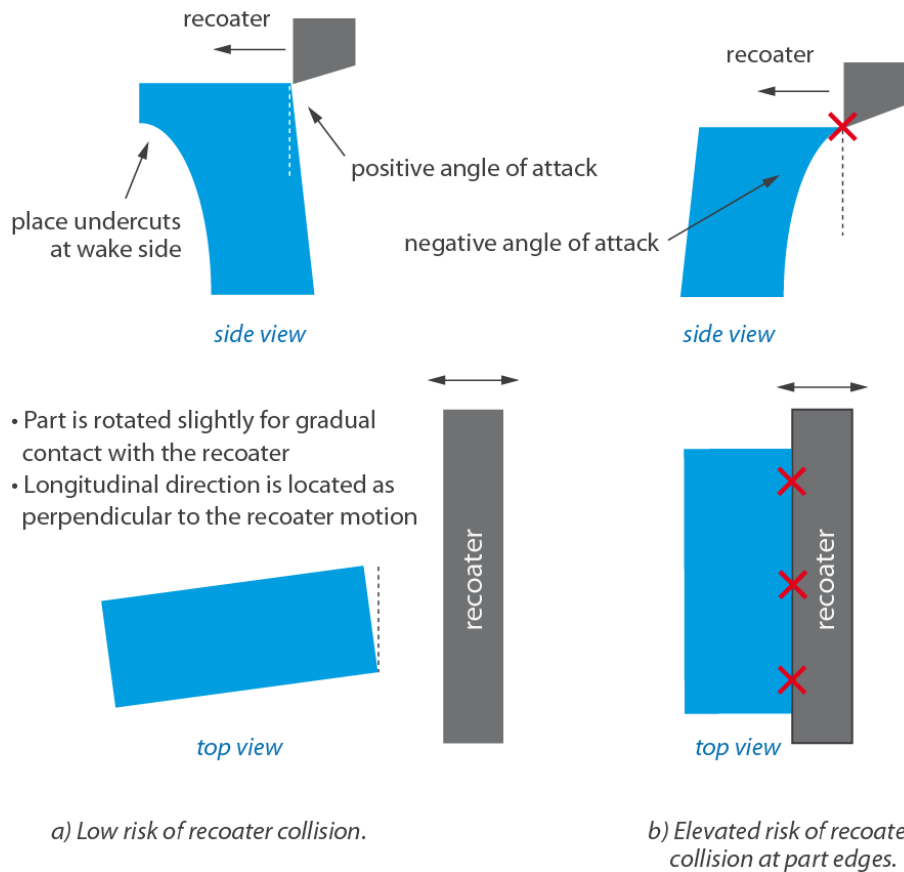


Figure 4. The basic instructions after VDI [1] for placing the components for printing. The basic idea is to place the part so that the wiper spreading the powder passes the edges in a slight angle, to lower the risk of collision and risk of interrupt of the printing process.

The local support condition of the melt pool is handled by defining the limit angle for design. The sufficient thermal conduction is ensured by avoiding overhangs and using appropriate supports in design. The surface quality resulting from the SLM depends on the geometry. These conditions and design principles are illustrated in the following figures.

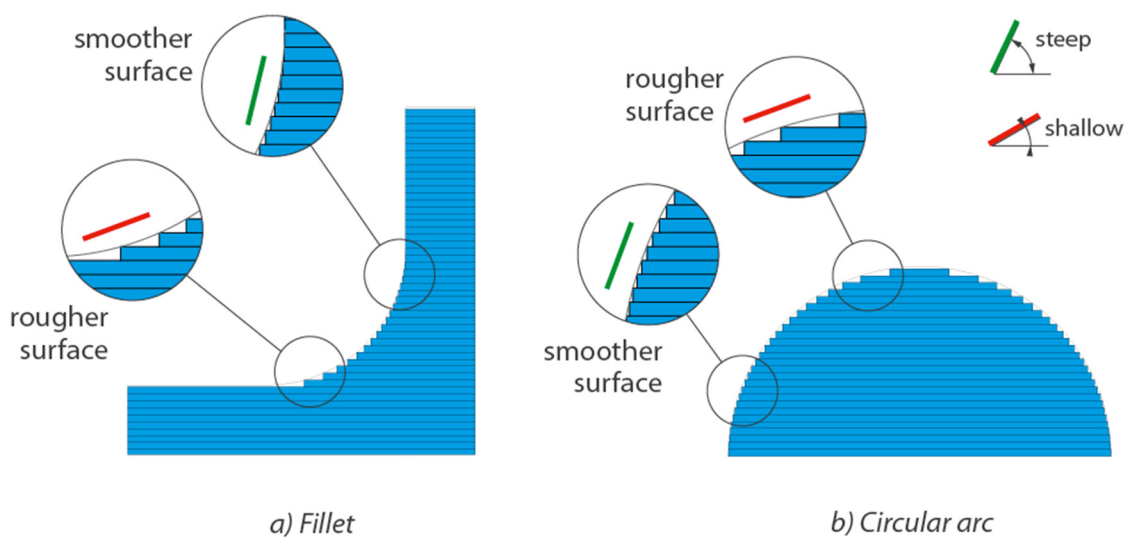


Figure 5. Effect of layered structuring on the surface quality.

The effect of layerity on the resulting surface quality follows basic trigonometry and the step length and rise can in principle be estimated by simple calculus.

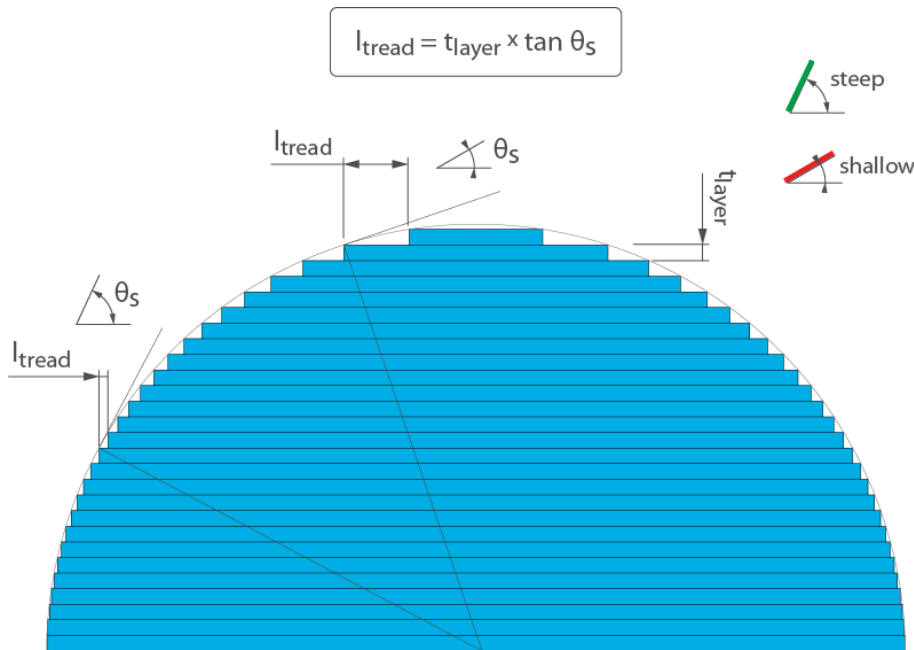


Figure 6. Effect of layered structuring on the surface quality. Geometrical dependence.

The effect of layered structuring on the surface quality and local supporting conditions is illustrated in the following figure at a few inclination angles.

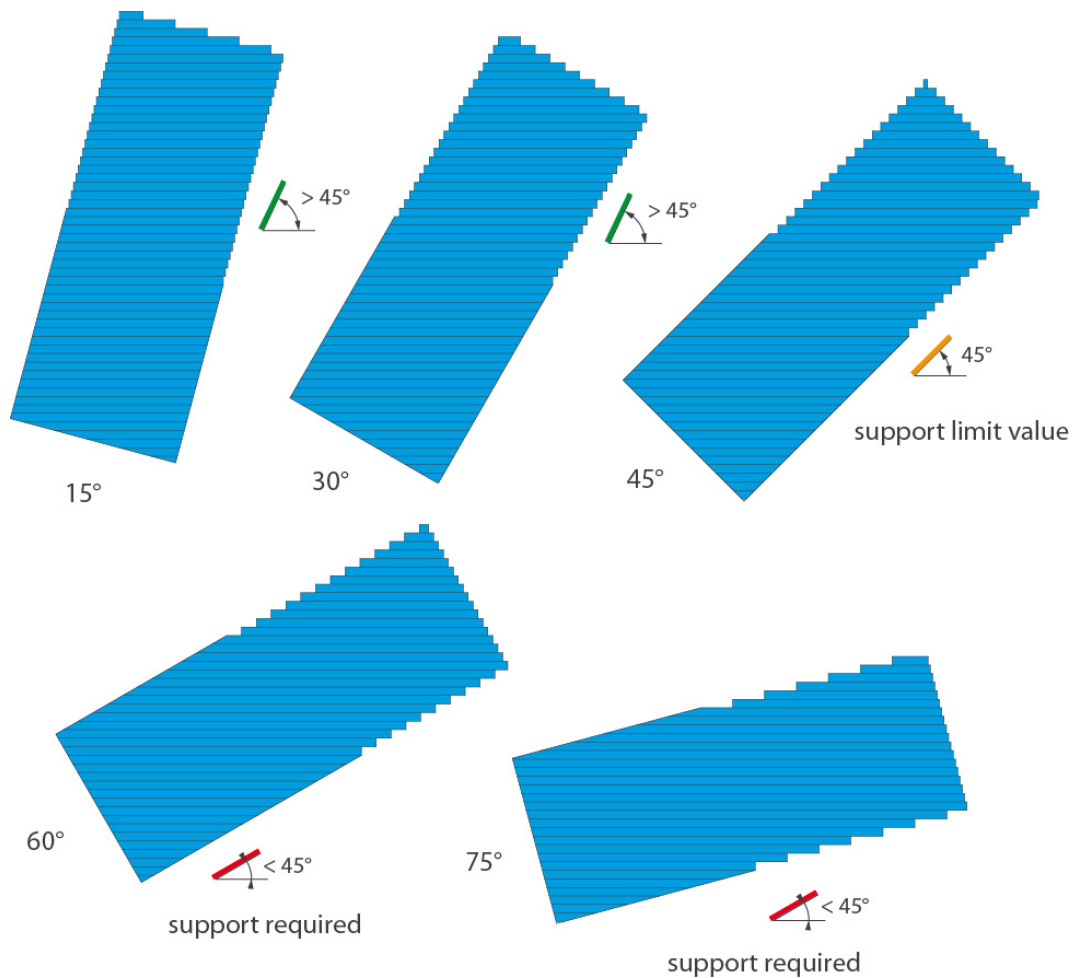


Figure 7. Effect of layered structuring on the surface quality and local supporting conditions.

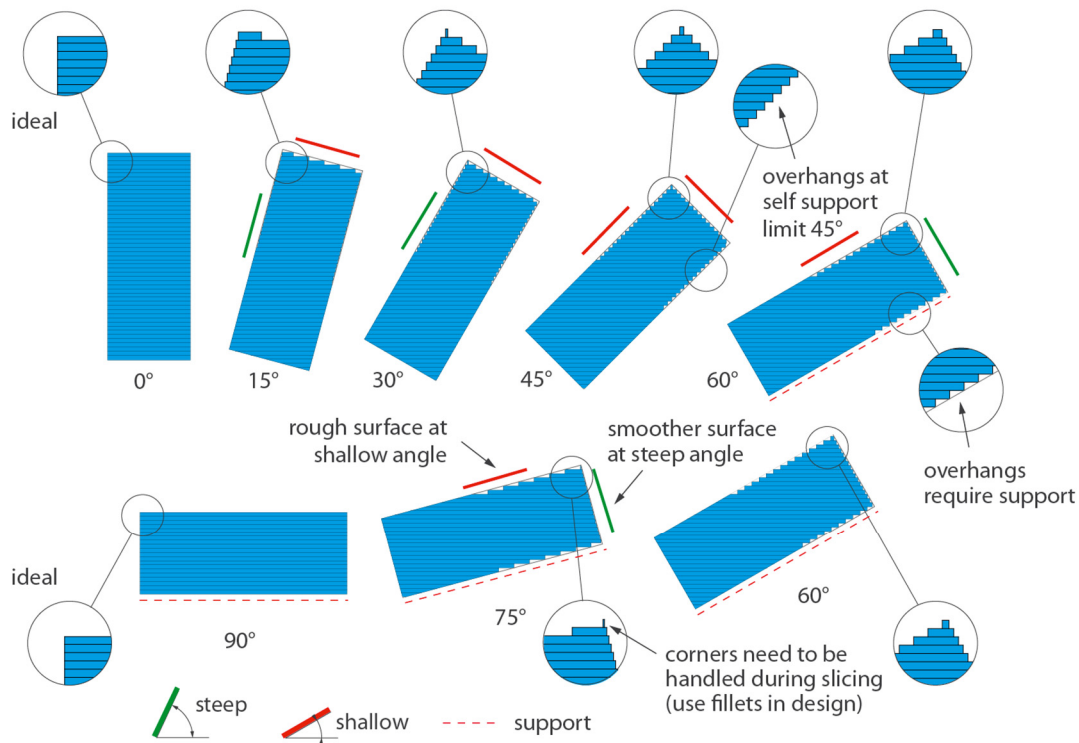


Figure 8. Effect of layered structuring on the surface quality and local supporting conditions.

Based on the brief layerity studies, it is seen that the layer thickness defines the minimum limit angle below which the structure requires supports. This is illustrated in the following figure. If the step length (depending on slope and layer thickness) is short enough, the preceding layer provides enough support for the melt pool. If not, the melt pool mixes with the below powder bed and dross formation occurs. To prevent this, supports are used after the limit angle. The limit angle depends on the material type (alloying) and process parameters. It was learned from the test prints that distortions are more significant than the sagging.

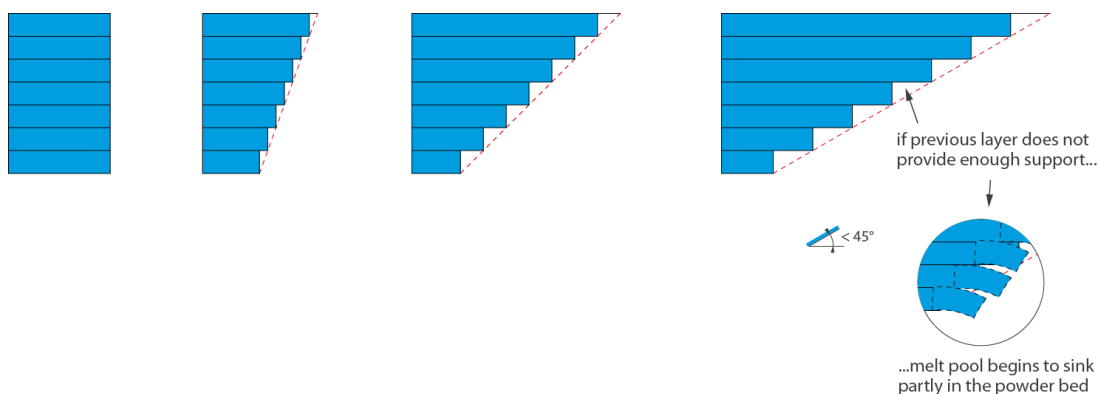


Figure 9. The condition defining the limit angle for minimum unsupported printing angle.

The mechanism of the dross formation is illustrated in the following figures. Heat conductivity of metal powder is much lower than of the solid metal, the ratio is about 1/100. At overhangs less heat is transferred away from the melted region than at vertical or slightly inclined orientations. The heat trapped at overhangs causes the melt pool to mix partially with the below powder, leading to the dross formation at such locations.

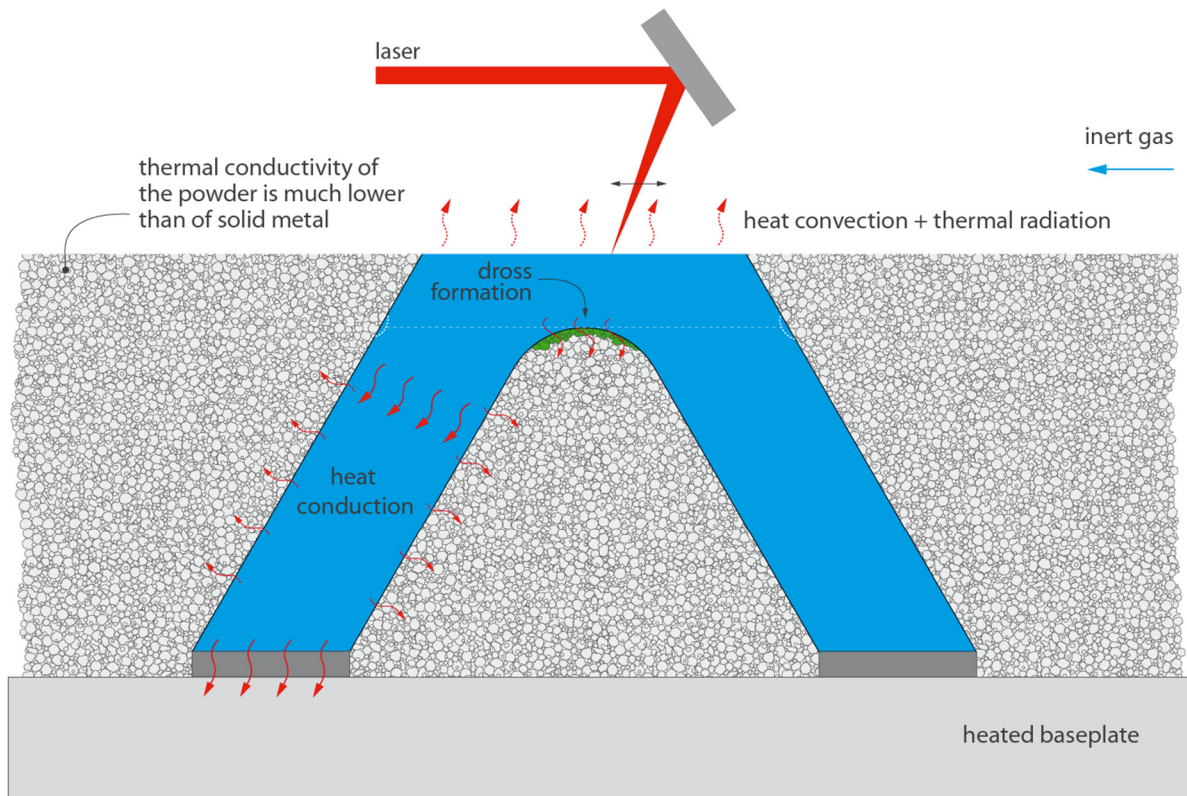


Figure 10. The mechanism of the dross formation. The powder is sintered partially over the layer thickness at locations with poor heat transfer, such as overhangs. The partially melted powder is attached to the component and is called dross, after the similar term used with castings. Dross can be ground off and typically small amounts of dross is allowed.

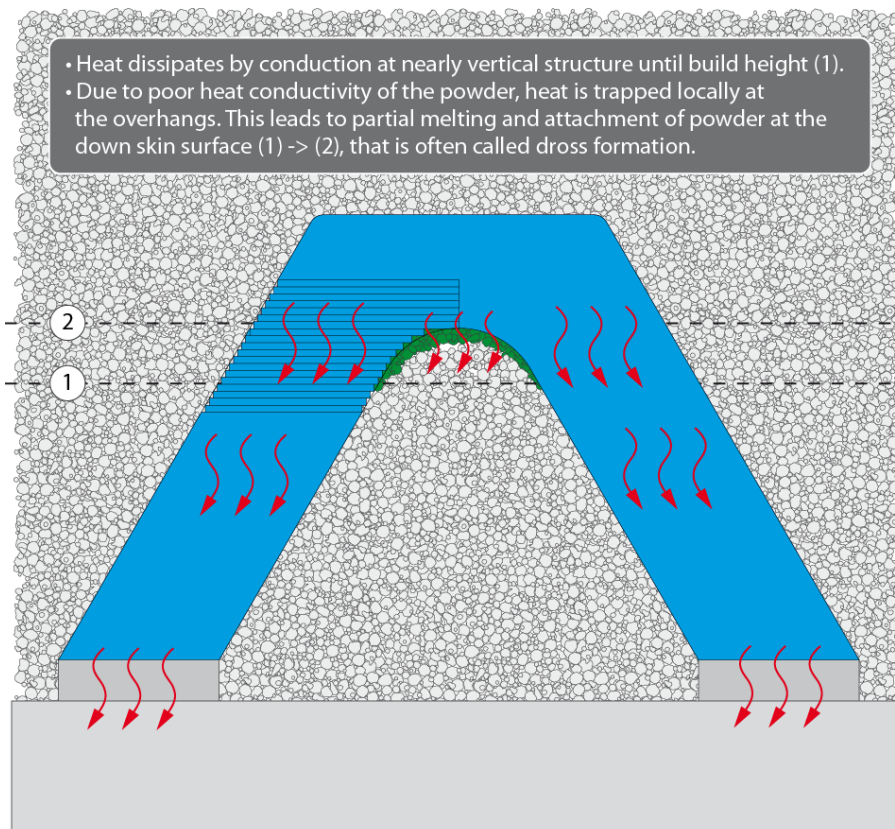


Figure 11. The mechanism of the dross formation explained.

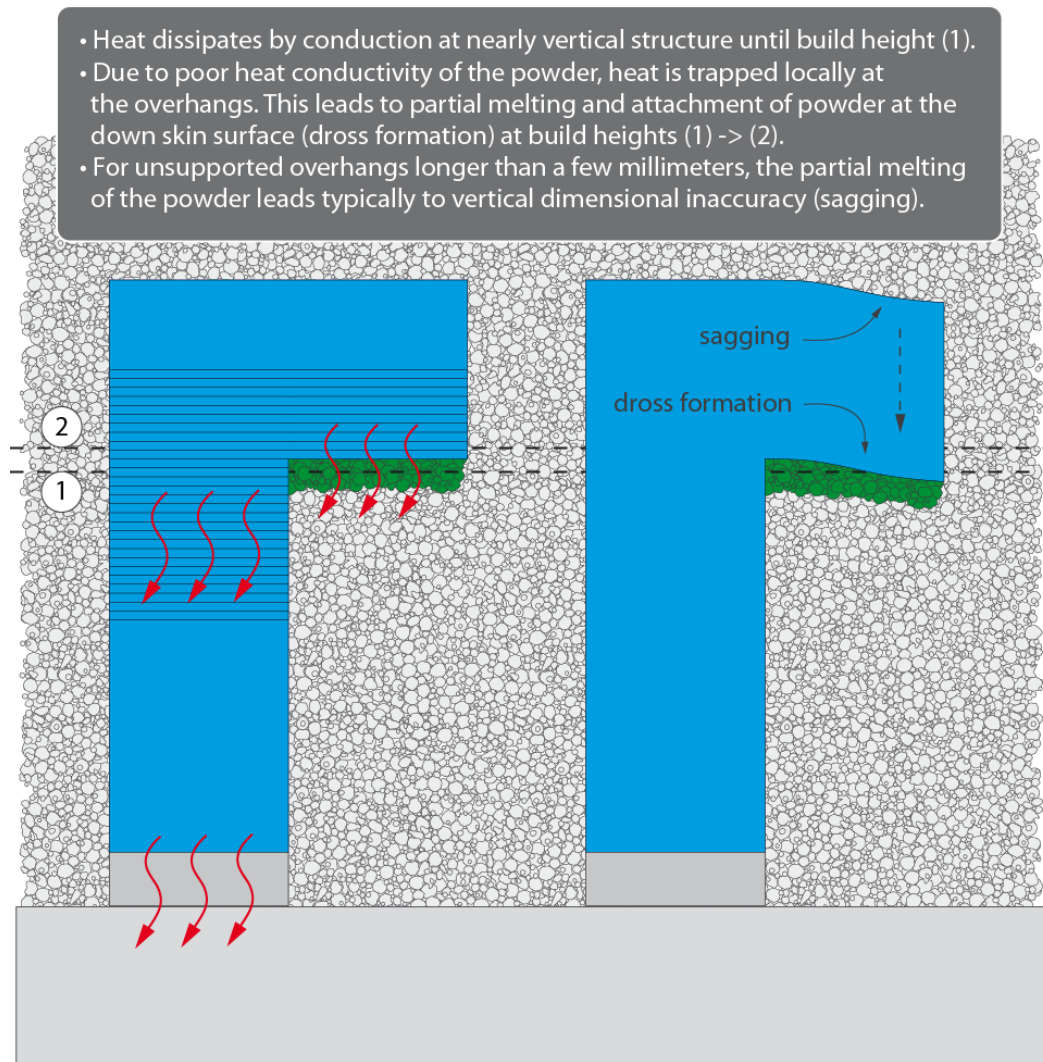


Figure 12. The mechanism of the dross formation explained.

Dross formation, distortions and sagging can be prevented in design by using fillet to support the overhang and increase thermal conduction from the overhang to the base plate. This is illustrated in the next figure.

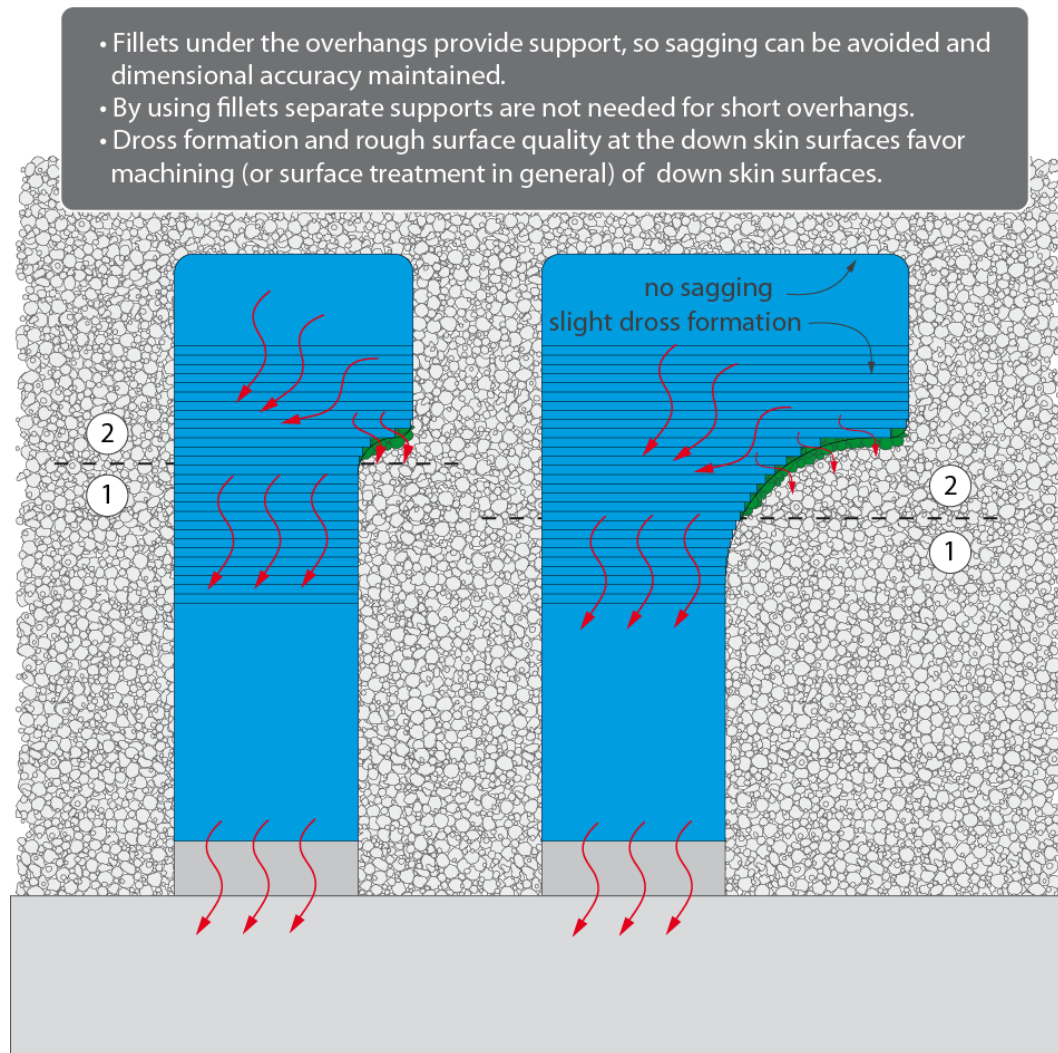


Figure 13. Preventing dross and sagging by using fillet to support the overhang and increase thermal conduction from the overhang to the base plate.

The effect of printing orientation on the heat input per layer with a plate like geometry is illustrated in the next figure. The part can be tilted to decrease the heat input per layer (less lasering per layer), so that the heat has time to spread to the component before the next layer is melted.

However, when considering tilting of the component, the designer needs to consider the support conditions of all the surfaces of the component. One field of research in design for AM is to develop computer software to optimize the printing orientation (minimize supports and heat input).

The printing orientation should in practice be fixed quite early in the design phase, to avoid excessive iteration of the design. Just like in casting design, the casting position is typically decided quite early in the design process.

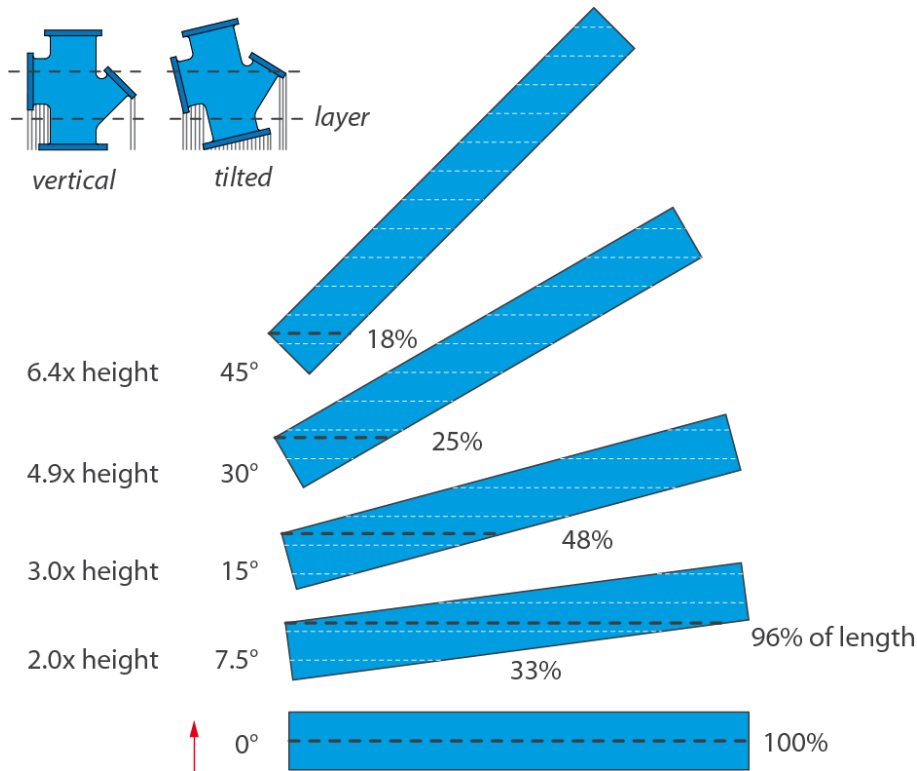


Figure 14. Effect of printing orientation on the heat input per layer with a plate like geometry.

The laser spot diameter defines the practical minimum radius of sharp end tips and the basic resolution of the process. This is sketched in the following figure.

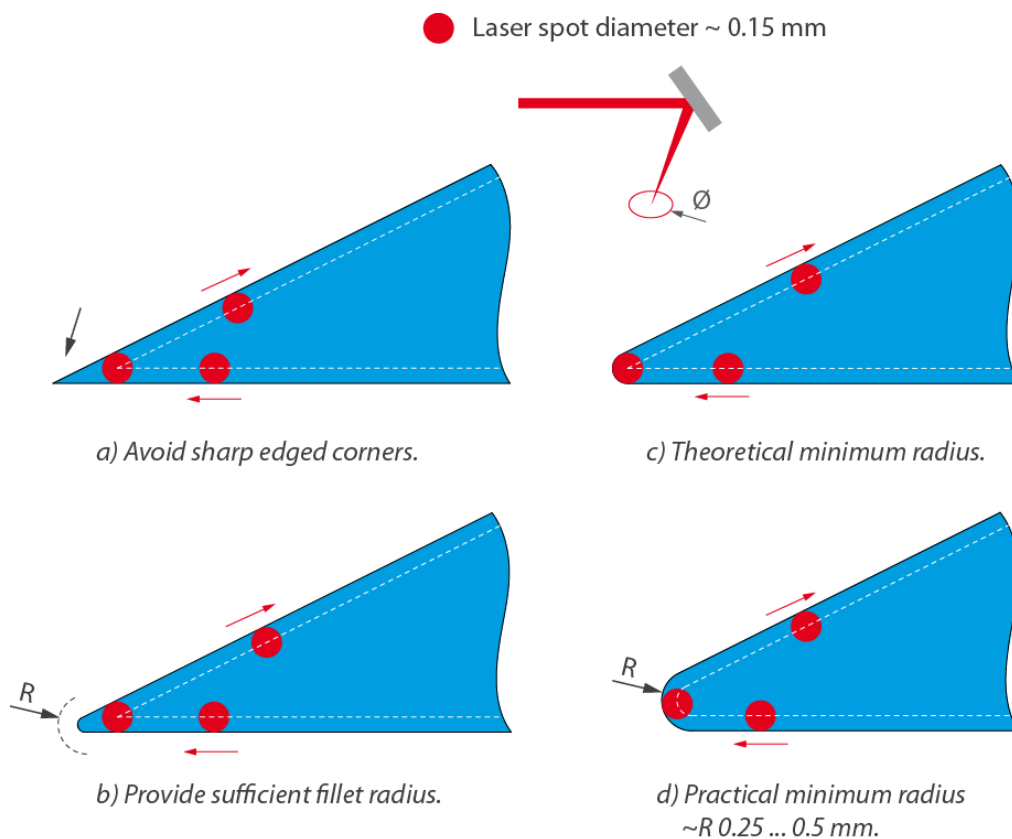


Figure 15. The laser spot diameter defines the practical minimum radius of sharp end tips. Similarly printing very thin blade like structures are limited by the laser spot diameter.

2.5 Basic design example

A candle holder shown in the figure below is a simple structure and it is used here to demonstrate the use of the basic support design rule on a component.

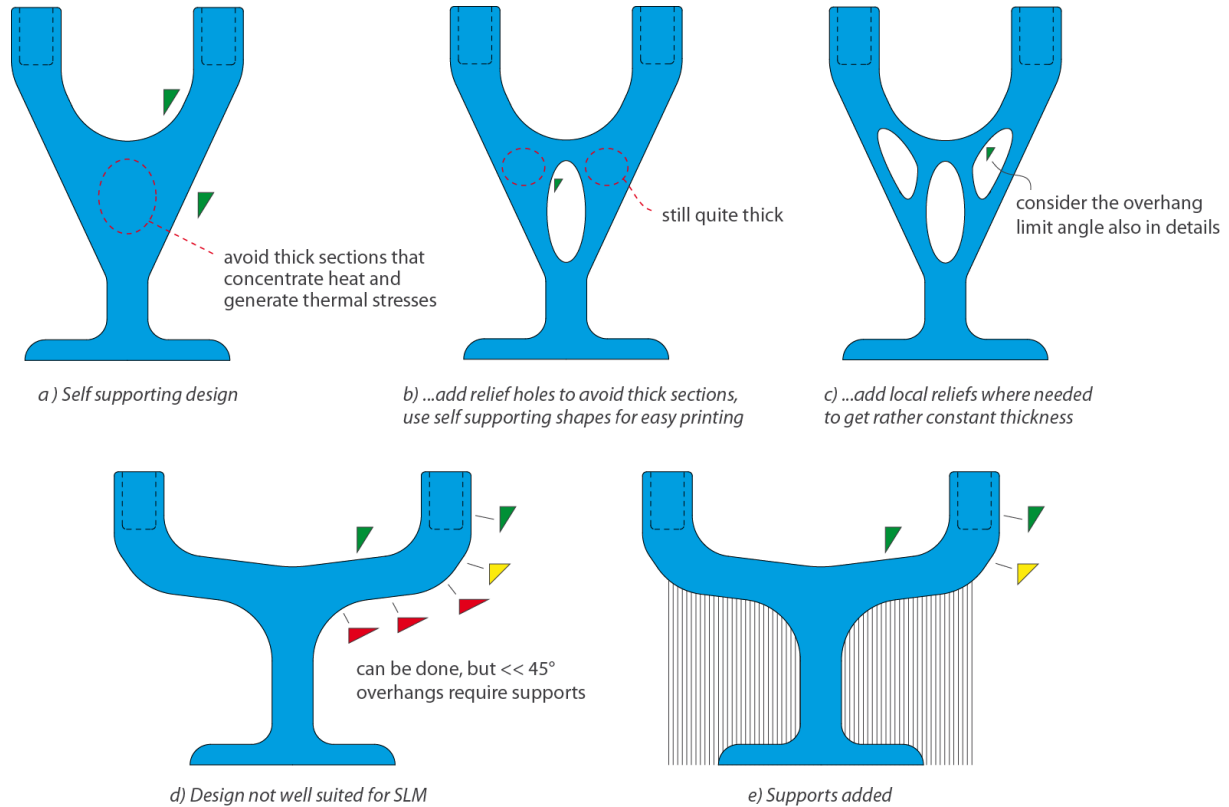


Figure 16. Basic example of component design considering the SLM support design rules.

The symbols for indicating the need of support at the component surfaces are explained in the figure below.

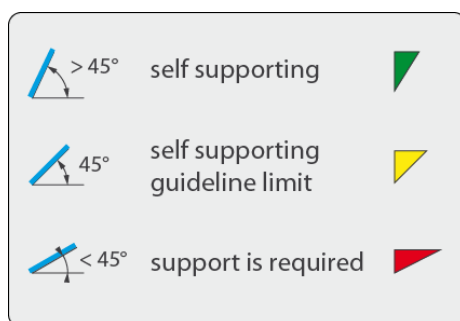


Figure 17. Symbols for need of support.

2.6 Support design

During the powder based, layer by layer laser melting of the component by the SLM process the downward orientated surfaces (at angle less than 45 degrees to platform) of the component have to be supported by additional support structures. This is due to the fact that the melt pool needs the support of the previous layer during solidification to avoid local geometrical deviations, that would accumulate in the following layers and lead to excessive geometrical deviations, thermal problems or even printing failures. The support structures are discussed in depth for example in [7] and [9].

2.6.1 Supports for build jobs

When designing supports for a build job the first rule of supporting is that you can't build on nothing. Some kind of supporting is always needed.

To minimise need of supporting the self-supportivity is recommended when designing the parts, so the printing direction should be considered in CAD. This is highly essential for inner channels so that those should not be fulfilled with supports not able to be removed after the build job finished. Heat treatments should be also taken into account when designing the inner supports. The powder stacks easily to small supports and channels during heat treatments.

It is recommended to try to achieve self-supporting printing orientations for the parts when positioning those to platform and build space for printing. This printing orientation optimisation is highly case sensitive and should be considered individually for each case and at restrictions.

The first primary of supporting is to attach parts to the building platform to lead the heat out from the structure. The second primary of supporting is to carry the bending stresses caused by the heat to create non-bended and dimensionally accurate parts. Adequate attaching for the structure is needed for the powder recoater functionality and laser accuracy to be filled. Thirdly, supports make non-self-supporting surfaces printable.

In general some parts might be able to start building directly from the platform. In these kind of cases the part needs additional material under the lowest positioned surface of the part. This extra material should be enough to saw it out and to be machined to dimensional accuracy. Typically big parts are considered to print directly to platform since those will have a lot of bending caused by the laser generated heat. In these cases there is typically still some need for supporting of smaller details.

It should be noted that heat conduction and heat caused bending stresses are different for each material. This means that adequate supports are different for each material.

For example, even big aluminium piece builds well in 45 degrees angle with only minimal supports on platform. The same part printed from Inconel needs very stiff supports to be able to print without support cracking and to achieve dimensional accuracy.

Stiffness for supports of one type should also be adjusted according the material in use.

2.6.2 Support design principles and support types

The support design principles typically used in designing SLM components are clarified in the following figures by examples.

The basic support design rules by Materialise NV are shown in the following figure. Materialise NV is the software house that provides the Magics and 3-Matic software used in this project for printing preparation and editing polygon models.

The basic idea in the support design rules by Materialise is to fix the part at the middle or the lowest point and the outermost corners by rod type supports. The leading principle of this idea is to carry the bending loads caused by the heat generated in the laser melting process. The downward orientated surfaces (downskin surfaces for short) are then supported by block supports. The rod supports are solid bars, while the block supports are cellular (lattice) structures.

Golden rules for support design by Materialise NV

1. Use cone supports for entire part and thermal stresses
 - always place a cone support at lowest point of part
 - and at the ends, where bending deflections are the largest
2. Use block supports for SLM layers
 - easy removal, many contact points
 - add break points and perforations
 - application of block supports is material and scan strategy dependent
3. Specifically for lattice / light weight structures
 - horizontal members:
 - safe to print span up to 1 mm
 - with fillets at ends even wider span can be printed without supports

According to discussions with
Manuel Michiels, Materialise NV

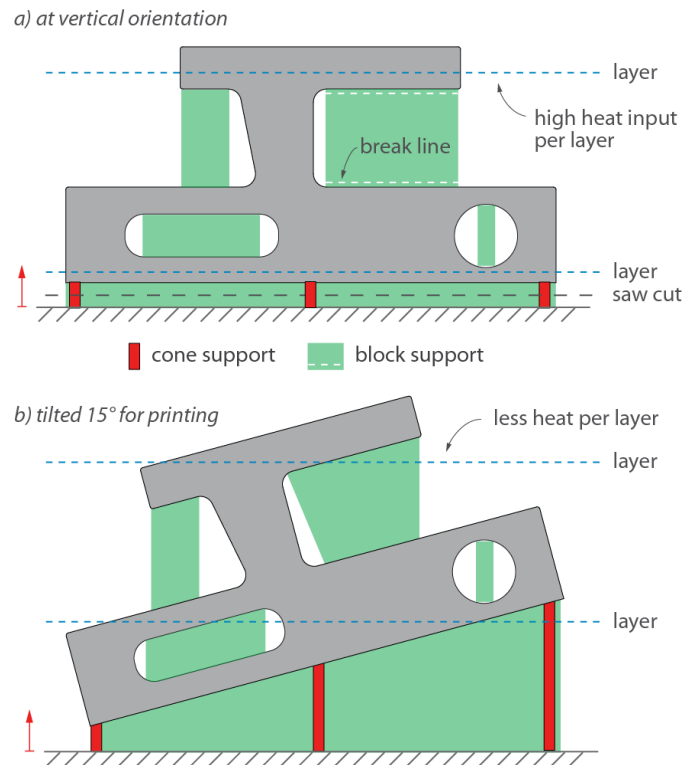


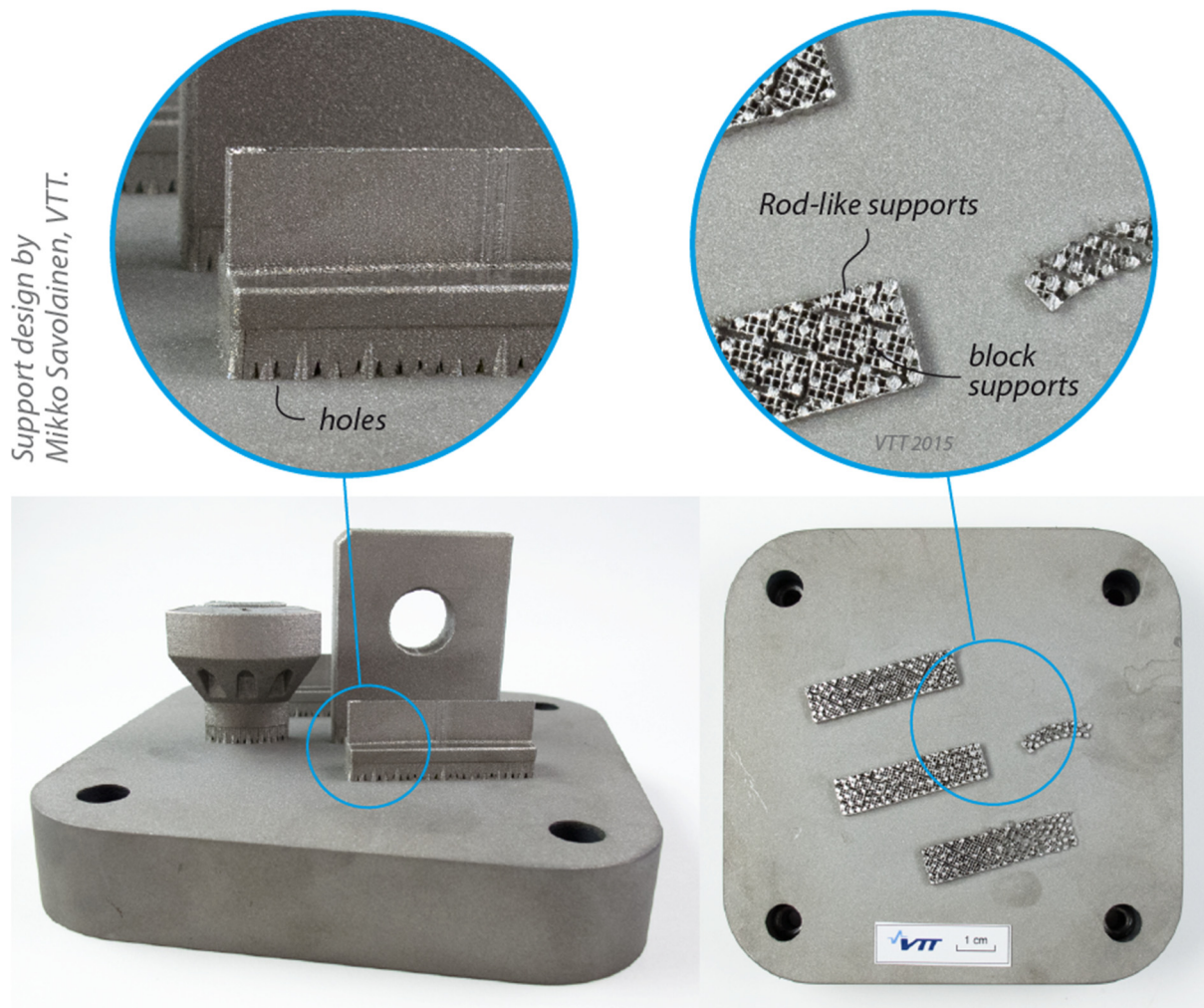
Figure 18. The basic support design rules by Materialise NV, Belgium.

The block support are easy to remove, but the stiffness and heat conductivity is lower that of the solid bars. The more the rod type supports are used, the stiffer the supporting structure becomes (and need of block support hatch condensing diminishes for some materials with low heat conductivity).

Figure 18 presents basic support design rules. As a note to consider, some of the presented block supports are located on-part which could be avoided using angled supports rising directly from the platform. Angled supports give better surface quality at (part's earlier) lower end of the support when on-part surface heat conduction effect is removed from the part. On-part starting supports are also more time consuming when removing and sometimes not possible to remove by machining.

An example of block supports used in printing of a set of small test prints is presented in Figure 19. The printed pieces were detached by machine saw from the base plate, and the support structures can be seen in the figure. This kind of support structures worked well for the small pieces. At larger pieces and components the block supports were often torn and heat markings and distortion were present in the prints. The solid support structures modelled in CAD were used in this project for larger pieces and components to provide additional stiffness and thermal conductivity.

Examples of the use of block (lattice) supports are presented in Figure 20. The block supports can be added between the downskin surfaces and the base plate, or between the downskin surfaces and the part itself. Tilting the part for printing decreases in principle the heat input per layer and is often considered to decrease the thermal distortions. Tilting of the part may however complicate the support design in complex structures. The limit angle concerns also the block supports and shallow build angles may lead to printing failures of the support structures. High block type support structures have poor thermal conductivity that may lead to heat build-up in the upper locations of the printed part.



a) Test pieces printed with typical block supports prepared with the Materialise Magics software.

b) Cross section of the supports are revealed after saw cutting.

Figure 19. Example of the block supports used in printing of a set of small test prints.

The attachment locations of the support structures have typically very rough surface quality after removal of the supports. Some working allowance is often added at the functional surfaces that are machined. Such machined locations can be often safely used as support locations, if the orientation suits for printing. The printing orientation and locations of the supports are recommended to be considered early in the design phase to get the best results.

The solid supports can be modelled directly in CAD to provide both good stiffness and good thermal conductivity for the support structures. Wire cutting can be used to cut the support structures. As the wire cutting machines are often numerically controlled the cutting can be done along curved (but planar in the other direction, not double curved) surfaces. By this approach the designer has also full control of where to locate the supports. An example of using the solid supports is presented in Figure 21.

The various possible arrangements for support structures are illustrated in Figure 22. The most applicable arrangement of the support structures depends on the component to be printed, the material and the process settings. A good practice may be to model an in-house test piece with reasonable complexity and typical geometric features and print a test serie varying the supports.

- Lattice supports are typically added to the part in the manufacturing phase.
- Lattice supports have lower stiffness and are less effective for heat transfer, and can be used when high dimensional accuracy is not required or with materials with high heat conductivity and low melting point (e.g. aluminium).
- Heat input per layer is often compensated by tilting the part so that the melted area per layer is kept minimal. Tilting of the part requires typically more build space than at flat position.
- Risk of thermal distortions can be compensated by increasing the machining allowances. Rod like supports are often used to fix the part properly.
- Lattice supports are often removed simply by hand or power tools.

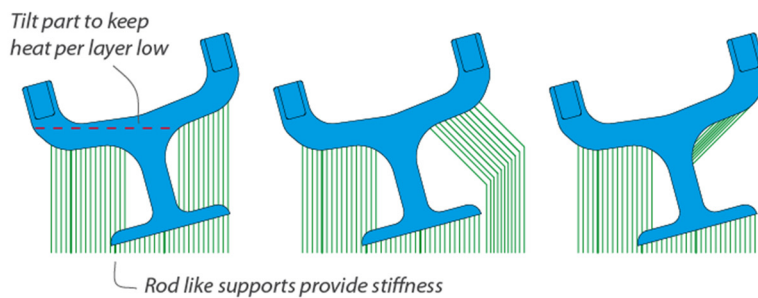


Figure 20. Lattice (block) supports and tilting the part for printing to decrease the heat input per layer.

The representation of the intended support structures when the printing is bought from a supplier is an open question. The geometry of the part is typically delivered as .stl or .step file, and the support design is up to the supplier that does the printing. The use of solid support modelled directly in CAD is one solution to this challenge while the printing practices are developing.

- Solid supports provide the best stiffness and heat transfer, and are recommended when high dimensional accuracy is required or with material with low heat conductivity (such as stainless steel).
- Flat position is suited for this case, as the part is symmetric and has a wide circular bottom flange. Higher heat input is compensated by the good heat conduction of solid supports.
- Solid supports can be removed by machining or wire cutting. Cutting and machining allowances need to be added before manufacturing.

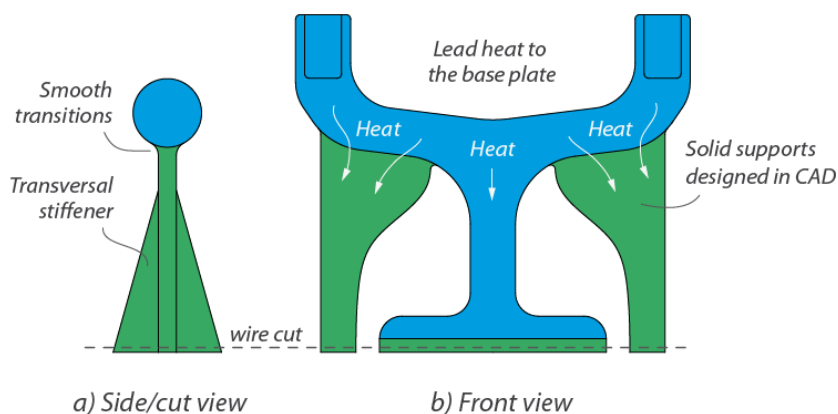


Figure 21. Example of using the solid supports.

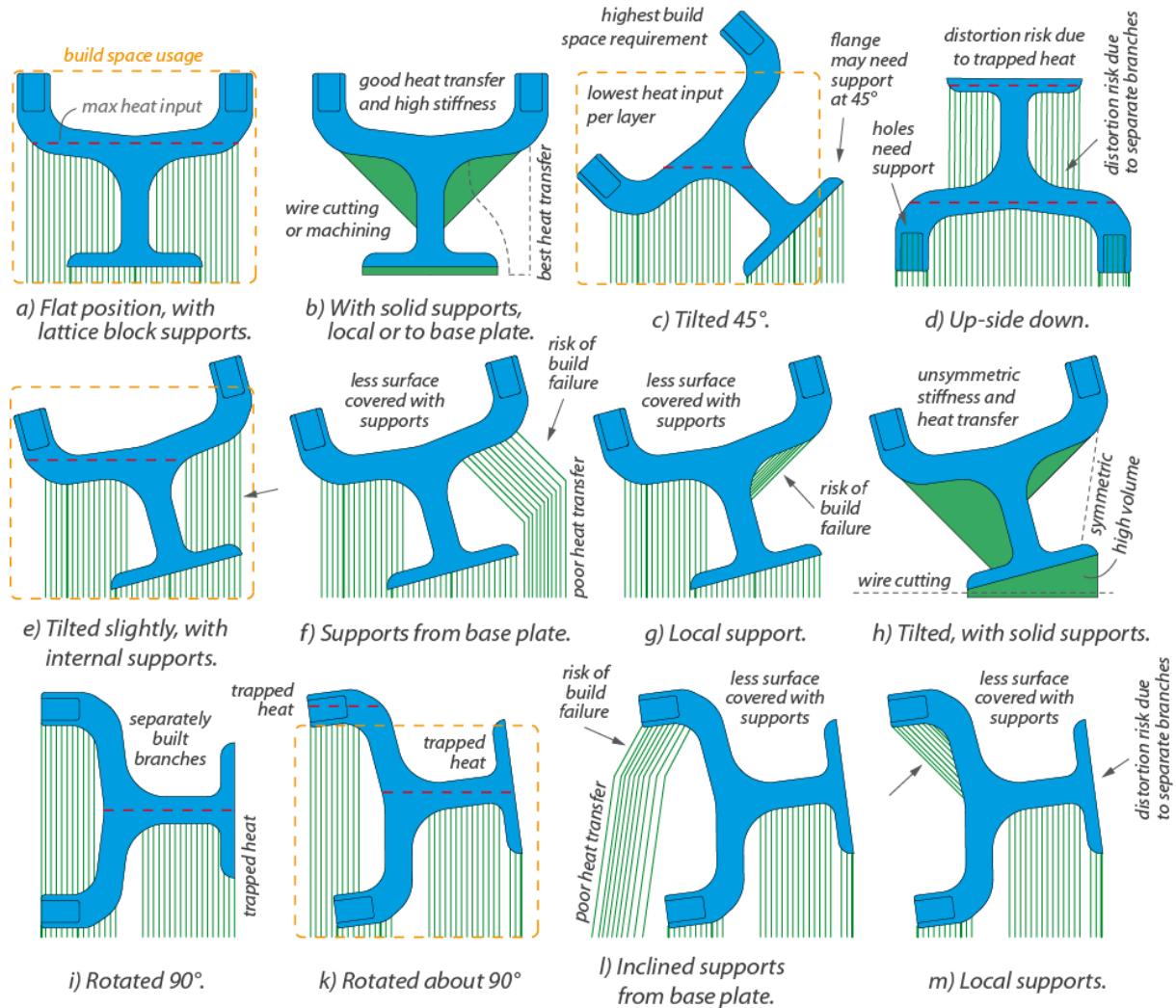


Figure 22. Illustration of the various possible arrangements for support structures.

2.7 Thermal stresses and distortions

The SLM process is prone to thermal stresses and distortions. A few examples of such printing failures encountered early in the project are presented in the following. Adding rod type supports among the block type supports provided additional supporting stiffness to prevent the excessive distortions in the test print series.

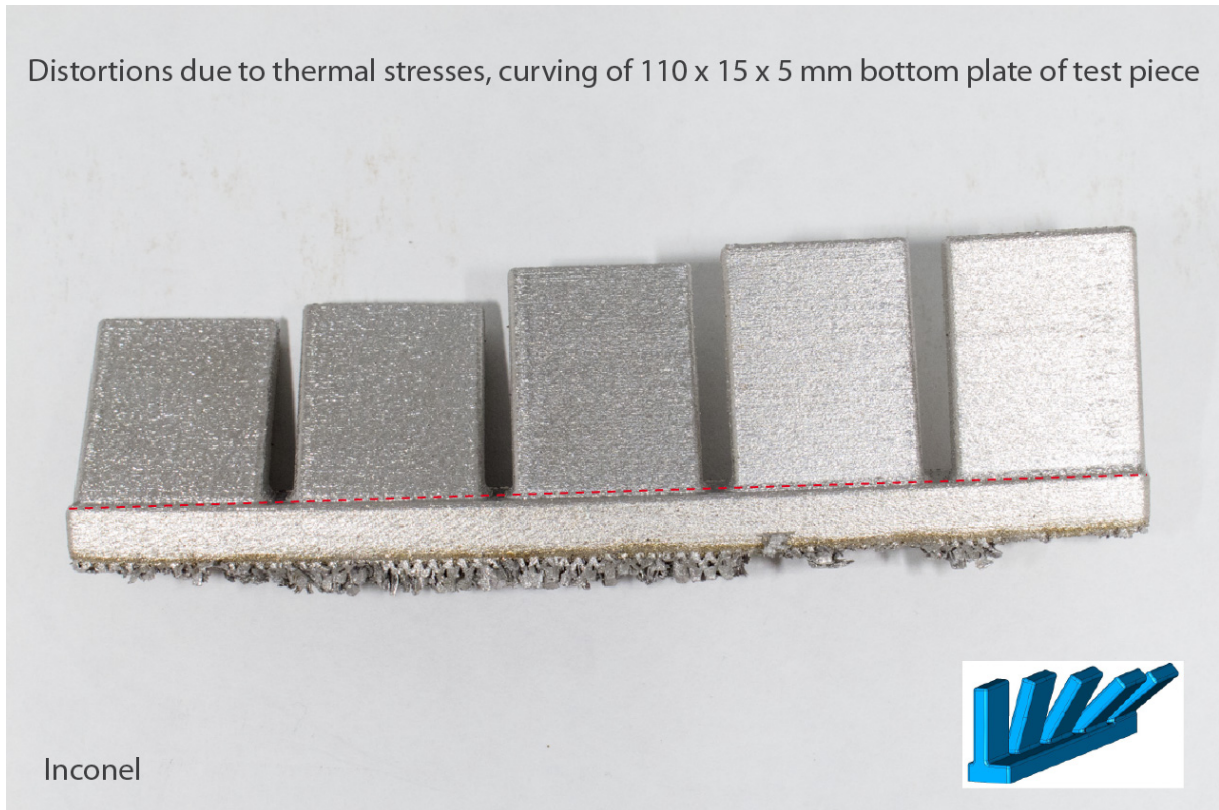


Figure 23. Example of distortions due to thermal stresses.

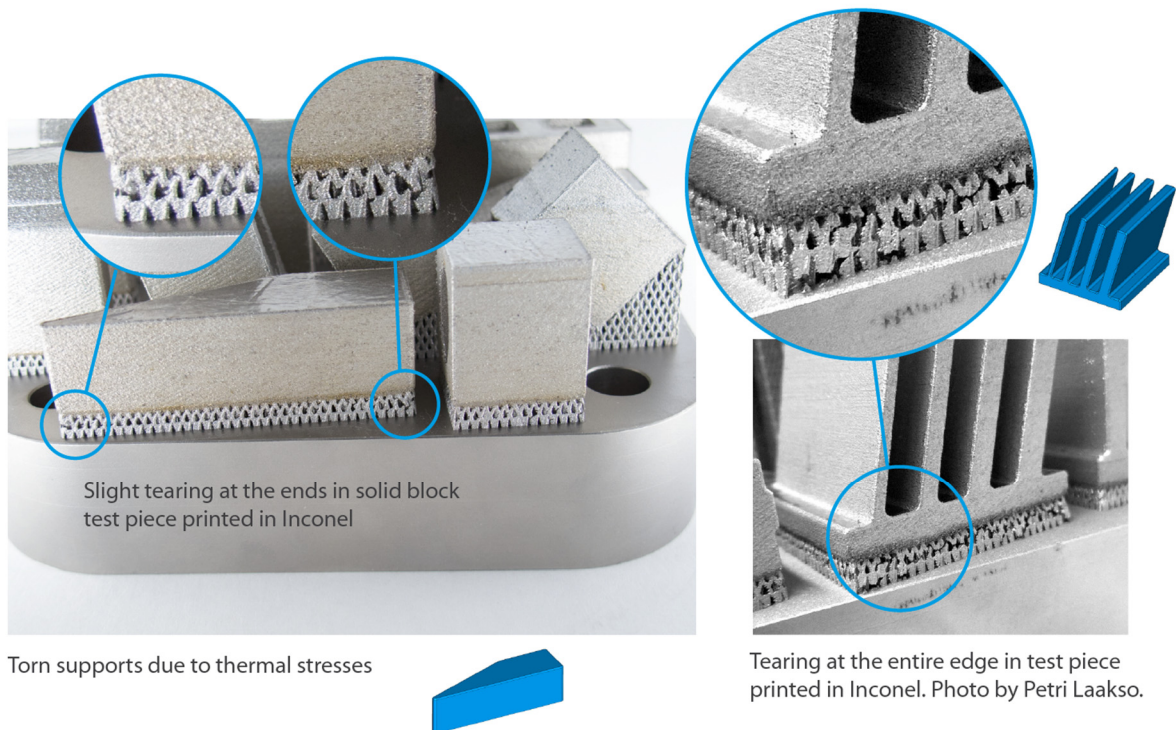


Figure 24. Example of torn block supports due to thermal stresses.

The geometrical accuracy of the 3D-printed test pieces was evaluated using FARO laser scanner and analysis software.

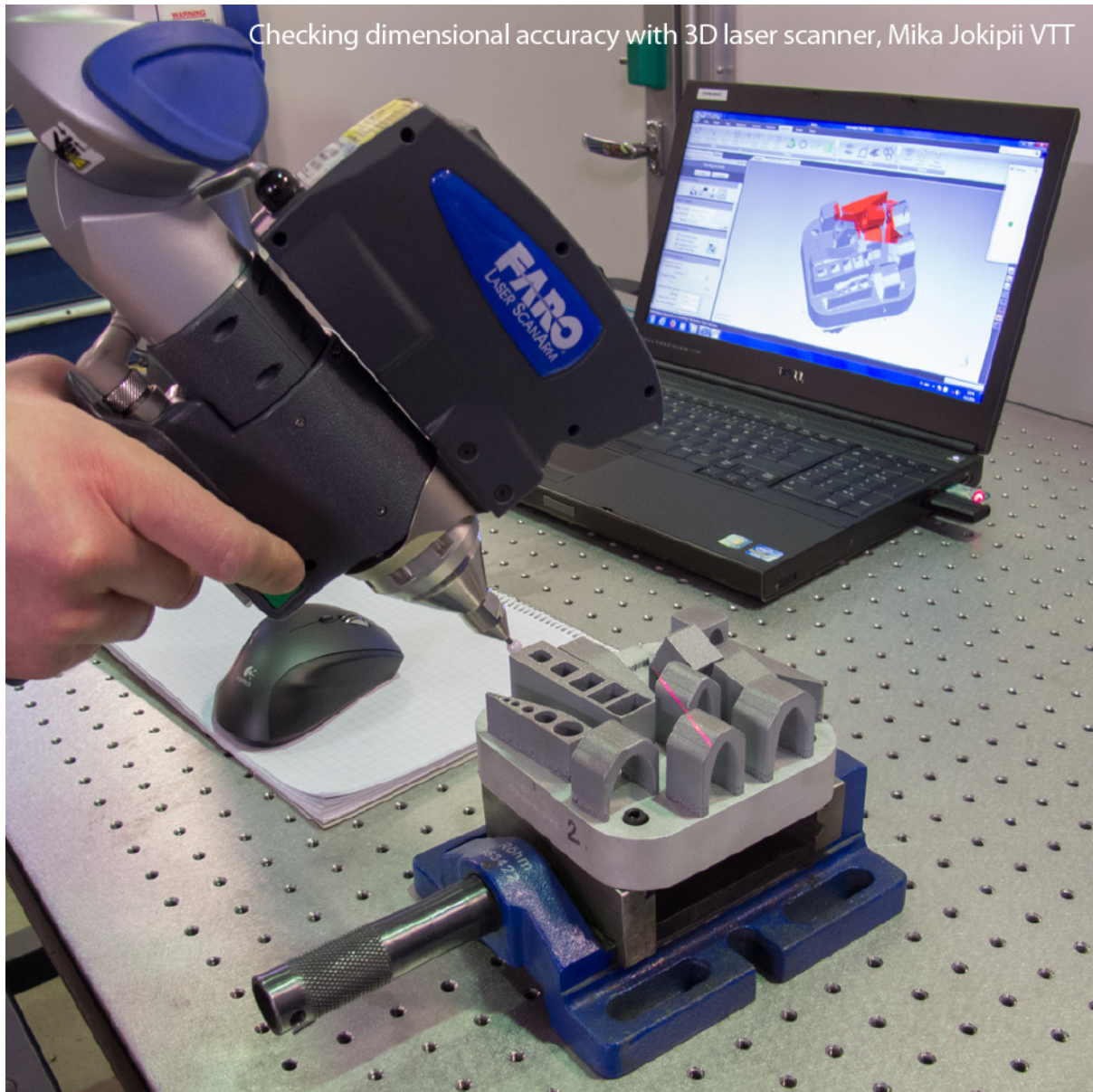


Figure 25. Checking dimensional accuracy of the test prints with FARO laser scanner.

3. Test series of individual design features

A series of individual design features were modelled using I-Deas CAD software. The test print series of several materials were evaluated to assess the manufacturing constraints related to the SLM process. The details of the test geometries are summarised in the following.

The main dimensions of the test pieces are typically below 50 mm. The wall thickness is typically 3 ... 5 mm. Maximum wall thickness used is 15 mm. The dimensions were needed to keep small due to the chamber size of the SLM125 HL printer (125 x 125 x 125 mm³) and to keep the printing times reasonable.

Systematic design and assessment of test prints for basis of SLM design rules

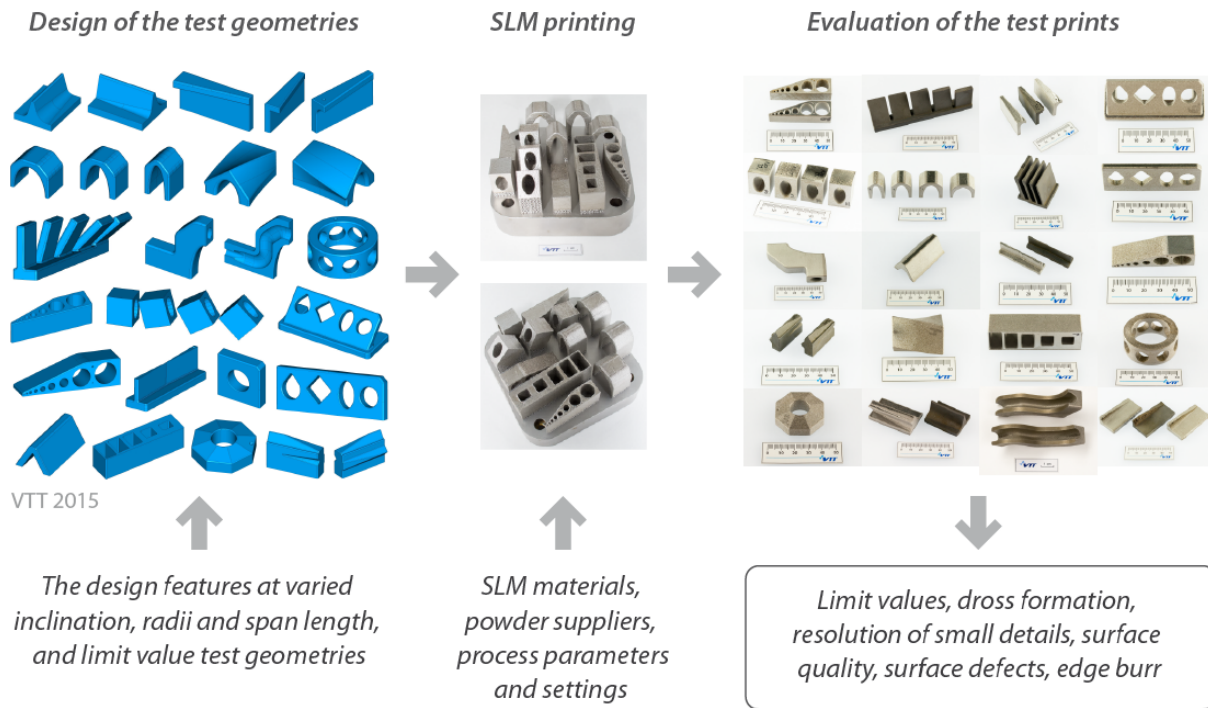


Figure 26. Overview of the approach used for determining the SLM design rules.

3.1 Inclined plates with varying angles and arch like junctions

The inclination angles are varied to assess the self-supporting limit angle and surface roughness versus the inclination. Inclined plates at constant angle of 75 degrees with varying thickness were printed to estimate the effect of plate thickness on the distortions. The span lengths of the archs are varied to assess the self-supporting limit of the down skin surface at the junction location.

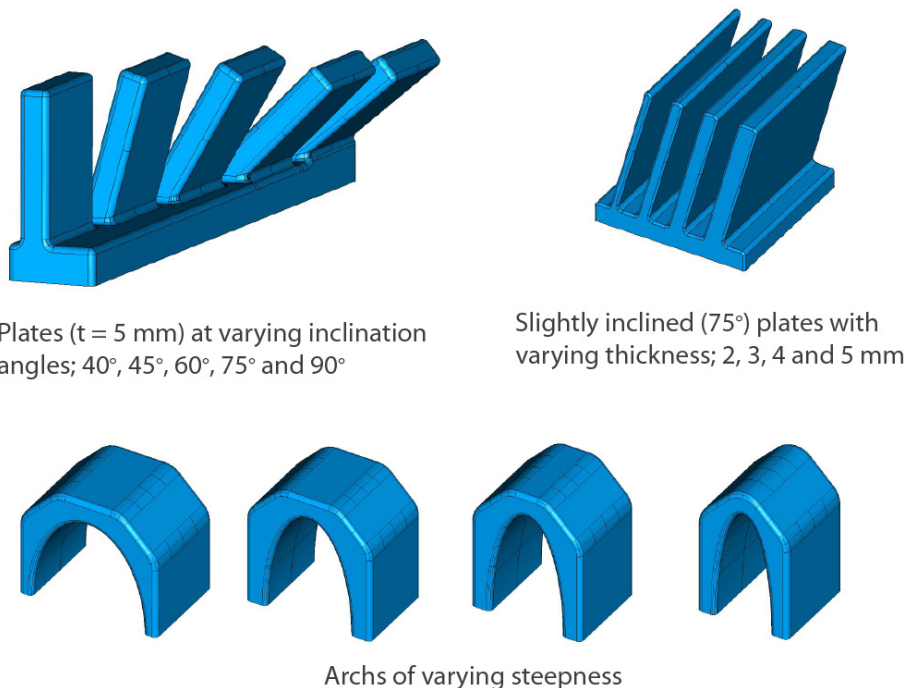
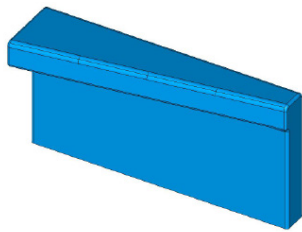


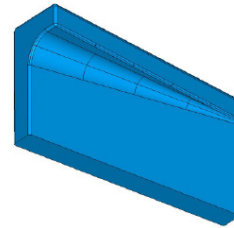
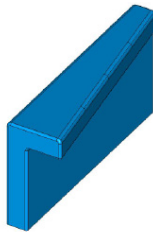
Figure 27. Test pieces for studying printability of inclined plates with varying inclination angles and arch like junctions.

3.2 Overhangs and small details

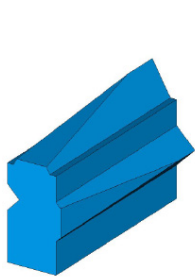
The cantilever plate with and without a supporting fillet was designed to study the behaviour of overhangs in SLM metal printing.



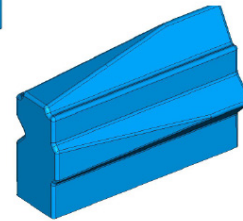
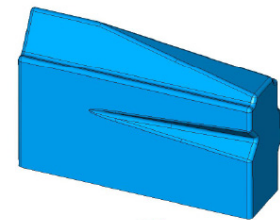
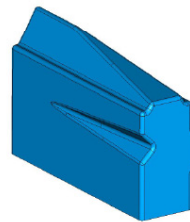
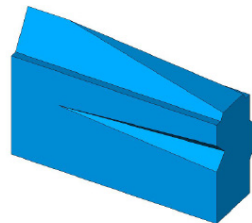
Overhang with varying length



Overhang with varying length and radius



Sharp and thin edges



Sharp and thin edges with overall fillet R0.5

Figure 28. Test pieces for studying printability of overhangs and small details.

3.3 Fillets and junctions with smooth transitions

The print quality at varying sizes of fillet radii was studied by test pieces with smoothly varying radii at various orientations.

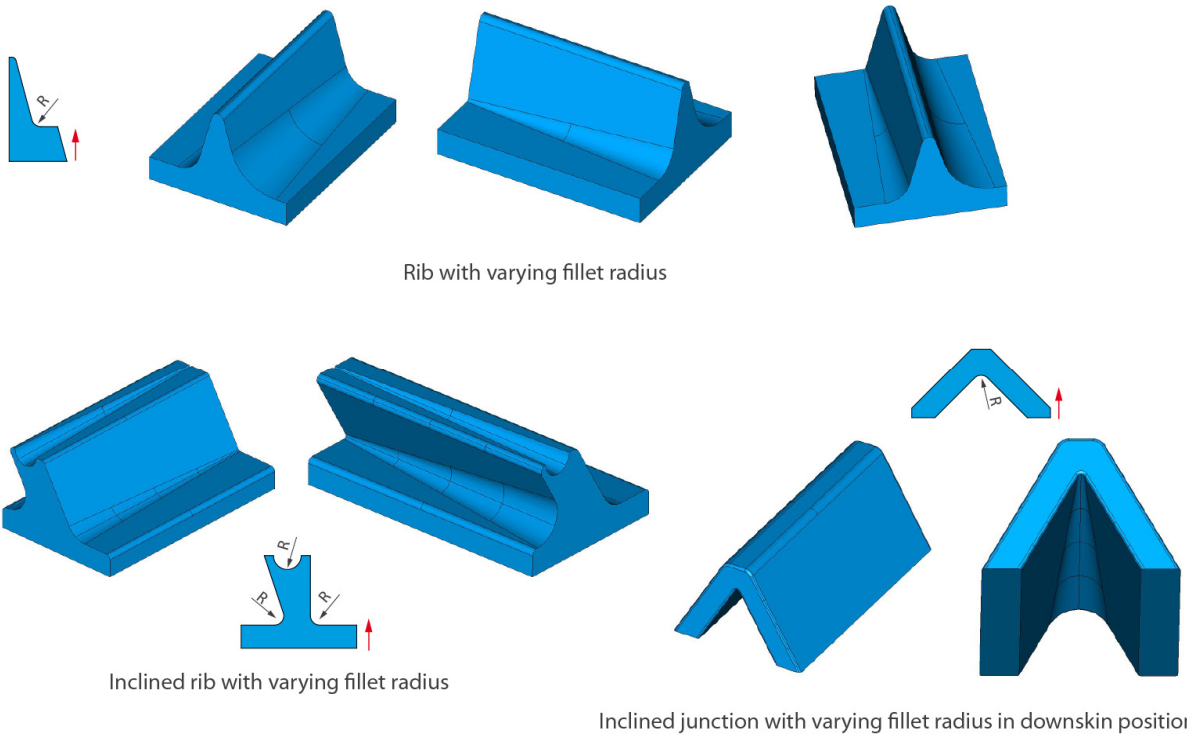


Figure 29. Test pieces for studying printability of fillets and junctions of separately grown branches with smooth transitions.

3.4 Holes

Test geometries with series of holes at varying diameter and inclination angle were designed. These are presented in the following figure.

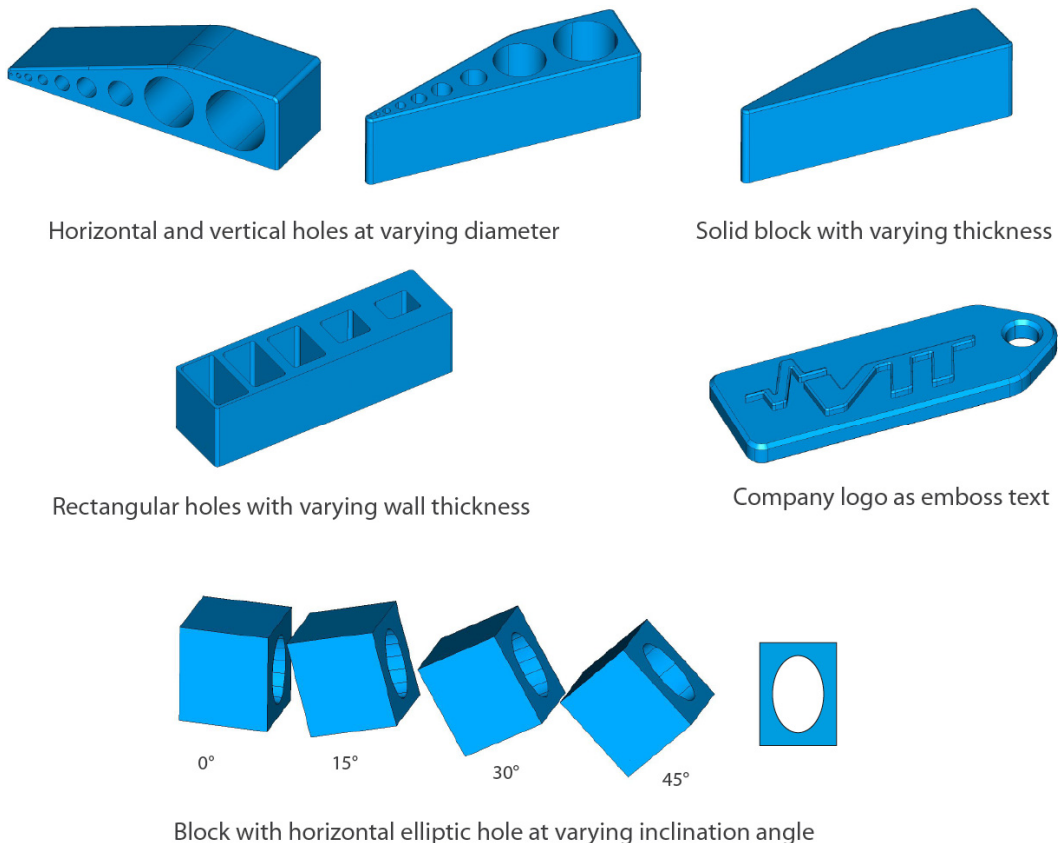
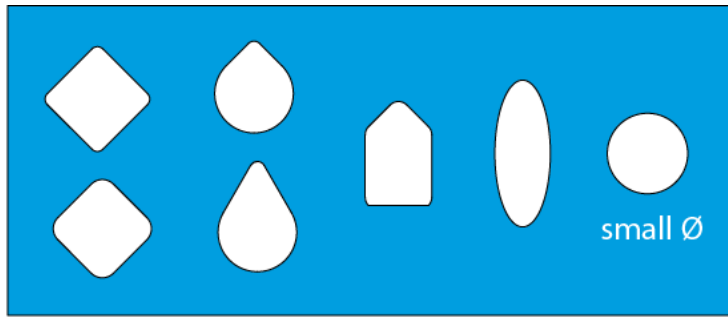
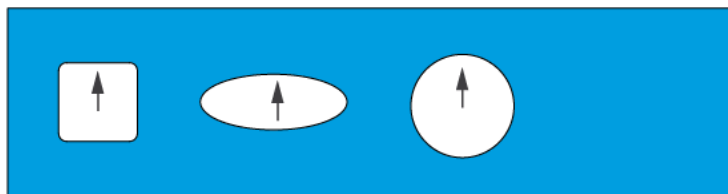


Figure 30. Test pieces for studying printability of holes.

Self-supporting holes and holes that require support during printing were both studied.

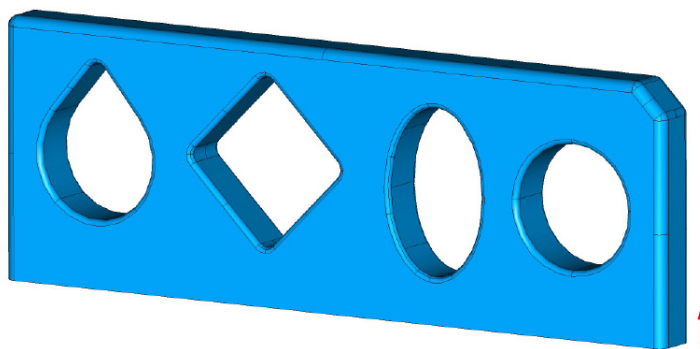


a) Self supporting cross sections for holes and channels

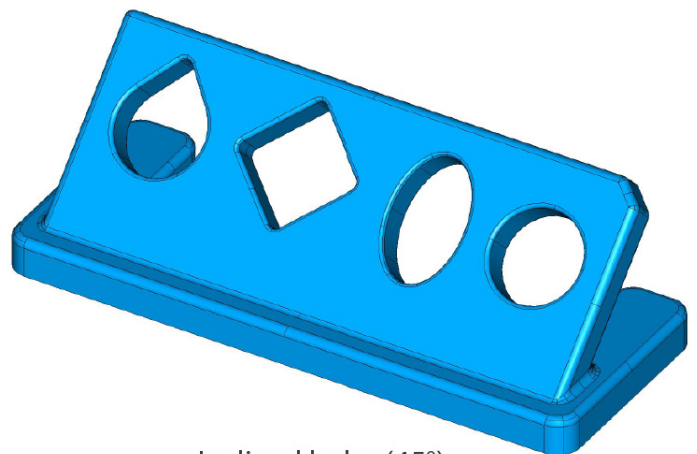


b) Holes requiring support during printing

Figure 31. Self-supporting holes (a) and holes that require support during printing (b). The self-supporting holes are naturally favoured in design.



Horizontal holes



Inclined holes (45°)

Figure 32. Test pieces for self-supporting holes.

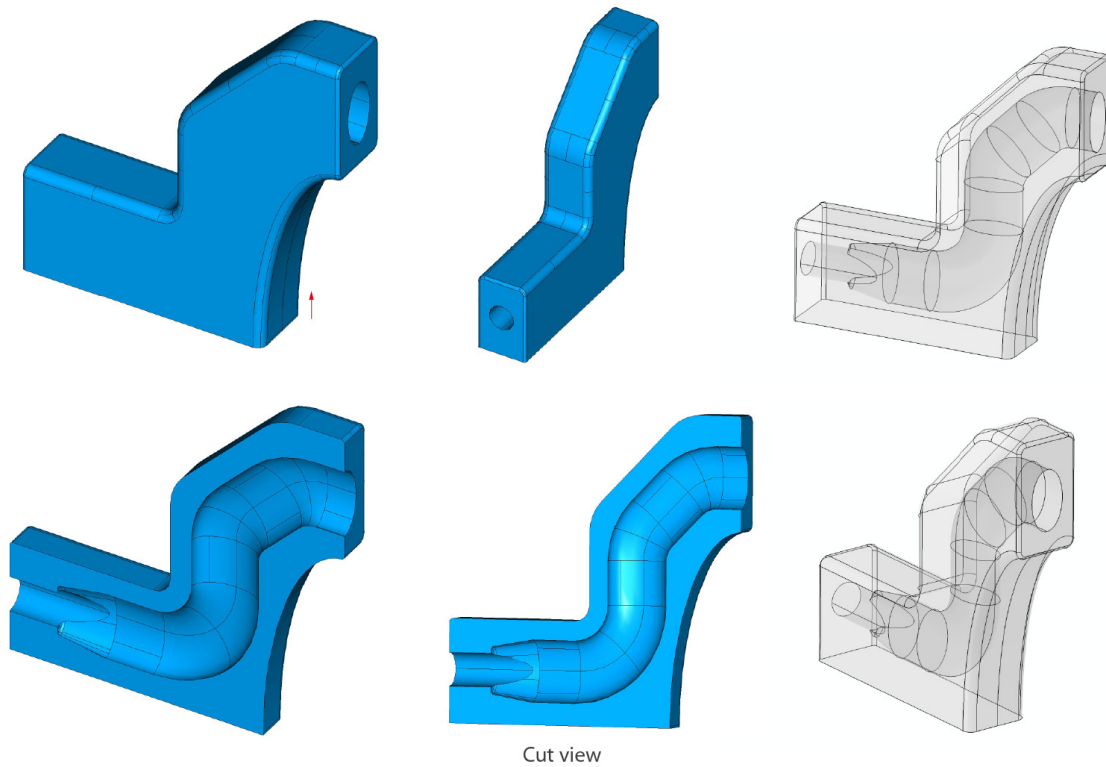
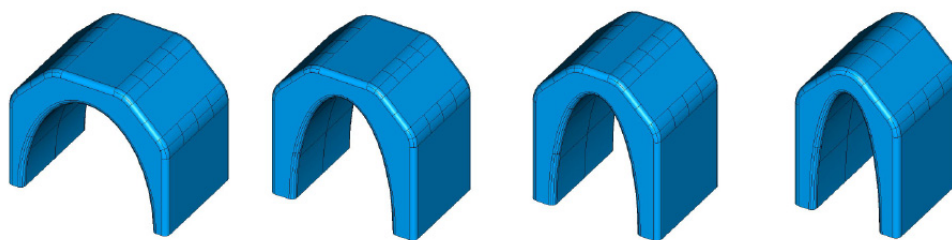
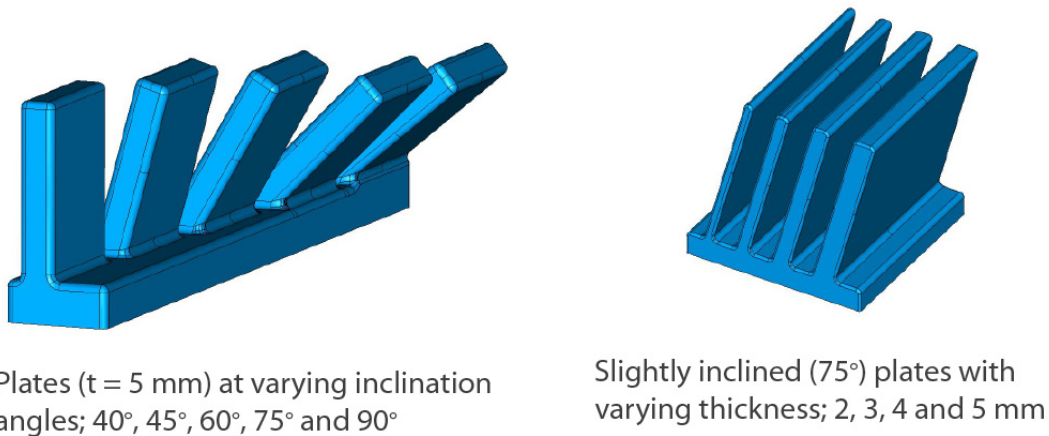


Figure 33. Test piece for internal channel. Self-supporting elliptic profile is used for the channel. Straight hole at the bottom left end was planned for testing threading.

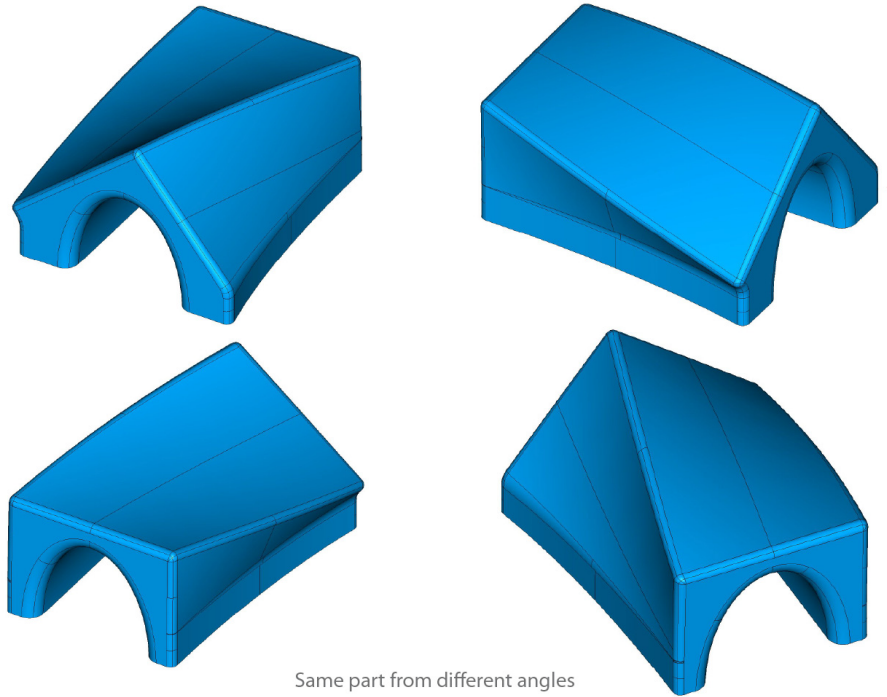
3.5 Surface quality

Surface quality was studied using the following test prints.



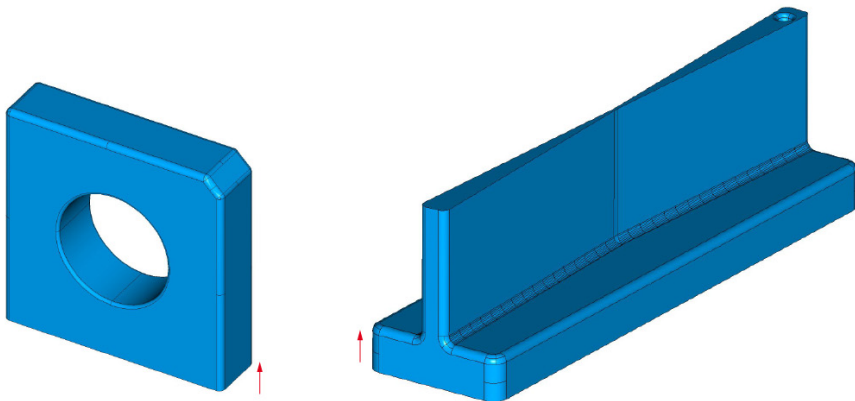
Archs of varying steepness

Figure 34. Surface quality was studied by profilometer using the top left test geometry, and visually of the other test pieces.



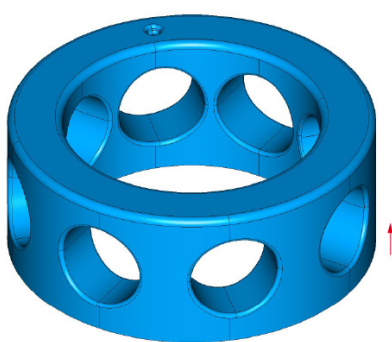
Same part from different angles

Figure 35. The test pieces with varying surface angle were used for assessing the surface roughness dependency of the inclination angle visually.

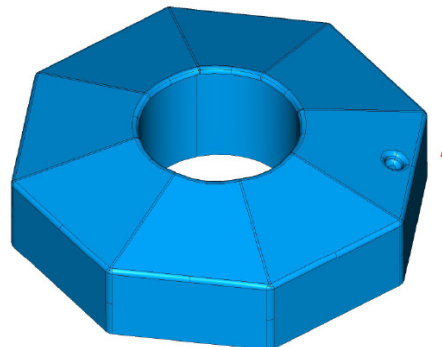


Large hole ($\varnothing 20$)

Thin vertical plate, with varying thickness 2 ... 0.2 mm



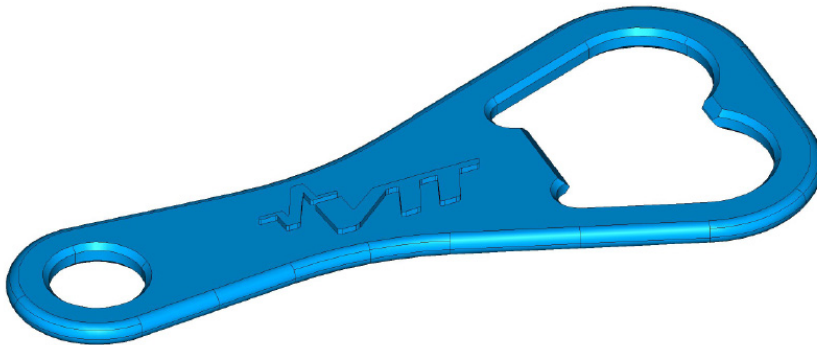
Holes, variation of angular orientation



Tilted and vertical flat surfaces, variation of angular orientation

Figure 36. Additional test pieces made after the first test print series. A larger diameter transversal hole was printed fine at $D = 20$ mm.

A Bottle opener was drafted in CAD after a common GWS opener to study how a company logo can be printed. The logos and texts can be added on parts in most CAD software and on .stl geometry for example in the 3-Matic software.



Company logo as emboss text

Figure 37. Bottle opener with company logo.

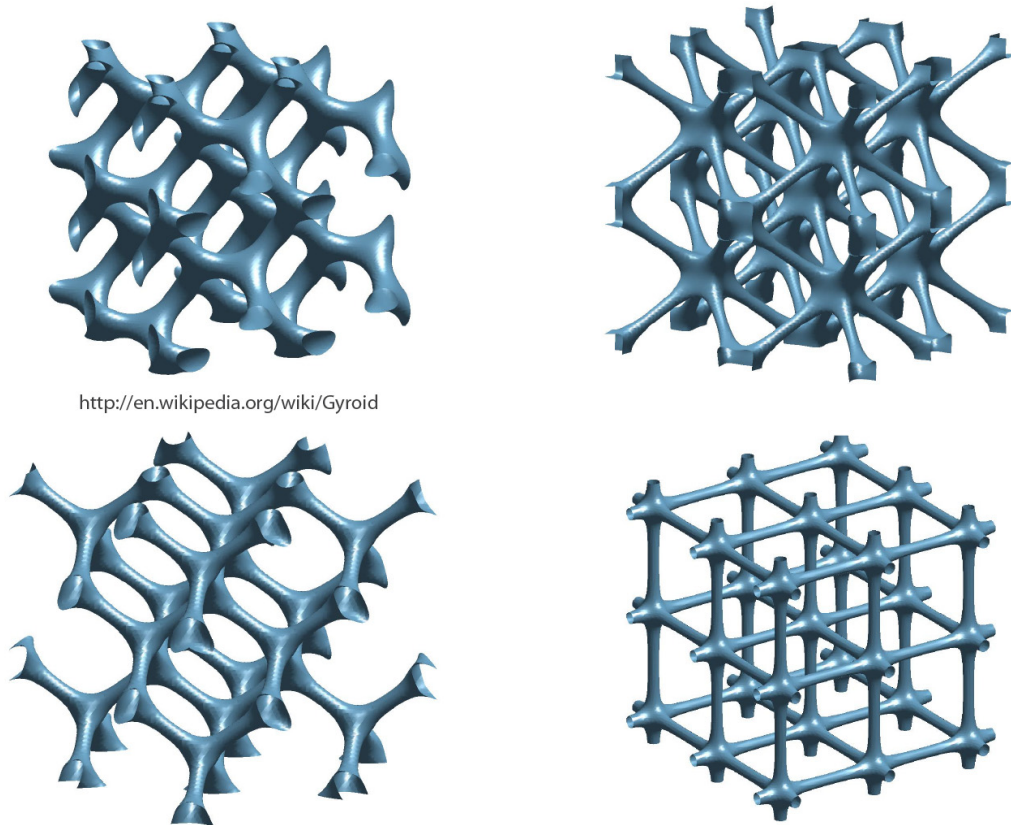
The bottle opener with company logo was printed in Inconel 625. A photo of the test print is presented in the next figure.



Figure 38. Bottle opener with company logo printed in Inconel.

3.6 Lattice structures

The lattice (cellular) structures allow design of light weight structures with additive manufacturing. The typical lattice structures were modelled in MATLAB using the mathematical formulas describing the shapes, and are presented in the following figures with comments. The cellular and lattice SLM structures are discussed in depth in for example [6].



<http://en.wikipedia.org/wiki/Gyroid>

Figure 39. Examples of lattice structures modelled at VTT in MATLAB.

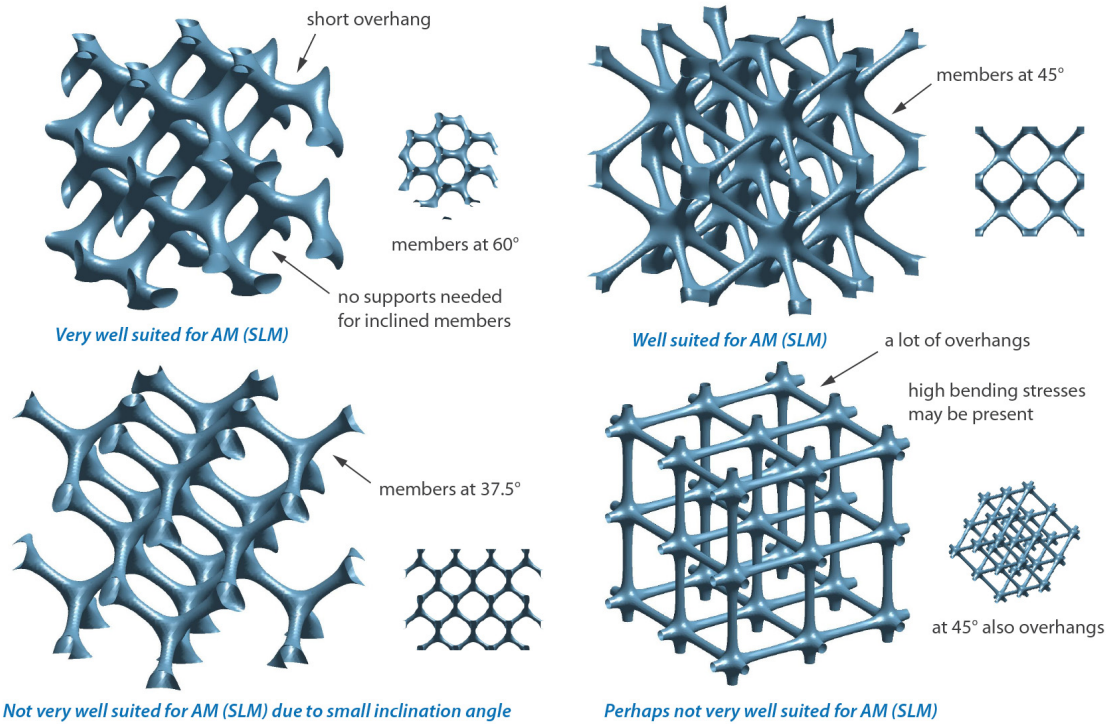
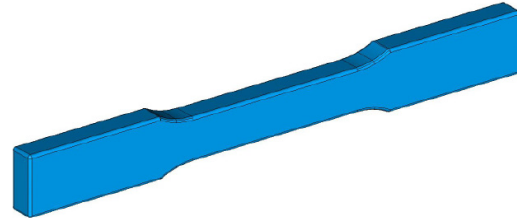


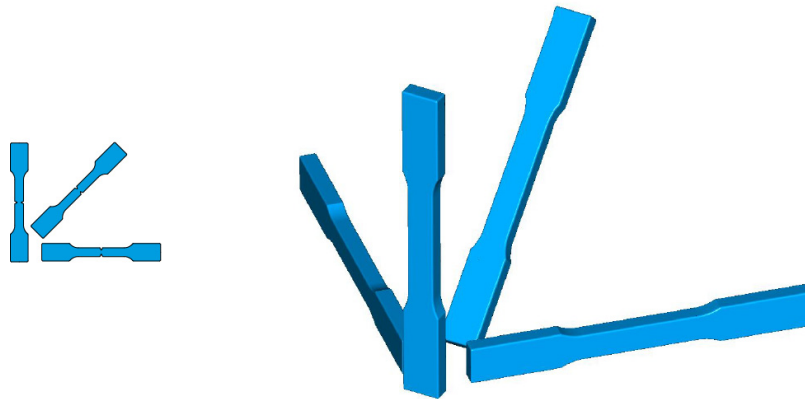
Figure 40. Assessment of lattices for printing in metal based on self-supporting properties. The gyroid on the upper left corner was seen the best choice for metal AM.

3.7 Tensile test specimen and tensile test results

Flat tensile specimen geometry was modelled by shortening a standard specimen to fit the SLM125 HL chamber. The flat tensile specimen is intended for fast tensile testing in as-built condition after each print batch to determine the mechanical properties resulting from the powder batch and at the printing parameters used. The materials used in the AM-Liito project are studied by Antero Jokinen and Tuomas Riipinen in report [19] (in Finnish).



Flat tensile test specimen



Flat tensile test specimens at four directions
(with supported downskin surfaces)

Figure 41. Tensile test specimen with typical arrangement for assessment of unisotropic mechanical properties due to the layered manufacturing process.

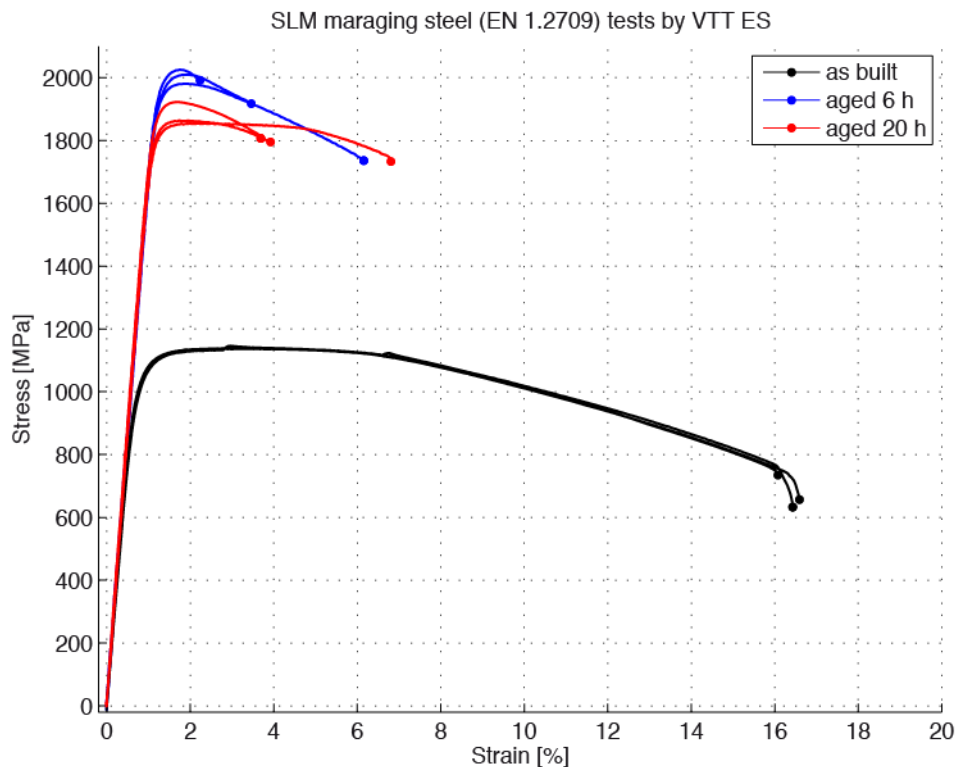


Figure 42. An example of tensile test results of SLM material as an excerpt from [17]. Due to the fast cooling rate of the melt typical to the SLM process many of the alloys used in SLM have typically high strength and high hardness. The elongation at fracture is typically rather low with many SLM materials.

3.8 Process settings used in the test series

The printing of the test series was started at SLM factory settings readily after receiving the SLM125HL printer at VTT November 2014.

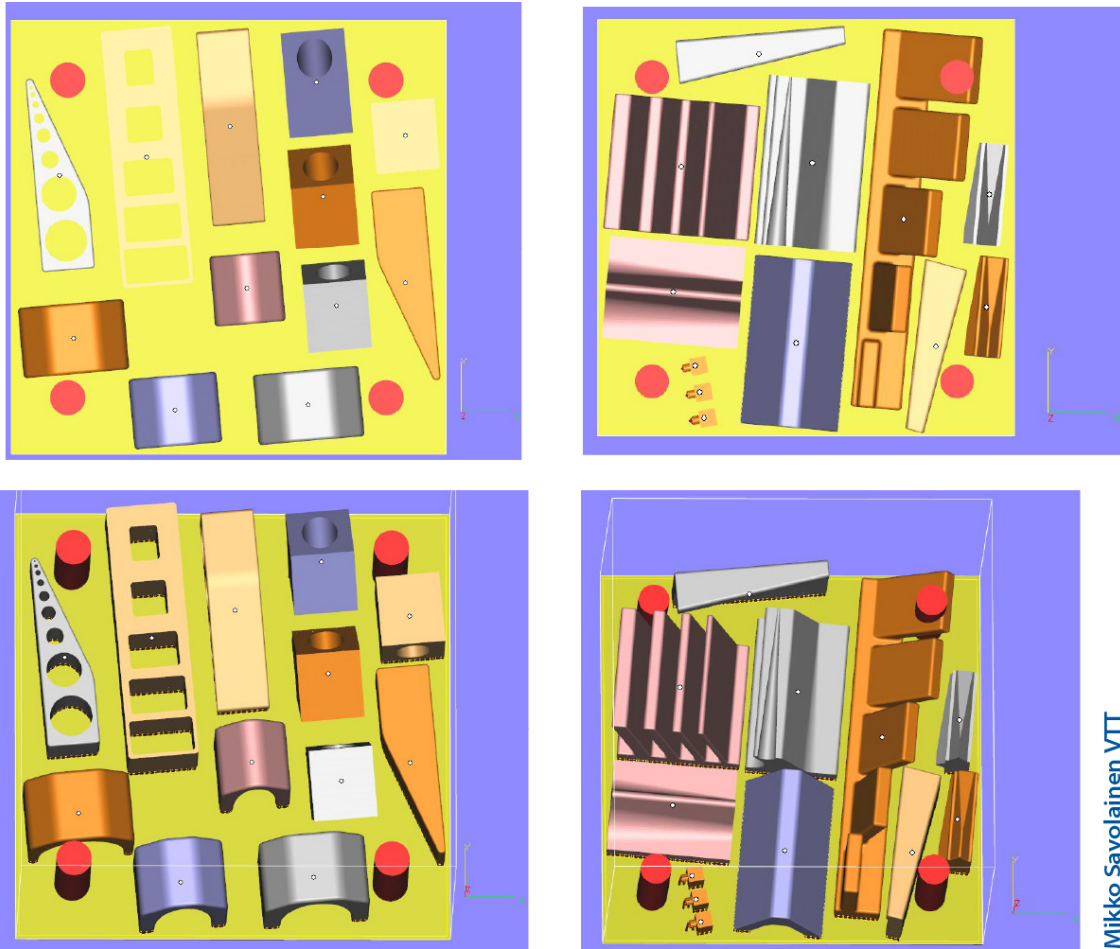
The first test series printed in AISi12 and Inconel 625 were printed at 50 μm layer thickness and at varying laser power and scanning speeds. The interlayer cooling time was also varied between batches. The later test series printed in H13 and AISI 316L were printed at 30 μm layer thickness. The process settings are discussed in detail in report [19].

The 50 μm layer thickness of the first test print series show as higher surface roughness in comparison to the later prints at the 30 μm layer thickness.

The printing parameters were optimised in AM-Liito project [19], but no test prints were printed using the optimised printing parameters due to the project schedule. For example the porosity studied of the test prints in this report is therefore considered a conservative example of the SLM materials.

3.9 Examples of the test prints

Examples of the nesting of .stl models in the Materialise Magics software for printing and the test prints before detaching the parts of the base plate are presented in the following figures. The base plate provides stiff platform for the building process and participates in the cooling or providing preheat to the part during build.

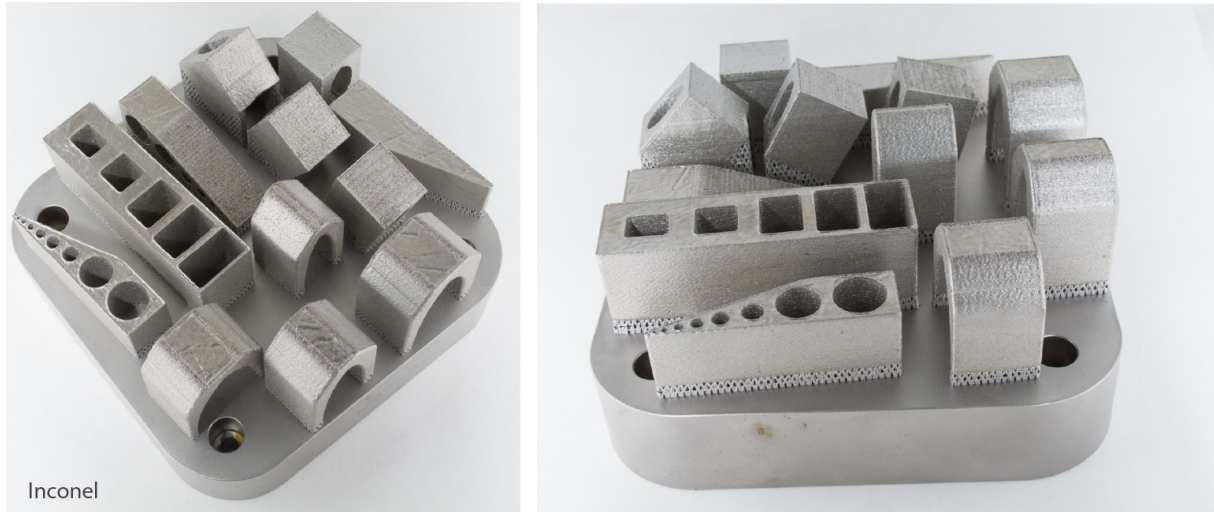


Mikko Savolainen VTT

Figure 43. Example of nesting of the components for printing.



Figure 44. First test serie printed in AISi12.



Inconel

Figure 45. Test serie printed in Inconel 625.



Figure 46. Test serie printed in Inconel 625.

3.10 Evaluation of the test prints

The photographs of the test print series are presented with remarks in the following.

3.10.1 Inclined plates

Evaluation of the inclined plates –test serie prints forms the basis of assessing the support limit angles for each material and the downskin surface of settings used.

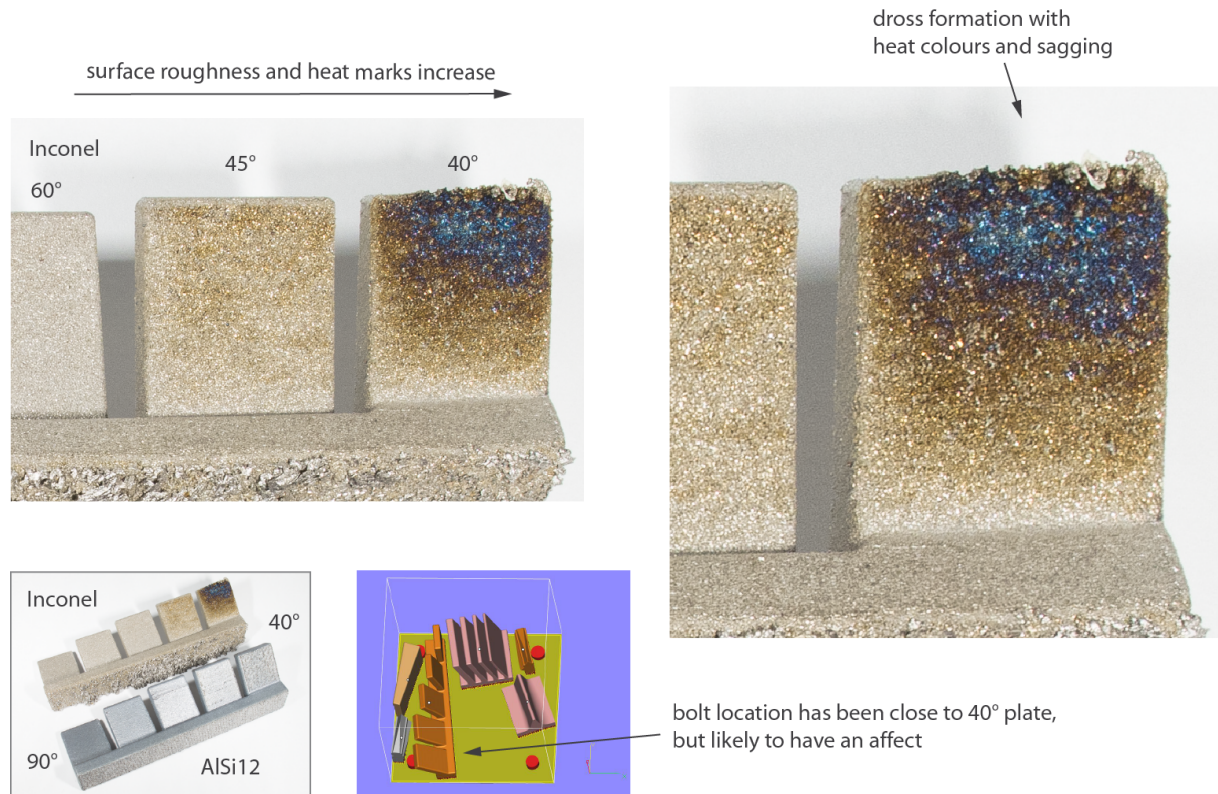


Figure 47. Evaluation of the inclined plates –test serie prints for AISi12 and Inconel printed at the SLM125 factory settings spring 2015.

3.10.2 Holes and channels

outermost beads next to edges form an elevated rim at up skin surfaces

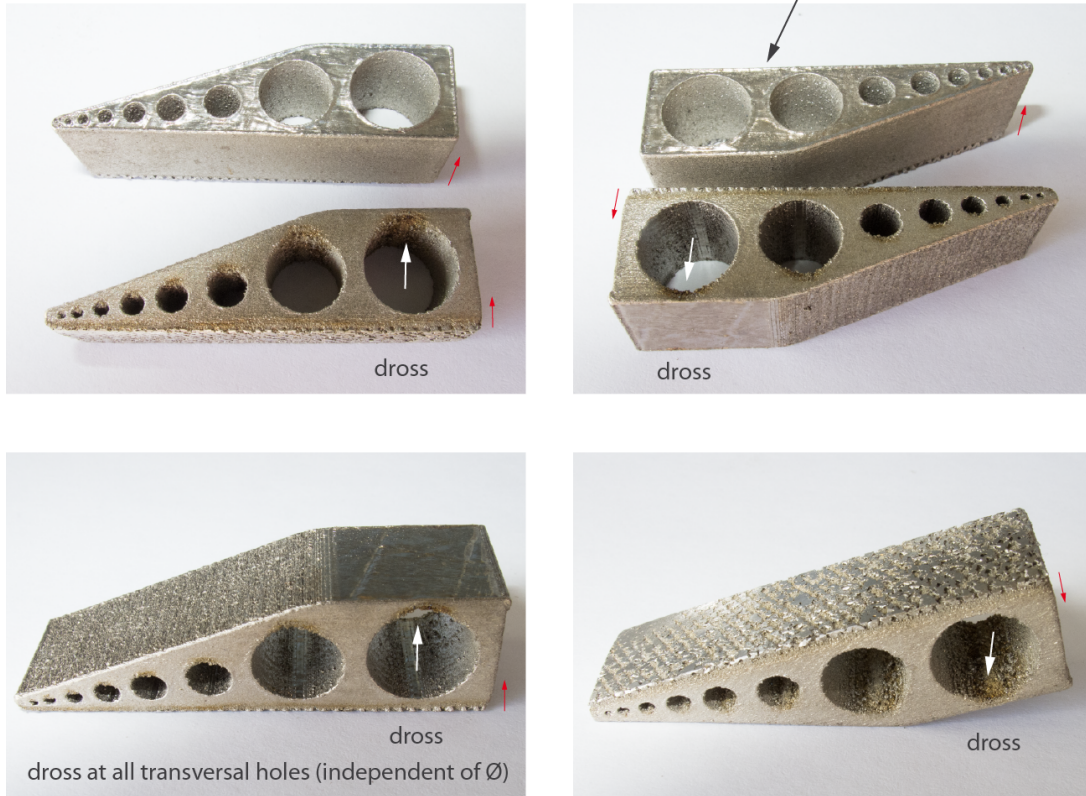
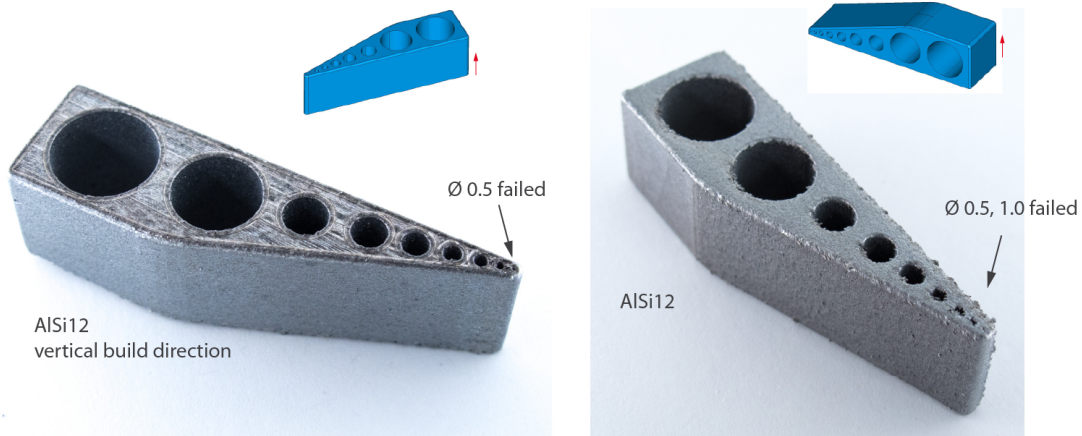


Figure 48. Evaluation of the vertical and transversal holes –test serie prints for Inconel printed at the SLM125 factory settings spring 2015.



Horizontal and vertical holes at varying diameter, Ø 0.5, 1.0, 1.5, 2, 3, 4, 5, 10, 12 mm

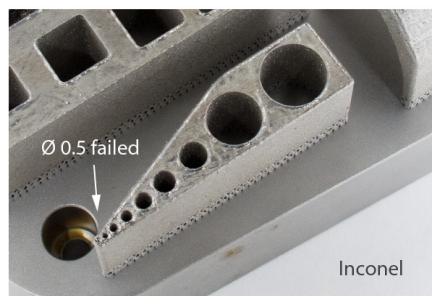


Figure 49. Evaluation of the vertical and transversal holes –test serie prints for AISi12 printed at the SLM125 factory settings spring 2015.

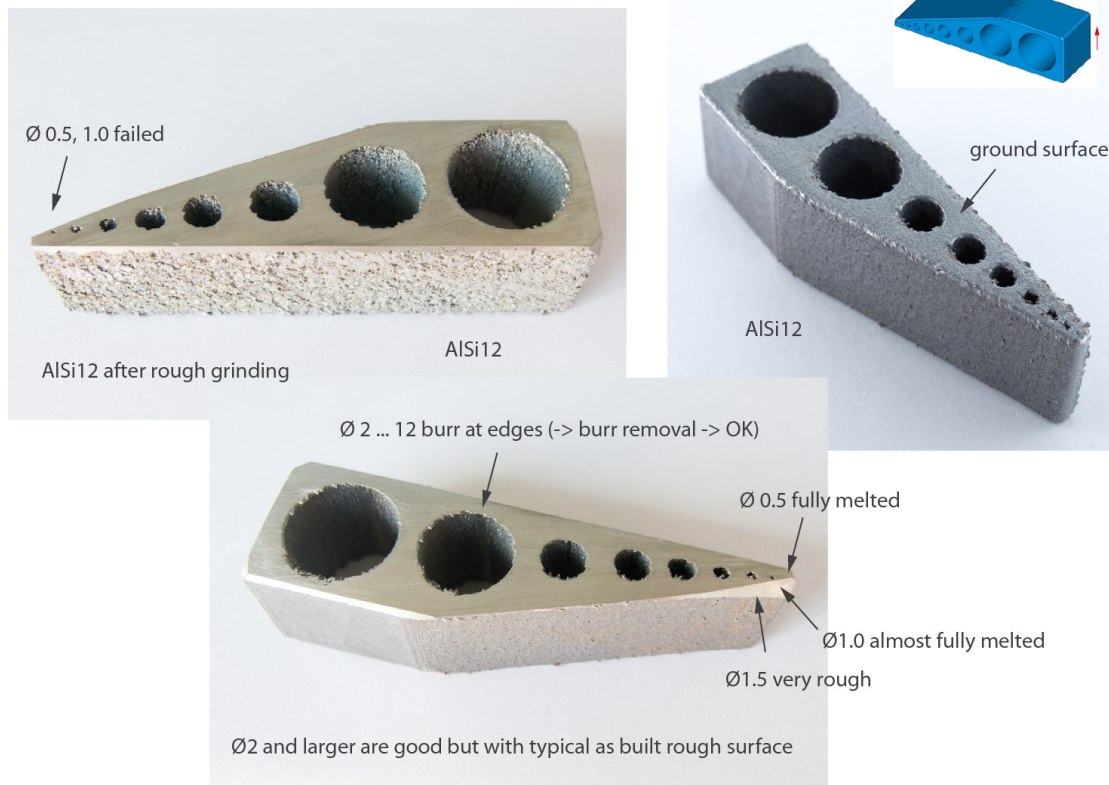


Figure 50. Evaluation of the vertical and transversal holes –test serie prints for AISi12 printed at the SLM125 factory settings spring 2015. Surfaces are ground roughly by belt grinder to reveal the small holes under the burr.

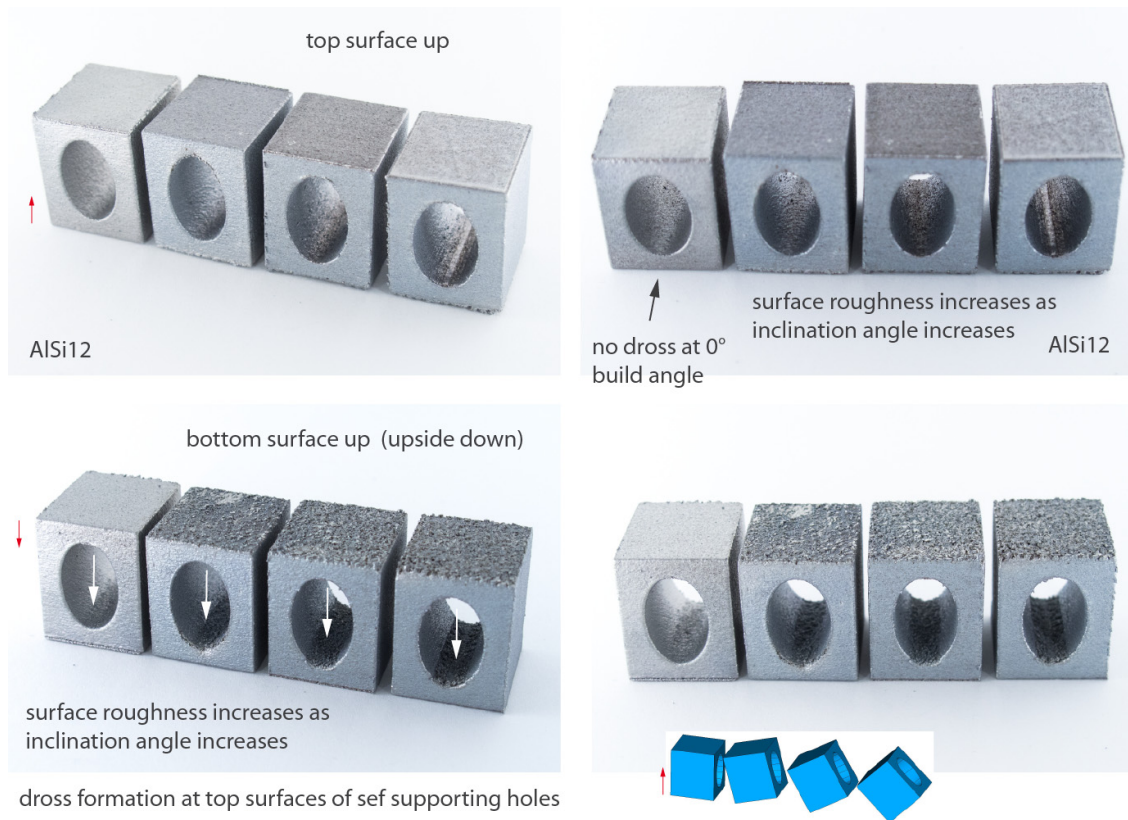


Figure 51. Remarks of the elliptic hole test pieces, AISi12.

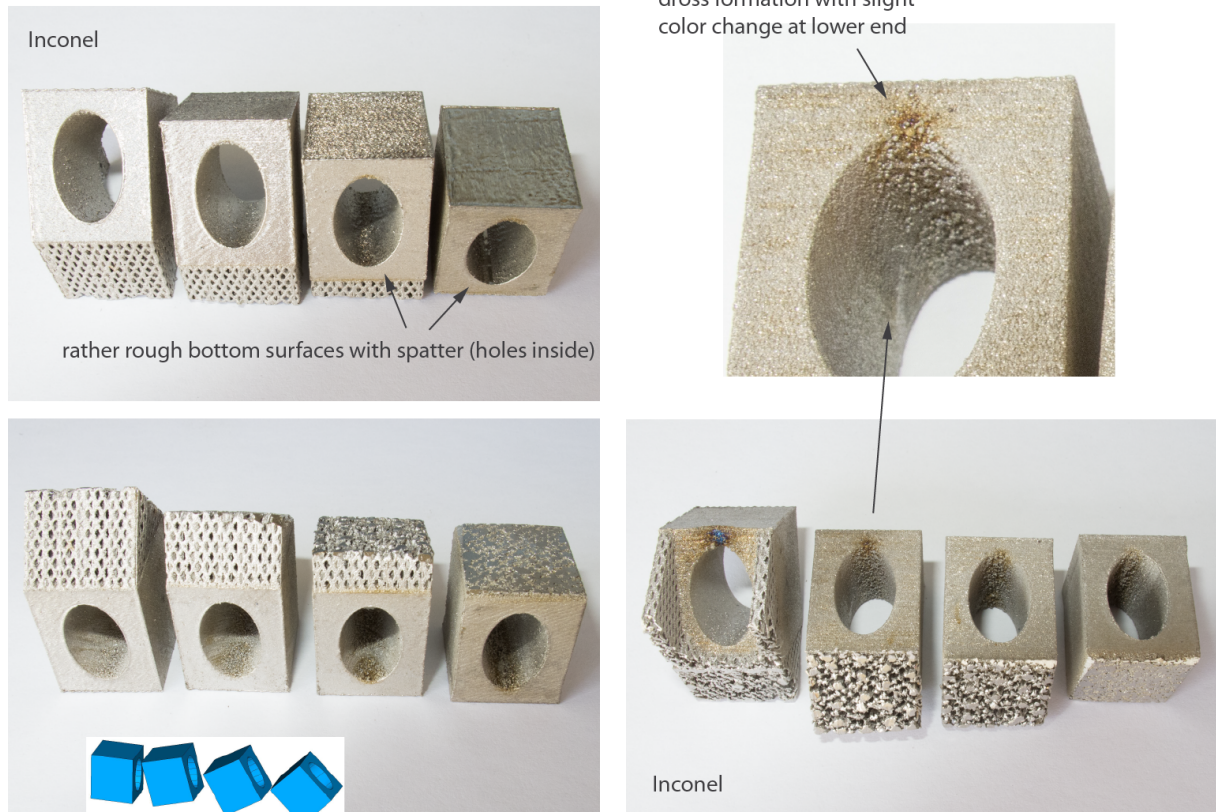


Figure 52. Remarks of the elliptic hole test pieces, Inconel.

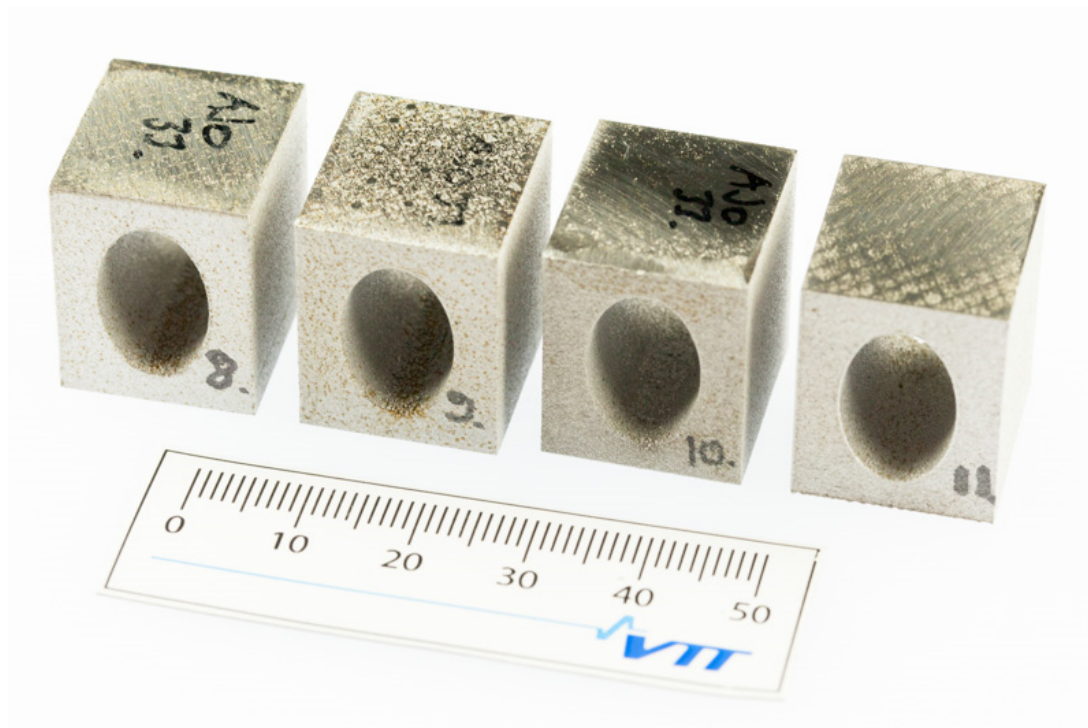


Figure 53. The elliptic hole test pieces printed in H13 tool steel at 30 μm layer thickness.



Figure 54. The transversal self-supporting holes test geometry printed in H13 tool steel at 30 μm layer thickness.



Figure 55. The 45 degrees tilted self-supporting holes -test geometry printed in H13 tool steel at 30 μm layer thickness.

3.10.3 Slots and grooves

Case study of O-ring (or seal in general) dove tail groove was done as part of printing a test series for assessing the various alternatives for support structures. The dove tail groove is difficult to manufacture with traditional production but can be printed easily by the SLM process. Photos of the test prints in AISI 316L are shown the following.



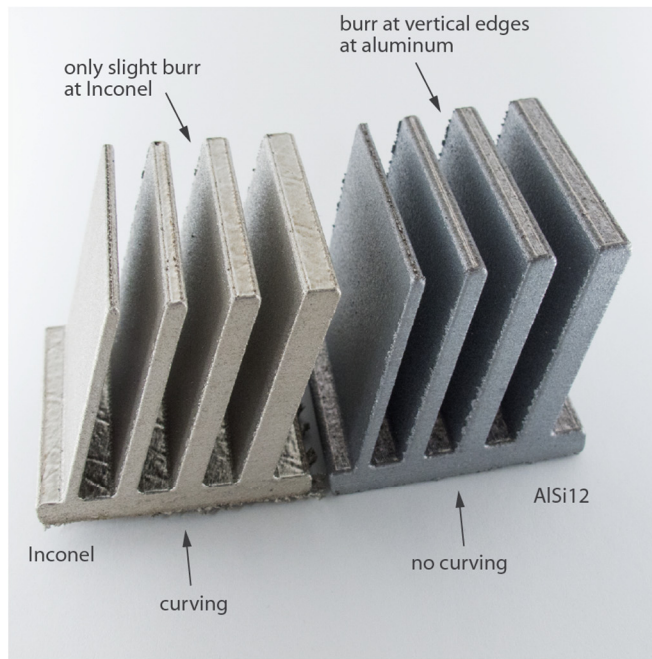
Figure 56. Test print study of O-ring dove tail groove (together with test print serie in which the support structures were evaluated).



Figure 57. Test print study of O-ring dove tail groove.

3.10.3.1 Edge burr and surface roughness dependency on transition angle

Edge burr and surface roughness dependency on transition angle is seen on the test pieces shown in the figure below.



not allowed in fatigue critical locations, or finishing required

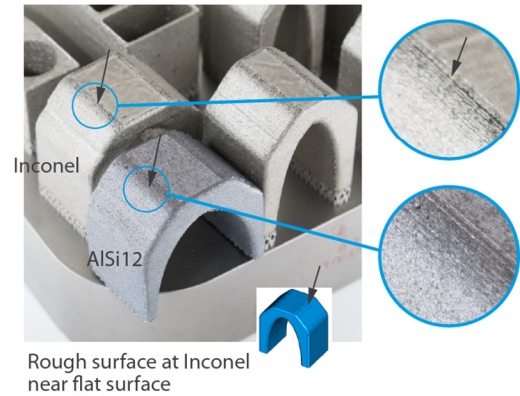
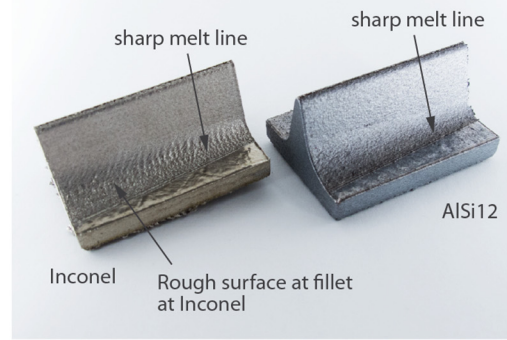


Figure 58. Remarks on the inclined plates with varying thickness test pieces.

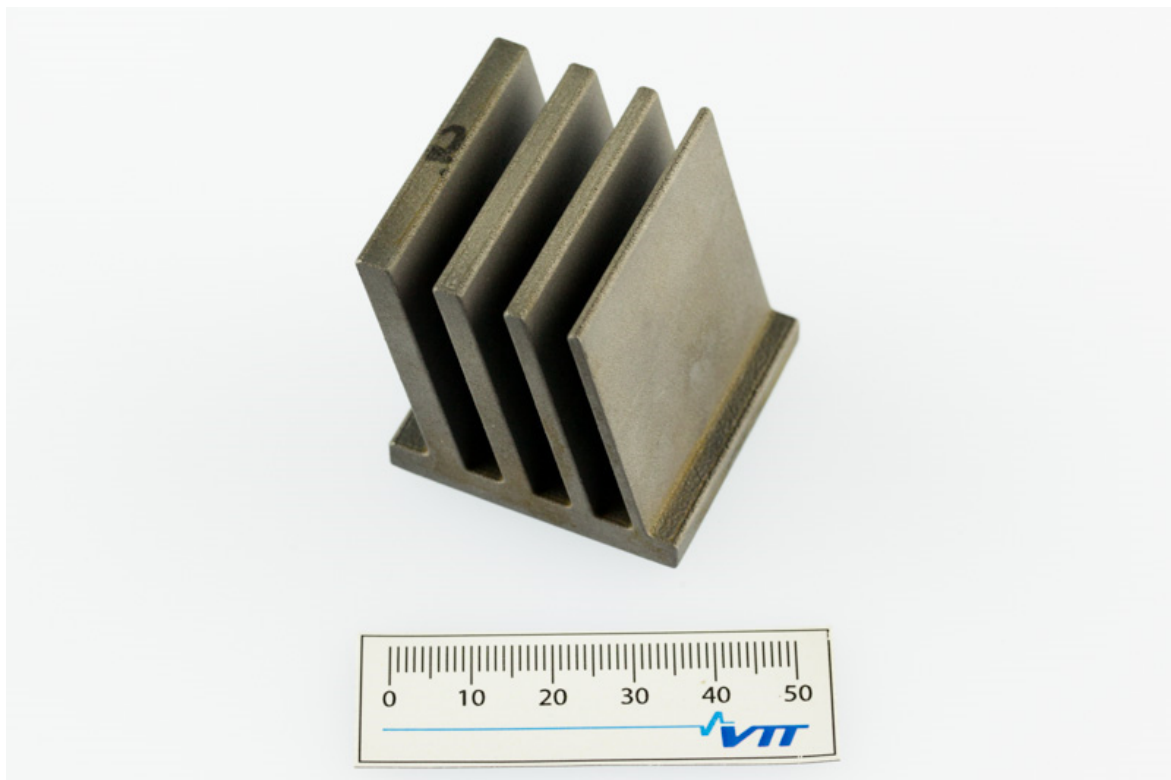


Figure 59. The inclined plates printed in H13 tool steel at 30 μm layer thickness. No defects were detected.



Figure 60. The inclined plates printed in Inconel. Burr can be seen at the sharp edges.

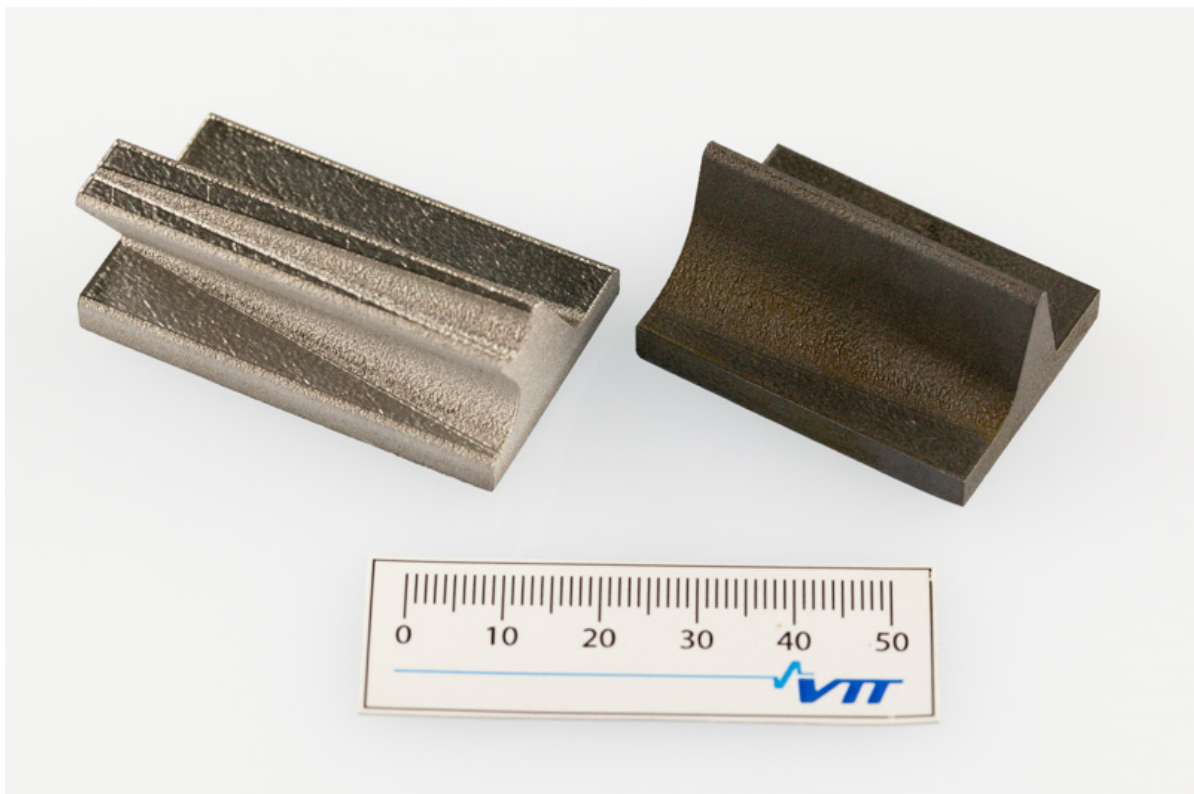


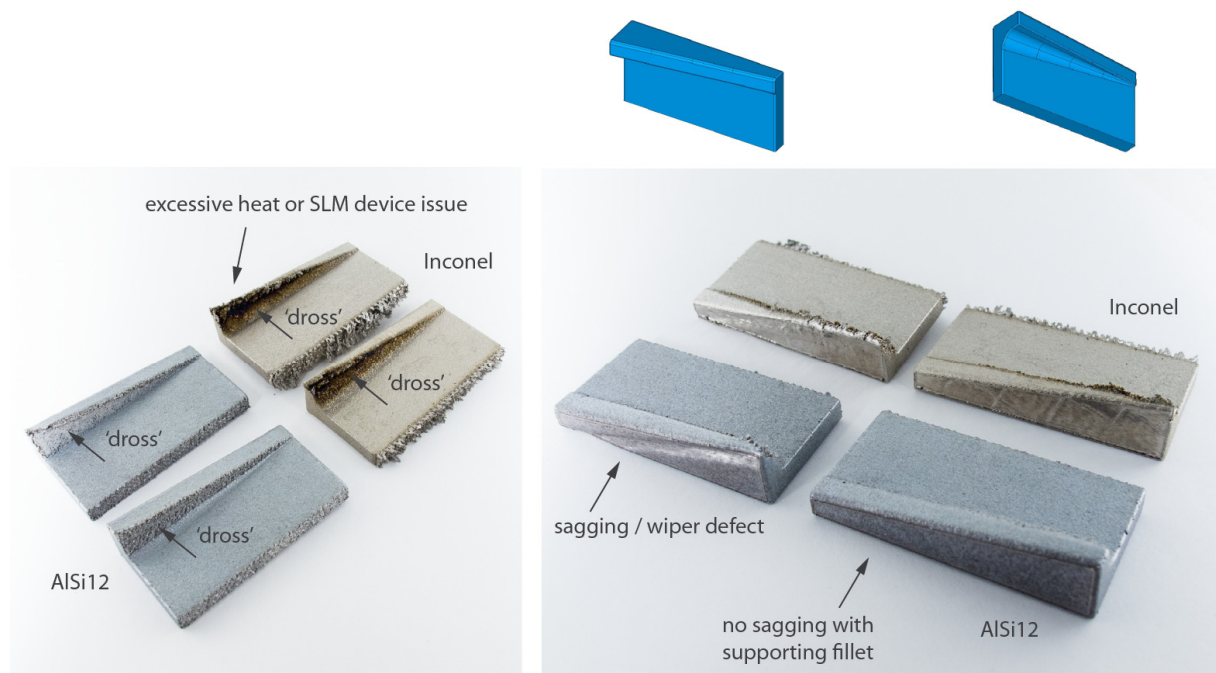
Figure 61. The varying radius fillet test pieces in Inconel and H13. No defects were detected.



Figure 62. The varying radius fillet test pieces in Inconel (back) and AISI12 (front). No defects were detected.

3.10.3.2 Overhangs

Dross is typically formed at the bottom surface of the overhangs. In addition, sagging occurs together with the dross at the top surfaces.



Overhang with varying length

Figure 63. Remarks on the overhang test pieces.

3.10.3.3 Junctions

The transversal shrinkage shows in all specimens with separately grown branches. The transversal shrinkage shows as a ridge at the level where the separately grown branches meet. The typical size of the ridges noted in the test prints was estimate to be about 0.5 mm.

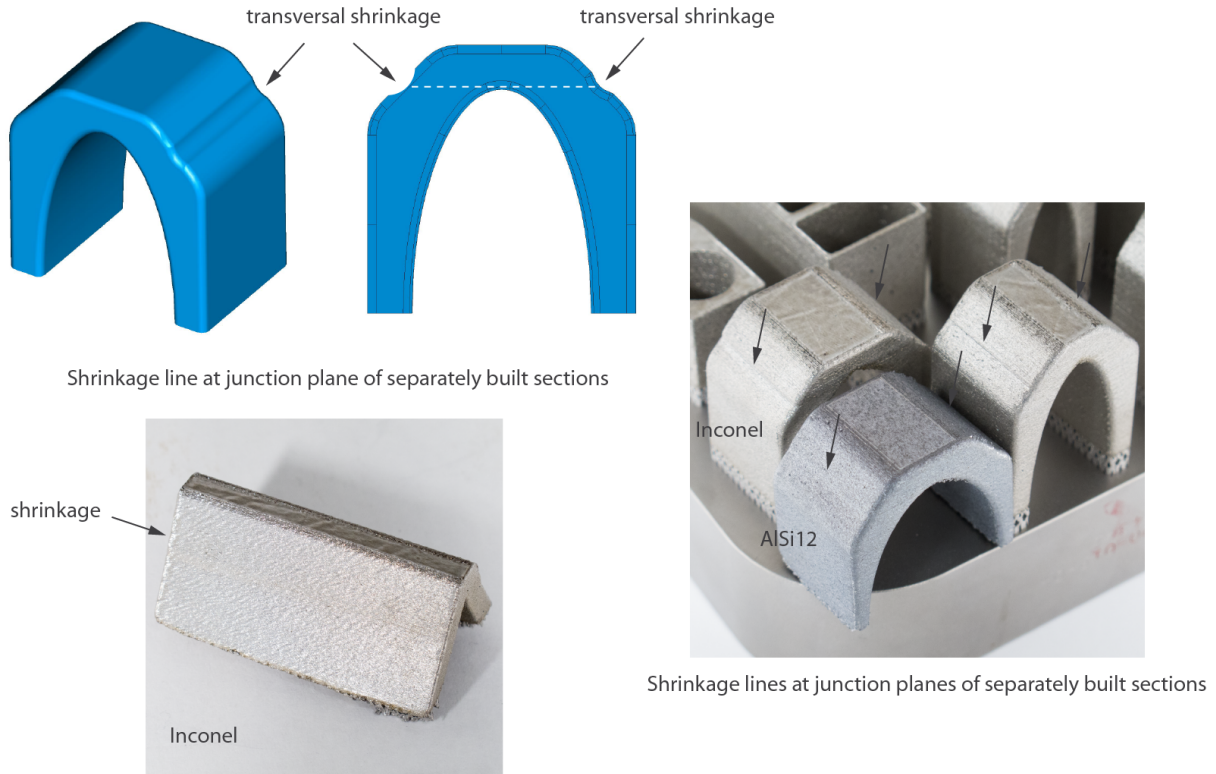


Figure 64. Remarks on the junction test pieces. The transversal shrinkage shows in all specimens.

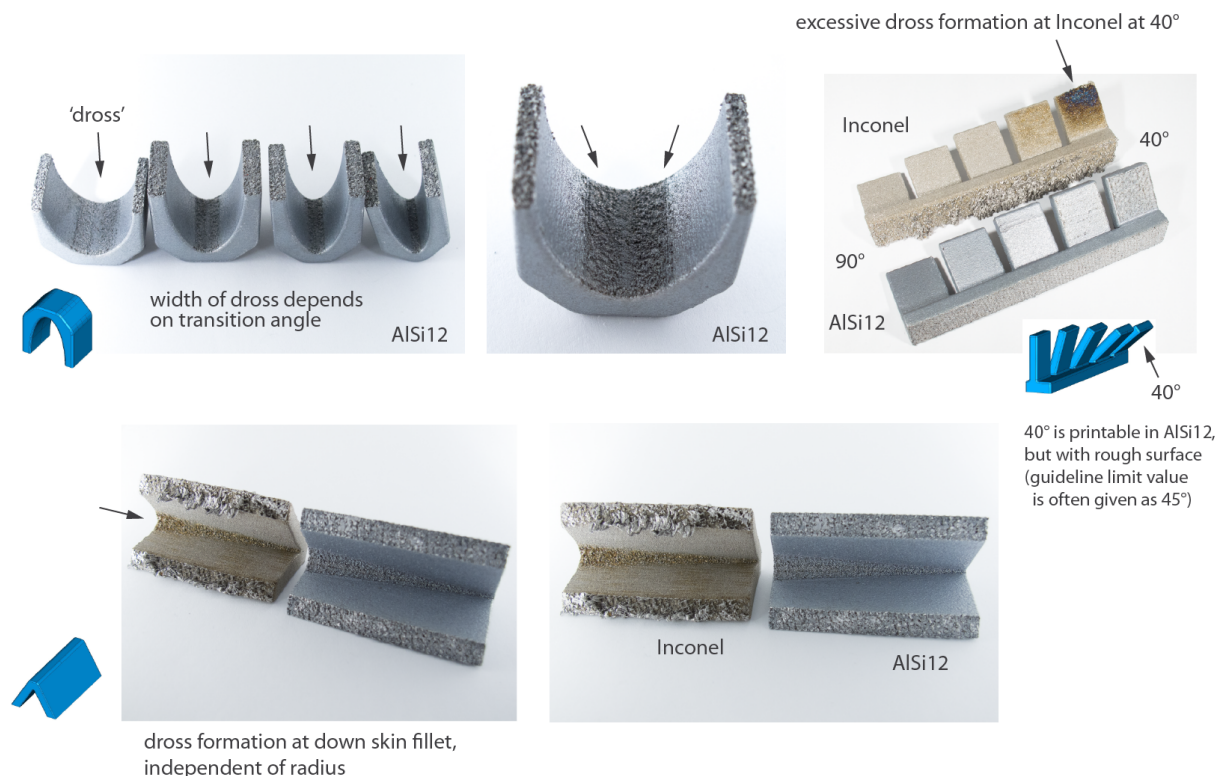


Figure 65. Remarks on the junction and inclined plate test pieces. The dross locations are indicated by arrows.

The dross formation takes place at the top locations of downskin surface of arch type structural details.

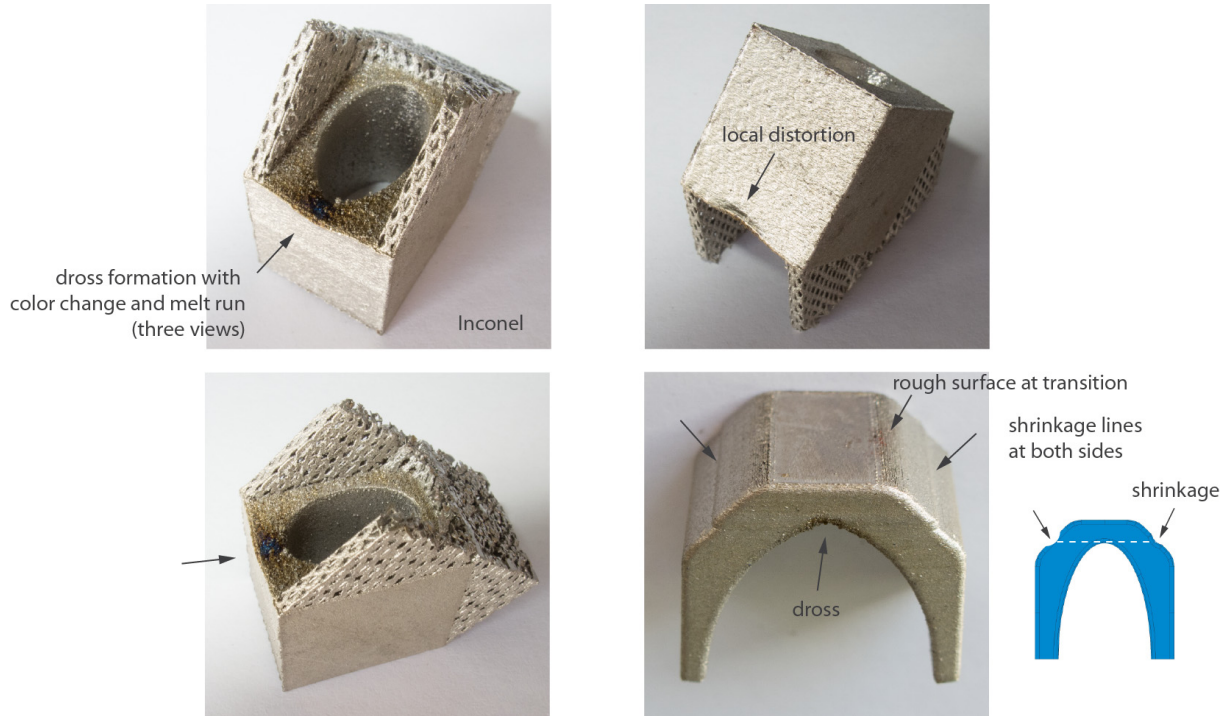


Figure 66. Remarks on the Inconel junction and elliptic hole test pieces. The dross and transversal shrinkage locations are indicated by arrows.

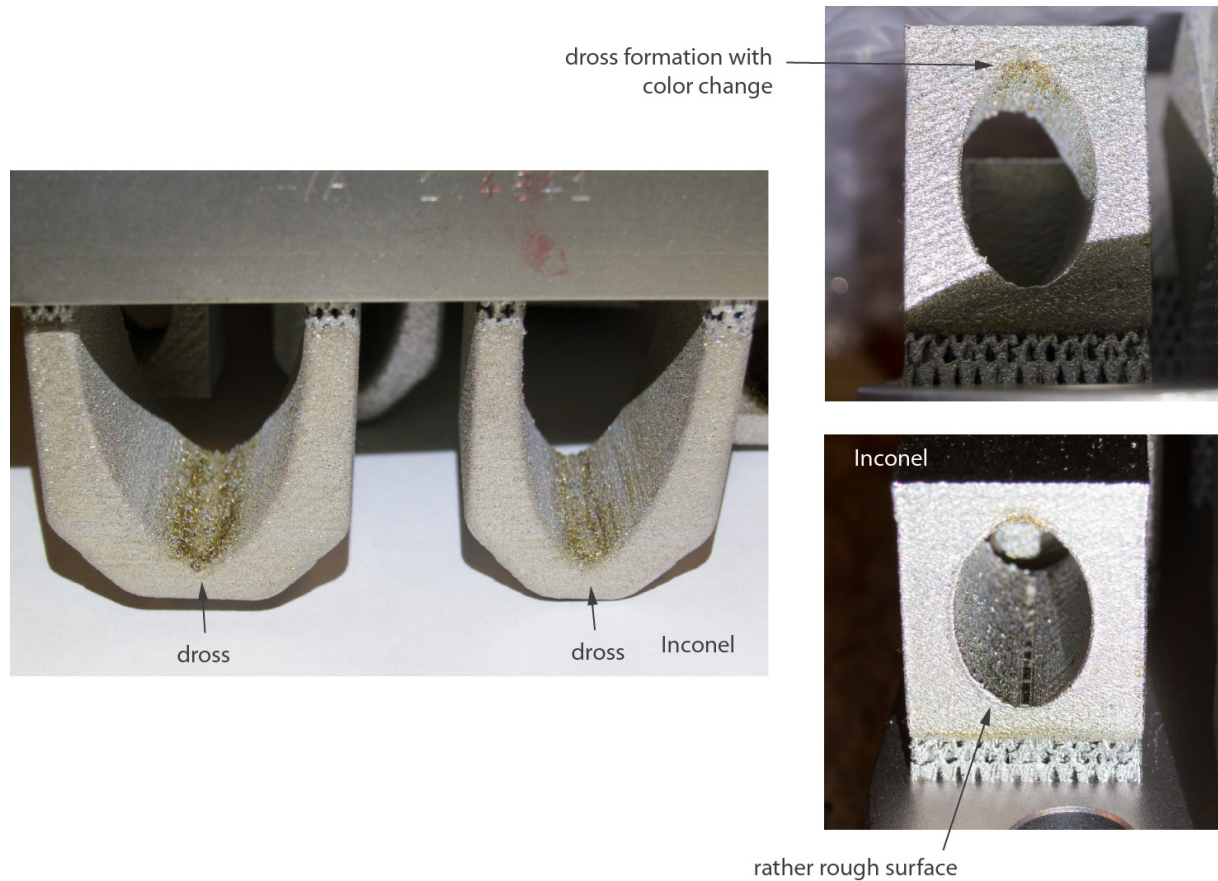


Figure 67. Remarks on the Inconel junction and inclined plate test pieces. The dross and heat mark locations are indicated by arrows.

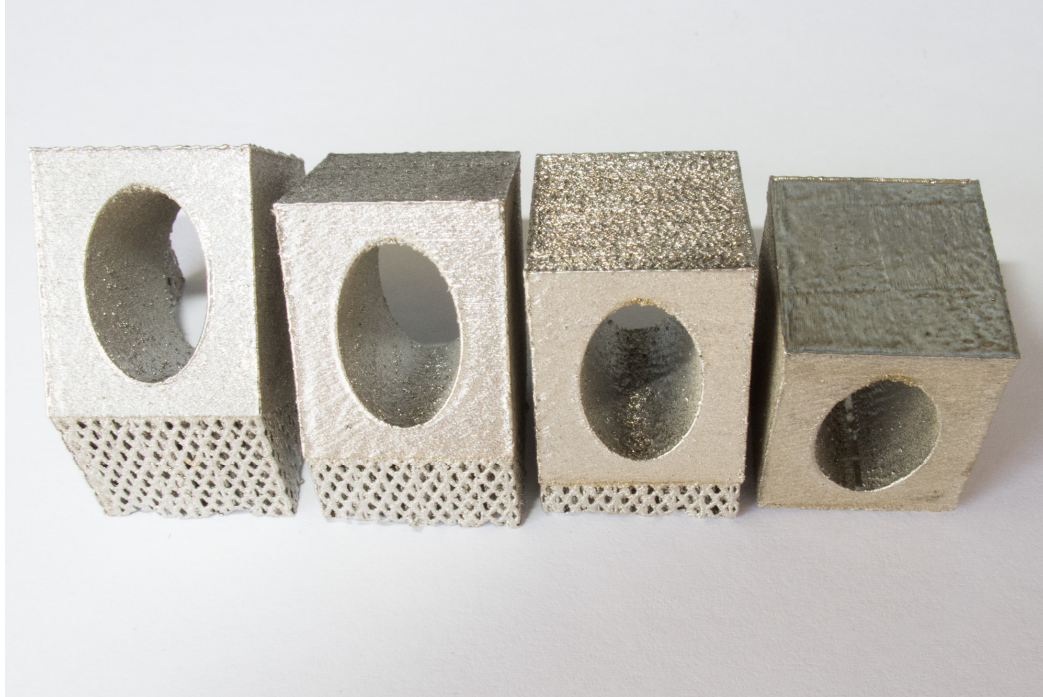


Figure 68. The inclined elliptic holes printed in Inconel.

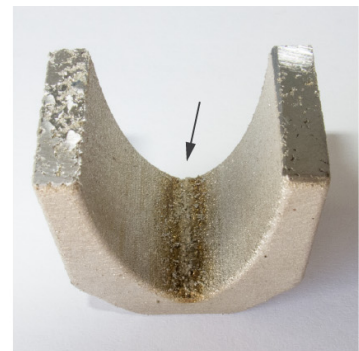


Figure 69. Remarks on the Inconel junction test pieces. The dross locations are shown.



Figure 70. The junction test pieces printed in H13 tool steel at 30 μm layer thickness seen from above.



Figure 71. The junction test pieces printed in H13 tool steel at 30 μm layer thickness seen from above. The rough surface quality at the transitions at top surfaces and the ridges due to the transversal shrinkage can be seen in the test pieces.

Transversal shrinkage is a local defect caused by thermal stresses, occurring at locations where separately grown regions meet.

1. No visually detectable sagging at short overhangs.
2. Check from macro specimens if local sagging occurs.
3. Transversal shrinkage at junction plane, depth $\sim 0.1 \dots 0.5$ mm (visual estimate).
4. Dross formation at the down skin surface.

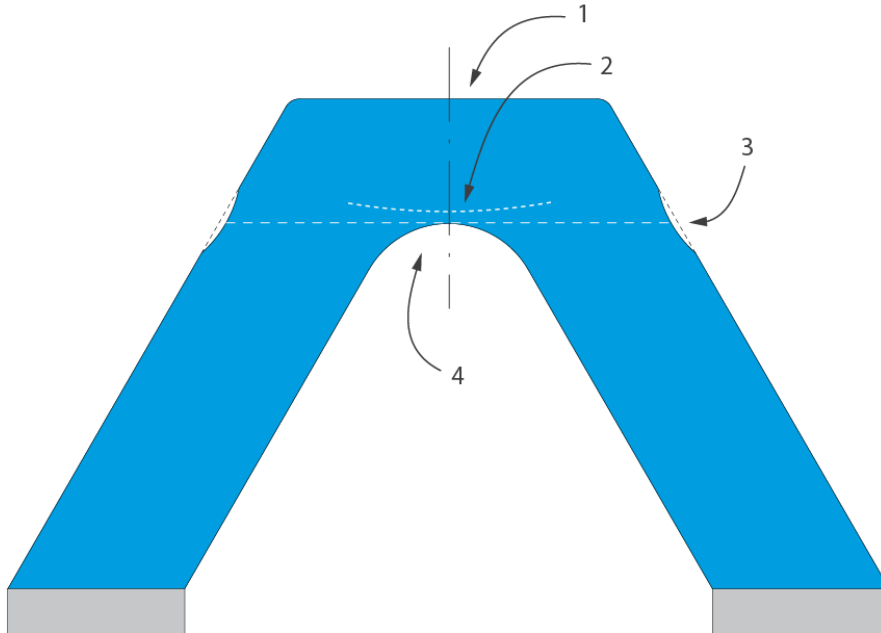


Figure 72. Summary of the remarks. The formation of sagging at location 4 was studied by microscopic examination of the macro specimen and no significant sagging was detected. The transversal shrinkage lines are visible to naked eye in the test prints with separate branches. Local curving (2) (sagging) occurs within the part based on the microscopic examination of the macro specimens.

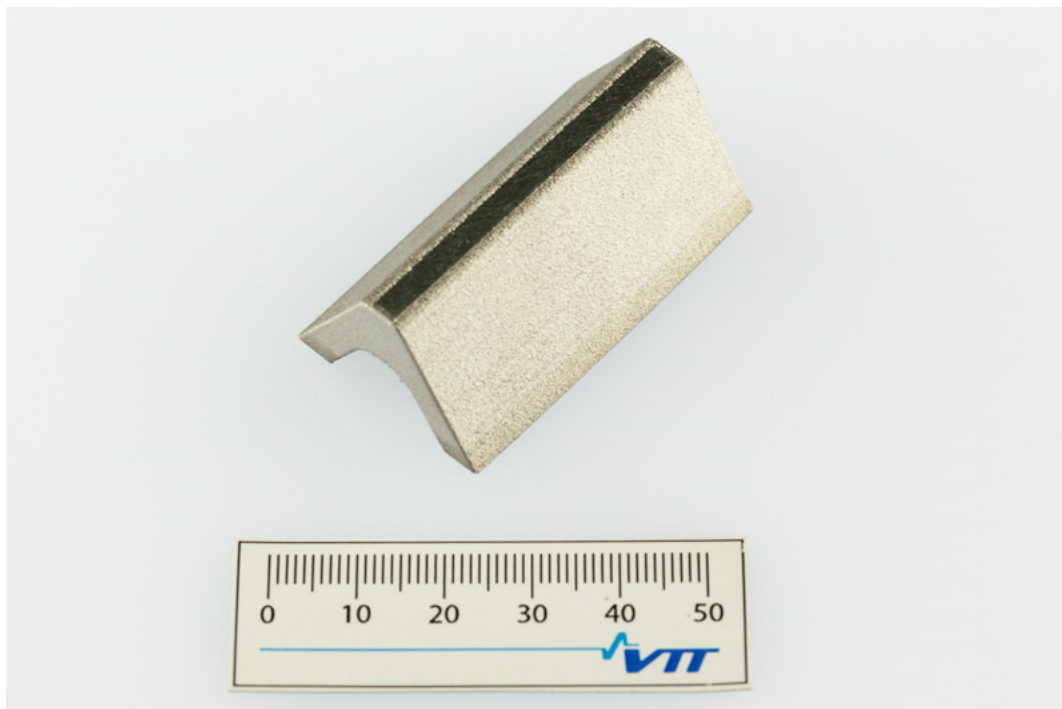


Figure 73. The branched inclined test geometry printed in H13 tool steel at 30 μ m layer thickness.

3.10.4 Unsupported overhangs

The overhang test pieces with and without fillet were printed in 316L and H13. The overhang test prints are presented in the following figures.

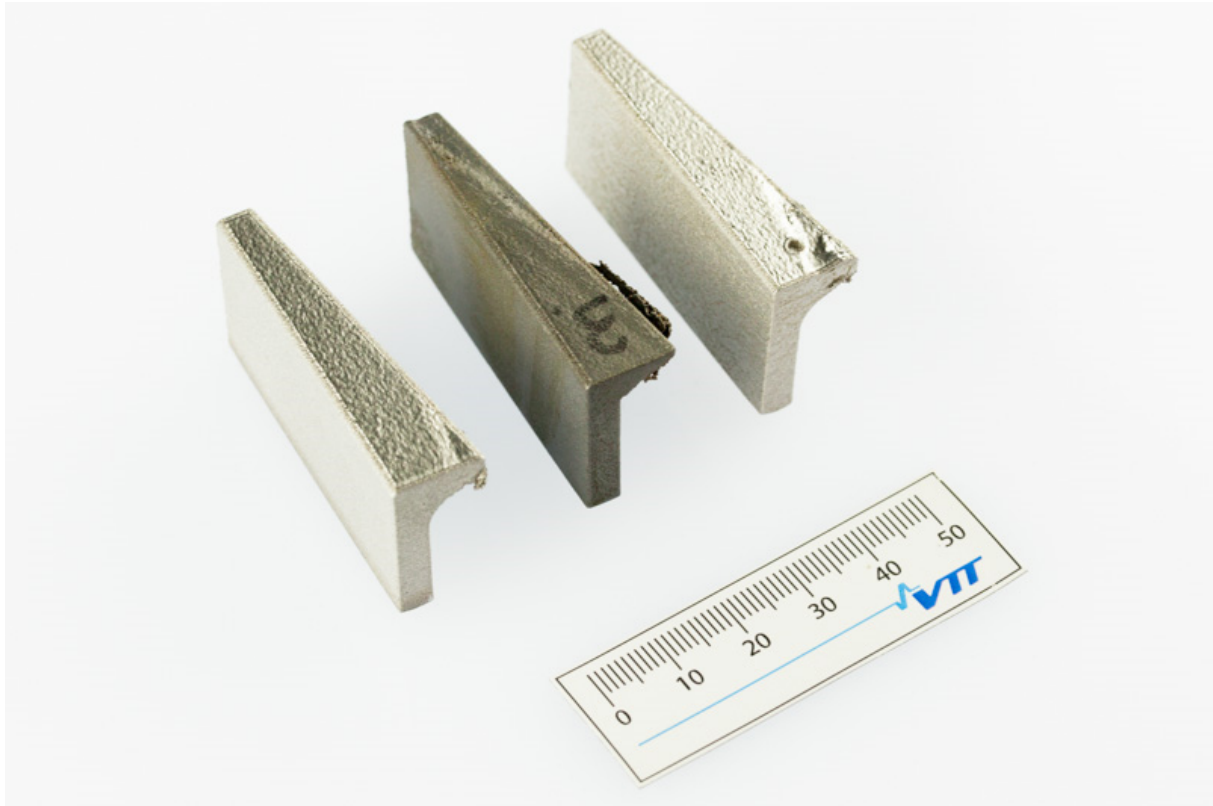


Figure 74. The overhang test pieces with and without fillet printed in H13 (middle) and 316L.

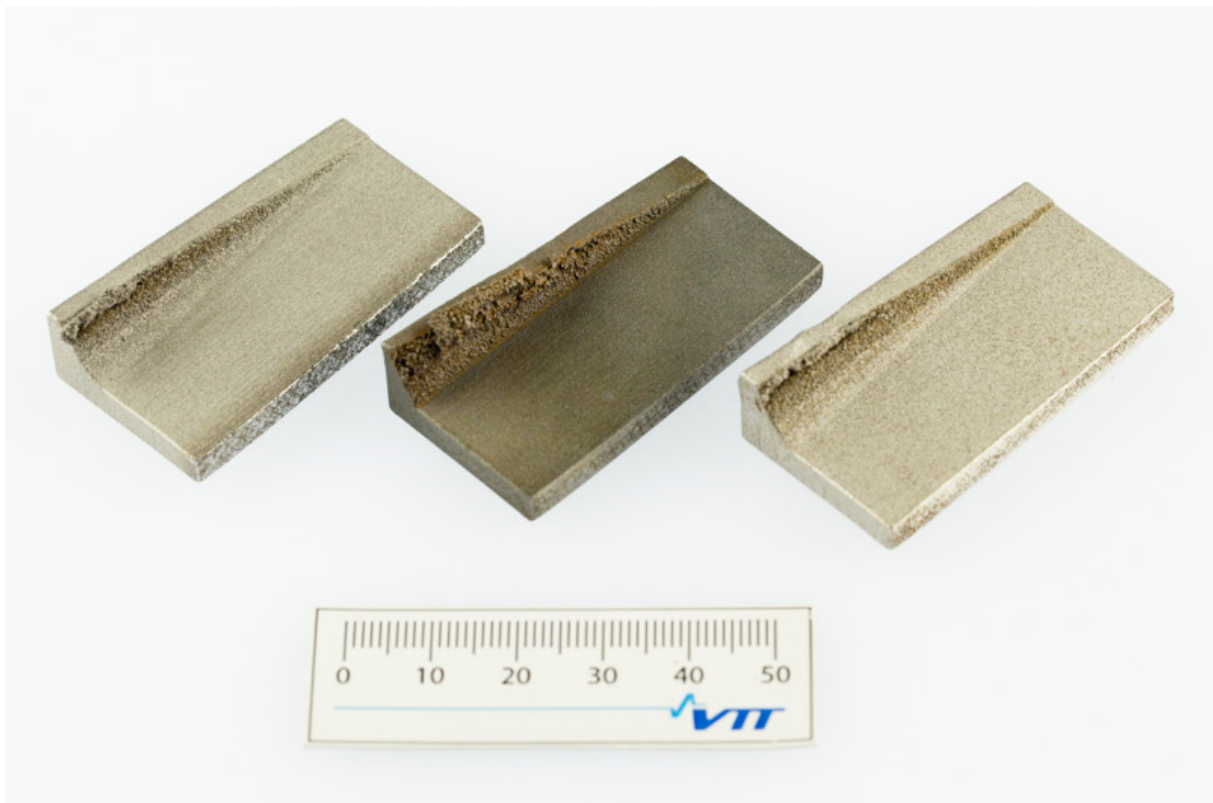


Figure 75. The overhang test pieces with and without fillet printed in H13 (middle) and 316L.

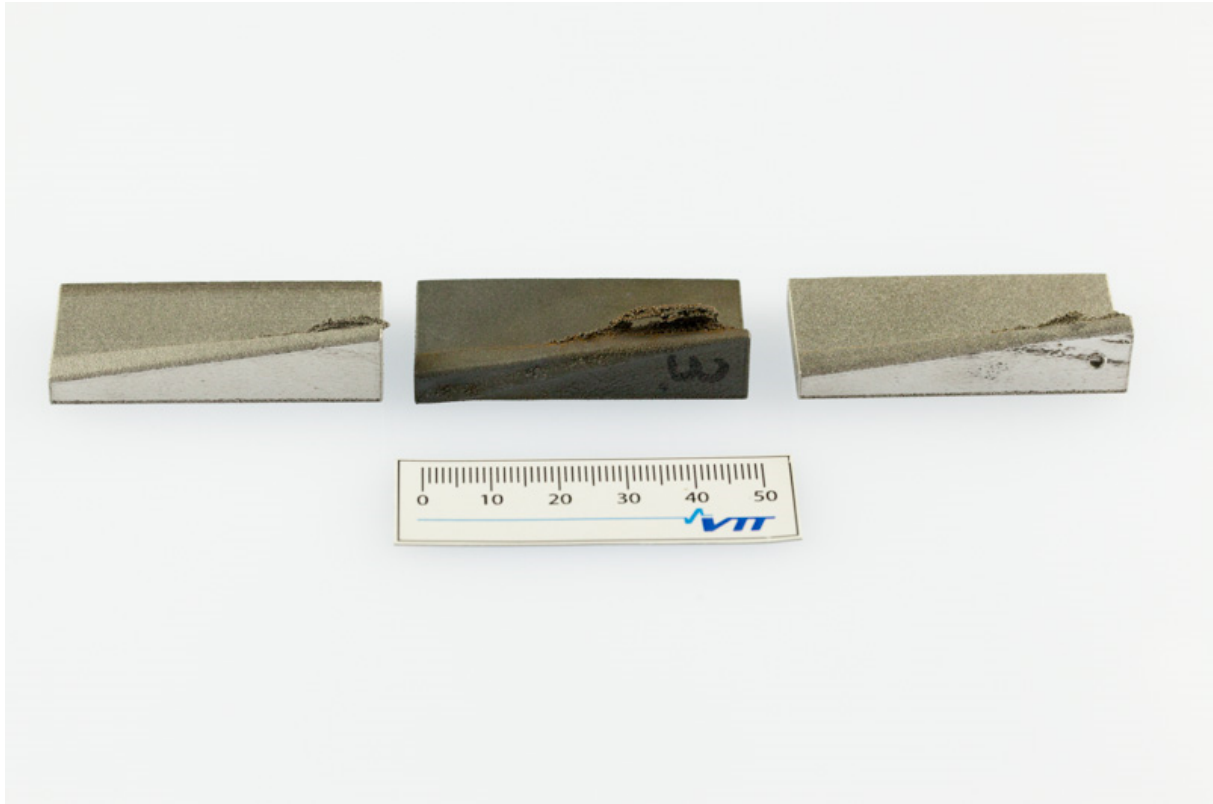


Figure 76. The overhang test pieces with and without fillet printed in H13 (middle) and 316L.

The overhang test pieces show that the limiting value for unsupported overhang is one to two millimeters. A small fillet increases the printable overhang distance. Overhang distance of several millimeters leads to wiper defect and poor quality or printing failure. Dross formation occurs at the downskin surfaces of the overhang details.

The wiper defects were quite common with the overhang test prints. The long overhang leads to heat build-up at the overhang region and results in wiper defect or print failures. The unsupported overhangs longer than the one to two millimeters are therefore not recommended in design.

3.10.5 Surface quality

Remarks on the surfaces of the test pieces are discussed in the following.

overhang test piece with sagging close to the 60° plate, most likely causing the surface defect

surface roughness increases →

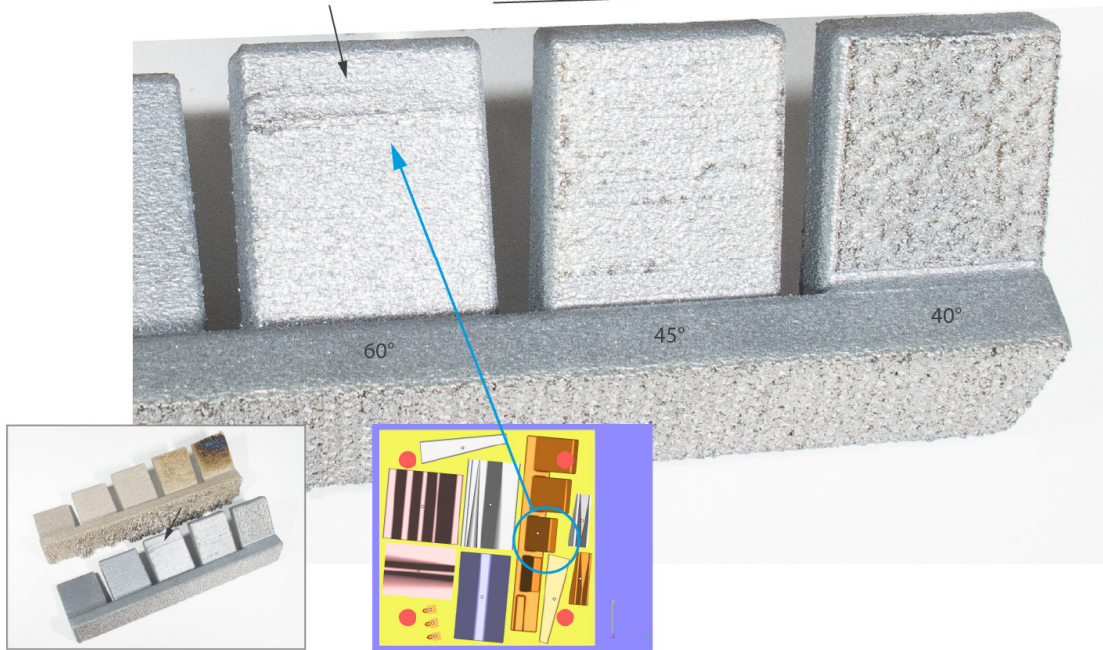


Figure 77. Remarks on the bottom surfaces of AlSi12 inclined plates.



Figure 78. The test prints of the inclined plates in Inconel and AlSi12 at 50 µm layer thickness. Wiper defect is seen at the AlSi12 piece downskin surface at the middle member. Surface roughness increases as the inclination angle decreases (shallow angle is worse).

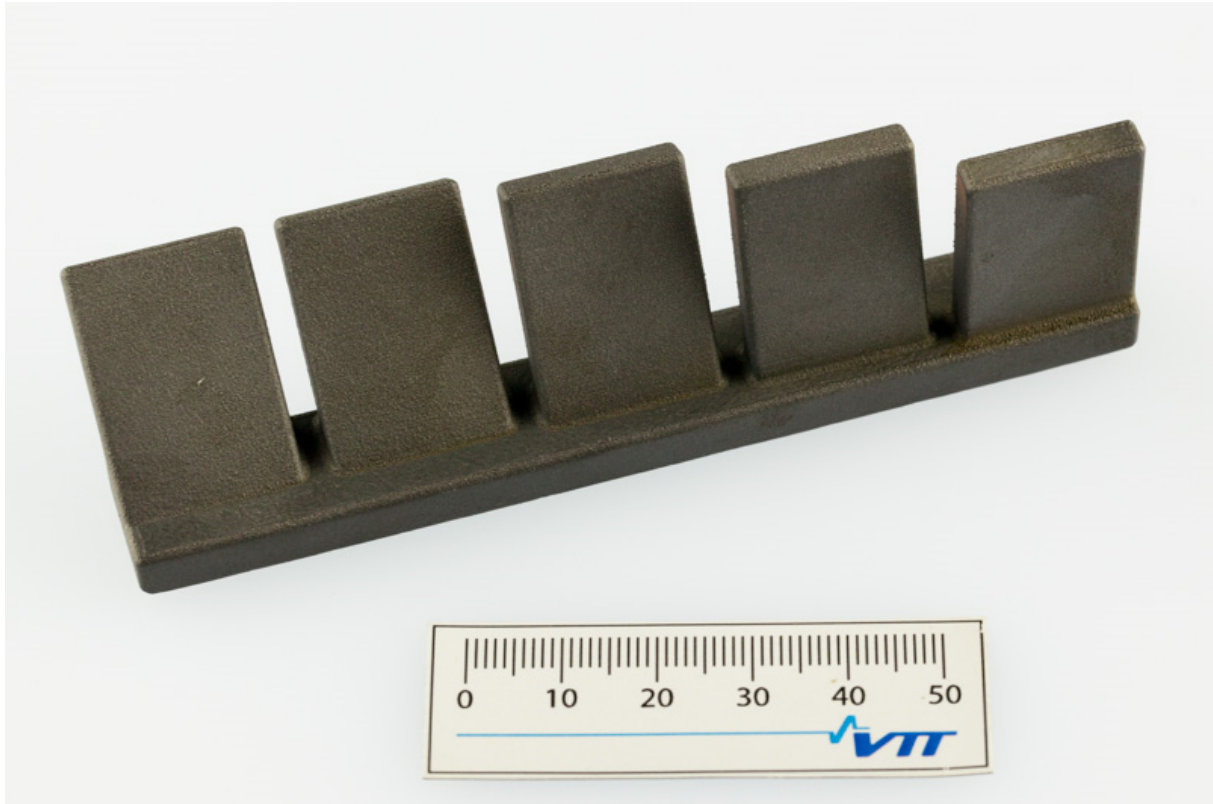
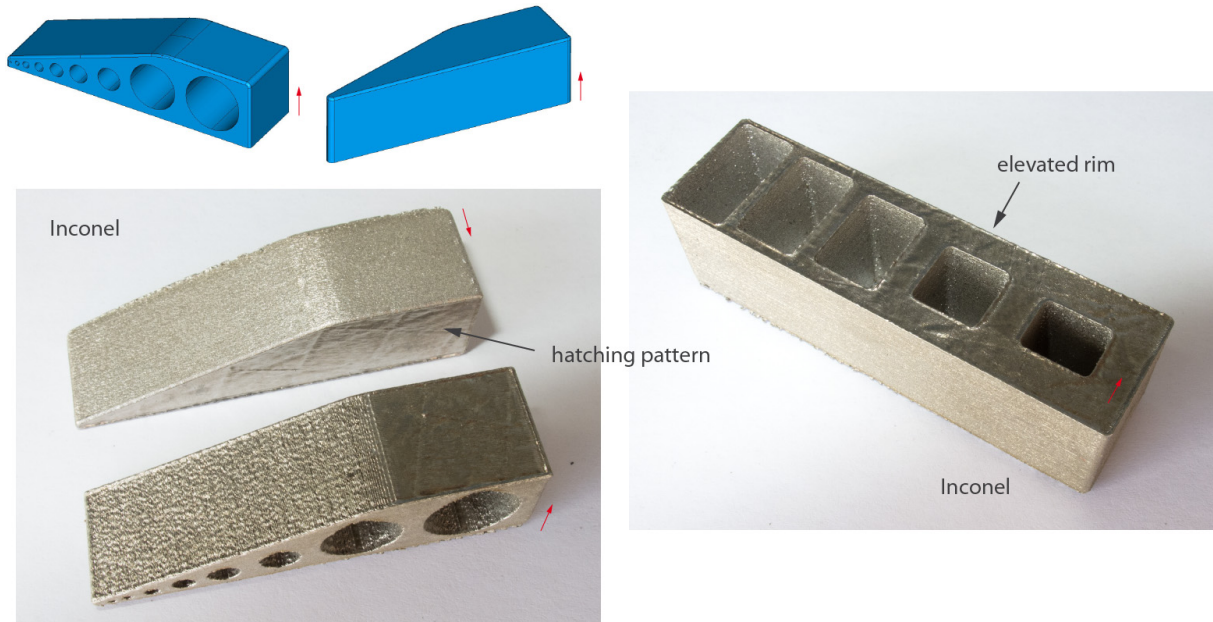


Figure 79. The test print of the inclined plates in H13 tool steel at 30 μm layer thickness. No defects were noted at the surfaces. The good heat conductivity of steel together with the small layer thickness result to very good printing quality.



difference in surface roughness of inclined surface

Figure 80. Remarks on the surfaces of Inconel test pieces.



Figure 81. Round holes test print in Inconel. The small diameter holes are better left drilled.

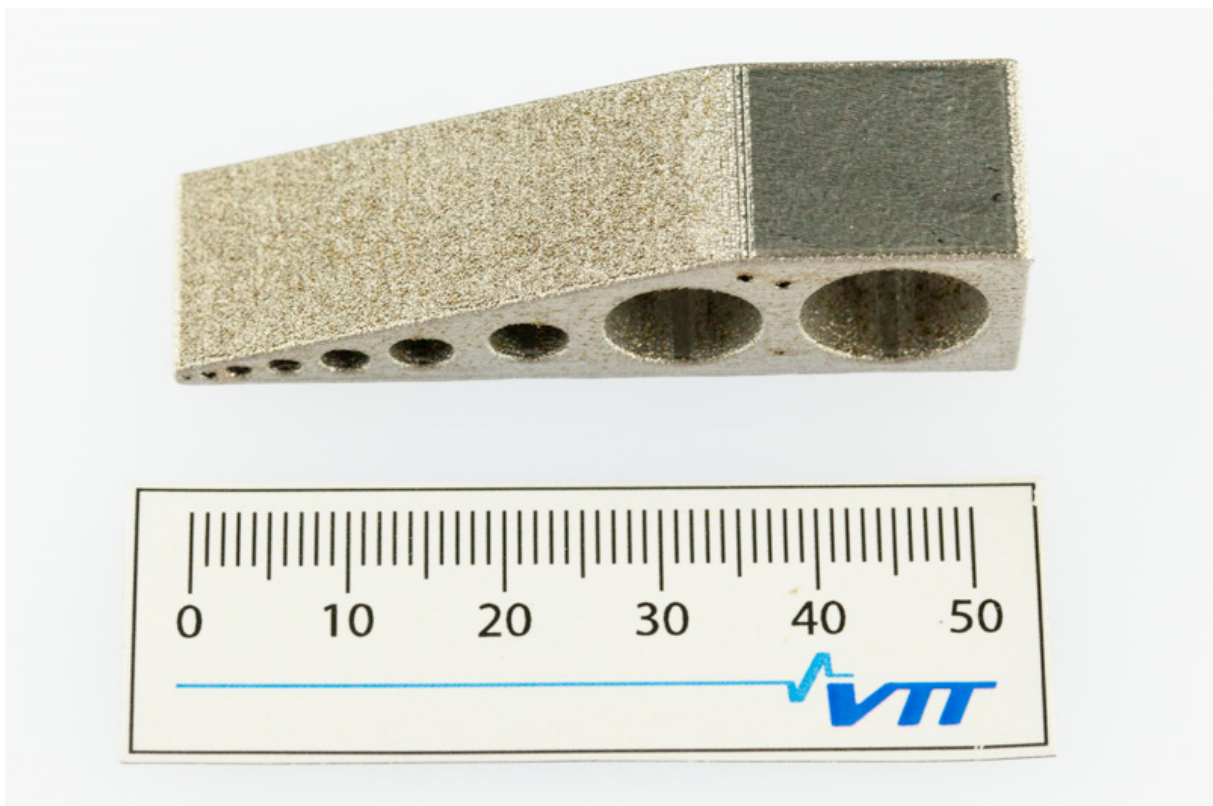


Figure 82. Transversal round holes test print in H13 tool steel at 30 μm layer thickness.

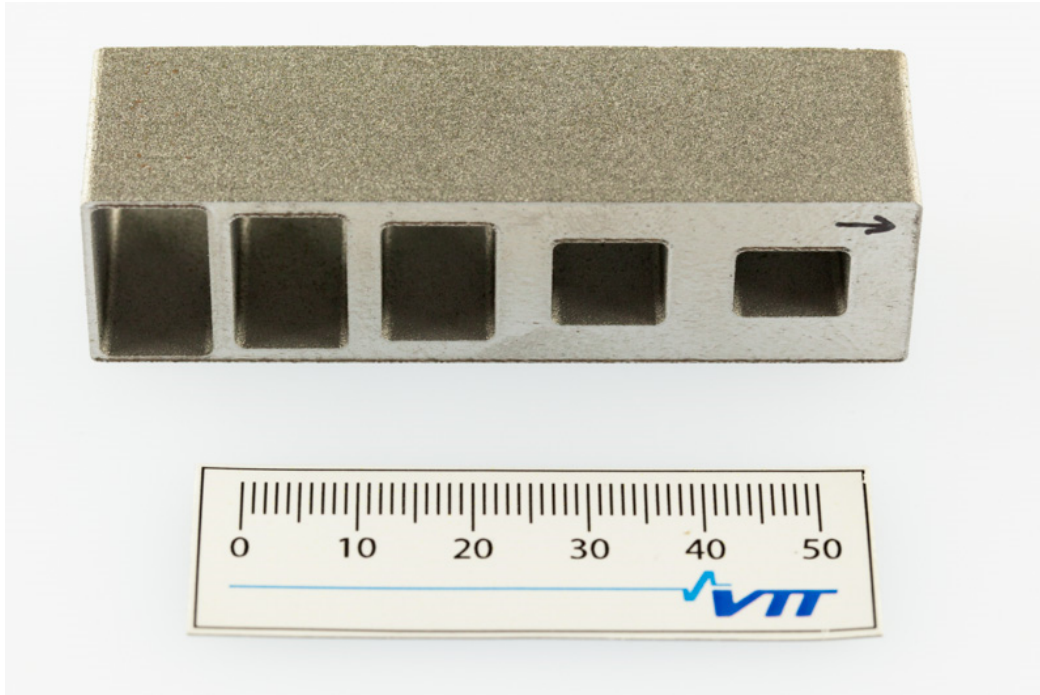


Figure 83. Rectangular holes test print in H13 tool steel at 30 μm layer thickness. No defects or distortions were noted.



Figure 84. The S-curve elliptic channel test geometries printed in H13 tool steel at 30 μm layer thickness. Dross is formed at the horizontal top locations (bottom piece at both ends) but otherwise the prints are defect free. Piece was wire cut in halves along the channel center line.

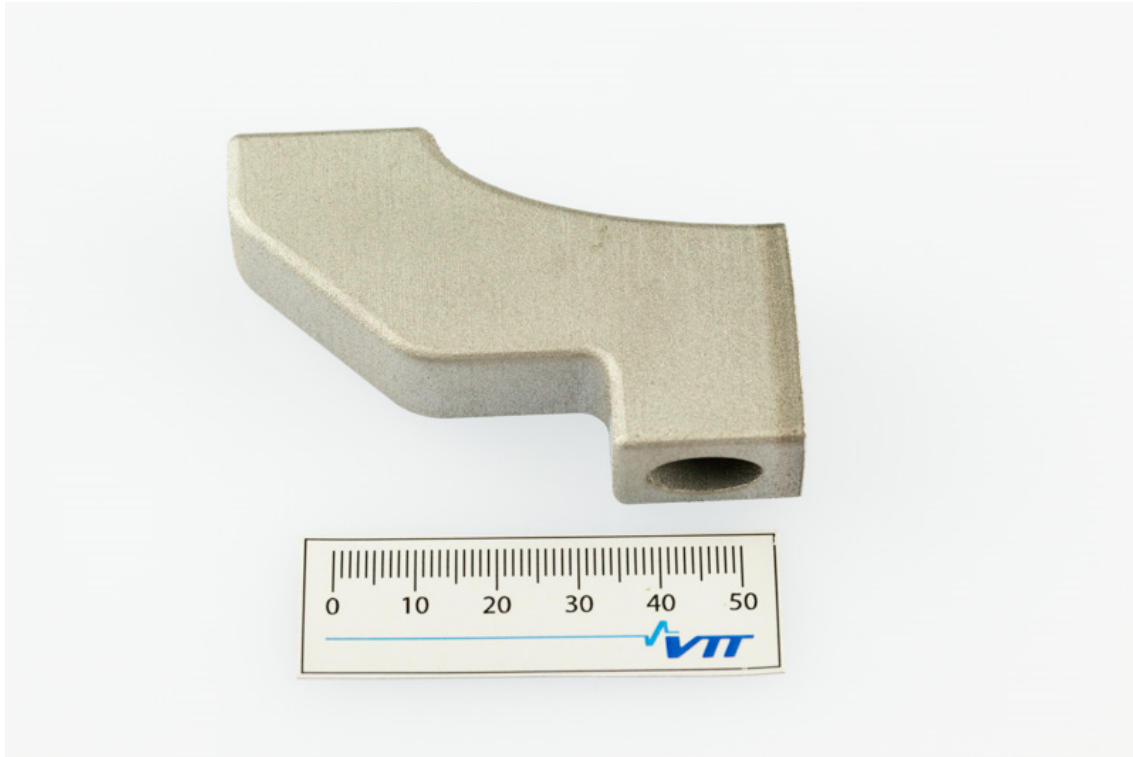
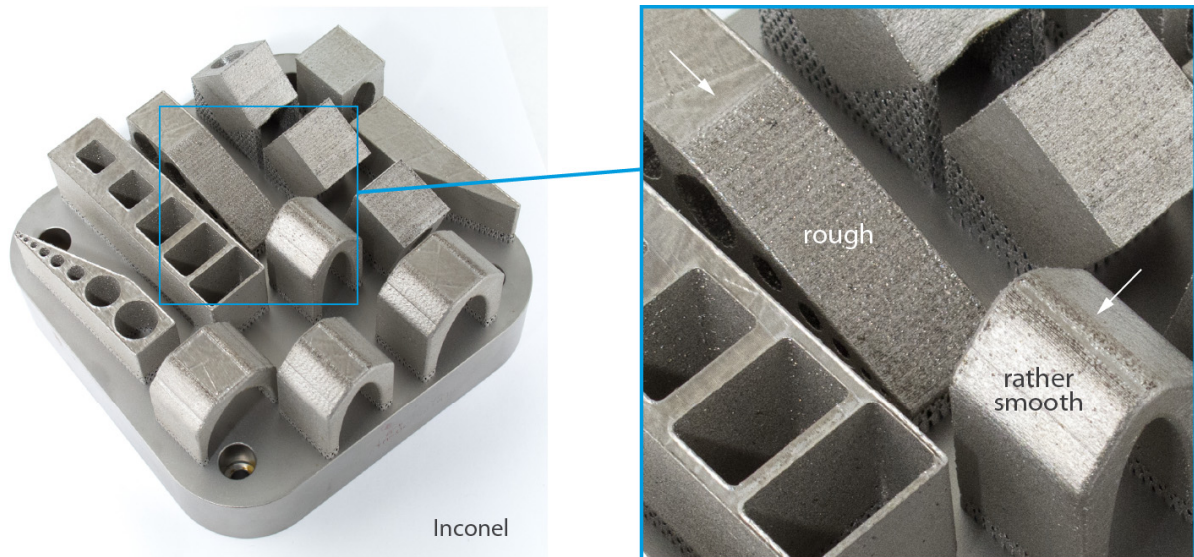


Figure 85. The S-curve elliptic channel test piece printed in H13 tool steel at 30 μm layer thickness before wire cutting.

Remarks on surface quality of Inconel test pieces are shown in the following figure.



surface roughness seems to depend on angular position

Additional test geometries to study effect of angular orientation

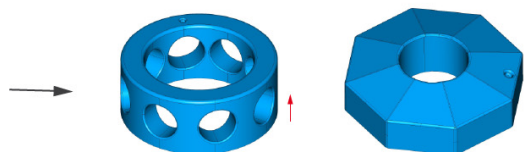


Figure 86. Remarks on surface quality of Inconel test pieces. Additional test geometries were prepared to evaluate the mechanism behind the surface roughness further. In these additional pieces no significant dependence was detected between the surface roughness and angular, in plane direction.



Figure 87. Additional test geometry for evaluating the dependence of surface roughness on the angular direction, printed in H13 tool steel at 30 μm layer thickness. No significant dependence was detected. The printed piece is upside down to show the cross at the top locations of the holes.

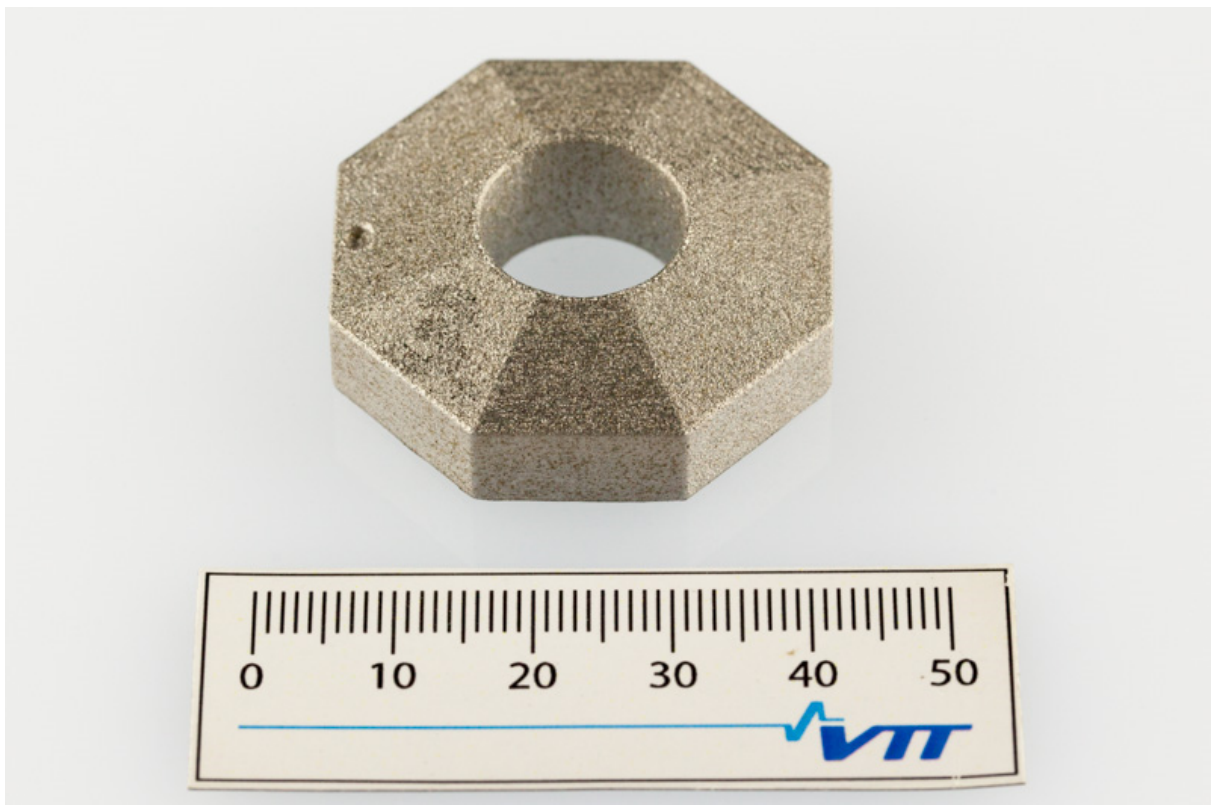


Figure 88. Additional test geometry for evaluating the dependence of surface roughness on the angular direction, printed in H13 tool steel at 30 μm layer thickness. No significant dependence was detected.



Figure 89. The varying inclination warped test geometry printed in H13 tool steel at 30 μm layer thickness. A Moiré type surface pattern can be seen at the left, at center line. This pattern is caused by the layered representation of a double curved geometry.

3.10.6 Wall thickness

Remarks on the wall thickness test pieces are presented in the next figure.

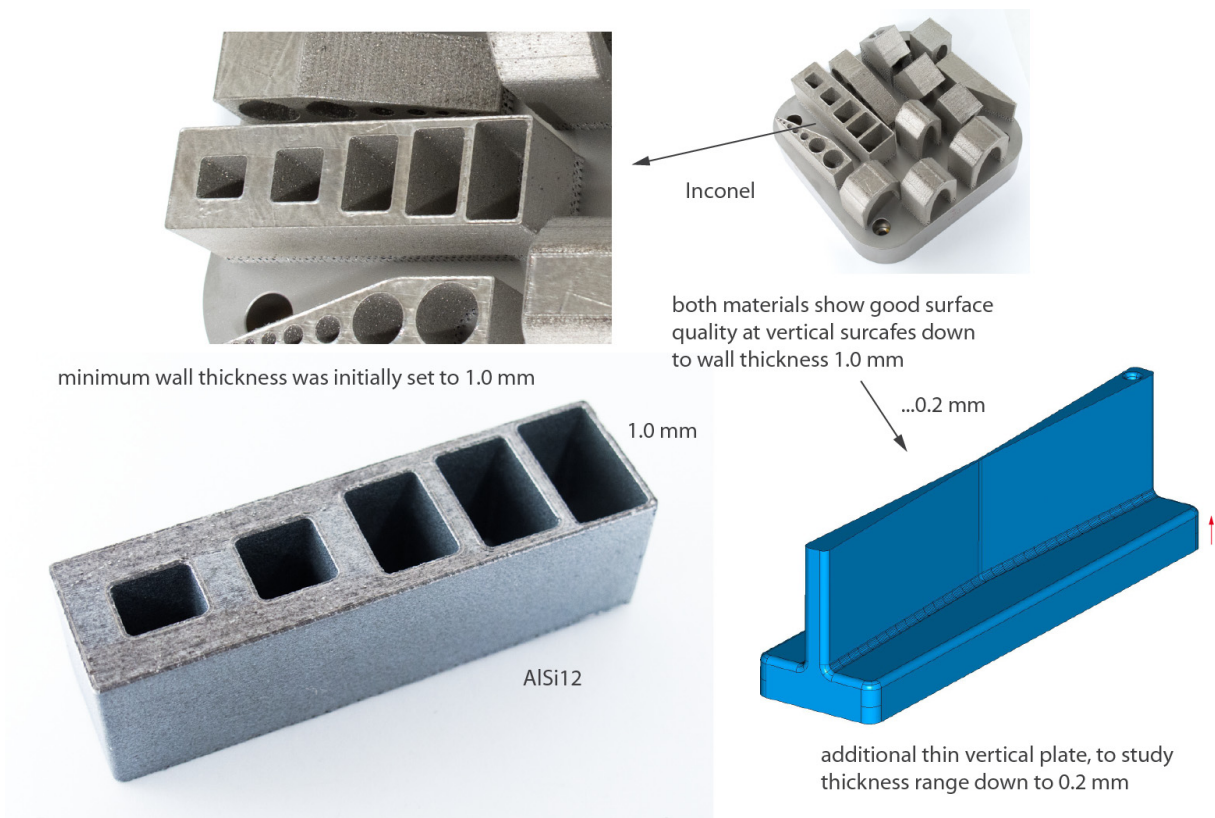


Figure 90. Remarks on the wall thickness test pieces. The vertical walls showed all to print fine, and additional test geometry was prepared to evaluate the limit value for wall thickness further.



Figure 91. Thin vertical blade test piece in 316L (left) and H13 (right). The narrow location is printed fine in H13 but shows slight offset in 316L (defect).

3.10.7 Small details

Remarks on the small detail –test pieces are presented in the following figure.

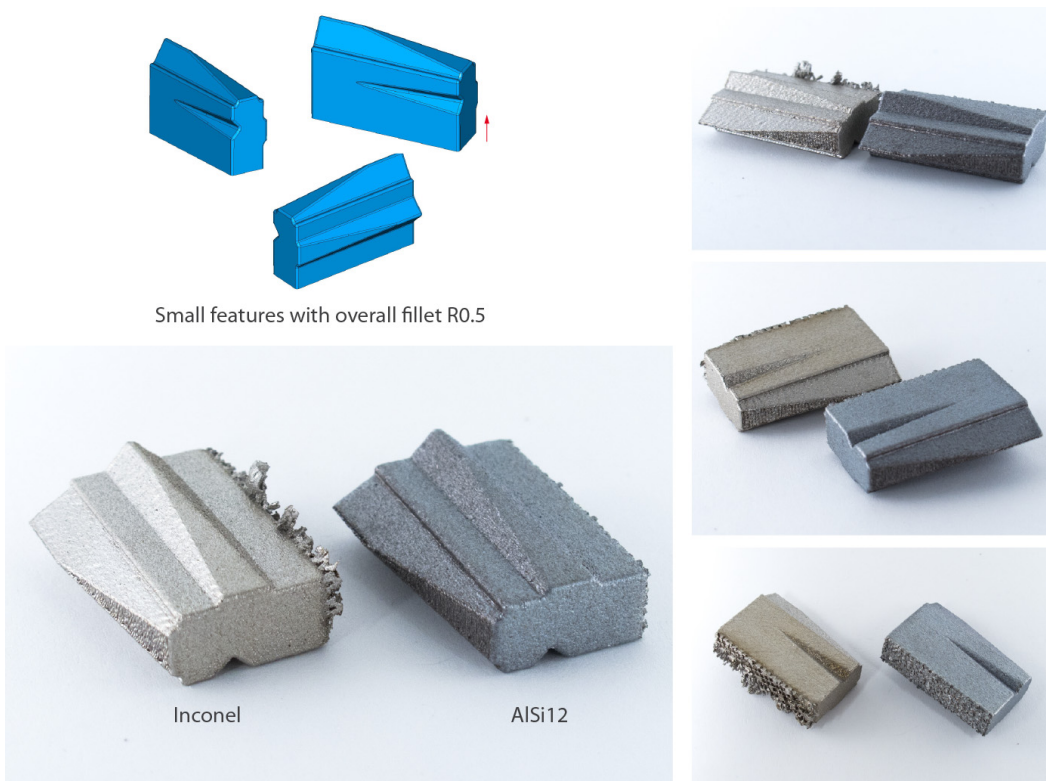


Figure 92. Remarks on the small detail –test pieces. The small details print fine. The AISi12 shows slight burr at sharp edges, and less burr at edges with fillets.



Figure 93. Small detail –test pieces printed in H13 tool steel at 30 μm layer thickness.

3.10.8 Lattice structure test prints

The gyroid type lattice structure was modelled in MATLAB based on the common mathematical formula describing the repeating gyroid geometry and exported into .stl file format for printing. The gyroid is self-supporting and is therefore well suited for metal 3D-printing.

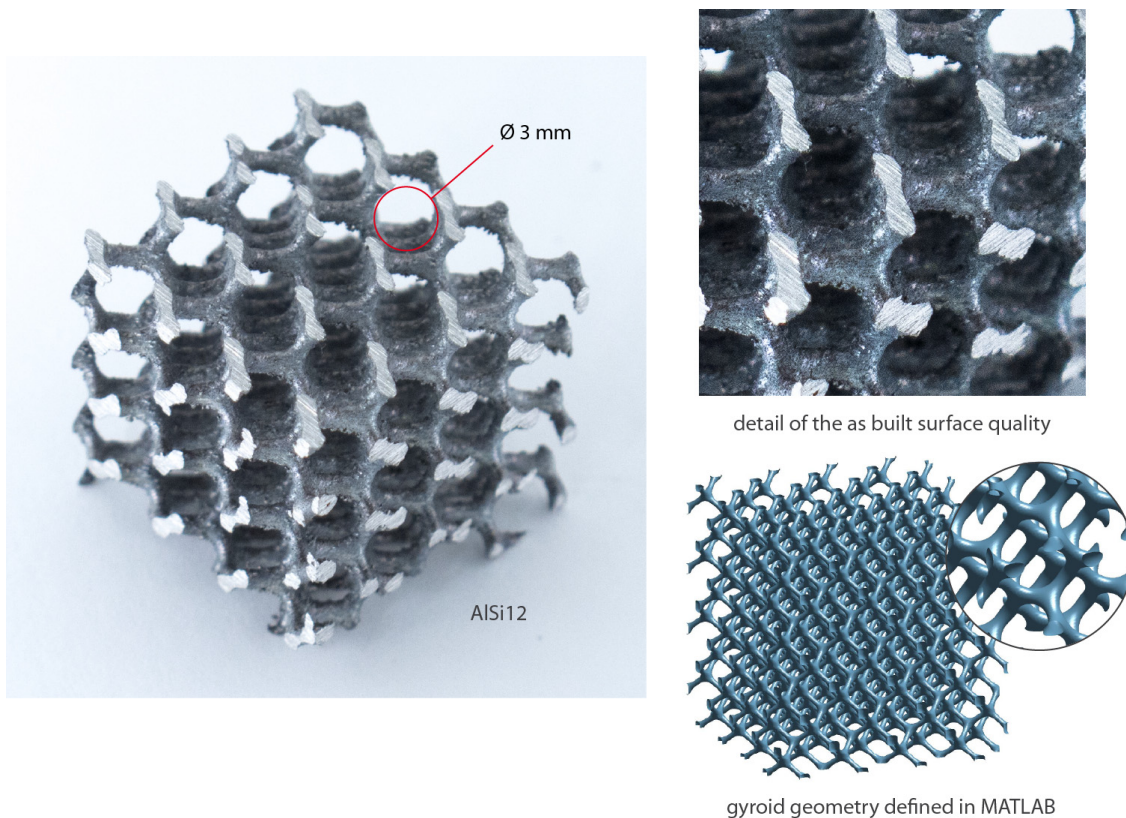


Figure 94. The gyroid test geometry printed in AISi12. The surfaces are quite rough, but the piece was printed fine.

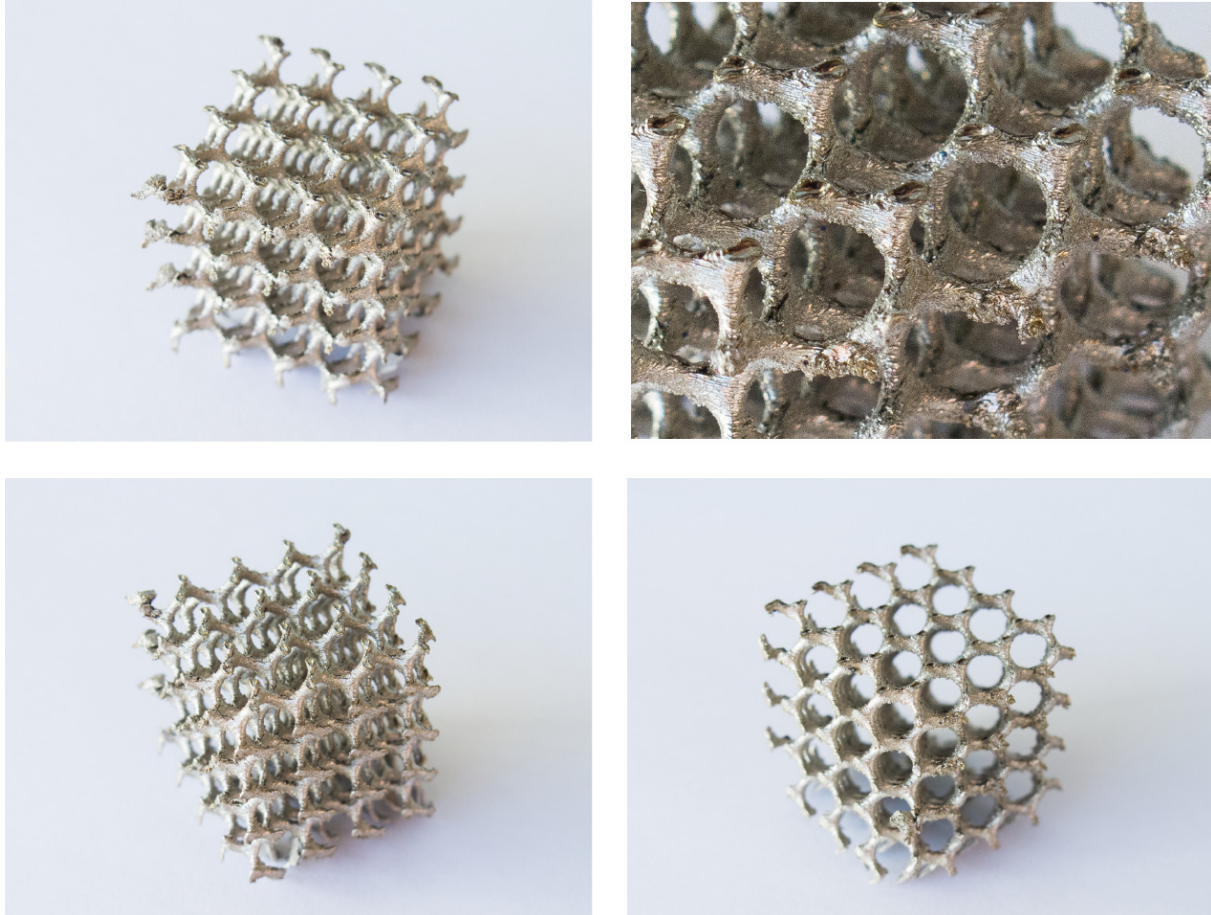


Figure 95. The gyroid test geometry printed in Inconel. The surfaces are quite rough, but the piece was printed fine.

3.11 Logos, texts and markings

Logos and texts can be added on parts before printing in many CAD software and in for example the Materialise 3-Matic software directly to the .stl geometry.

3.12 Patterns and textures

Patterns and textures have both functional and esthetic use.

For example patterns mimicing denticles at shark skin are used to reduce drag at surfaces due to fluid flow. The lotus leaves have microscopic pattern creating hydrophobic effect that can be used for self cleaning surfaces in products. The feet of a gecko lizard are famous for their ability to stick to smooth surface with help of the van der Waals force. Most of the biomimic surface patterns are below the reach of the current resolution and accuracy of AM, but may become relevant as the AM develops further.

The patterns for securing grip on tools and handles traditionally made by knurling (pyällys in Finnish) or by molding can be printed on the product surface in AM.

For esthetic use, figures and 3D shapes can be printed as patterns on the product surface in AM. For example the 3-Matic software has efficient tools for adding such patterns on the models.

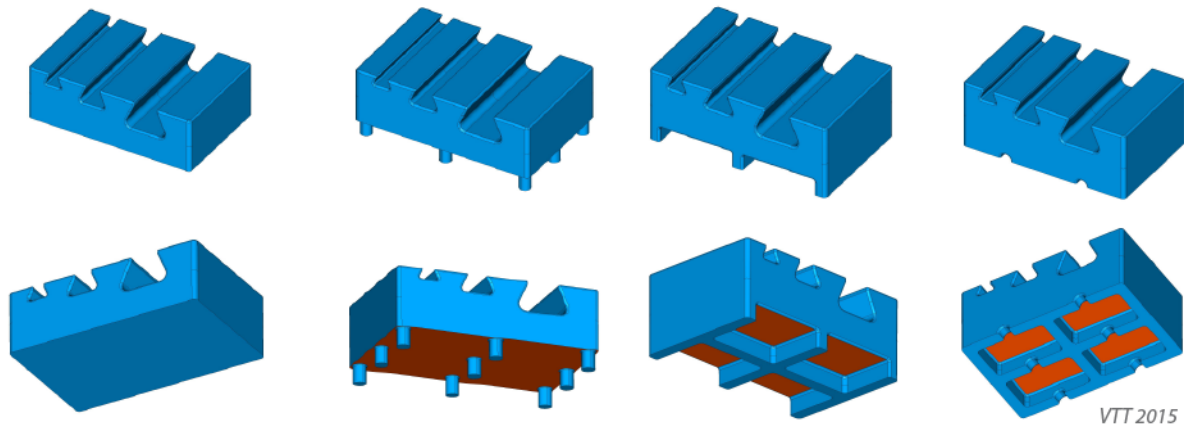
3.13 Test serie of various support types

A test serie was prepared for assessment of the behaviour of a plate like structure at different types of support designs. The test geometries and the varied support designs are presented

and commented in the following. The dove tail type seal grooves were added to the top surface of the test piece to bring some unsymmetry to the test geometry.

The case a) in Figure 96 is printed directly from the base plate and as a variant with the block and rod supports added in Magics software before printing. The case b) is with 3 mm diameter rods added in CAD and block supports added in Magics. The case c) is an open grate modelled in CAD and block supports added in Magics. The case d) is a closed grate modelled in CAD and block supports added in Magics. The 'rat holes' were added to the closed grate for powder removal.

Block supports are added at the orange surfaces in Magics before printing.



a) Direct build from platform,
and with Magics supports.

b) Rods added
in CAD.

c) Open grate.

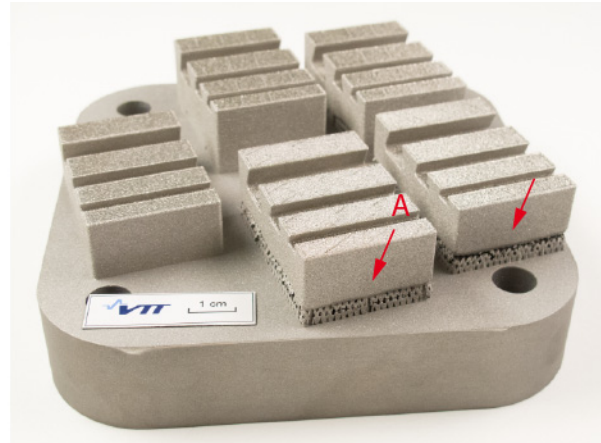
d) Closed grate.

Figure 96. Test serie for assessment of different types of support designs.

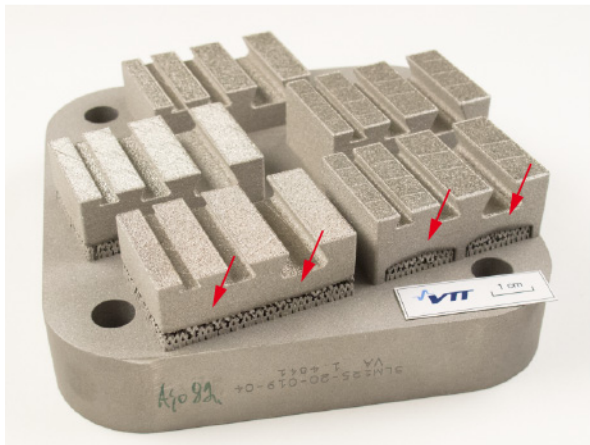
Test prints of different types of support designs in AISI 316L is presented in Figure 97.



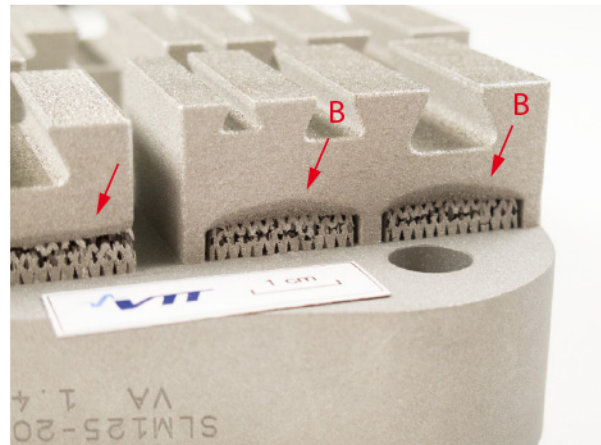
a) Support test serie printed in AISI 316L, view showing the grate versions and the piece printed directly from the base plate.



b) The burning marks and torn supports in the block support pieces. The heavy rods modelled in CAD (A) prevent distortions.



c) The burning marks and torn supports in the block support pieces. The torn supports lead to distortions and geometrical inaccuracy.



d) The burned edges and torn supports in the block support pieces, details. The open type grate (B) shows excessive edge burning.

Figure 97. Overview of the test prints of different types of support designs in AISI 316L.

The block supported test pieces show heat colors and local distortions at the bottom edges. The closed grate and the case printed directly from the base plate printed out fine.

Side views of the test prints of different types of support designs in AISI 316L are presented in Figure 98.



Figure 98. Side views of the test prints of different types of support designs in AISI 316L.

Bottom views of the test prints of different types of support designs in AISI 316L are shown in Figure 99.

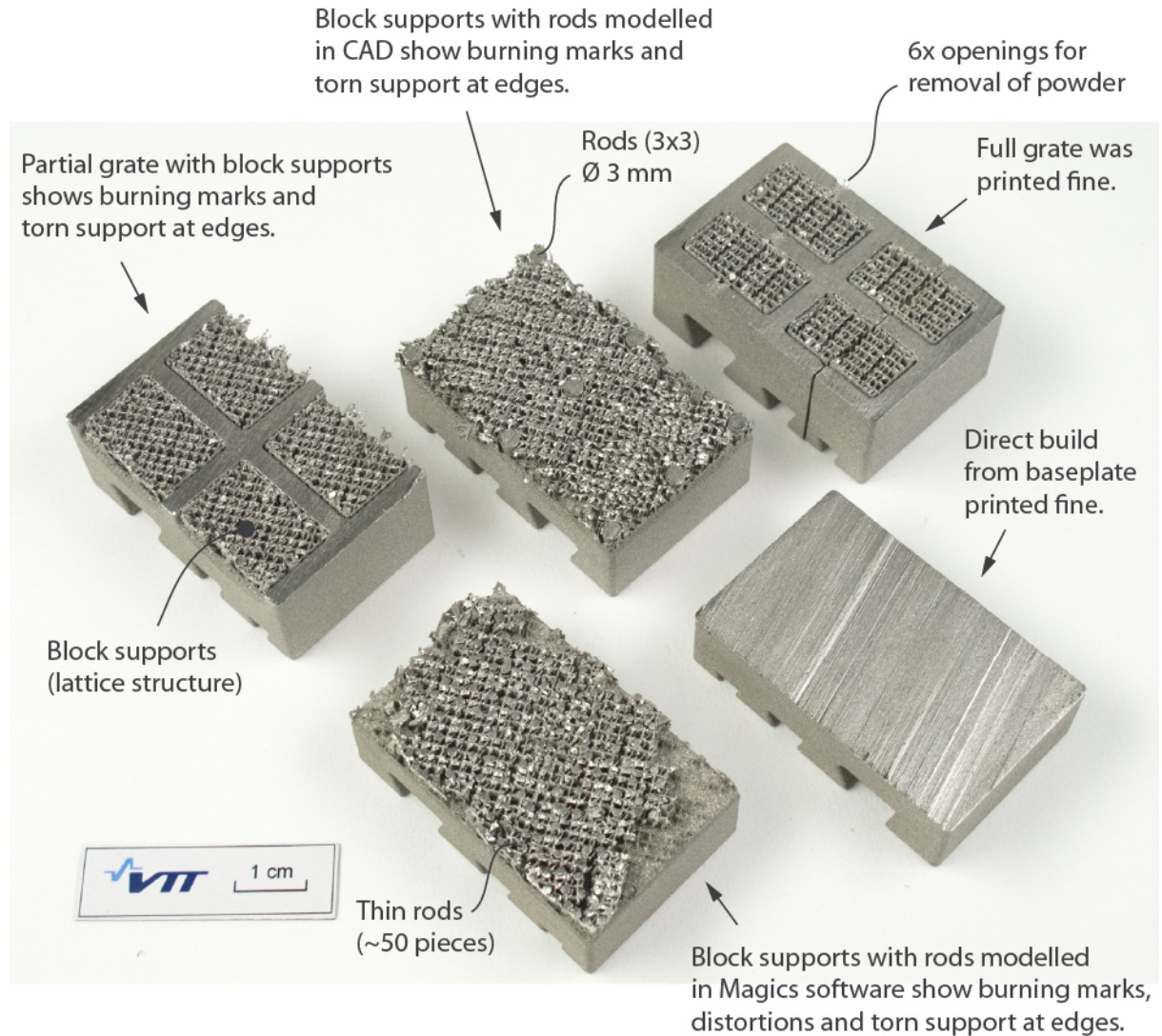


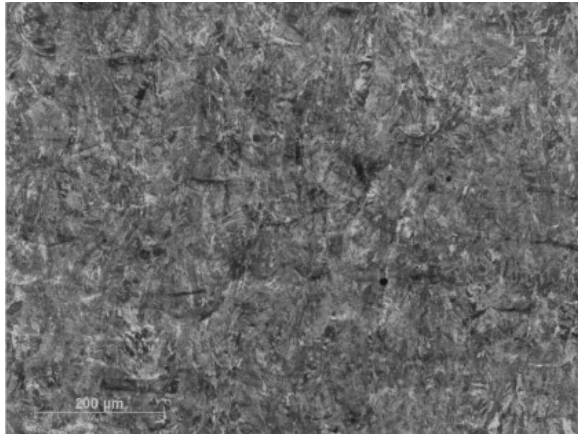
Figure 99. Bottom views of the test prints of different types of support designs in AISI 316L.

Based on the test series, the open grate type support structure with block support or direct build from base plate with cutting allowance are recommended as support types for SLM components for mechanical engineering applications.

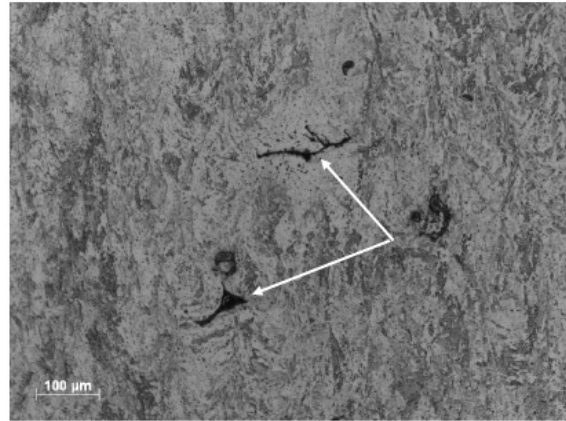
3.14 Manufacturing defects

Examples of possible material/manufacturing defects typical to SLM are presented in the following figure as excerpts of the earlier metallurgical analysis by Reetta Riihiaho in VTT ES report [17].

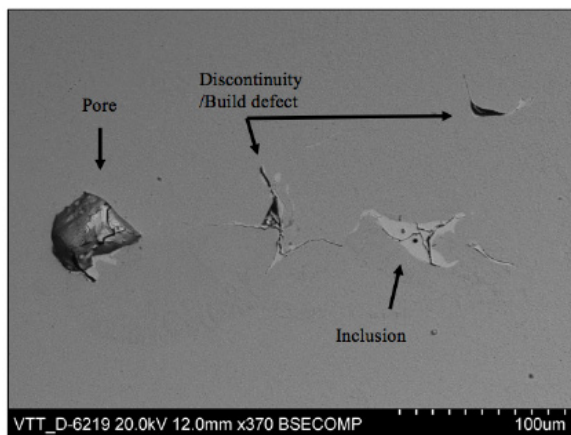
The manufacturing defects typical to SLM are also listed in Appendix E.



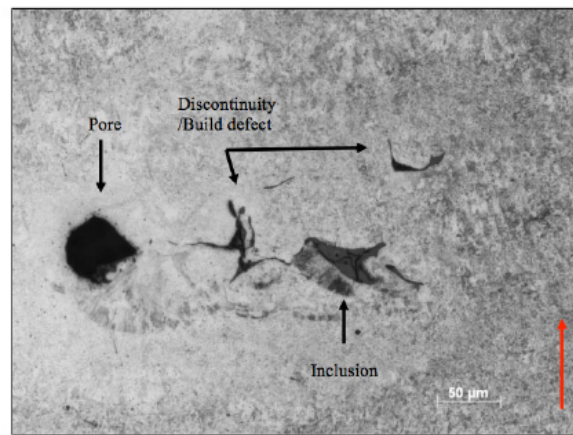
Microstructure of the heat treated Maraging steel sample (6h) the arrow shows the 3D printing direction.



Non-metallic, sharp inclusions and/or pores were observed in the microstructure, see arrows.



Picture 15. Scanning electron microscopy (BE) image of the pores, inclusions and discontinuities detected in the Stainless steel PH1 specimen (see previous image). The white substance that is in the inclusion was also observed in the bottom of the pore.

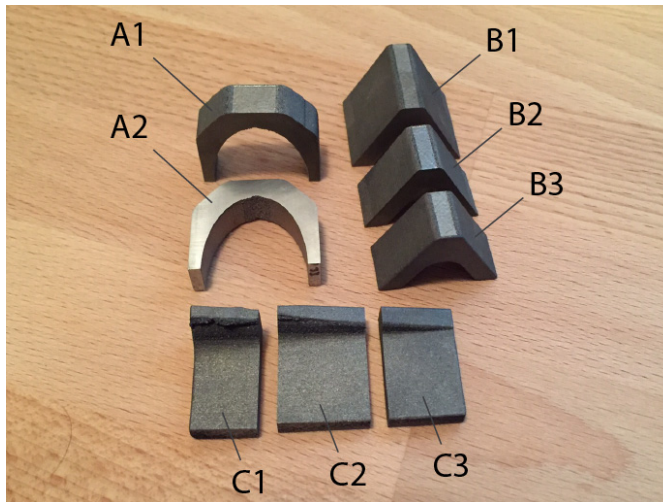


Picture 14. Pores, inclusions and discontinuities were detected in the Stainless steel PH1 specimen. Red arrow shows the building direction. Optical microscopy image.

Figure 100. Examples of possible material defects typical to SLM are presented in the following figure as excerpts of the earlier metallurgical analysis in VTT ES report [17]. The analysis by Reetta Riihiahio demonstrates the various defect types typical to the SLM process.

3.15 Porosity

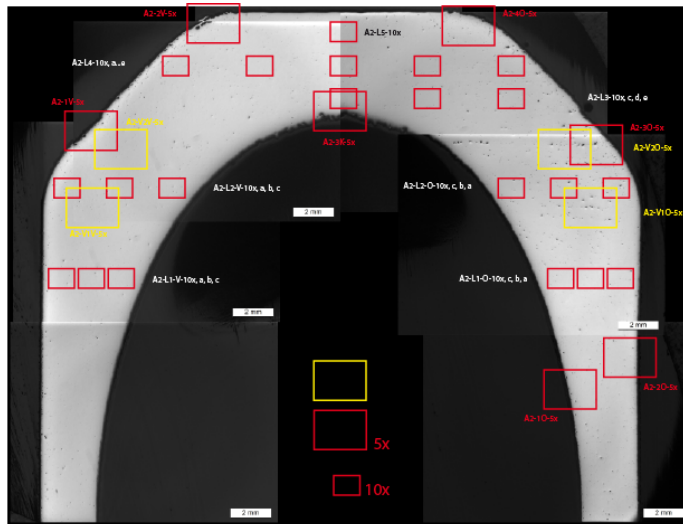
The porosity common to SLM prints was studied by microscope of three H13 tool steel test prints. The test pieces were printed early in the project using the default process settings, leading to higher porosity than is possible to achieve at optimised process settings. The test prints were wire cut to pieces by KTS-mekano Oy and ground and polished at VTT.



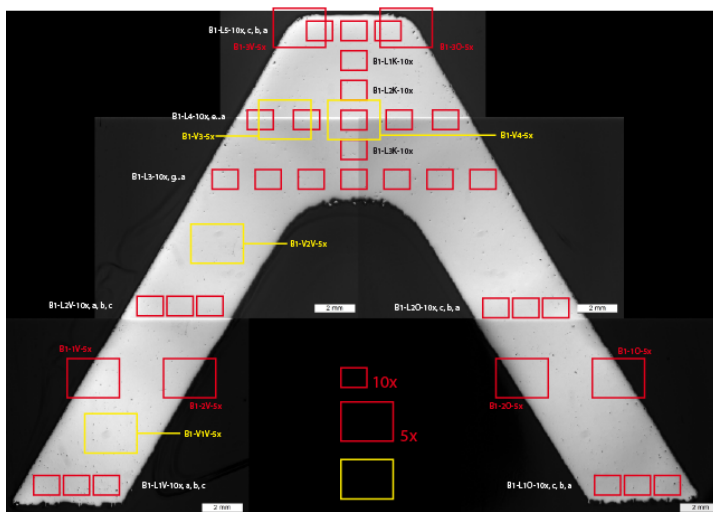
Wire cutting by KTS-Mekano Oy

Figure 101. Three H13 tool steel test prints used in the microscope study.

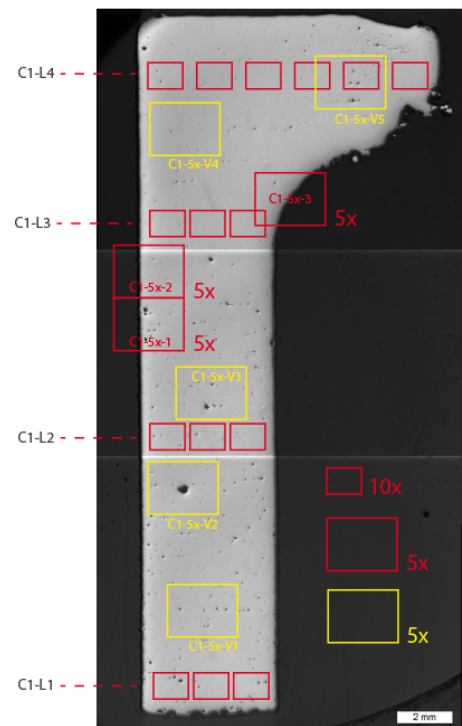
The cross sections of the samples and the studied locations are presented in the following figures.



Cross section of specimen A.



Cross section of specimen B.

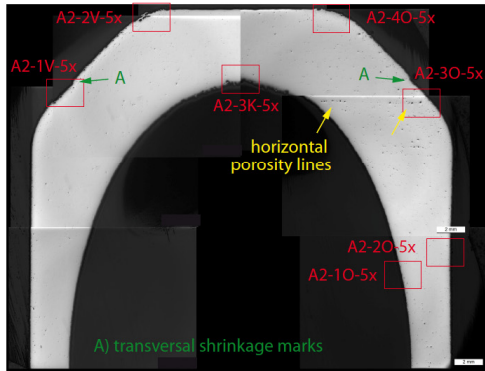


Cross section of specimen C.

Figure 102. The cross sections of the samples and the locations studied by optical microscope.

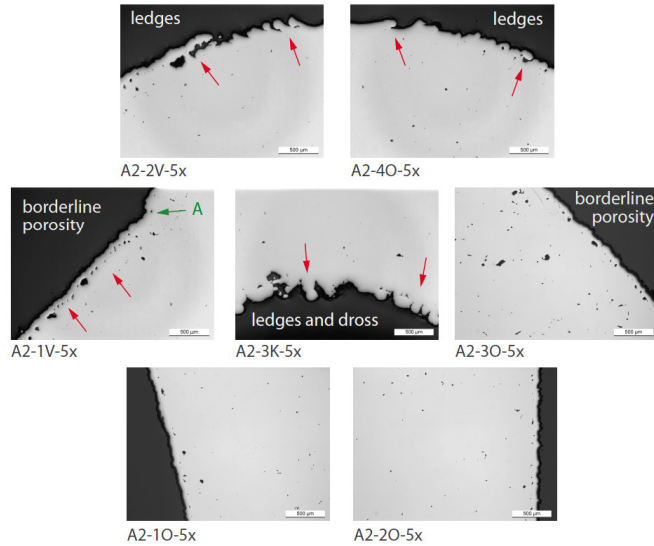
The cross sections of the specimens and the optical microscope (OM) figures at 5x magnification are presented with remarks in the following figures. The microscope studies were conducted by Seija Kivi, VTT.

- Legdes (protrusions) and notches result at locations of large step size, at transition angles close to flat, horizontal surface.
- Borderline porosity occurs at inclined upskin surfaces, but only slightly at inclined downskin surfaces.
- Ledges can be seen at downskin surfaces, but not as much at upskin surfaces.



Surface evaluation locations of SLM H13 macro specimen A2

Stair step effect shows as ledges (protrusion, elevated edges, cold lap type formation) at near horizontal transitions at upskin surfaces.



Slight borderline porosity can be seen at vertical and near vertical surfaces.

Figure 103. The cross sections A2 of specimen A and the OM figures at 5x magnification.

- Legdes (protrusions) and notches result at locations of large step size, at transition angles close to flat, horizontal surface.
- Borderline porosity occurs at inclined upskin surfaces, but seemingly not at inclined downskin surfaces.
- Ledges can be seen at downskin surfaces, but not as much at upskin surfaces.

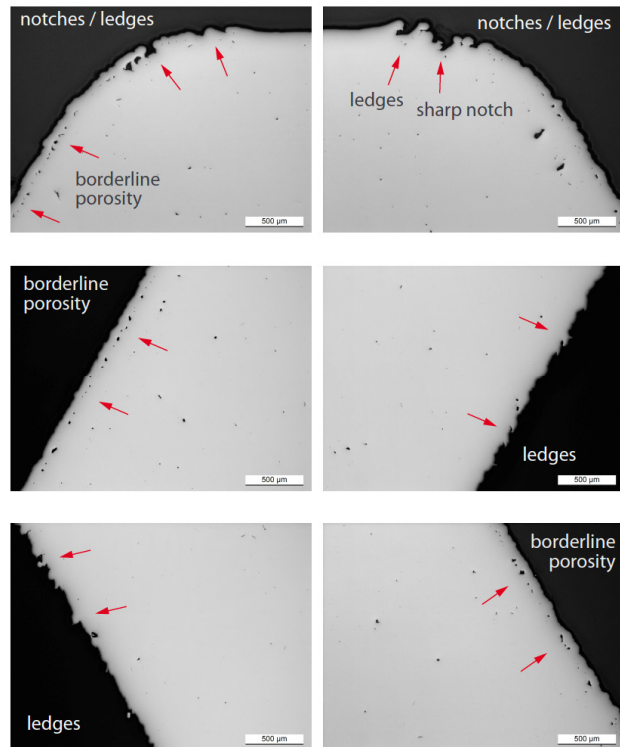
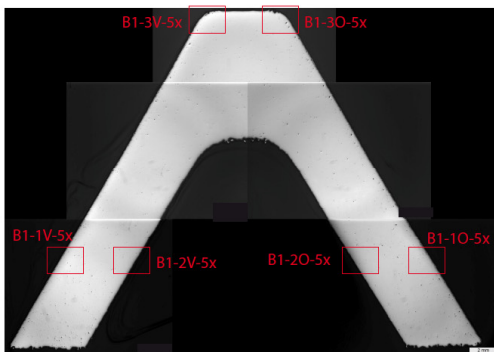


Figure 104. The cross sections B1 of specimen B and the OM figures at 5x magnification at the edge locations.

-> Low porosity, only a few larger voids.
 -> Voids are nicely distributed (separated).

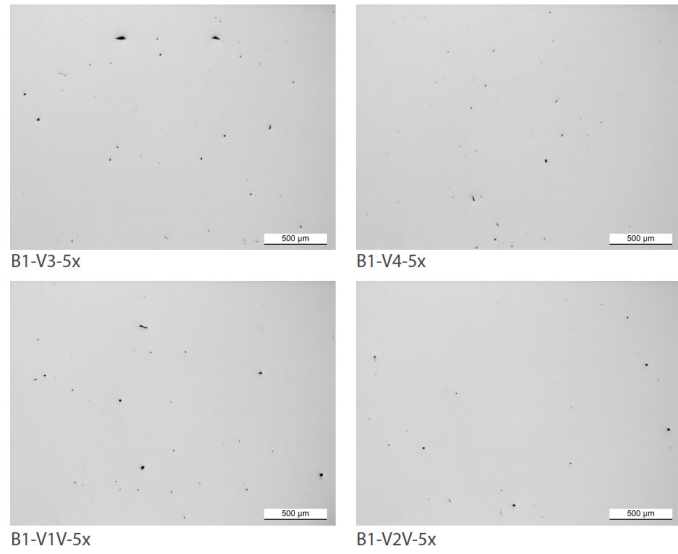
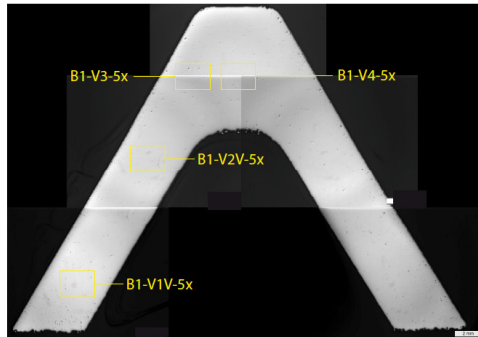


Figure 105. The cross sections B1 of specimen B and the OM figures at 5x magnification at the internal locations.

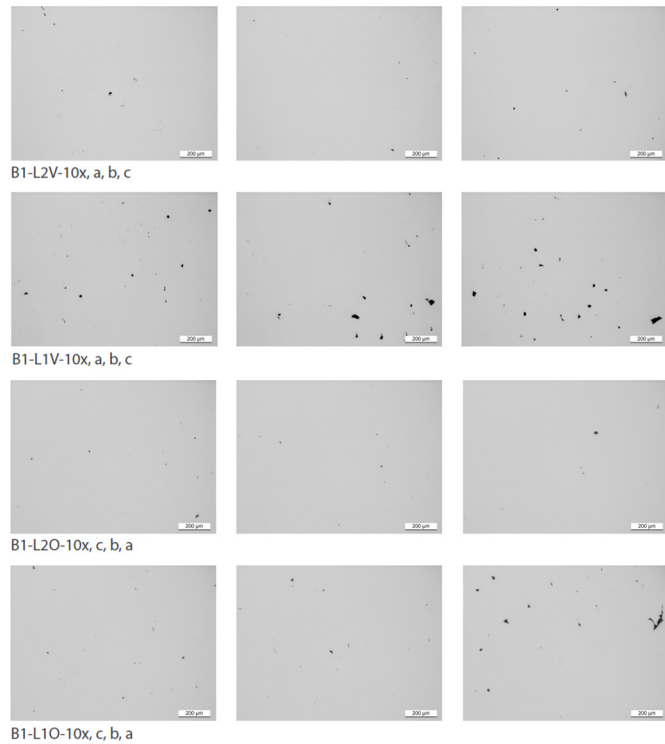
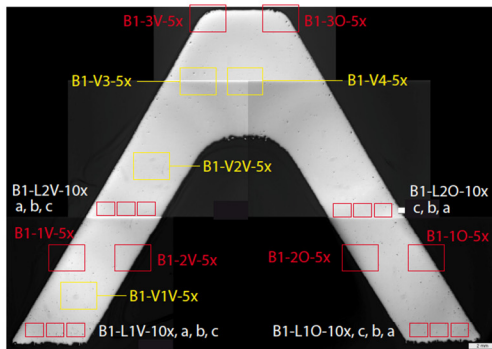


Figure 106. The cross sections B1 of specimen B and the OM figures at 10x magnification.

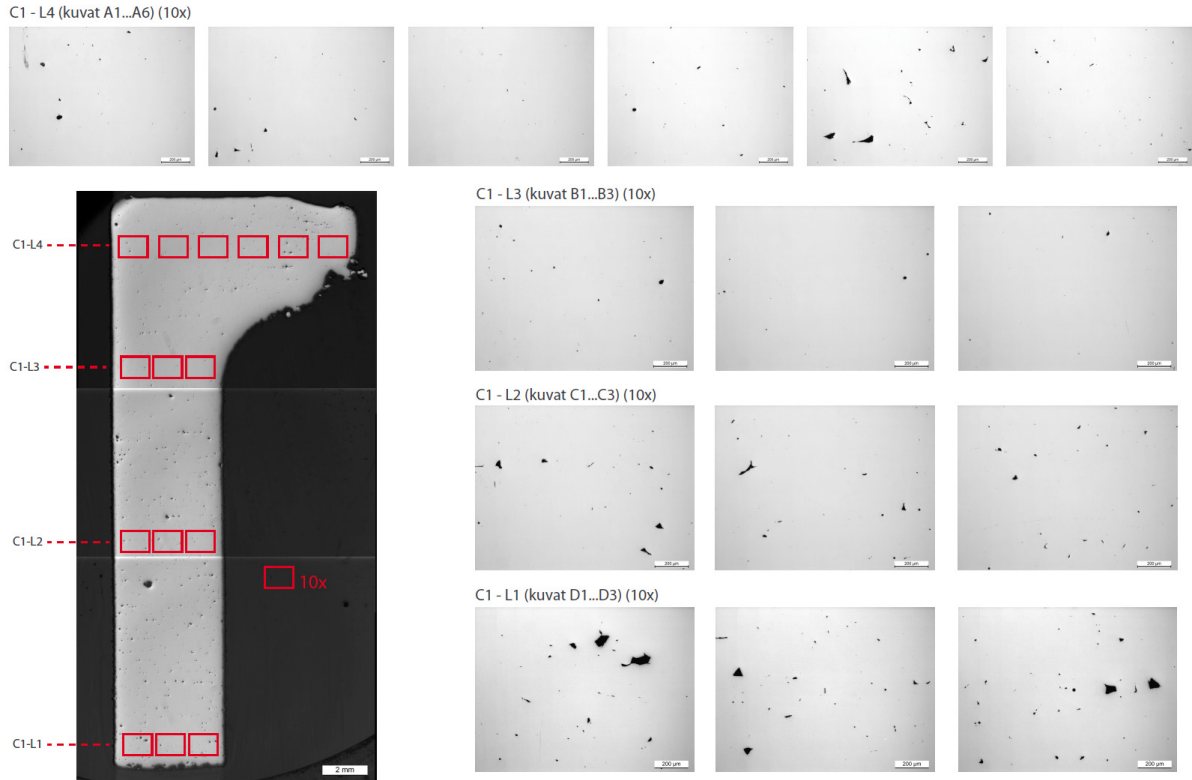


Figure 107. The cross sections C1 of specimen C and the OM figures at 10x magnification.

Surface quality at vertical surface, with typical porosity.

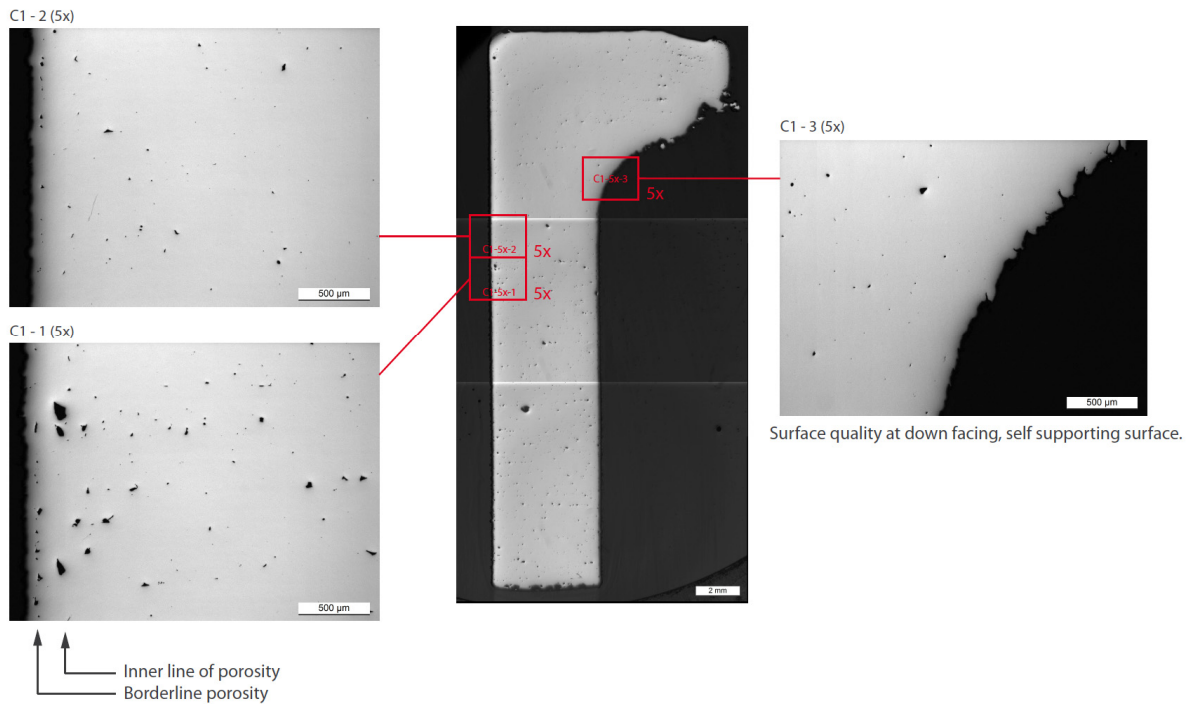


Figure 108. The cross sections C1 of specimen C and the OM figures at 5x magnification, edge locations.

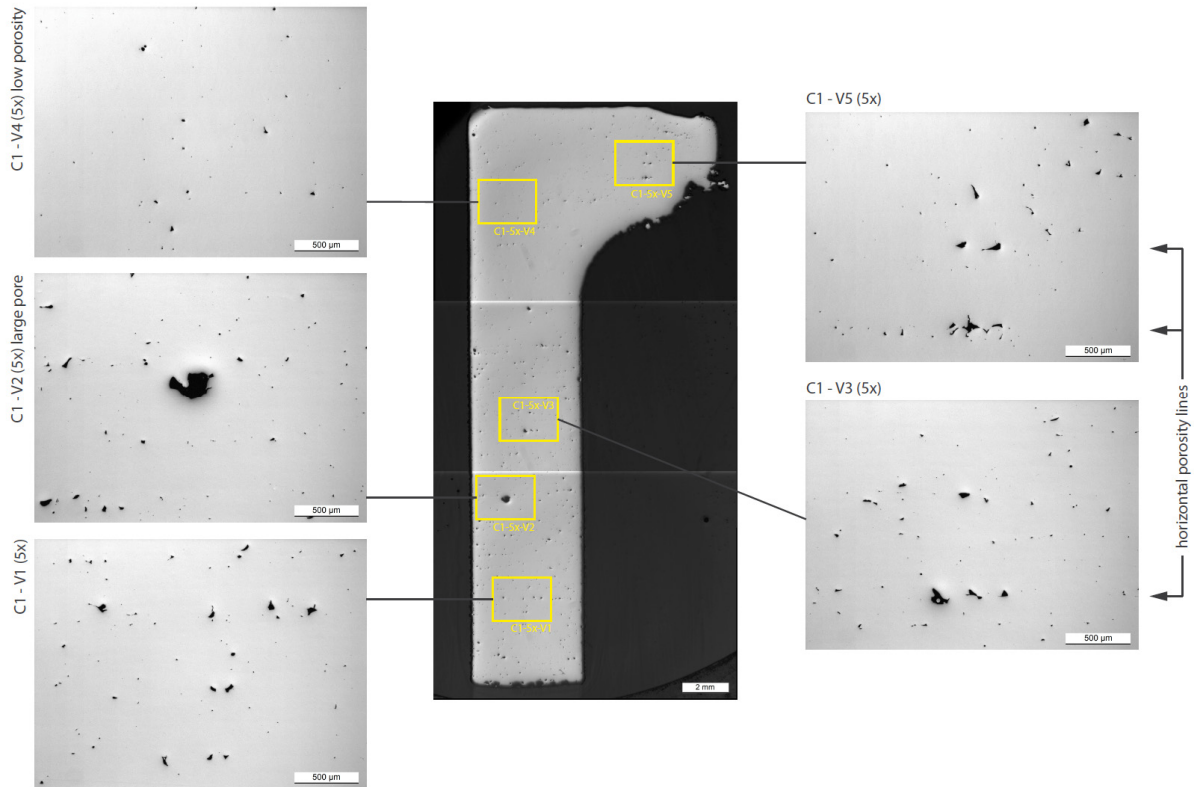


Figure 109. The cross sections C1 of specimen C and the OM figures at 5x magnification, internal locations.

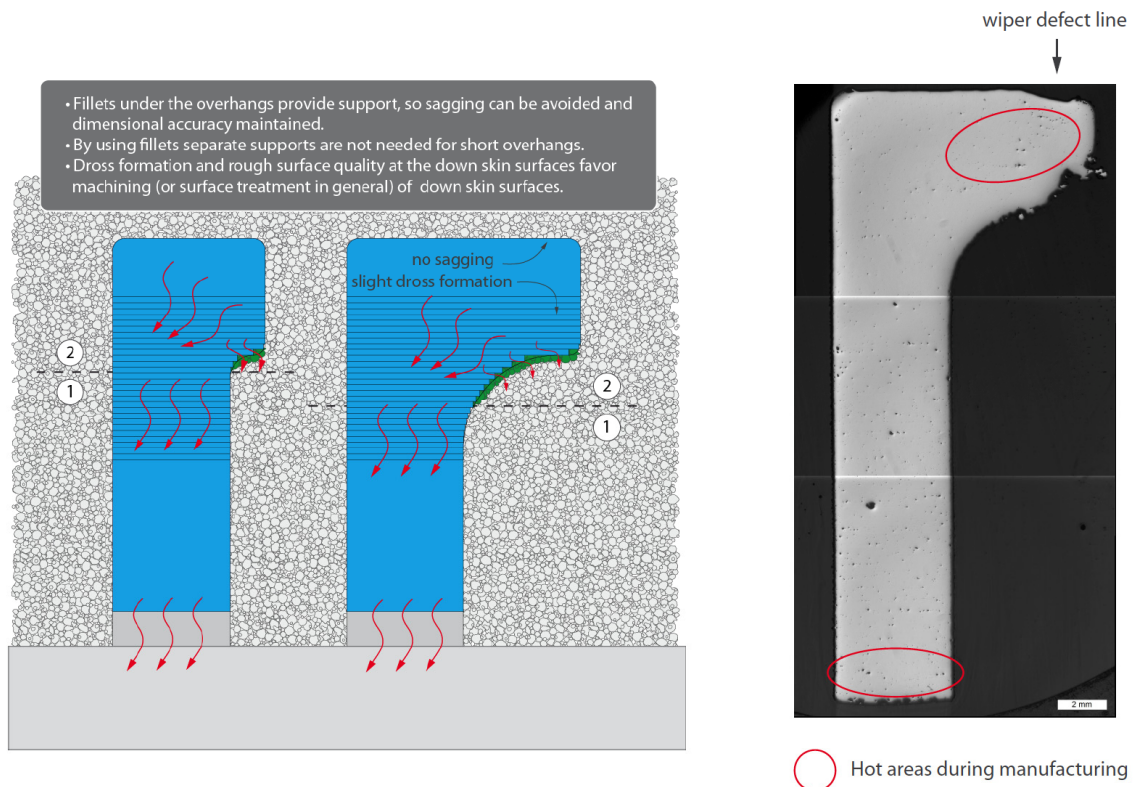


Figure 110. The cross sections C1 of specimen C and the locations with the highest heat build-up. The bottom location takes heat due to the block supports that conduct heat poorly. Solid metal supports are recommended to avoid heat build-up in critical components. This test piece has experienced damage after a wiper defect.

3.16 Etched macro specimens

After studying the porosity, the macro specimens were etched to reveal the boundaries of the weld passes (scanning lines). The remarks are commented on the figures. The local curving of the layers can be seen in the microscope figures of the etched macro specimens. However, no sagging was indicated by the study.

Remarks on the etched specimen A2 are presented in Figure 111. The stair step effect, borderline porosity and dross can be seen in the microscope figures of the etched macro specimen.

Macro specimen A2, etched, microscopy by Seija Kivi, VTT

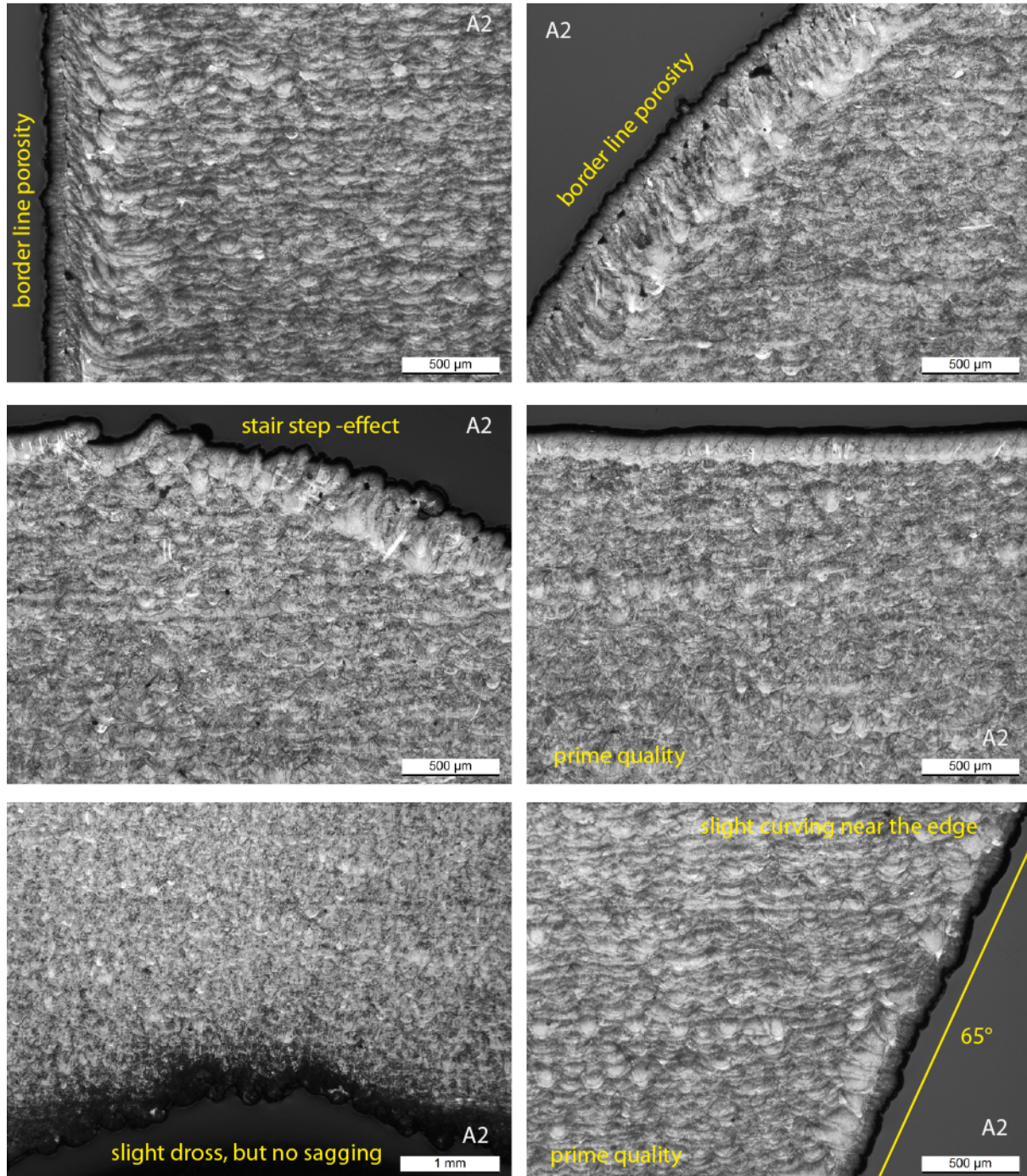


Figure 111. Remarks on the etched specimen A2.

Macro specimen A2, etched, microscopy by Seija Kivi, VTT

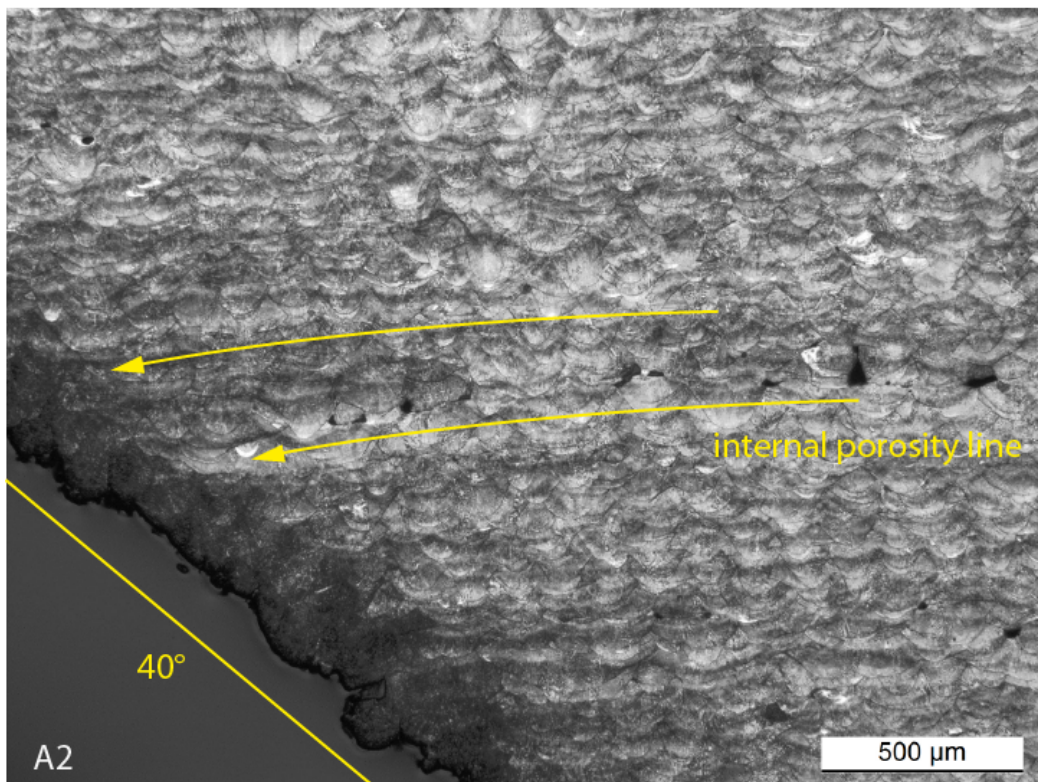
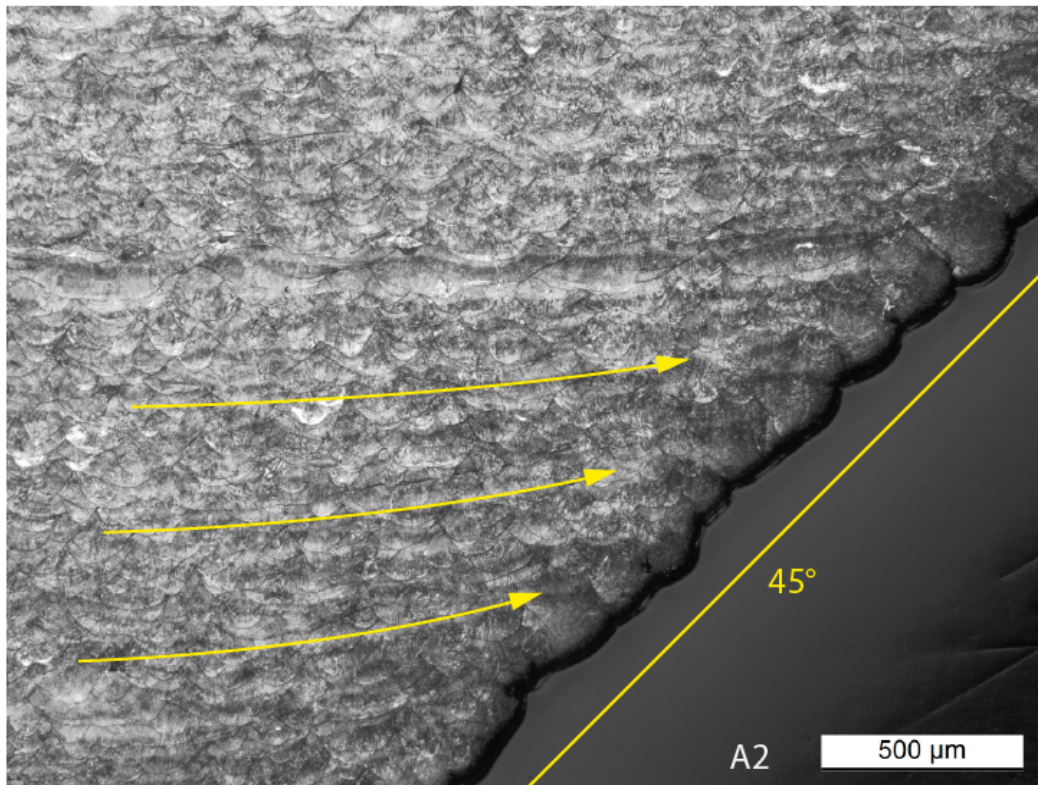


Figure 112. Remarks on the local distortions, etched specimen A2.

Local distortion of the layers due to the inclined geometry and lines of internal lack of overlap type defects are seen in the microscope figures in Figure 112. Both upwards and downwards curving are seen at the layers.

Macro specimen B1, etched, microscopy by Seija Kivi, VTT

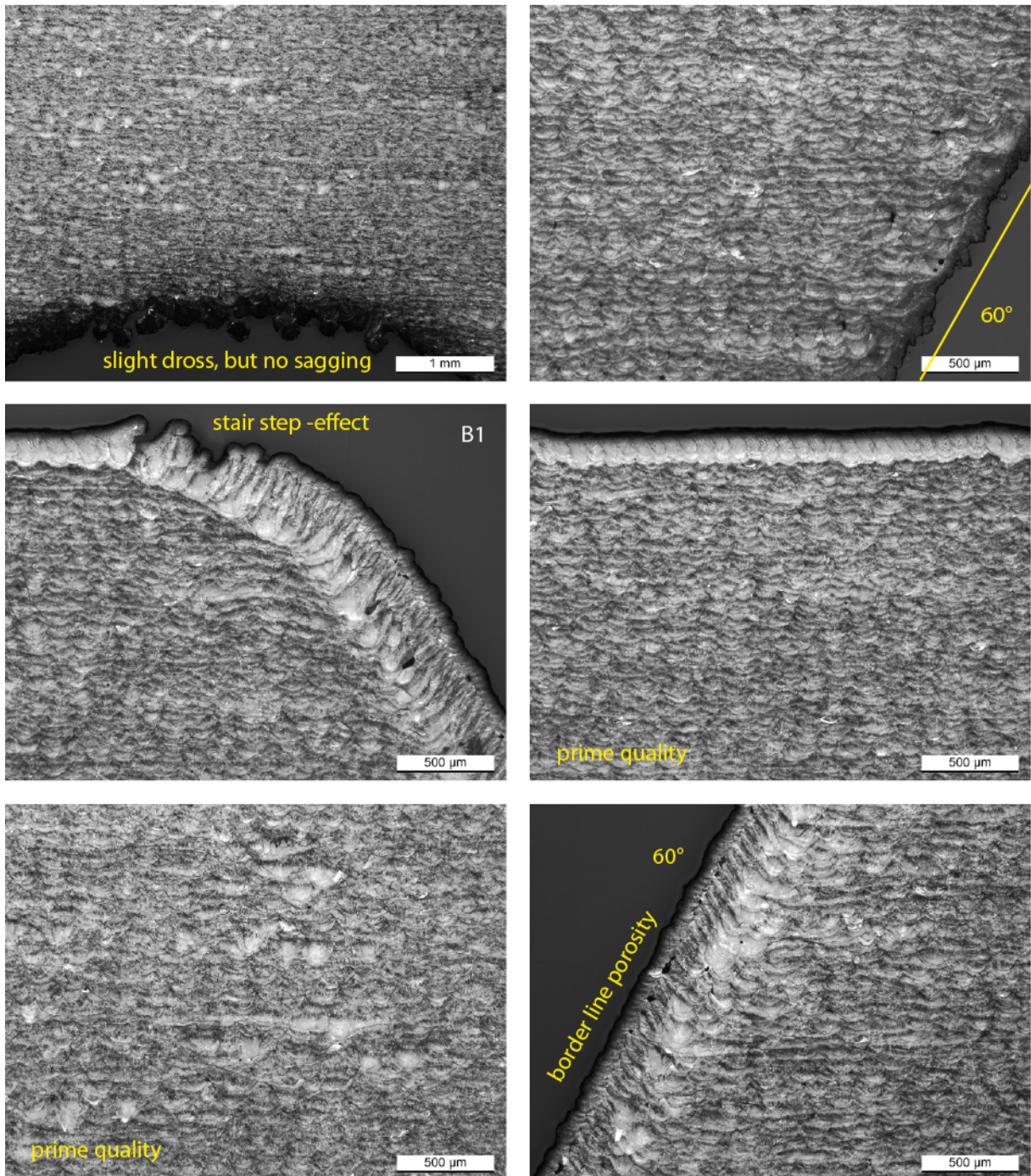


Figure 113. Remarks on the etched specimen B1.

Macro specimen C1, etched, microscopy by Seija Kivi, VTT

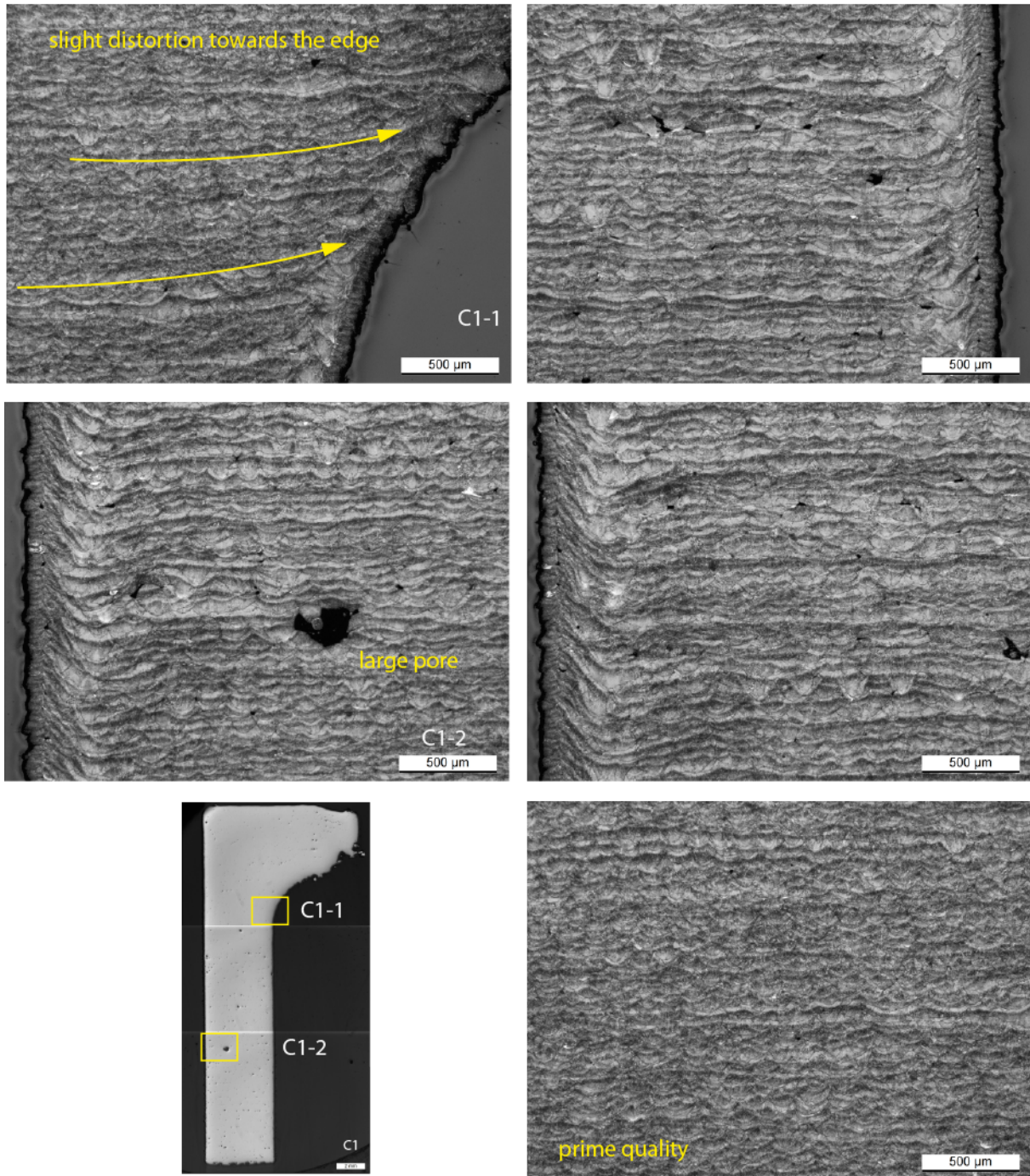


Figure 114. Remarks on the local distortions and defects, etched specimen B1.

The large pore in Figure 114 is considered to be caused by malfunction in the powder feed. The size of the pore is of several layer thicknesses. Local layer distortions are seen again at the locations near inclined edges of the part.

Macro specimen C1, etched, microscopy by Seija Kivi, VTT

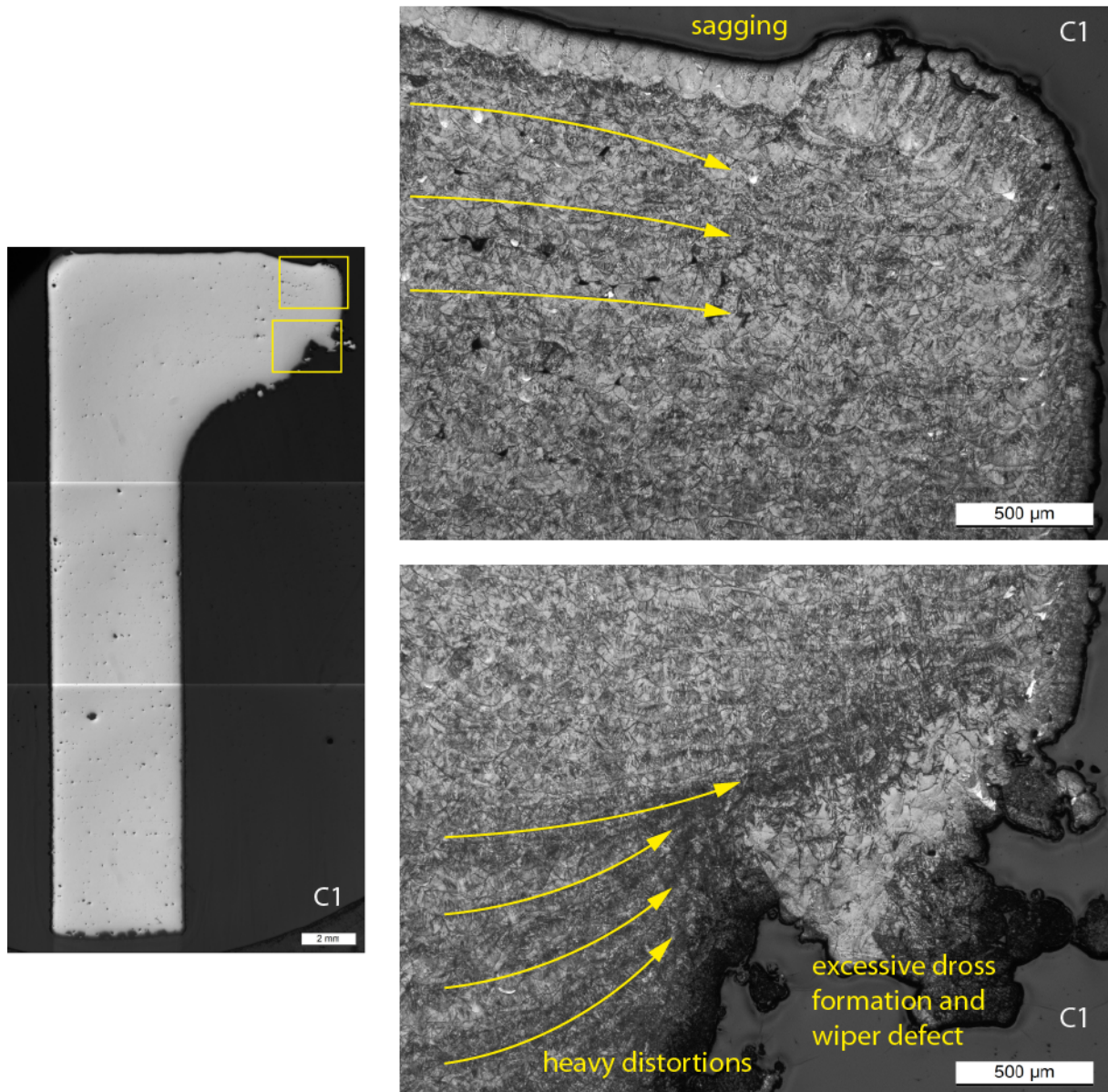


Figure 115. Remarks on the local distortions, etched specimen C1 at the wiper defect location.

Excessive local distortions are seen at the overhang section of the test piece C1. The heavy local distortions are interpreted to have been accumulated layer by layer and lead to wiper defect. The wiper defect has then caused the main damage on the part. This is considered the main cause of printing failures leading to interrupt of the printing process in SLM. Unsupported overhangs with excessive length and poor heat control are recommended to be avoided in design to avoid local distortions and printing failures.

3.17 Lack of fusion type defects

The lack of fusion type defects and occasional clusters of porosity are explained by a brief CAD exercise. The SLM printing proceeds by changing the orientation of the hatching between layers at 67° increments. The incremental change of hatching orientation is illustrated in the following figure.

Stripe hatching at circular section, three consecutive layers at incremental hatch rotations 67°-67°-67°

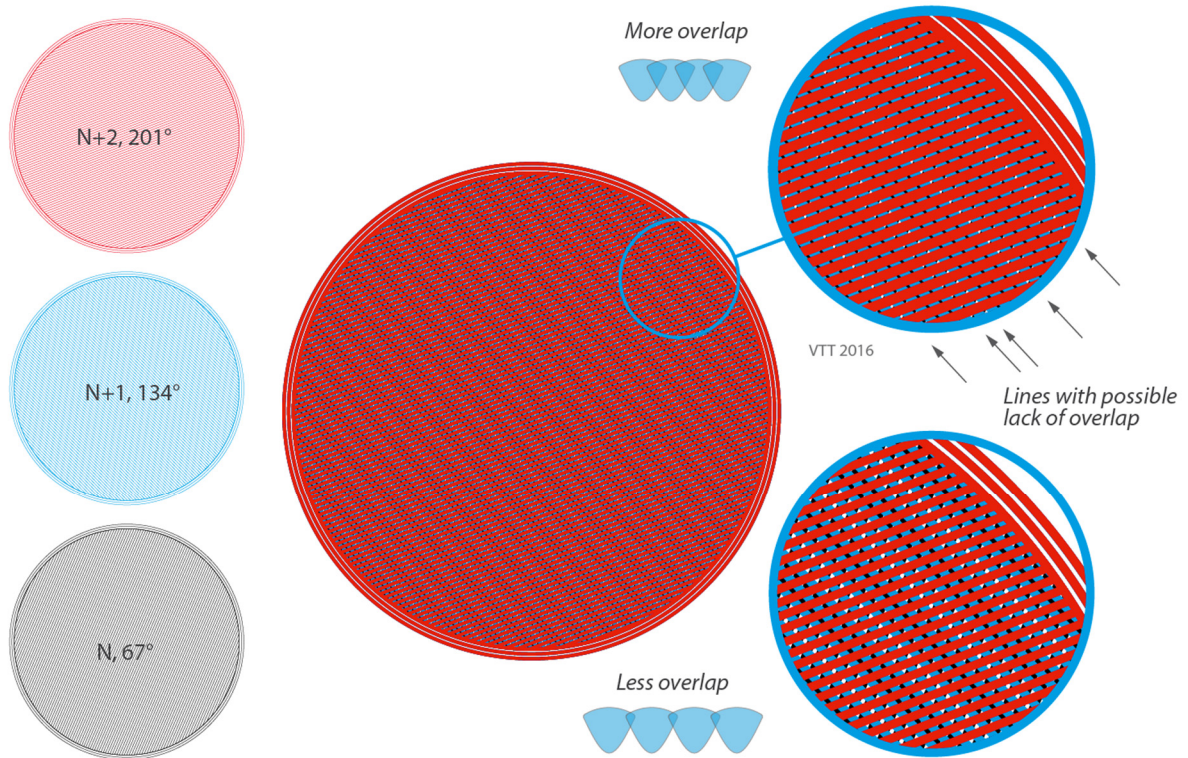


Figure 116. Brief CAD exercise of hatching of three consecutive layer rotated from layer to layer and variation of the overlap between the individual passes. The lack of overlap can be seen to occur as a repeating pattern.

The hatching was then studied in 3D CAD by modelling three layers. The geometry is illustrated in the next figure. The 3D CAD study shows the formation of internal porosity or lack of fusion lines and clusters.

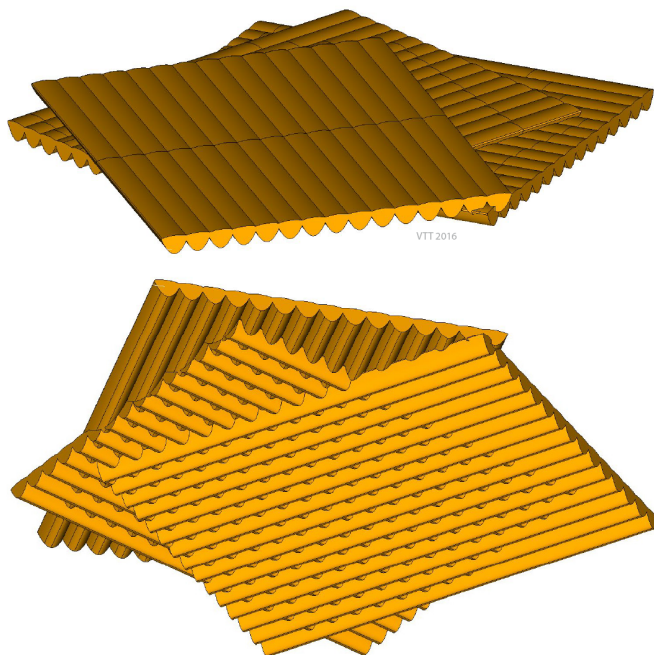


Figure 117. Three layers of weld passes at incremental rotation of 67 degrees between layers.

The cut views of the solid geometry shown in the following figures reveal the defect patterns.

Three layers in CAD (67°-67°-67°), cut views

- The repeating patterns indicating lack of overlap revealed in 2D figures shows in the 3D model also.
- These void patterns are the likely cause of the internal porosity lines in the studied SLM samples.
- Cut views along the hatch and porosity line directions presented as examples below.

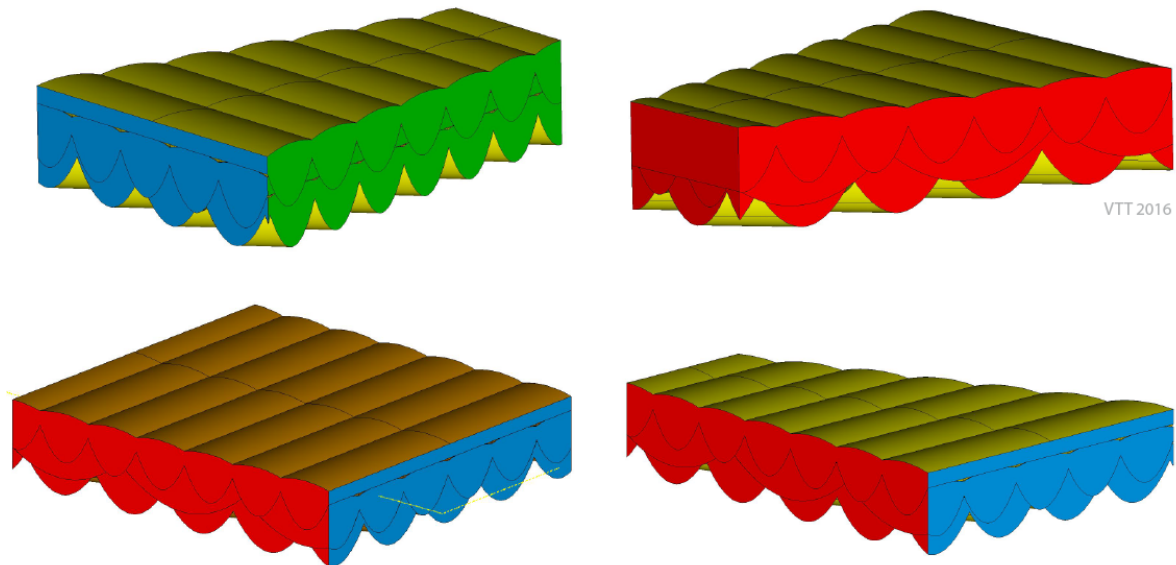


Figure 118. The cut views of the 3D model of hatching reveals the typical patterns of the melt lines.

Three layers in CAD (67°-67°-67°), cut view along the porosity lines

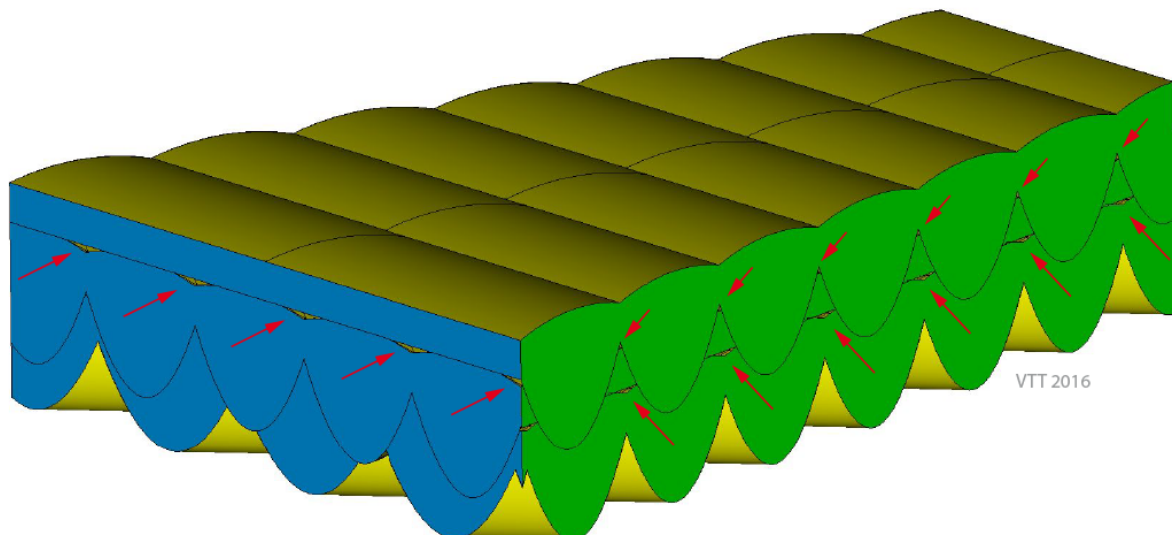


Figure 119. The lack of fusion type defects are seen in the geometry after joining the layers. This type of patterns of holes can be seen in the macro specimens as clustered porosity inside the material (different from the borderline porosity).

The overlap type defect is a geometrical effect caused by the hatching. The extent of the lack of overlap can be controlled by the overlap setting in the process parameters.

Increasing overlap between passes improves the soundness of the fabricated material.

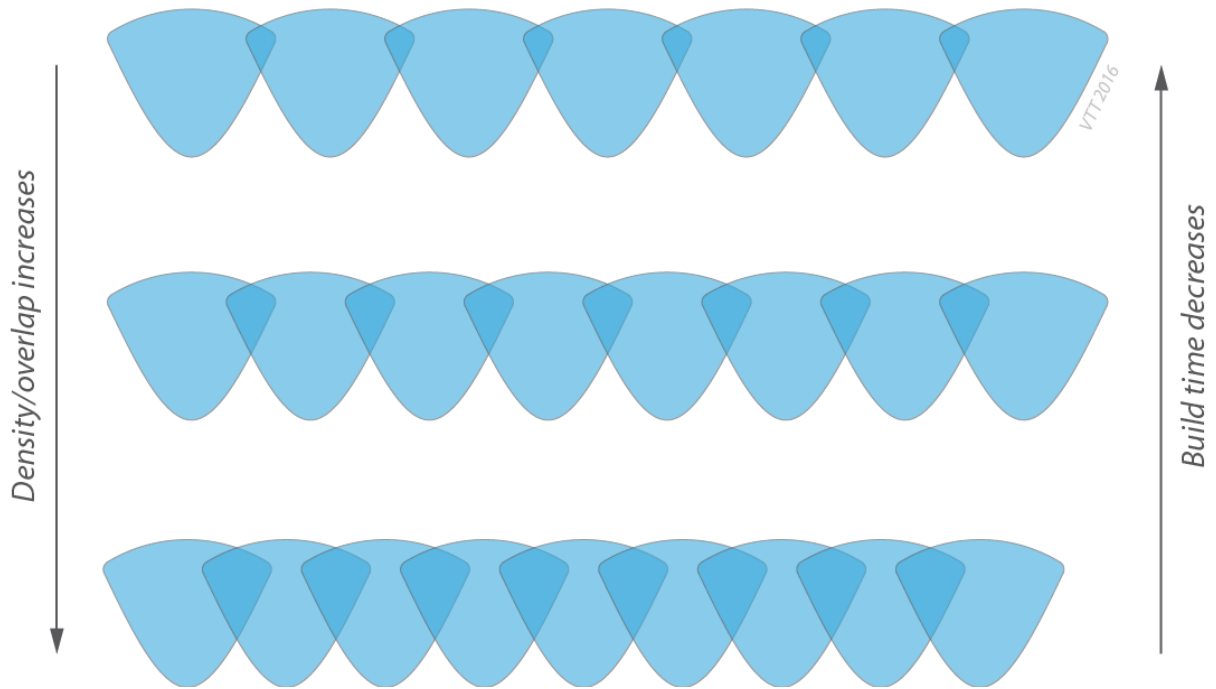


Figure 120. Illustration of the effect of overlap of weld passes on the density of the printed material. Material density (soundness) can be increased by using more overlap, but this increases the build time.

3.18 Study of required amount of machining allowances

The guide values for machining allowances for the SLM process defined in the VDI guideline [1] are consistent with the findings in this work. The key findings of the test prints related to the required machining allowances to meet sound material and to account for thermal distortions are discussed in the following with example figures and schematic illustration presented in the following figures.

Microscope figures by Seija Kivi, VTT

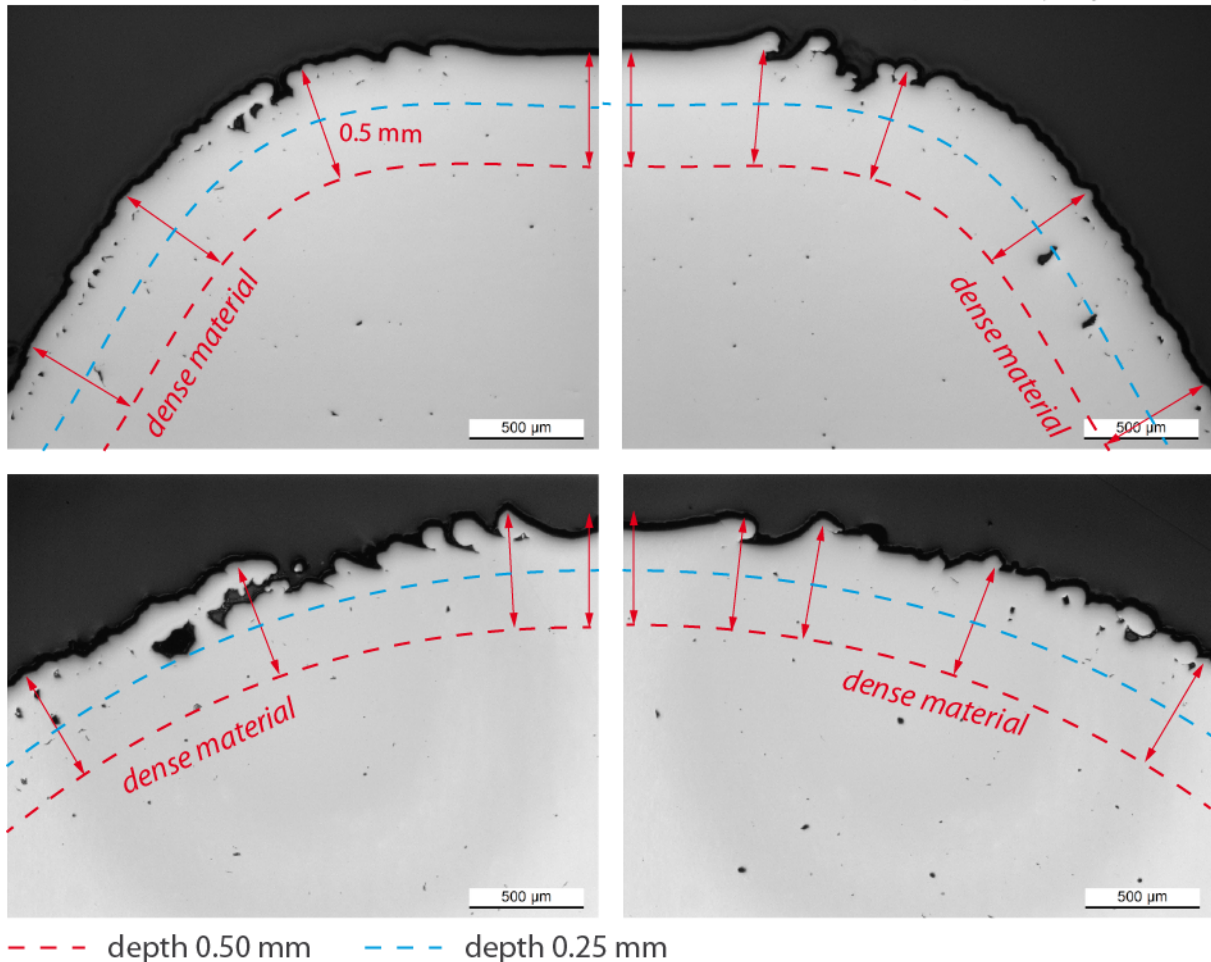


Figure 121. The fillet locations of a H13 test print. Dense material is met after removing 0.5 mm material of the surface.

The effect of the layerity on the surface roughness at smooth transition locations can be seen in the optical microscope figures in Figure 121. The 0.25 mm machining (or other finishing) depth about just covers the surface irregularities. The 0.5 mm depth would serve as machining allowance to cover the surface irregularities and meet sound material for such locations based on these samples.

The inclined, close to vertical and downskin locations have slightly larger surface irregularities and porosity near the surface. These locations are studied in the next two figures. The geometrical deviations such as ridges due to the transversal shrinkage require additional machining allowances. The ridges due to the transversal shrinkage met in the test prints and the test component in this project were rather small, and about 0.5 ... 1.0 mm additional machining allowance is estimated to cover these local geometrical deviations. The magnitude of the transversal shrinkage depends on the span length between the separately built branches, stiffness of the printed component and thermal conditions during printing. The larger component require therefore most likely bigger machining allowances to cover the local geometrical deviations.

The component level thermal distortions and large functional surfaces may require higher additional machining allowances. The component level thermal distortions are best to be simulated by numerical methods. Larger components have in principle larger thermal distortions.

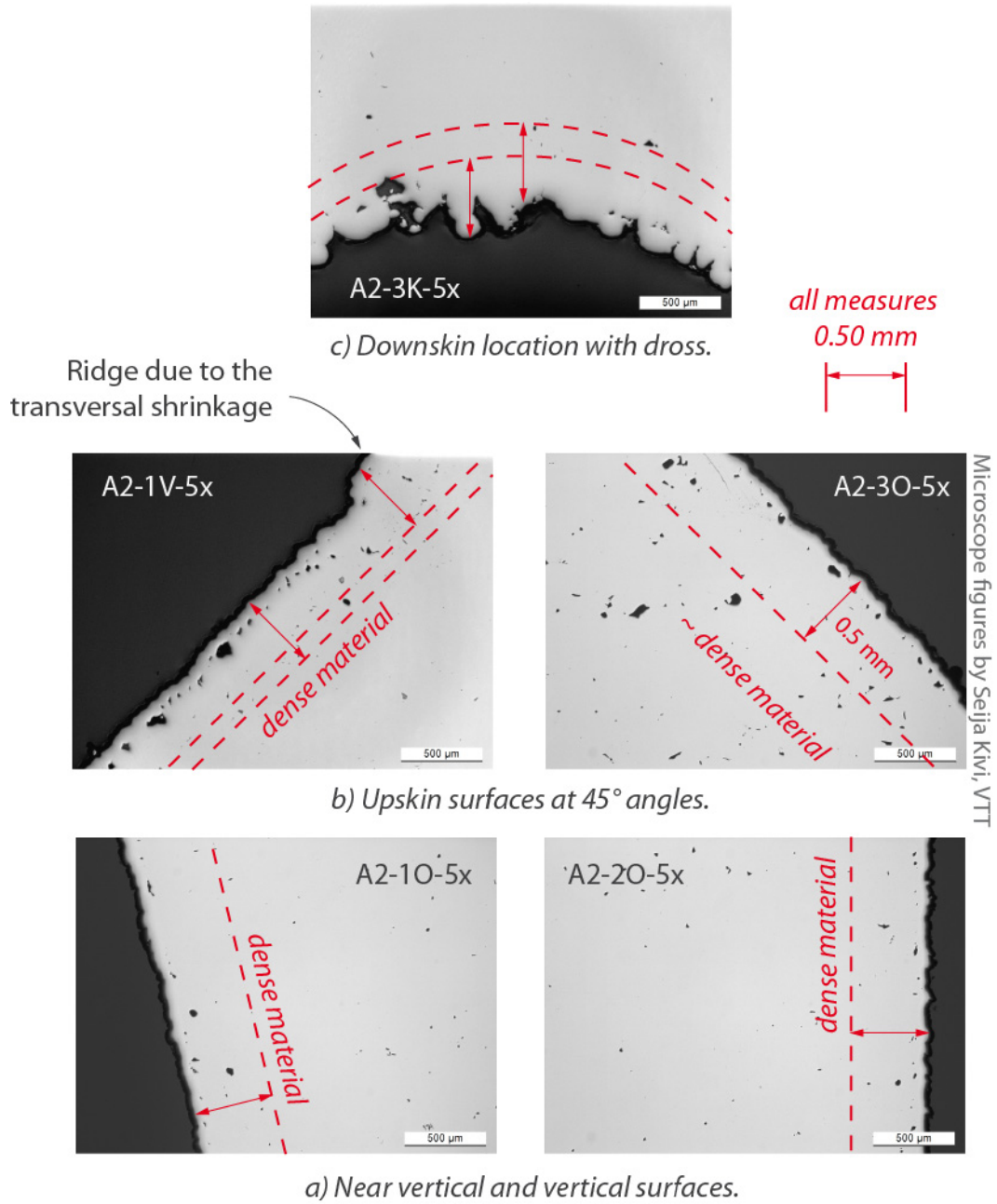
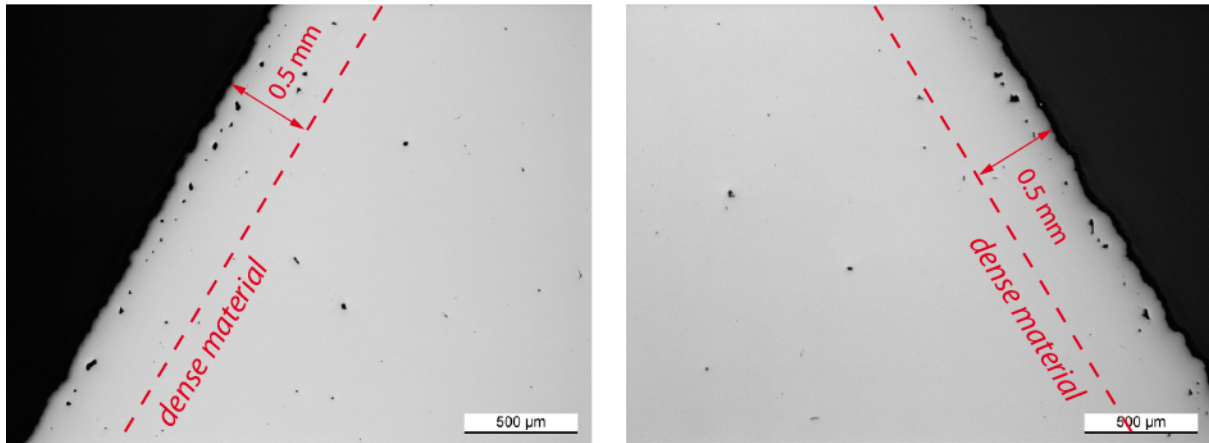
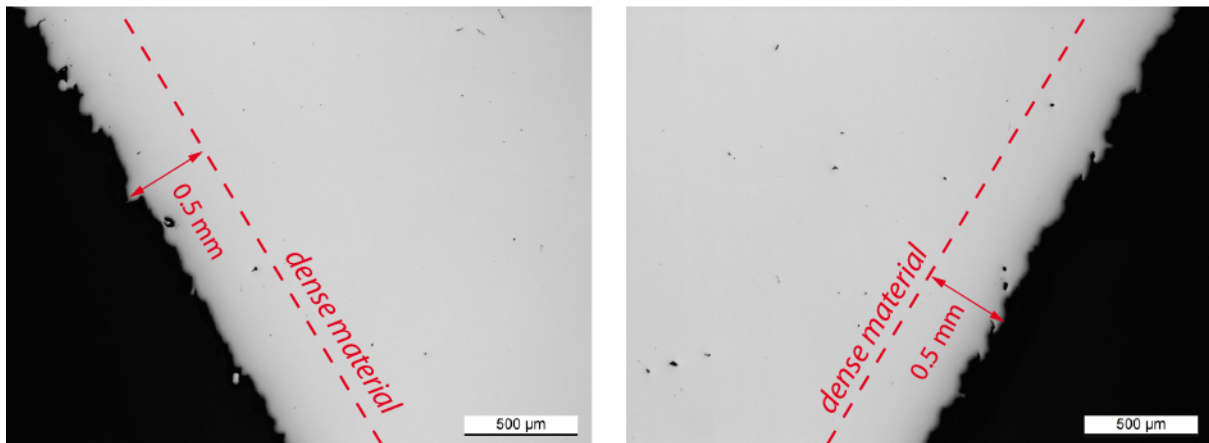


Figure 122. The locations of a H13 test print. Dense material is met after removing 0.5 mm material of the surface at most locations. The distortions and ridges need to be accounted in assessment of the required machining depth. The 1.0 mm machining allowance covers the surface effects and slight distortions of a small component.

Microscope figures by Seija Kivi, VTT



b) Upskin surfaces (specimen B1).



a) Downskin surfaces (specimen B1).

Figure 123. The inclined locations of a H13 test print. Dense material is met after removing 0.5 mm material of the surface.

The assessment of required machining allowance of a component manufactured by SLM are illustrated in the next figure.

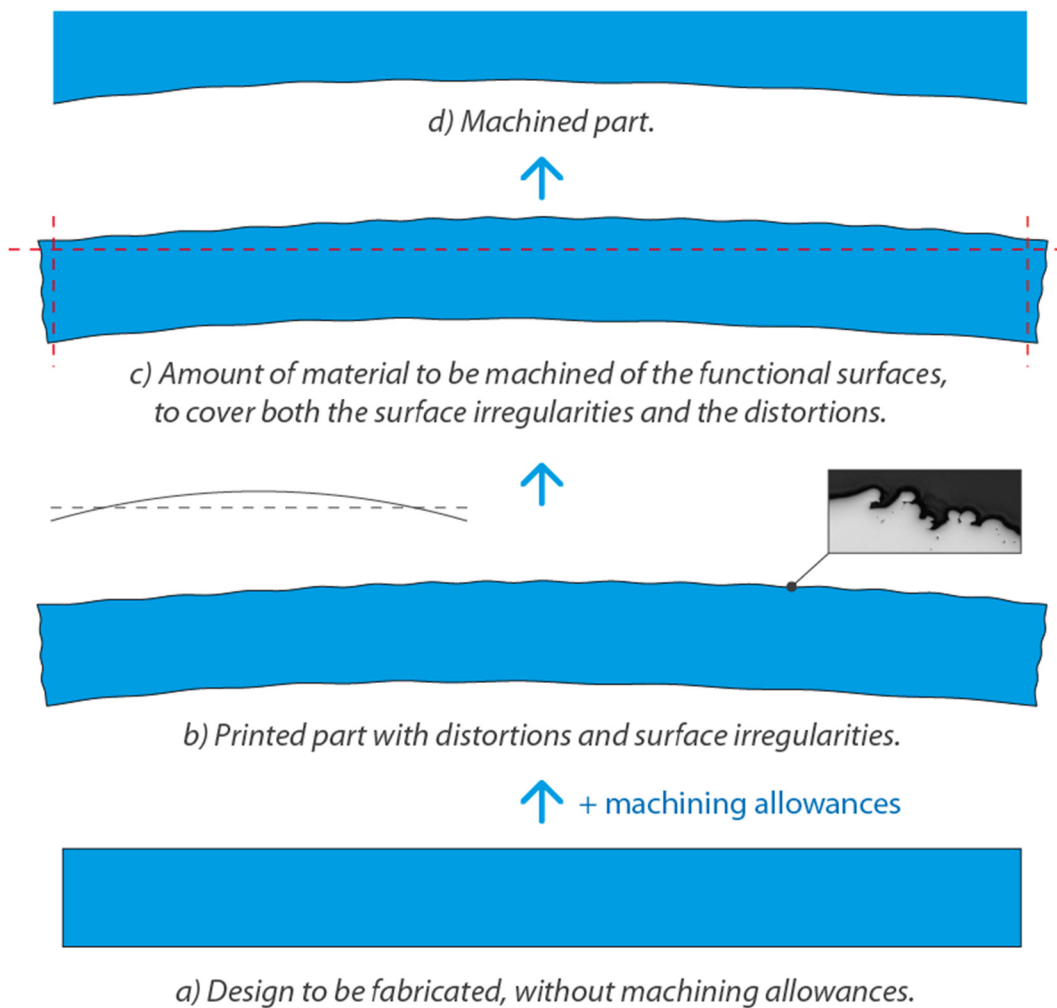


Figure 124. Illustration of the effect of distortions typical to SLM process, that need to be considered in assessment of the suitable machining allowance for a 3D printed component in addition to the surface irregularities and subsurface porosity.

3.19 Study of effect of porosity on fatigue strength of SLM H13 steel

The effect of porosity on fatigue strength of SLM H13 tool steel was studied in brief by image analysis, FEA and the Murakami-Endo approach [11]. The image analysis was done in MATLAB. The results of the study are presented in the following figures and in Appendix F.

The brief study indicates that the porosity typical to SLM is not after all necessarily detrimental to material fatigue strength when the sizes of the pores are kept small and the porosity is evenly distributed. The situation is in principle similar to inclusions and small defects in traditionally manufactured materials. Quality control and material testing are required for safe and durable products for SLM as in all manufacturing.

The brief study of the macro specimens by the Murakami-Endo method and image analysis show that the majority of the pores have little impact on the fatigue limit estimate. The majority of the fatigue limit estimates are above the Murakami-Endo upper limit estimate $1.6 \times H_v$. Only the larger pores lead to fatigue limit estimates below the Murakami-Endo upper limit estimate $1.6 \times H_v$. A more detailed study with more comprehensive sampling and including the effect of residual stresses in the assessment of fatigue strength need naturally to be done for forming understanding of SLM materials, with validation by fatigue tests.

An example of the Murakami-Endo fatigue limit estimate for the H13 tool steel test print at typical porosity is presented in Figure 125 and at larger manufacturing defects in Figure 126.

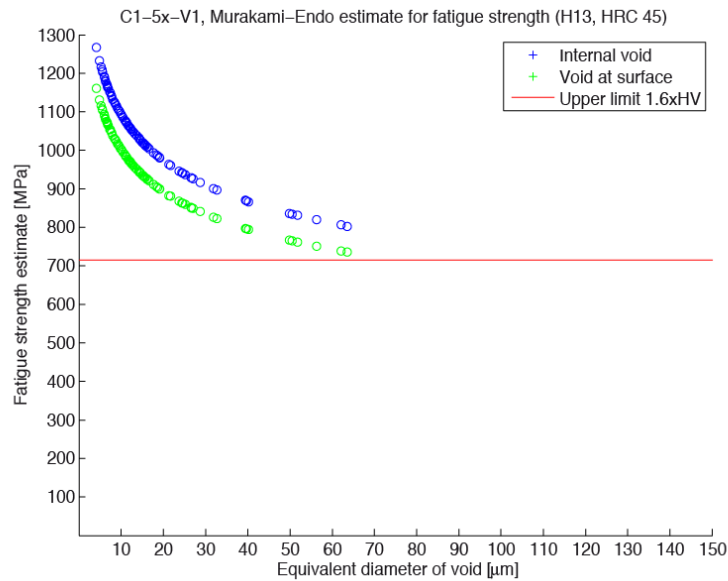
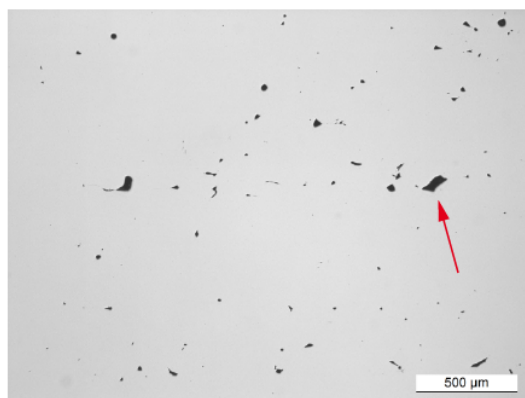


Figure 125. Example of the Murakami-Endo fatigue limit estimate for the H13 tool steel test print specimen C1, typical porosity, location V1 at magnification 5x.

Macro specimen A2, 5x magnification, classification of voids



A2-V20-5x

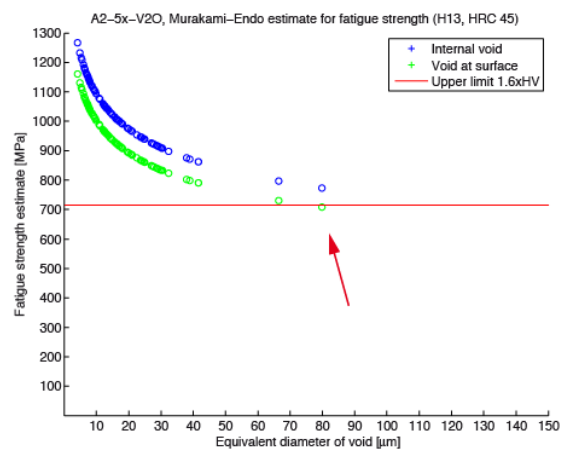
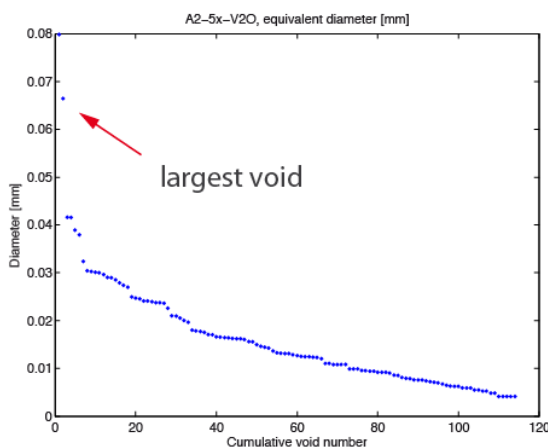
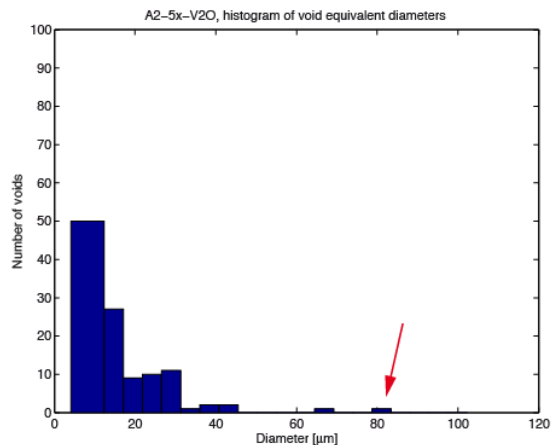


Figure 126. Example optical microscope image of a larger size internal defect at 5x magnification of H13 tool steel test piece, macro specimen A2, equivalent diameters of defects vs cumulative number of defects, histogram of defect sizes and resulting Murakami-Endo fatigue limit estimates (at stress ratio $R = -1$).

4. Test print of a mock-up component design

After evaluating the test prints and learning of the printability of the individual design features, the design features were applied to component design and the component test print was evaluated.

4.1 Basis of design of a structural test component

Dimensional and geometrical accuracy are important for mechanical engineering components. A test component was designed for assessment of various dimensional and geometrical measures commonly used in mechanical engineering. The various geometrical features studied in the test print series were included in the test component design, to see how the elementary features print as part of a component.

As the chamber size limits the maximum dimensions of the component, the four flanges were set at different orientations within the available printer space. The flanges are functional, machined surfaces, and determining the amount of machining allowances required for a component made by SLM was one objective in the component design and test print exercise.

The design intent was to prepare an example geometry of a load bearing machine element or structural component, with the following design principles and objectives:

- Including the features studied earlier by series of test prints into the test component.
- Design features suitable for SLM are used, such as self-supporting elliptic cross section for the horizontal pipes, additional ribs and local detailed design to modify overhang members to be self-supporting.
- Features such as thick sections and overhangs, that are challenging to manufacture by SLM due to the thermal distortions, are included in the test component.
- Smooth transitions are used at corners for good fatigue strength.
- Only functional surfaces are machined, and the smooth transitions are left at as-built surface as far as possible.
- Bolt holes are reamed utilising pre-fabricated holes, as suggested by Leevi Salonen from KTS-mekano Oy.
- Manual work needed for removal of supports is minimised.
- The SLM process is prone to thermal distortions, which needs to be considered in the machining allowances.
- The build chamber size of SLM125 HL limits the main dimensions of the component to 125 x 125 x 125 mm (nominal build space).

The component is designed with rather thick flanges and walls to seek a bit problems with the SLM process, as the process is prone to distortions. The basic design follows a common casting design but with AM design rules applied throughout the design work. The tube like basic structure is used to connect the flanges together and bear the structural loads. A topology optimized version was planned, but as the topology optimization provides only rather poor control of the geometry the traditional CAD was used in design. The tube like structure is symmetric and the junctions could be done with smooth transitions. Fluid flow is not considered in the design, and the tubes are just intended to represent a mock-up structure.

The thermal stresses are expected due to the rather high wall thickness. The thermal distortions are part of the SLM process and are therefore included in the study.

Two variants of the component were designed. First one is designed as symmetric, for moderate thermal distortions. The second part is designed as unsymmetric with a hole and a stiff bracket at opposite sides, for larger extent of thermal distortions. The hole provides a

locally open profile and the bracket provides local stiffness and a local heat concentration during the printing.

The first sketch follows the example design presented in EN-ISO 8062-3. The first sketch is presented in the following figure.

The dimensional and geometrical accuracy of the component is measured by MIKES after the printing and then after machining. The machining and wire cutting is done by KTS-mekano Oy. The dimensional and geometrical tolerances are then compared to EN-ISO 8062-3 accuracy classes to estimate how the SLM process compares to the casting process.

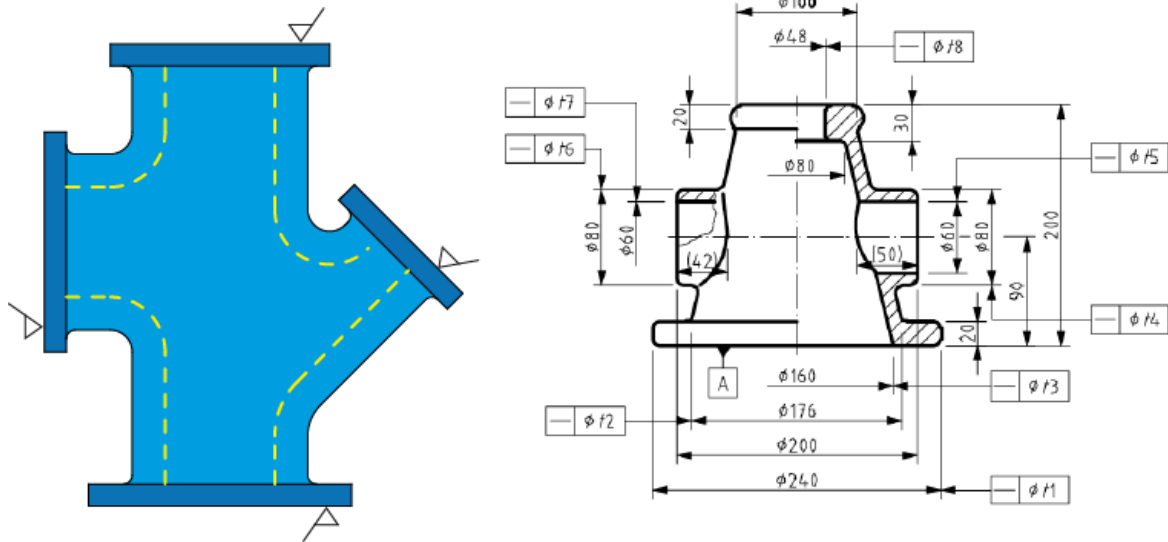


Figure 127. The first sketch of the SLM geometrical accuracy test component follows the example design presented in EN-ISO 8062-3.

The manufacturing accuracy tolerance classes defined for casting in the ISO 8062 standard are used in the assessment to the 3D-printed component geometrical accuracy. An example geometry described in ISO 8062 standard is used as basis of studying the geometrical tolerances of the 3D –printed test component.

- Standard SFS EN ISO 8062-3
Geometrical product specifications (GPS). Dimensional and geometrical tolerances for moulded parts. Part 3: General dimensional and geometrical tolerances and machining allowances for castings
- The geometrical tolerances covered by this part of ISO 8062 are:
 - tolerances for straightness, flatness, roundness,
 - parallelism, perpendicularity, symmetry, and coaxiality.
- ISO 8062-3 example structure (right) could perhaps *be used as test geometry for AM by scaling to fit for VTT SLM125HL printer?*
- ISO 8062-3 defines tolerance grades related to nominal dimensions (below)
 - *tolerance grades could be defined for AM products in a similar way?*

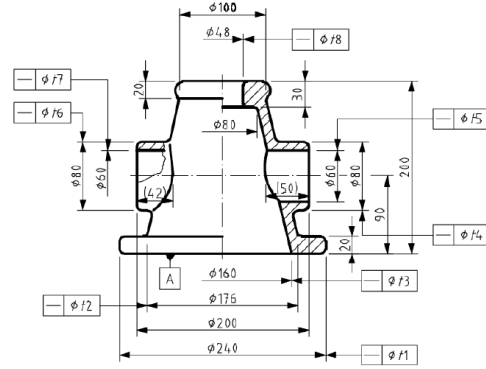


Figure E.2 General straightness tolerances

suited for AM test series (*)

Table 2 Linear dimensional casting tolerances (DCT)

Nominal dimensions related to the moulded part	Linear dimensional tolerance for dimensional casting tolerance grade (DCTG) ^a																Dimensions in millimetres														
	1	2	3	4	5	6	7	8	9	10	11	12	13	14	15	16 ^b	1	2	3	4	5	6	7	8	9	10	11	12	13	14	15
≤ 10	0.09	0.13	0.18	0.26	0.36	0.52	0.74	1	1.5	2	2.8	4.2	—	—	—	—	—	—	—	—	—	—	—	—	—	—	—	—	—	—	—
> 10 ≤ 16	0.1	0.14	0.2	0.28	0.38	0.54	0.78	1.1	1.6	2.2	3	4.4	—	—	—	—	—	—	—	—	—	—	—	—	—	—	—	—	—	—	—
> 16 ≤ 25	0.11	0.15	0.22	0.3	0.42	0.58	0.82	1.2	1.7	2.4	3.2	4.6	6	8	10	12	—	—	—	—	—	—	—	—	—	—	—	—	—	—	—
> 25 ≤ 40	0.12	0.17	0.24	0.32	0.46	0.64	0.9	1.3	1.8	2.6	3.6	5	7	9	11	14	—	—	—	—	—	—	—	—	—	—	—	—	—	—	—
> 40 ≤ 63	0.13	0.18	0.26	0.36	0.5	0.7	1	1.4	2	2.8	4	5.6	8	10	12	16	—	—	—	—	—	—	—	—	—	—	—	—	—	—	—
> 63 ≤ 100	0.14	0.2	0.28	0.4	0.56	0.78	1.1	1.6	2.2	3.2	4.4	6	9	11	14	18	—	—	—	—	—	—	—	—	—	—	—	—	—	—	—
> 100 ≤ 160	0.15	0.22	0.3	0.44	0.62	0.88	1.2	1.8	2.5	3.6	5	7	10	12	16	20	—	—	—	—	—	—	—	—	—	—	—	—	—	—	—
> 160 ≤ 250	—	—	—	—	—	—	—	—	—	—	—	—	—	—	—	—	—	—	—	—	—	—	—	—	—	—	—	—	—	—	
> 250 ≤ 400	—	—	—	—	—	—	—	—	—	—	—	—	—	—	—	—	—	—	—	—	—	—	—	—	—	—	—	—	—	—	
> 400 ≤ 630	—	—	—	—	—	—	—	—	—	—	—	—	—	—	—	—	—	—	—	—	—	—	—	—	—	—	—	—	—	—	
> 630 ≤ 1 000	—	—	—	—	—	—	—	—	—	—	—	—	—	—	—	—	—	—	—	—	—	—	—	—	—	—	—	—	—	—	
> 1 000 ≤ 1 600	—	—	—	—	—	—	—	—	—	—	—	—	—	—	—	—	—	—	—	—	—	—	—	—	—	—	—	—	—	—	
> 1 600 ≤ 2 500	—	—	—	—	—	—	—	—	—	—	—	—	—	—	—	—	—	—	—	—	—	—	—	—	—	—	—	—	—	—	
> 2 500 ≤ 4 000	—	—	—	—	—	—	—	—	—	—	—	—	—	—	—	—	—	—	—	—	—	—	—	—	—	—	—	—	—	—	
> 4 000 ≤ 6 300	—	—	—	—	—	—	—	—	—	—	—	—	—	—	—	—	—	—	—	—	—	—	—	—	—	—	—	—	—	—	
> 6 300 ≤ 10 000	—	—	—	—	—	—	—	—	—	—	—	—	—	—	—	—	—	—	—	—	—	—	—	—	—	—	—	—	—	—	

^a For wall thicknesses in grades DCTG 1 to DCTG 15, one grade coarser applies (see Clause 7).
^b Grade DCTG 16 exists only for wall thicknesses of castings generally specified to DCTG 15.

*) VTT's SLM125HL 3D-printer max printing size is 125 mm x 125 mm x 125 mm.

Figure 128. The manufacturing accuracy tolerance classes defined for casting in the ISO 8062 standard are used in the assessment to the 3D-printed component geometrical accuracy.

- Standard SFS EN ISO 1302
Geometrical Product Specifications (GPS). Indication of surface texture in technical product documentation
- Standard SFS EN ISO 1101
Geometrical product specifications (GPS). Geometrical tolerancing. Tolerances of form, orientation, location and run-out

Taulukko 1 Geometrysten ominaisuuksien tunnukset

Toleranssit	Ominaisuus	Tunnus	Tolerances	Characteristics	Symbol
Muoto	Suoruus	—	Form	Straightness	—
	Tasomaisuus	□		Flatness	□
	Ympyrämäisyys	○		Roundness	○
	Lieriömäisyys	ℋ		Cylindricity	ℋ
	Tasoviivan muoto	∩		Profile any line	∩
	Pinnan muoto	∪		Profile any surface	∪
Suunta	Yhdensuuntaisuus	//	Orientation	Parallelism	//
	Kohtisuoruus	⊥		Perpendicularity	⊥
	Kulma-asento	∠		Angularity	∠
	Tasoviivan muoto	∩		Profile any line	∩
	Pinnan muoto	∪		Profile any surface	∪
Sijainti	Paikka	⊕	Location	Position	⊕
	Samankeskiisyys (keskipisteille)	⊙		Concentricity (for centre points)	⊙
	Sama-akselisuus (akselille)	⊙		Coaxiality (for axes)	⊙
	Symmetrisyys	≡		Symmetry	≡
	Tasoviivan muoto	∩		Profile any line	∩
	Pinnan muoto	∪		Profile any surface	∪
Heitto	Heitto	↗	Run-out	Circular run-out	↗
	Kokonaisheitto	↗↗		Total run-out	↗↗

Figure 129. Examples of the geometrical tolerances studied in the work (FIN/ENG).

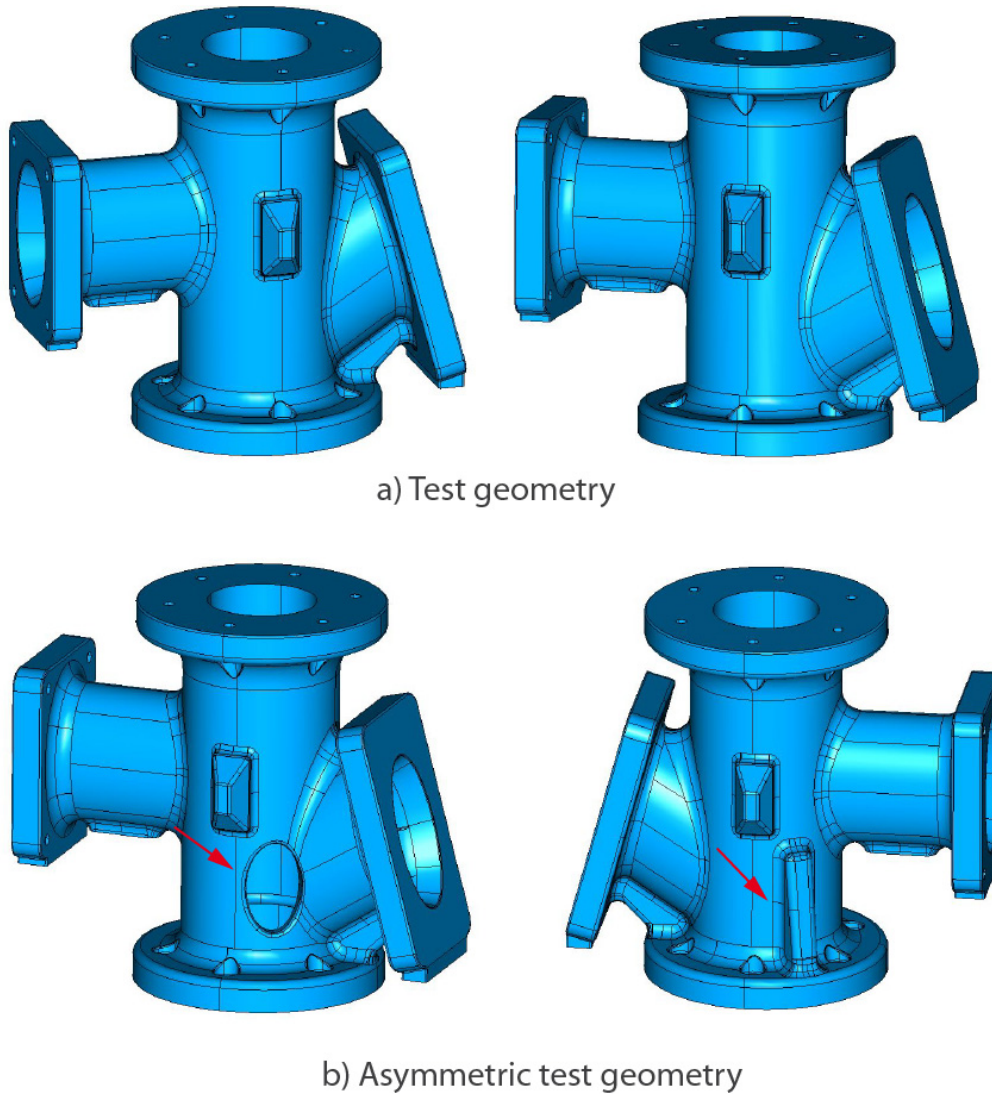


Figure 130. The initial designs of the test component.

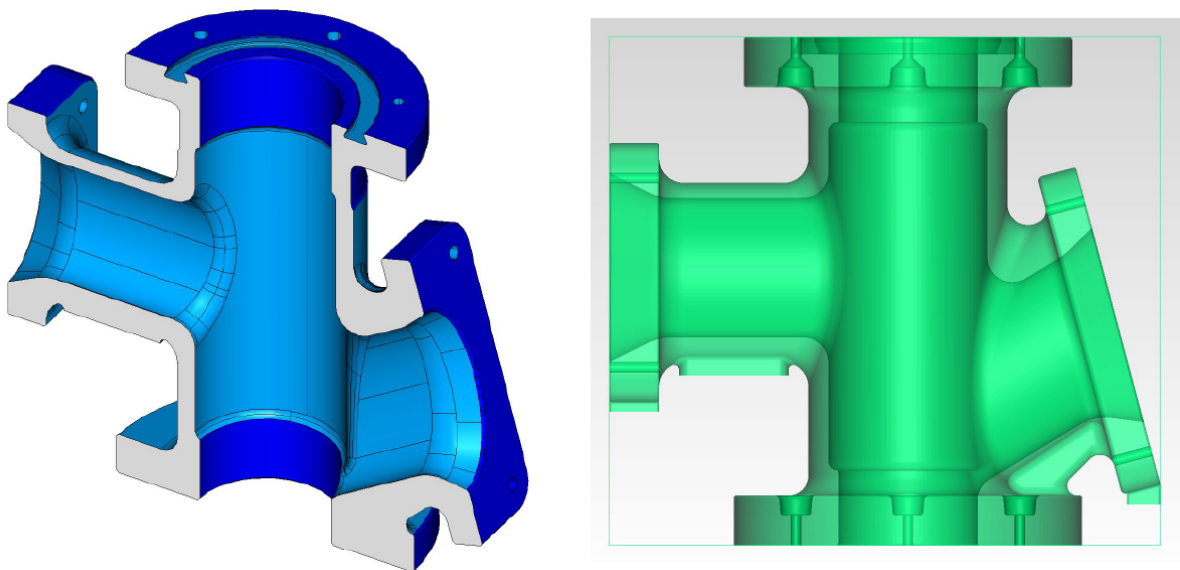
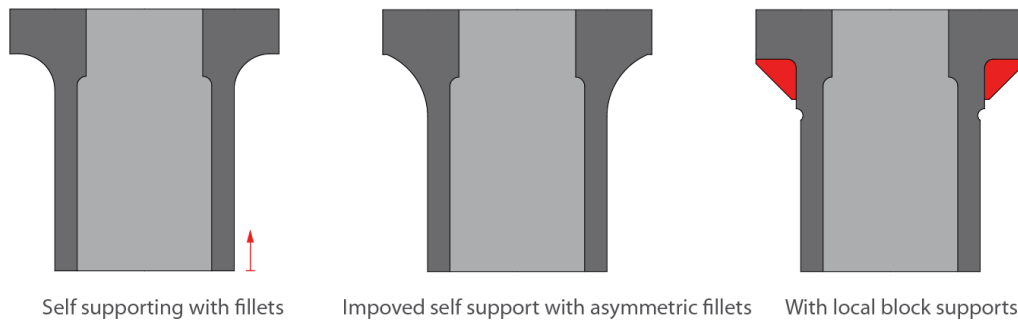


Figure 131. Cut view and transparent view of the test component. Self-supporting elliptic cross sections are used in the horizontal and inclined pipe branches. The vertical pipe is circular. Rather thick sections were intentionally designed to the component, to create heat concentration and include thermal distortion effects into the mock-up test component.

The AM specific design variations are presented in the following figures.

a) at vertical orientation



b) tilted 15° for printing

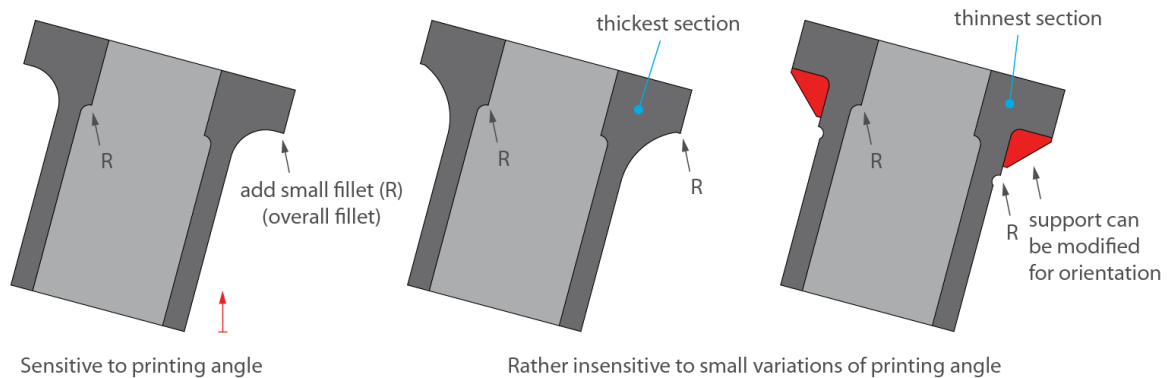


Figure 132. Study of effect of printing orientation on the local support angles and study of effect of support solution on the section thickness.

The printing orientation (tilting the part) has direct effect on the local support angles. The axisymmetric, large structure was considered to be best printed in vertical orientation. And as the objective was to intentionally seek thermal distortions, the vertical printing orientation was decided to be used in the study.

The inclined pipe branch with rather shallow angle would require additional support. An additional rib at 45 degree angle was attached below the inclined pipe branch to avoid the need of additional supports during printing. The solution worked fine in the test prints.

Additional rib to obtain self supporting overhang

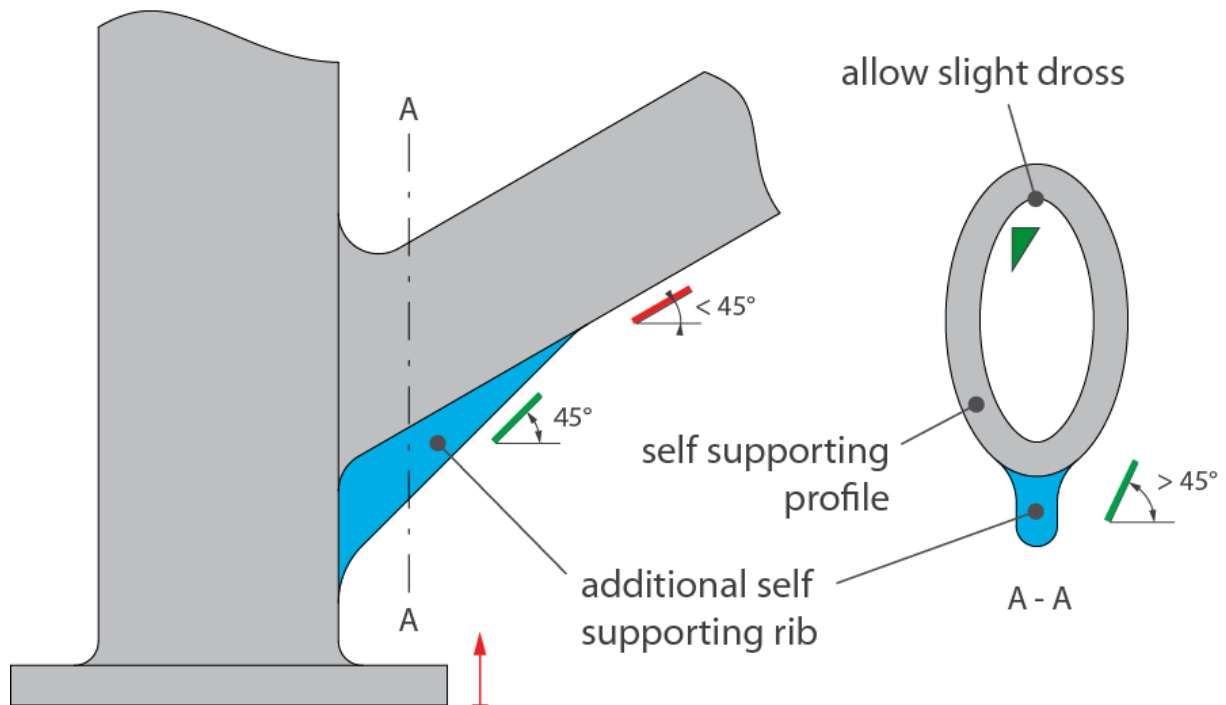


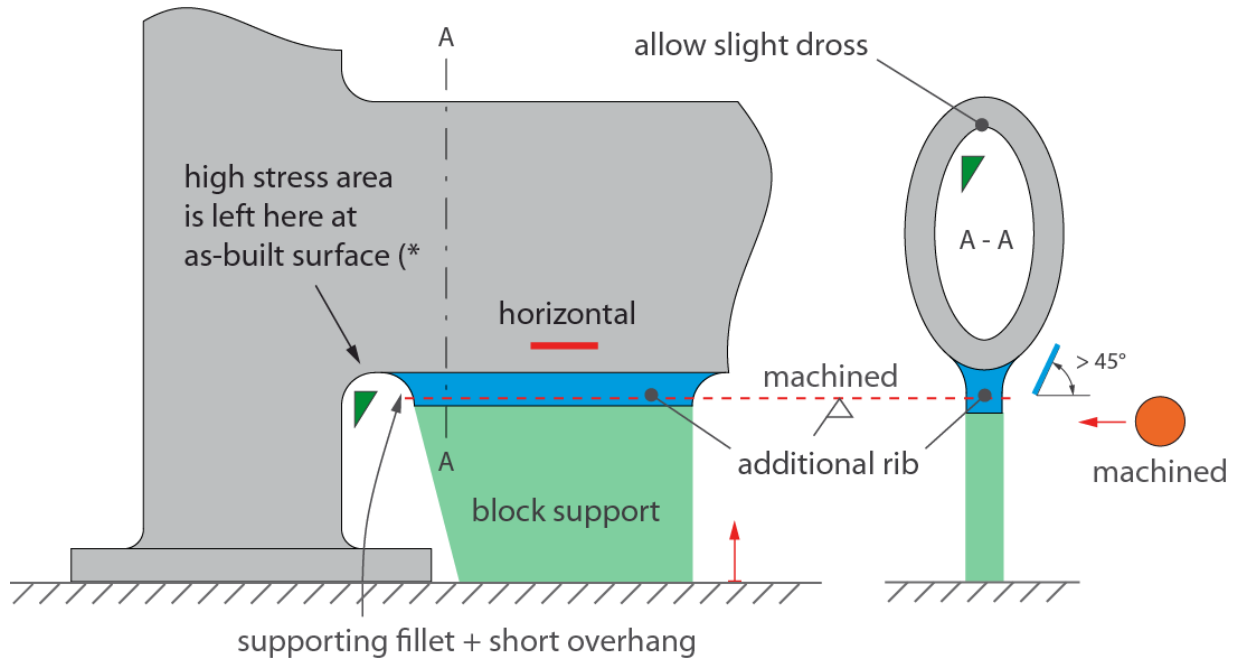
Figure 133. AM design features experimented with the component. An overhang structure can be printed without additional support structures in shallow angle by adding a rib with steeper angle below the overhang. The design is similar to the rib used in traditional watering can to reinforce the pipe of the watering can. This design feature was included in the final design of the test component and it worked fine.

The horizontal pipe requires also supports. In practice the transitions of the pipe branches are stress concentration locations and often fatigue critical. As machining of the fillet locations is difficult, the transitions are typically left to as-cast surface in castings, with large radii to ensure smooth transition and low stress. The same approach can in principle be adapted to AM design.

The horizontal pipe branch is supported by an additional rib below the pipe, but the transitions at the ends are left at smooth fillets. The transitions are therefore at as-built surface, without temporary supports during the printing that would leave rough markings on the surface. The transitions can be ground by manual power tools after printing during removal of supports and cleaning (as done in foundry).

The supports at the horizontal rib can be machined or wire cut, and the remaining rib left to the structure.

Using local flange to avoid need of supports at root fillets, supports can be removed by machining



*) alternative way is to add machining allowance and machine the transition

Figure 134. AM design features experimented in the mock-up test component.

The bolt holes of the top flange were designed as counter sunk bolt holes, to achieve a self-supporting solution at the overhang flange.

Countersunk bolts can be used at down skin surfaces
if embedded bolt heads are required

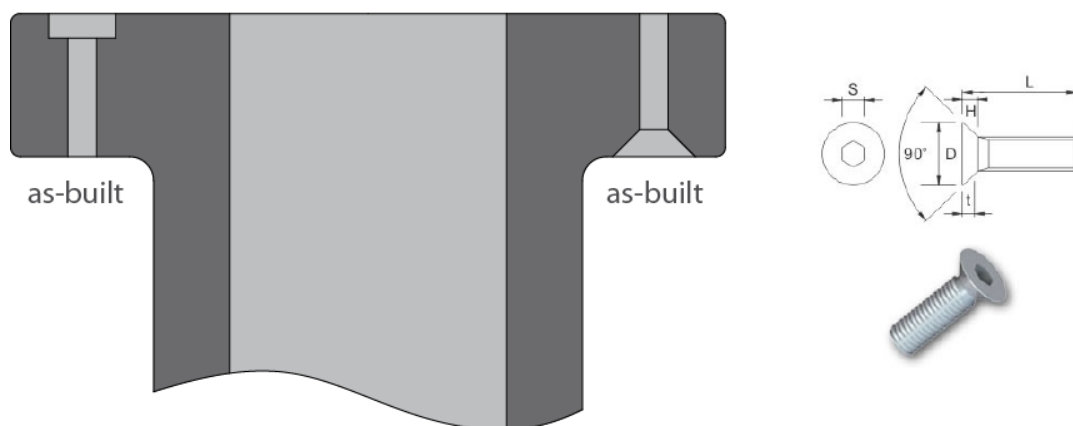
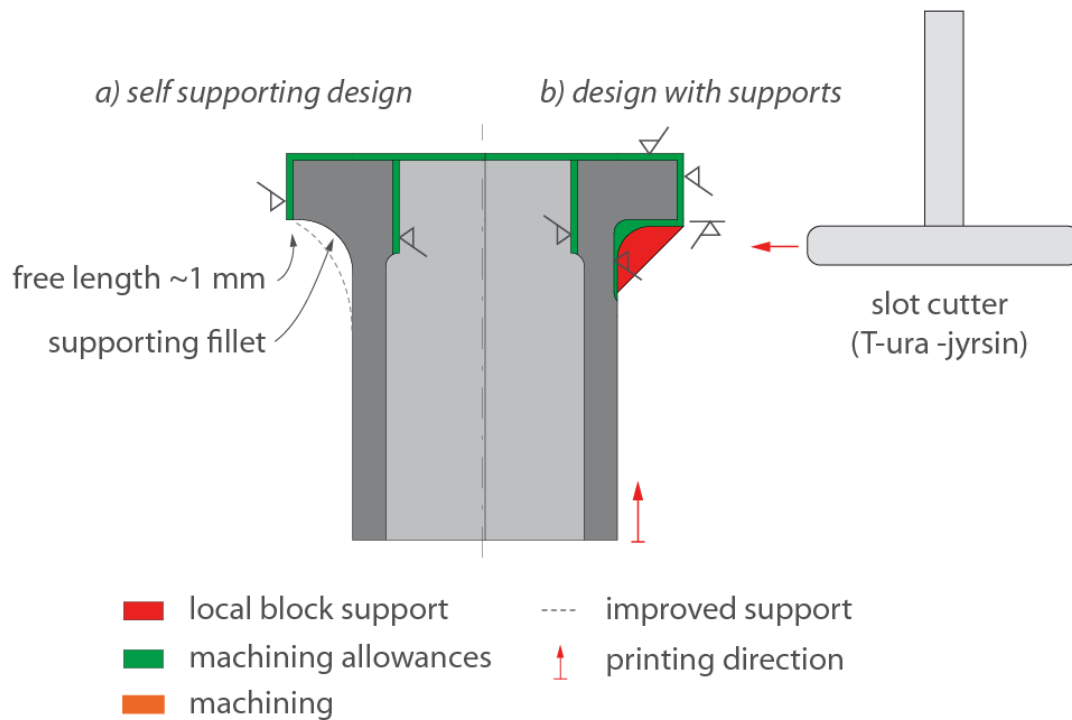


Figure 135. AM design features experimented with the component.

The overhang of the top flange requires support during printing. The typical solution would be to add temporary support between the bottom and top flanges. Instead of this, a local support was discussed with Leevi Salonen from KTS-mekano to be used, in order to achieve shorter printing time, save material, obtain better cooling for the overhang and maintain the surface quality of the top surface of the bottom flange. The local support and the removal of the support by machining is presented in the next figure.

Pipe flange with machining allowances, design variations for overhang support



Local supports / machining according to discussions with Leevi Salonen, KTS-Mekano

Figure 136. Using local support under the top flange overhang, and machining of the flange bottom surface by slot cutter tool.

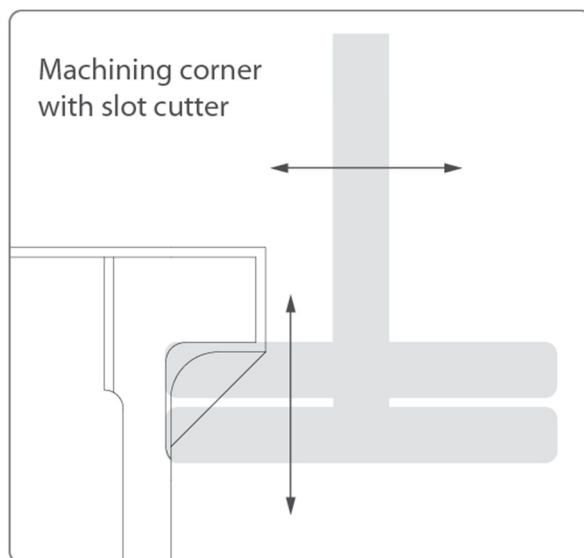


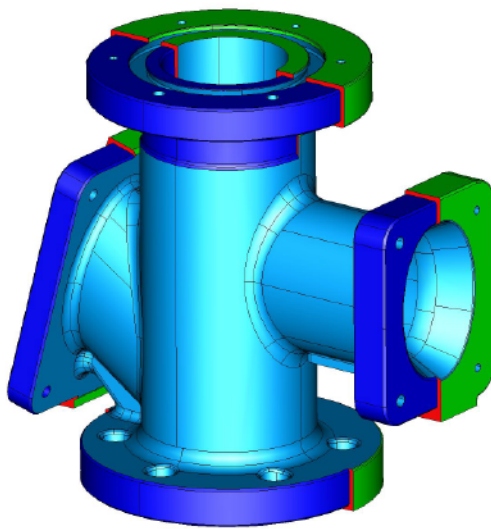
Figure 137. Detail of the top flange overhang with the illustrated tool path for machining the corner.

The design features included in the part are listed below.

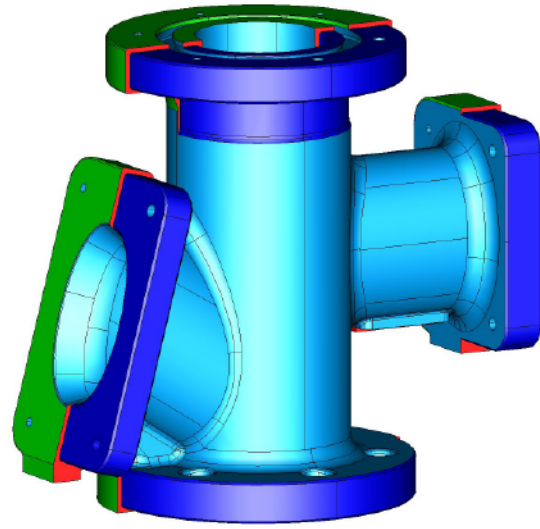
- Flanges at various positions and orientations, representing typical inclination angles; flat, vertical and inclined.
- Surfaces for assessment of required machining allowances by test machining and measurement of the dimensional deviations.

- Thick sections to represent conditions leading to heat build-up during the printing, for studying thermal distortions and sources of deviation of dimensional accuracy.
- Members at shallow inclination angle and overhang at top flange to study suitable support designs.
- Thick material sections to represent heat build-up during the printing at various heights from the platform.

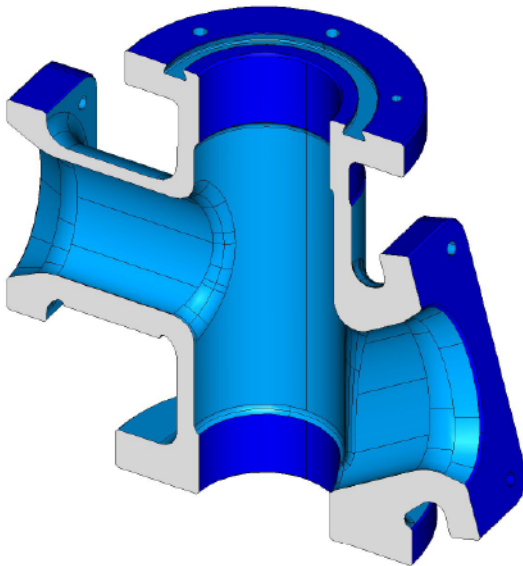
The machining allowances are presented in the next figure.



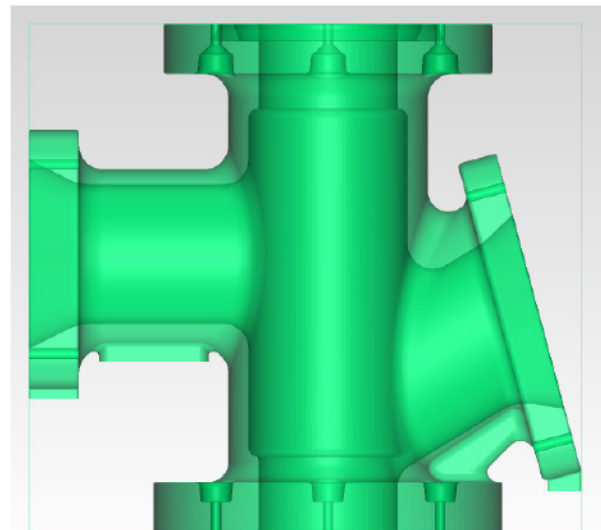
a) Machining allowances.



b) Machining allowances, from another side.



c) Cut view.



d) Transparent view.

Figure 138. The machining of the test component. The machining allowances are indicated by red color. One millimeter was used as the nominal machining allowance at all machined surfaces.

The preliminary machining and geometrical tolerance drawings by KTS-mekano Oy are presented in the following figures. The geometric tolerance values are analysed based on the geometric measurements by MIKES.

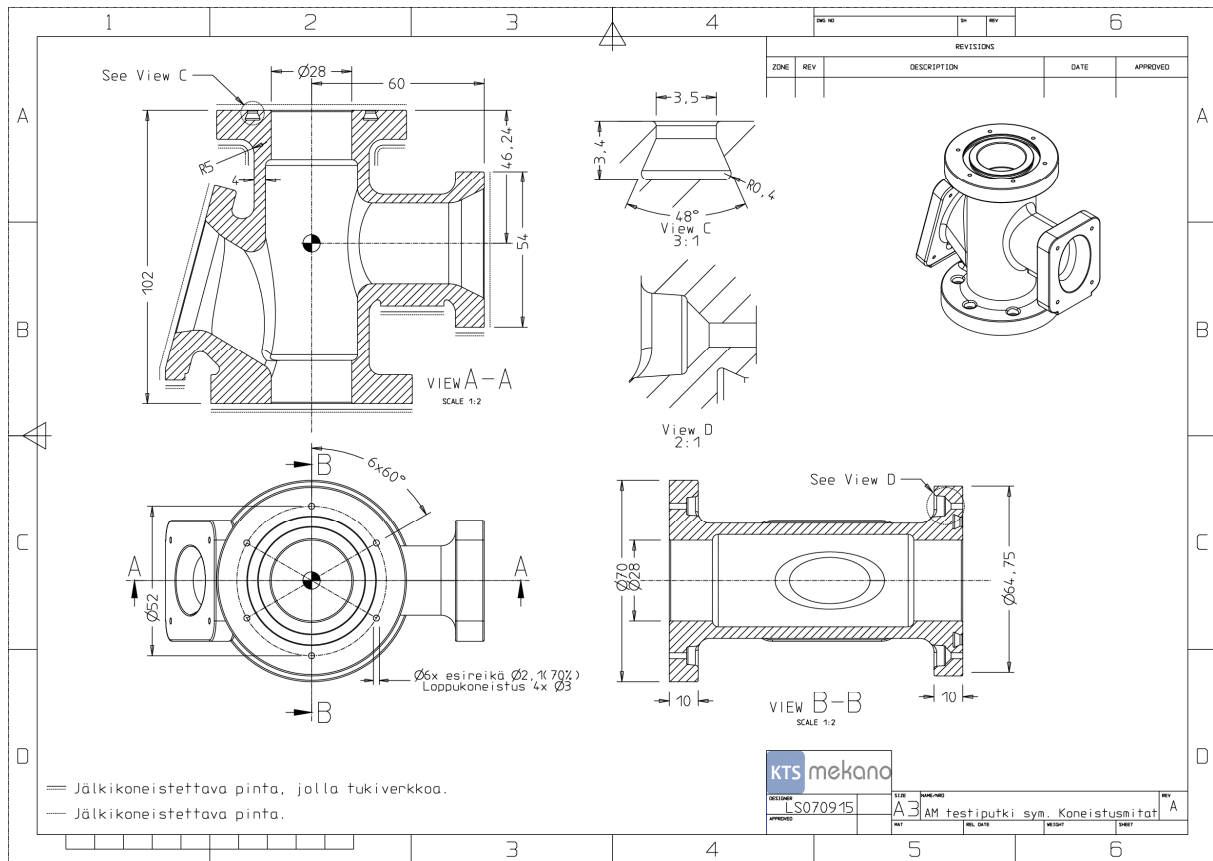


Figure 139. Machining of the test component. Preliminary drawing in the early design phase.

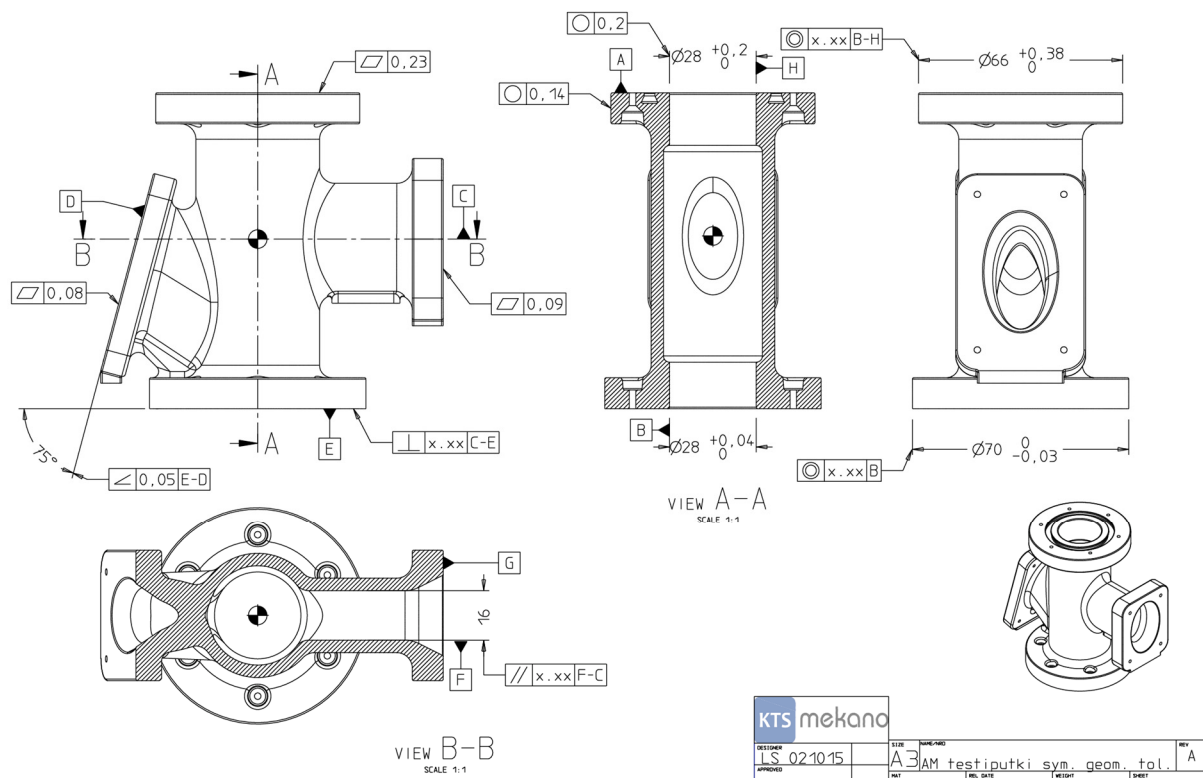


Figure 140. Target geometric tolerances with values according to geometric measuring of the test component by MIKES. The geometric tolerance values are analysed based on geometric measurements by MIKES with the coordinate measurement device. Geometric deviations were measured also at VTT using the FARO laser scanner.

4.2 Support design of the test component

The support angle analysis results presented in the figure below show the locations that are locally at less than the 45 degree inclination angle. The general guide value of 45 degrees was used in estimating the locations that would need temporary supports during the printing. The local short overhangs can typically be printed without supports. Some dross will result, but in this case the locations are machined or ground, and the local dross accepted. Use of temporary supports would in many cases lead to worse surface quality that the dross causes.

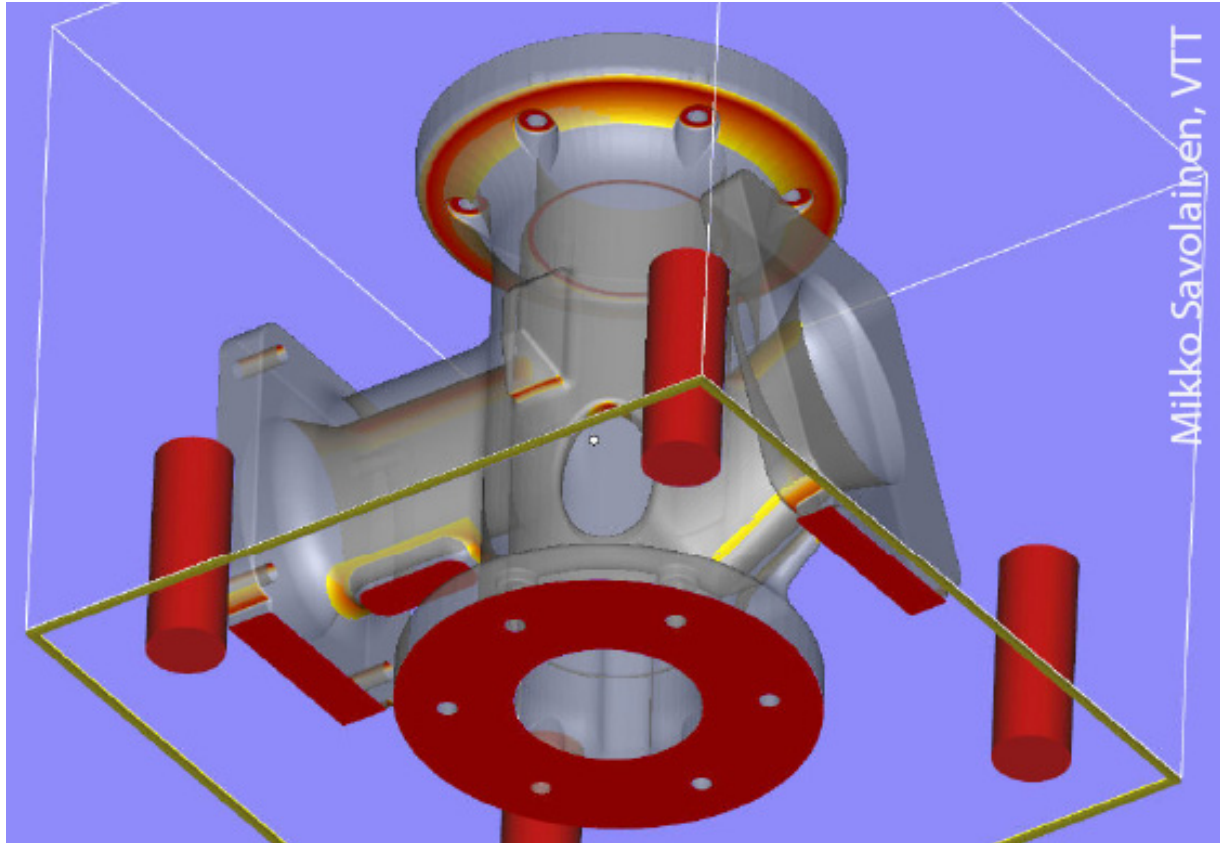


Figure 141. Support angle analysis results by the Magics software revealing the locations in red that require support during printing. The analysis is only indicative and typically some engineering judgement is needed in estimating the locations of supports.

The supports were done mainly directly in the CAD-software, rather than added to the polygon model in the Materialise Magics software. The solid metal CAD supports turned out to be the most straightforward approach and led to best results. The designer can define the solid supports already during the modelling, the supports are included in the geometry file for printing and the solid supports provide good heat conductivity to ensure failure free printing. The cutting lines for easy removal of the support structures are considered in the support design.

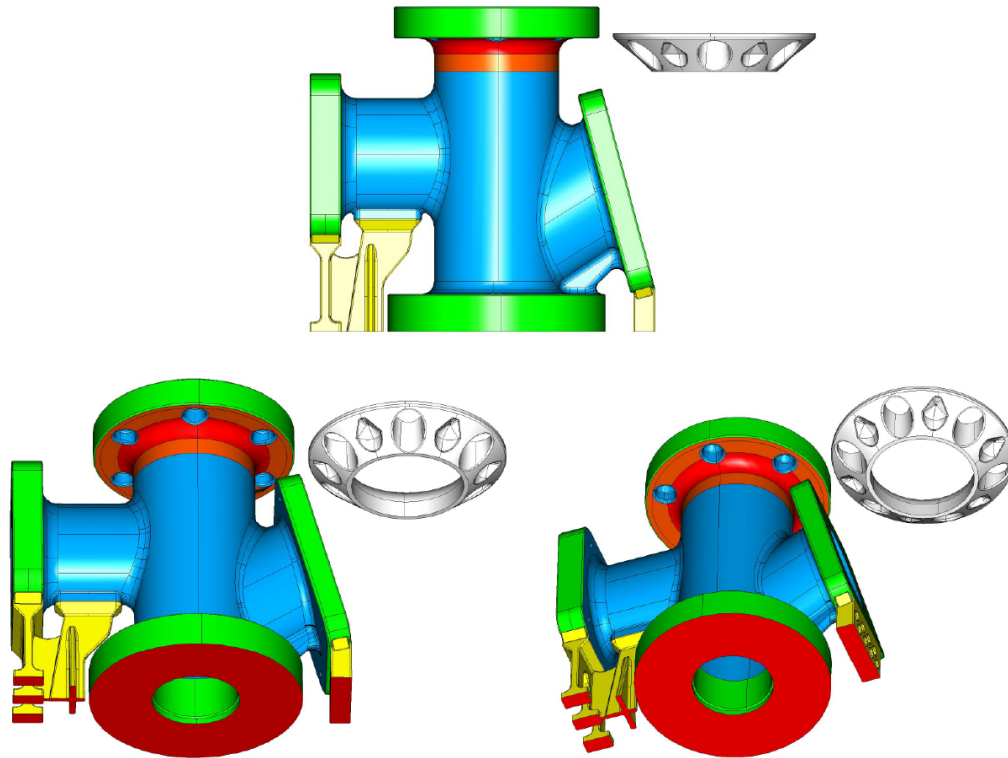


Figure 142. The support design for the top flange that has the overhang. The collar piece (white) and the other supports (yellow) are joined to the component part before exporting the model as .stl file for printing. The red surfaces are at the base plate level.

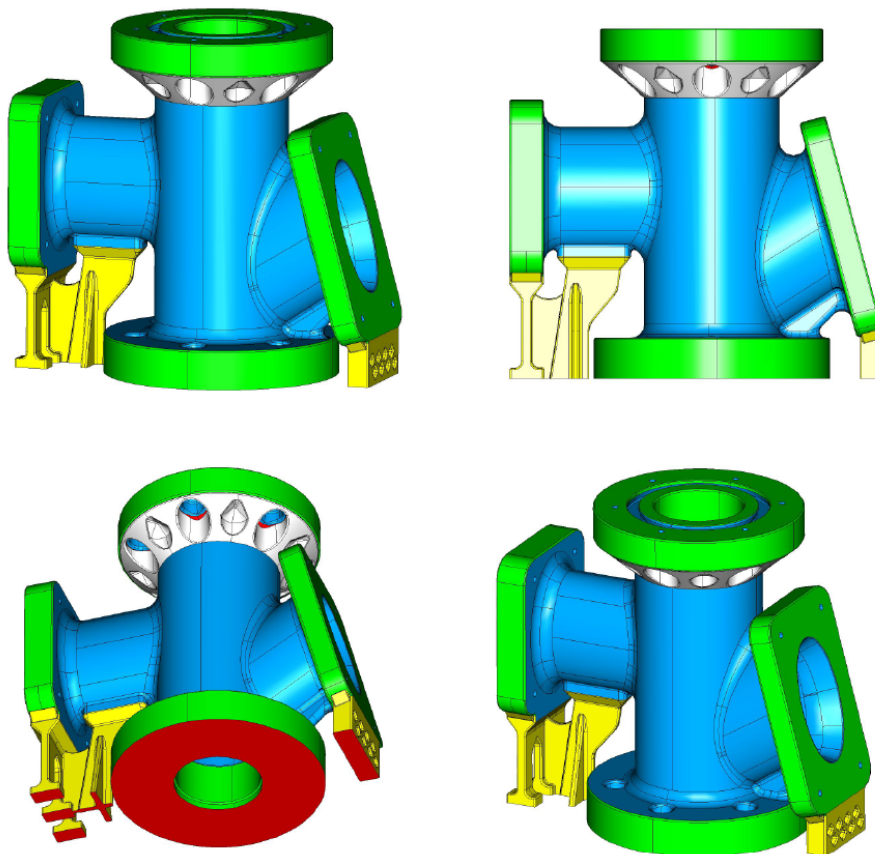


Figure 143. The support design for the test component. Collar is joined to the model.

4.3 Assessment of heat concentration locations

There was no simulation tool suited for SLM available at the time of this work to assessment of the locations of heat concentration. In order to get a rough estimate of the hot spots, the component was studied by traditional casting simulation. The result is of course not a perfect match due to the obvious differences between the processes, but this was considered better than nothing.

The roughly estimated heat traps of the component are shown in the following figures.

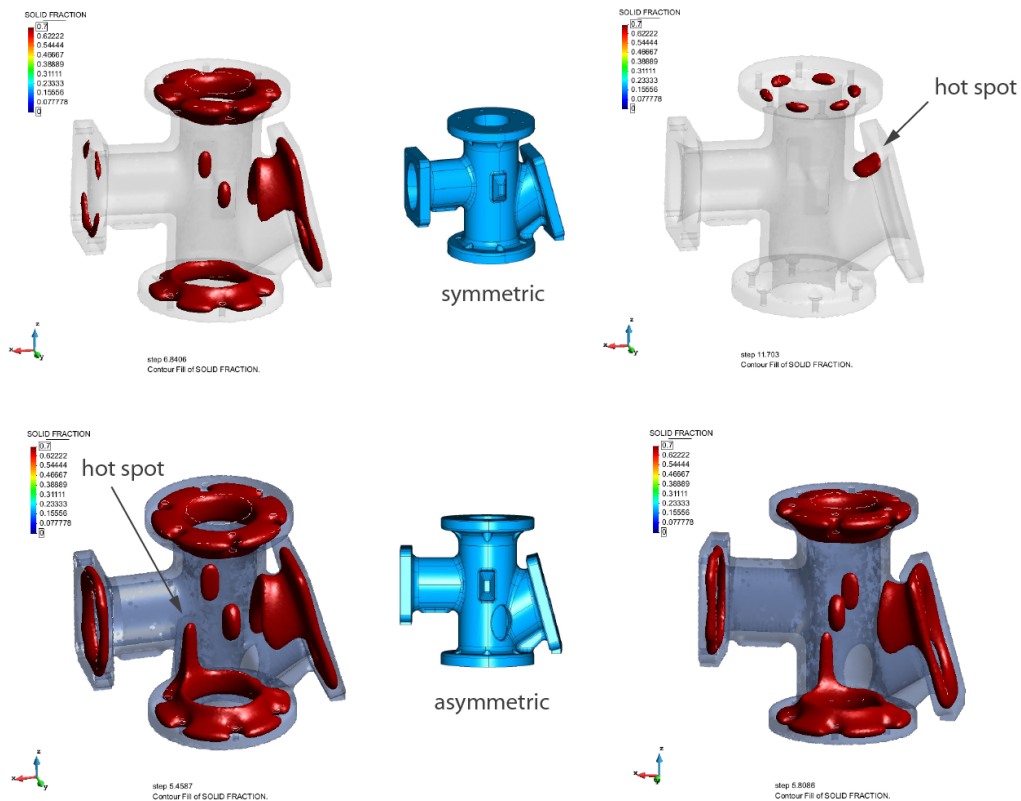


Figure 144. Brief cast simulation to see the heat gathering locations of the component.

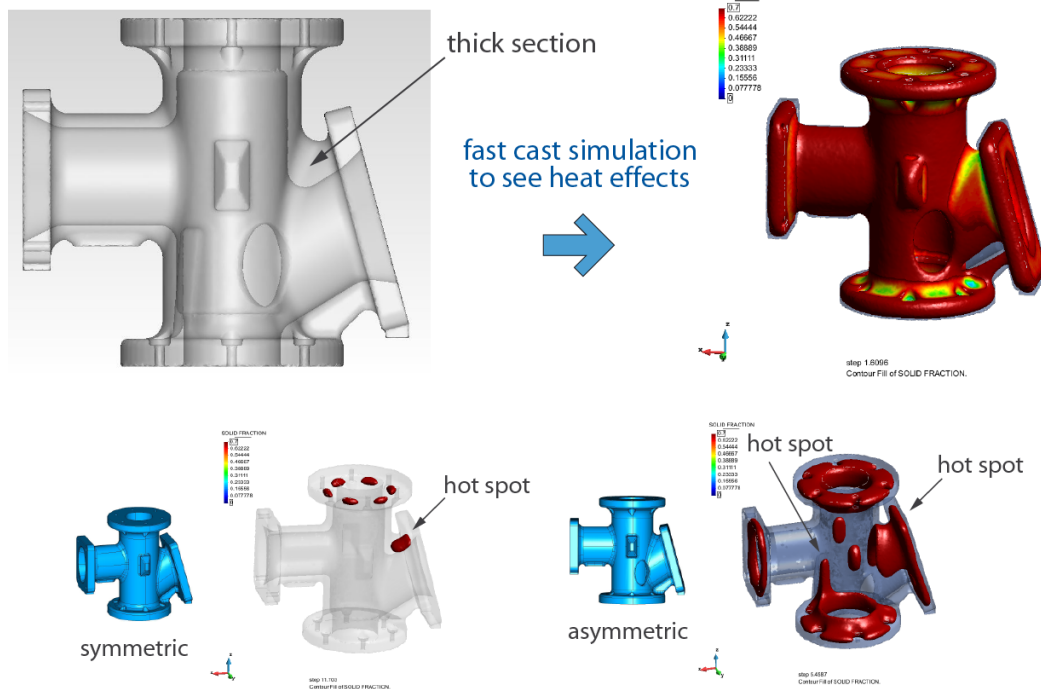
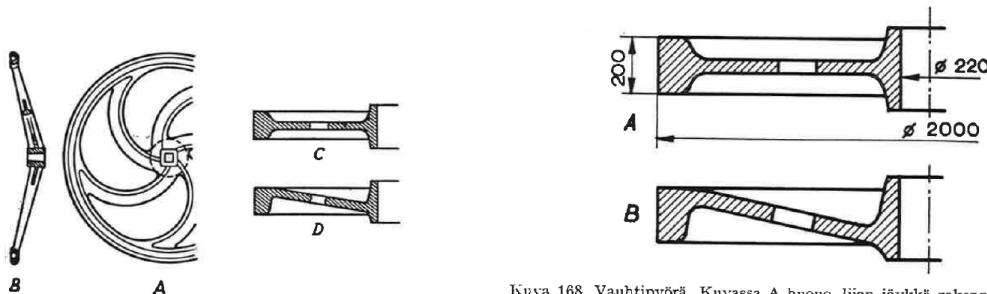


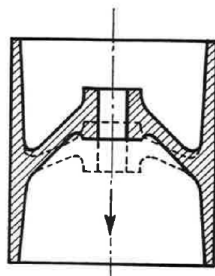
Figure 145. Brief cast simulation to see the heat gathering locations of the component.

The design guidelines for castings are in principle applicable also to component design using the SLM process. The favourable shapes for avoiding thermal stresses, distortions and cracking can be used in design as basic guidelines.

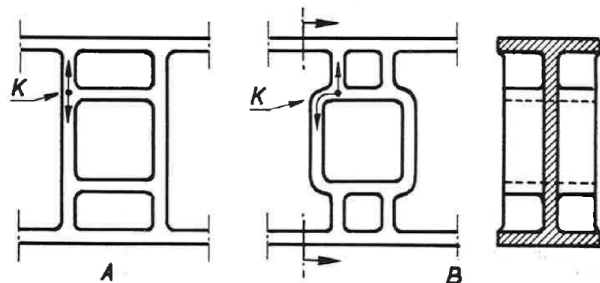


Kuva 166. Joustavia konstruktio-
muotoja. Fyörän puolien kaareviksi tekeminen antaa joustavuutta (A ja B). C = huono, jäykkä rakenne, D = hyvä, joustava rakenne. Ks. kuva 168.

Kuva 168. Vauhtipyörä. Kuvassa A huono, liian jäykkä rakenne. Kuvassa B joustava rakenne.

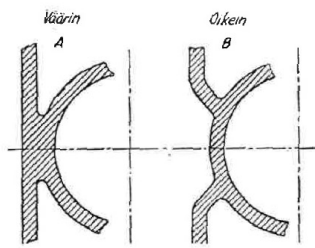


Kuva 167. Käyttöpyörä, jonka napa on joustava.



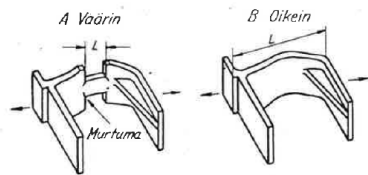
Kuva 169. Tukiripakonstruktio. Kuvassa A esitettyä rakennetta tulisi välttää. Sen sijaan suositellaan kuvan B mukaista rakennetta. K = kutistuminen.

Figure 146. Favouring flexible shapes to avoid thermal stresses and cracking [1].



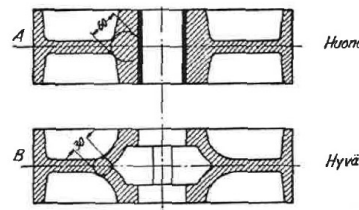
Kuva 40.

Avoid thick sections also in AM



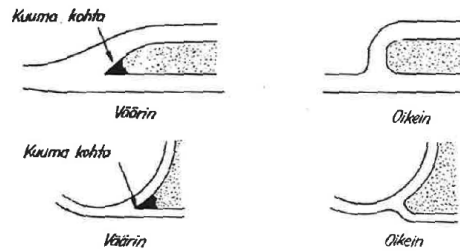
Kuva 56. A. Kutistumavoimat keskittyvät lyhyelle alueelle L. B. Kutistumavoimat jakaantuvat tasaisesti alueelle L.

Avoid abrupt changes in stiffness and sharp corners (stress concentrations) also in AM



Kuva 43. Hihnapyörä.

Avoid thick sections also in AM



Kuva 77. Muotin terävät kärjet muodostavat helposti kuumia kohtia. Näiden muodostuminen on vältettävä oikealla muotoilulla.

Avoid sharp corners and provide flexibility also in AM

Figure 147. Favouring smooth, equal thickness, and flexible shapes to avoid thermal stresses and cracking [16].

4.4 Fatigue critical locations

The fatigue critical locations are typically the transitions of structural members. To show the locations the component was studied by a brief FE-analysis with fictional loading at the flanges that represent bolted connections.

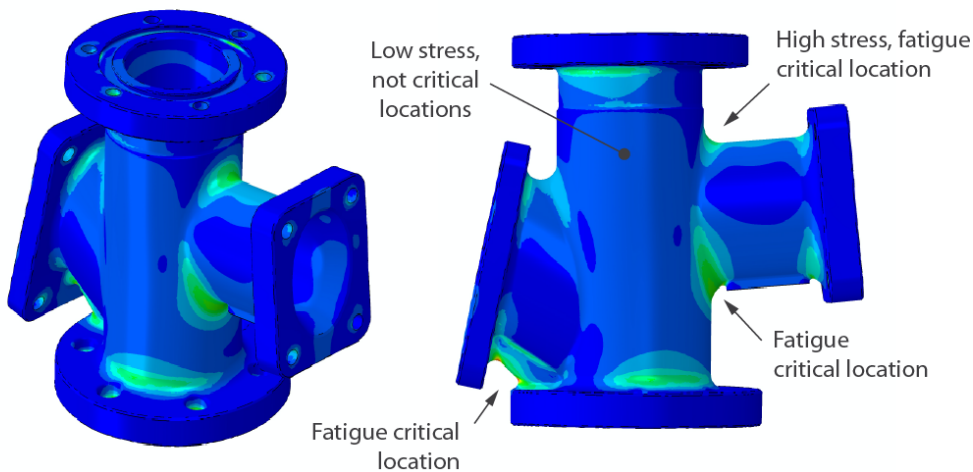
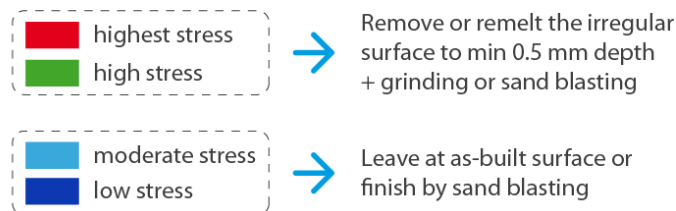


Figure 148. The fatigue critical locations are typically the transitions of structural members.

The locations of the highest (alternating) stresses can't be left at as-built surface in case of critical components and need grinding, machining, remelting or other finishing to remove the rough surface and the borderline porosity typical to SLM process.

4.5 Exporting the CAD model for printing

The accuracy of the polygon representation of the geometry was studied in brief. It was learned that very fine accuracy is best to be used in the export to .stl file format from CAD-software. Here I-Deas CAD software was used. The quality of the .stl file at different settings in I-Deas is presented in Figure 149. It is seen, that the vertical cylinder surface requires rather small (linear) triangles until the geometrical representation is accurate enough. This is due to the linear triangles used in the .stl file format, that represent curved geometry only approximately.

Based on the test prints, the .stl representation should be similar to the case d) in Figure 149 to avoid triangulation from showing up in the printed component. Human eye and shaded view in CAD software are a practical approach in evaluation of the accuracy of the triangulation. Many suppliers use .step files that use NURBS representation of the geometry.

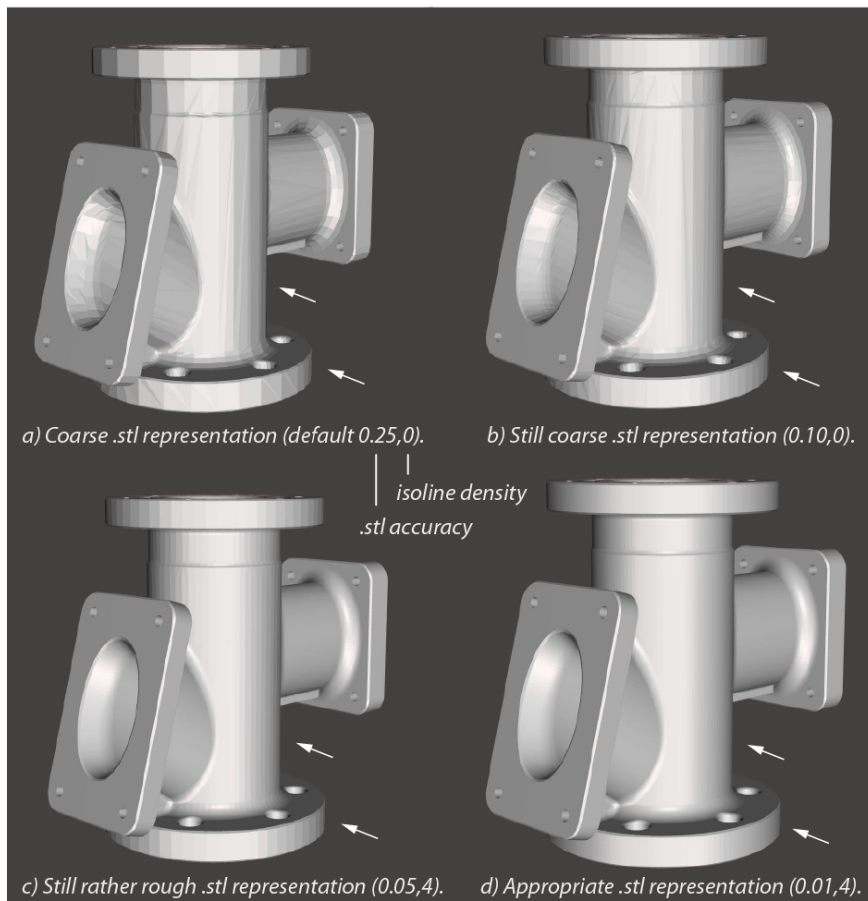


Figure 149. Effect of output resolution setting on the .stl representation.

There are different options in different CAD programs to adjust the accuracy of the stl-presentation provided as source of the laser parameter file to be sent for the printer.

In Materialise Magics preprocessing program it is possible to adjust stl triangle element presentation accuracy for surfaces and arbitrary selected areas of the surfaces. Typically this type of adjustment is needed and done to adjust some areas more suitable for support attachment areas.

The basic thing which should be considered and taken into account in CAD is the roundness of the part. If there is not enough triangle elements in the circular arch it will be seen as discontinuities of the circle and separations of the arc. The separations can not be eliminated from the stl when using Magics. In Magics the triangles could be added but the original lack of roundness is still there.

Then creating the stl the needful amount of elements should be checked just by eye since the circular arch and need of the elements grows as a function of the diameter of the arch, see Figure 150. In the figure angle tolerance for the both cylinders is 30 degrees. The smaller looks round and the bigger one is not anymore round when looking closer. The angle tolerance should be a lot smaller for the bigger cylinder to make it round. The geometry stl for a build job just have to be checked by eye.

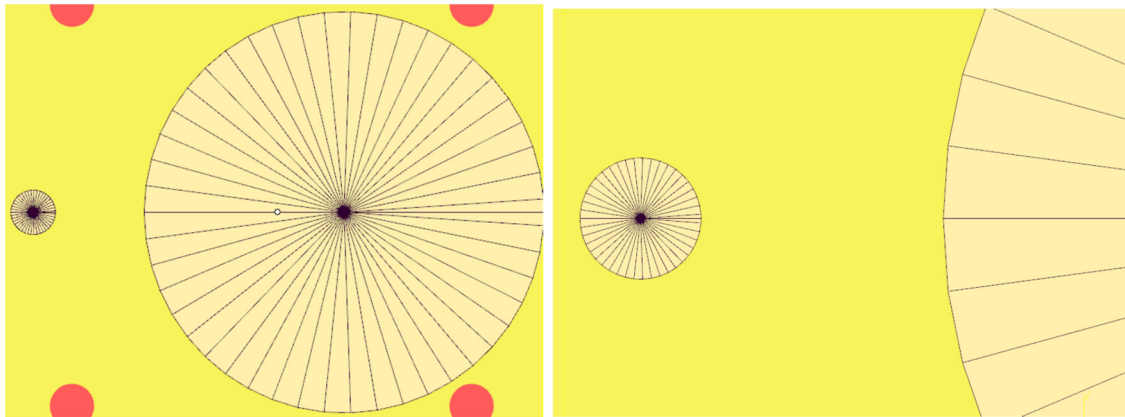
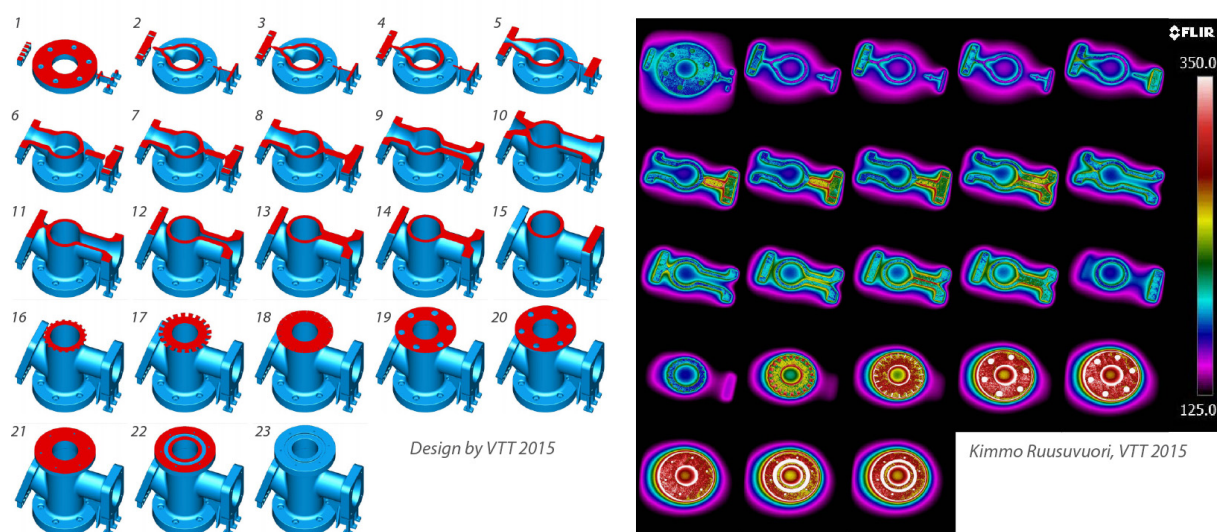


Figure 150. Element length at circular arch with two different radiuses, 5 mm and 45 mm. Angle tolerance for the both cylinders is 30 degrees.

4.6 Thermal imaging of the component during printing

Thermal images of 23 cross sections during the printing of the test component are presented in the following figure. The images were acquired using a FLIR thermal video camera.



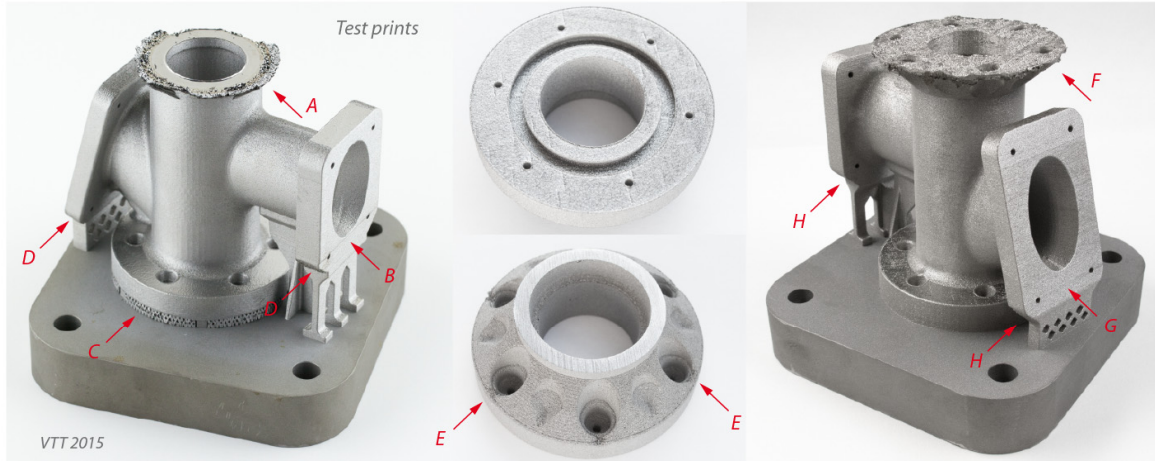
a) Studied cross-sections in CAD model.

b) The monitored temperature distributions at the end of melting of the layers.

Figure 151. Thermal images of 23 cross sections during the printing of the test component. Material is H13 tool steel.

4.7 Trial prints of the test component

The component was printed a few times as the learning process and the support design was improved gradually after learning how the component is best printed. The test prints ended typically at printing failures at the top flange support locations. The remarks of the test prints are presented in the following figure.



a) Component with lattice supports (A) at top flange. Failed test print in tool steel H13. Ridge 0.5 mm due to transversal shrinkage at vertical flange (B). Slight cracking at lattice supports below bottom flange (C). Slight dross at bottom corners of vertical flanges (D). Printing failure at location A due to heat build up.

b) Flange test piece printed separately in 316L. Only slight local dross at locations E.

c) Failed component test print in 316L. Same solid support collar design (F) as printed separately (b). Ridge 0.2 mm due to transversal shrinkage at vertical flange (G). Bottom flange printed from the base plate directly for increased support. Dross at bottom corners of vertical flanges (D). Printing failure at location F due to excessive heat build up.

Figure 152. Lessons learned during the trial prints of the test component. The block supports and shallow angle solid support of the top flange led to printing failures due to heat build-up. The shallow angle solid support of the top flange printed fine as a test piece directly from base plate (b), but failed as part of the component, as excessive heat builds up in the top of the component, as can be seen in the thermal images.

4.8 Printed test component

The printed test component and the support structures of the test component are presented in the following figures. The test component was printed in H13 tool steel. No other parts were printed simultaneously with the part, to keep the conditions simple and well defined for easy interpretation of the component print quality.

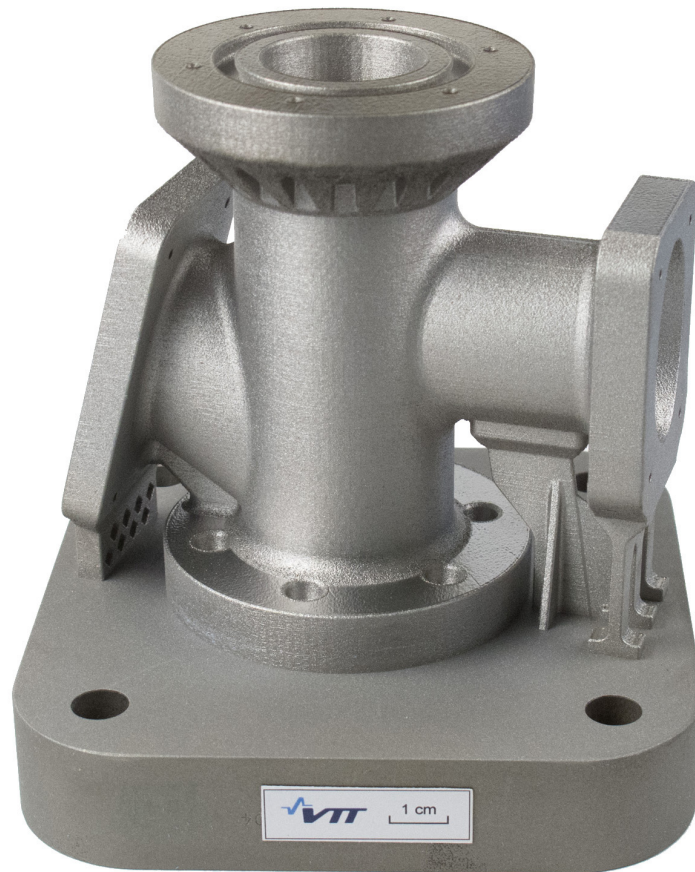


Figure 153. The test component and the support structures printed in H13 tool steel.

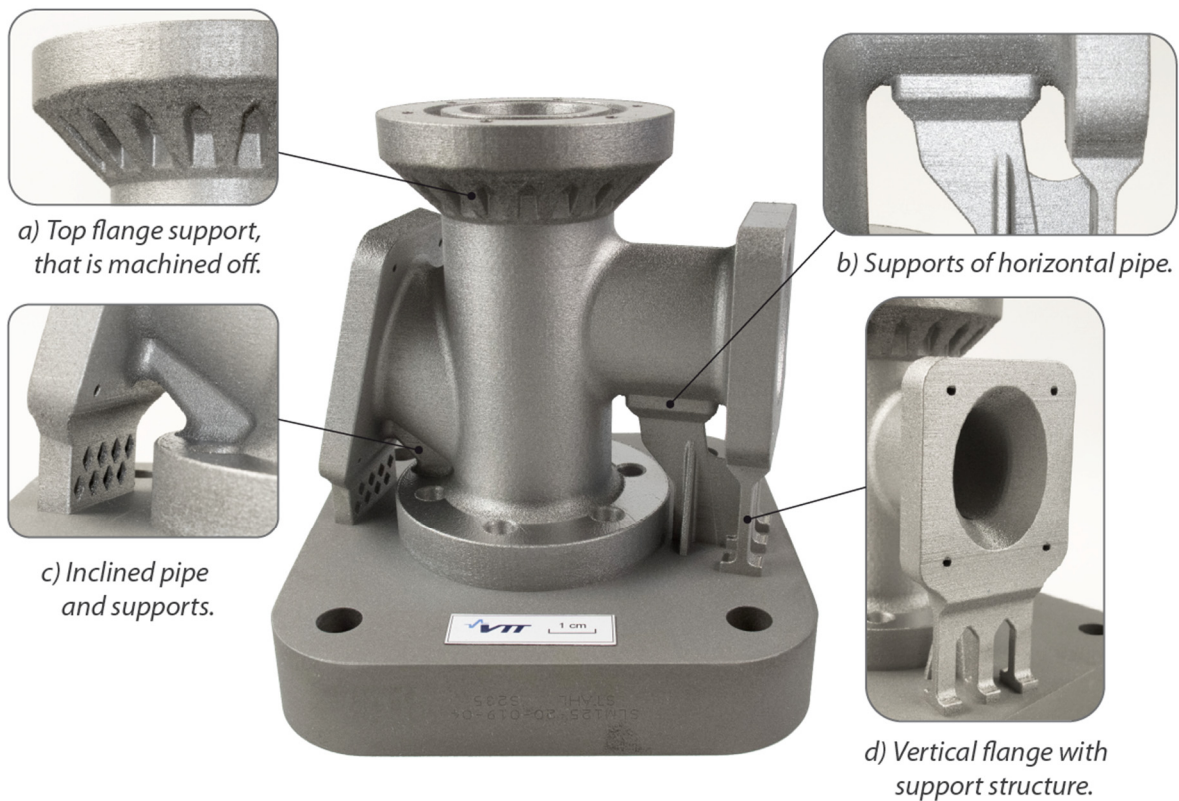


Figure 154. The printed test component and the support structures. All supports were designed as solid supports in CAD in the final design.

The geometrical measurement by FARO laser scanner and the analysed deviation [mm] of the printed part from the CAD part by Antti Vaajoki, VTT, are presented in Figure 155.

The heat build-up in the top of the part shows as slight distortion of the top flange. The geometrical deviations are within the intended machining allowances and therefore the printed part was considered acceptable for machining.

No component level distortion, all deviations are covered in machining allowances.

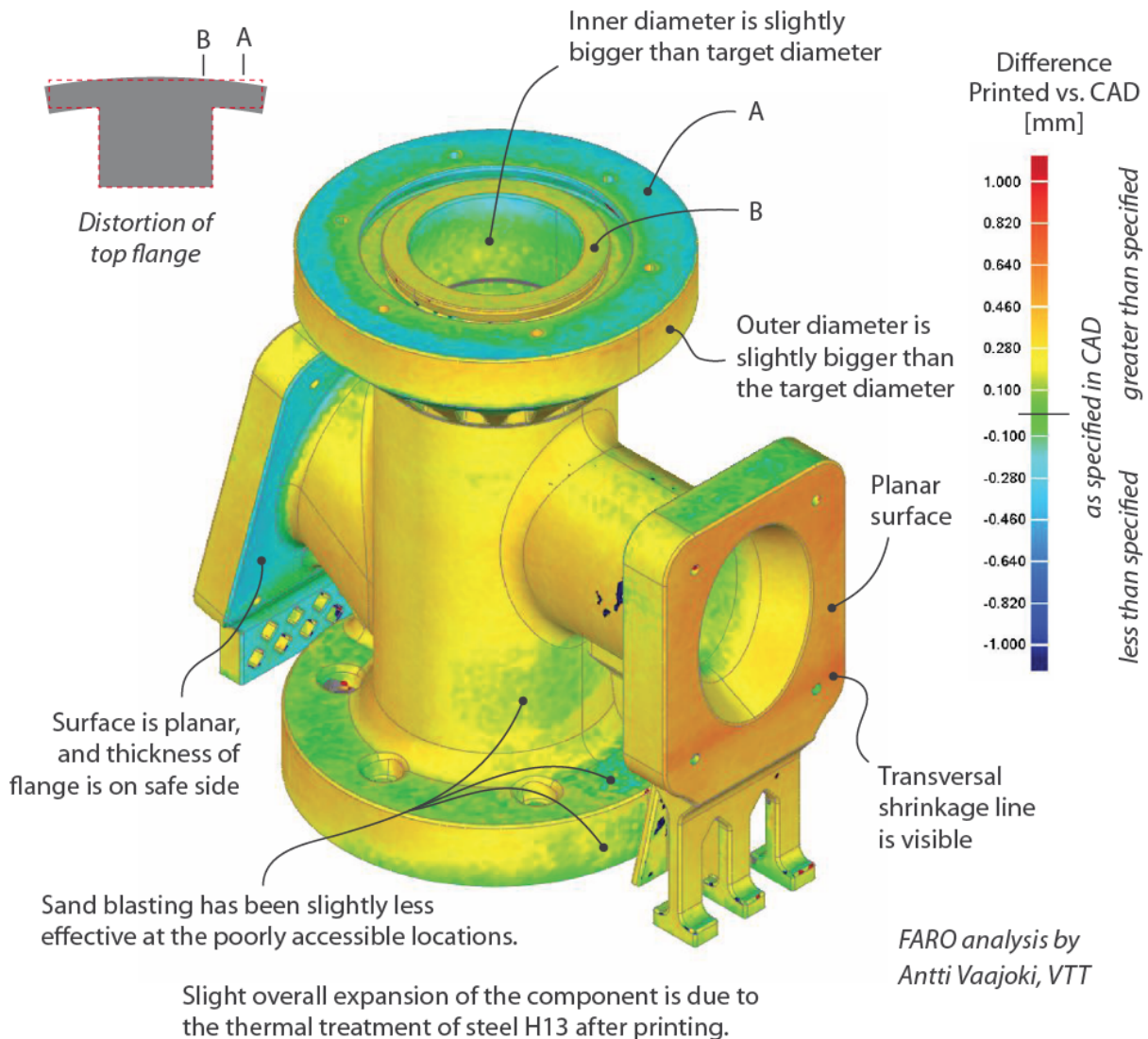
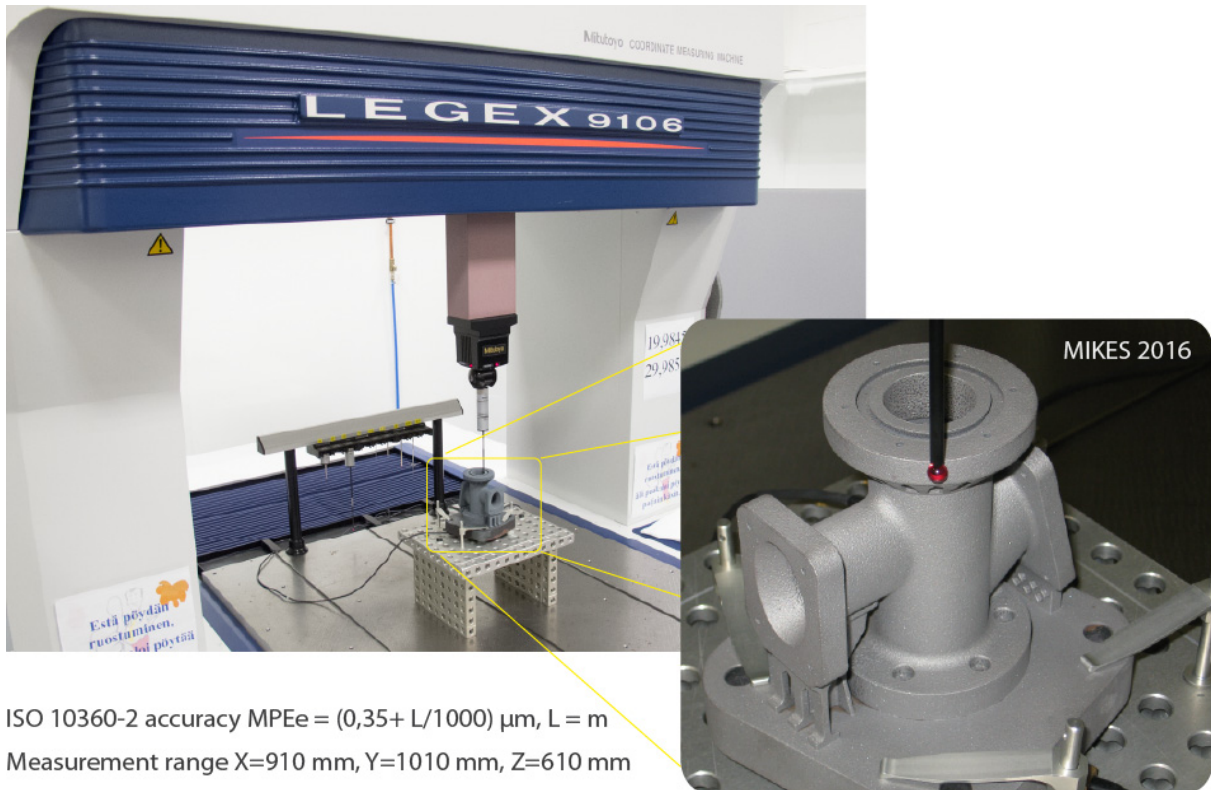


Figure 155. The geometrical measurement by FARO laser scanner and the deviation [mm] of the printed part from the CAD part. The heat build-up in the top of the part shows as slight distortion of the top flange. The geometrical deviations are within the intended machining allowances and therefore the printed part is acceptable for machining.

The geometrical measurement of the test component using the Mitutoyo Legex 9106 coordinate measuring machine is presented in the following figure.



ISO 10360-2 accuracy $MPE_e = (0,35 + L/1000) \mu\text{m}$, $L = \text{m}$
 Measurement range $X=910 \text{ mm}$, $Y=1010 \text{ mm}$, $Z=610 \text{ mm}$

Figure 156. Measurements of the test component using coordinate measuring machine Mitutoyo Legex 9106 at VTT-MIKES.

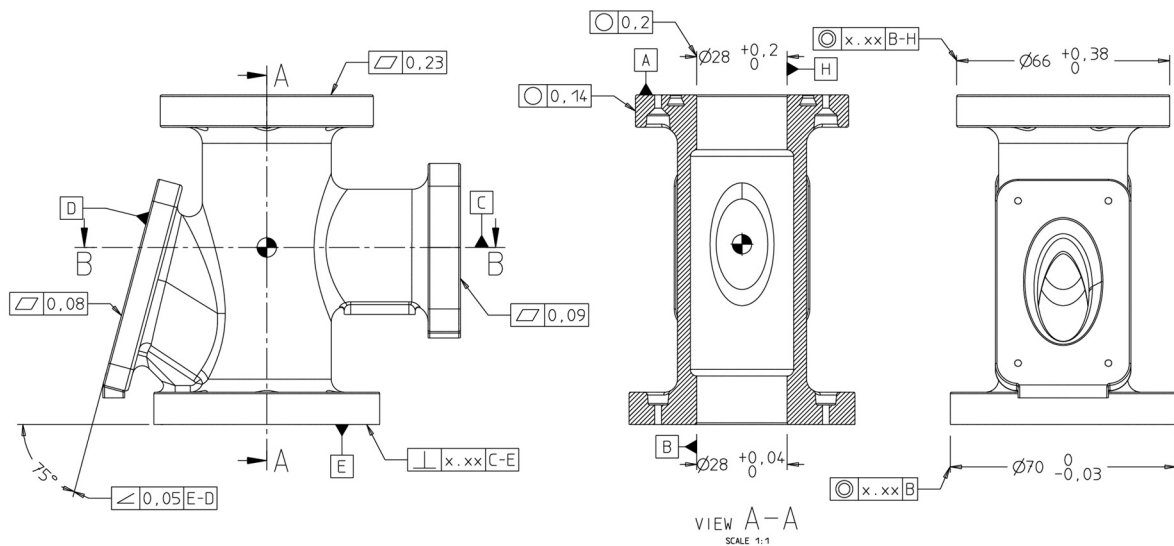


Figure 157. Examples of the measurement results by MIKES summarised by KTS-mekano Oy. The bottom flange was attached to the base plate and was not accessible to the measurement.

The linear dimension casting tolerance grades (DCTG) SFS-EN ISO 8062-3 are presented as an excerpt in Figure 158. The geometric accuracy of the test component printed in H13 was assessed to fall between SFS-EN ISO 8062-3 linear dimension casting tolerance grades (DCTG) 4 and 5 at component level. Even DCTG 1 and DCTG 2 accuracies were met at individual features.

SFS-EN ISO 8062-3 linear dimension casting tolerance grades (DCTG)

Dimensions in millimetres

Nominal dimensions related to the moulded part		Linear dimensional tolerance for dimensional casting tolerance grade (DCTG) ^a															
		DCTG 1	DCTG 2	DCTG 3	DCTG 4	DCTG 5	DCTG 6	DCTG 7	DCTG 8	DCTG 9	DCTG 10	DCTG 11	DCTG 12	DCTG 13	DCTG 14	DCTG 15	DCTG 16 ^b
–	≤ 10	0,09	0,13	0,18	0,26	0,36	0,52	0,74	1	1,5	2	2,8	4,2	–	–	–	–
> 10	≤ 16	0,1	0,14	0,2	0,28	0,38	0,54	0,78	1,1	1,6	2,2	3	4,4	–	–	–	–
> 16	≤ 25	0,11	0,15	0,22	0,3	0,42	0,58	0,82	1,2	1,7	2,4	3,2	4,6	6	8	10	12
> 25	≤ 40	0,12	0,17	0,24	0,32	0,46	0,64	0,9	1,3	1,8	2,6	3,6	5	7	9	11	14
> 40	≤ 63	0,13	0,18	0,26	0,36	0,5	0,7	1	1,4	2	2,8	4	5,6	8	10	12	16
> 63	≤ 100	0,14	0,2	0,28	0,4	0,56	0,78	1,1	1,6	2,2	3,2	4,4	6	9	11	14	18
> 100	≤ 160	0,15	0,22	0,3	0,44	0,62	0,88	1,2	1,8	2,5	3,6	5	7	10	12	16	20
> 160	≤ 250	–	0,24	0,34	0,5	0,7	1	1,4	2	2,8	4	5,6	8	11	14	18	22
> 250	≤ 400	–	–	0,4	0,56	0,78	1,1	1,6	2,2	3,2	4,4	6,2	9	12	16	20	25
> 400	≤ 630	–	–	–	0,64	0,9	1,2	1,8	2,6	3,6	5	7	10	14	18	22	28
> 630	≤ 1 000	–	–	–	–	1	1,4	2	2,8	4	6	8	11	16	20	25	32
> 1 000	≤ 1 600	–	–	–	–	–	1,6	2,2	3,2	4,6	7	9	13	18	23	29	37
> 1 600	≤ 2 500	–	–	–	–	–	–	2,6	3,8	5,4	8	10	15	21	26	33	42
> 2 500	≤ 4 000	–	–	–	–	–	–	–	4,4	6,2	9	12	17	24	30	38	49
> 4 000	≤ 6 300	–	–	–	–	–	–	–	–	7	10	14	20	28	35	44	56
> 6 300	≤ 10 000	–	–	–	–	–	–	–	–	–	11	16	23	32	40	50	64

^a For wall thicknesses in grades DCTG 1 to DCTG 15, one grade coarser applies (see Clause 7).

^b Grade DCTG 16 exists only for wall thicknesses of castings generally specified to DCTG 15.

Figure 158. The linear dimension casting tolerance grades (DCTG) SFS-EN ISO 8062-3.

4.9 Removal of support structures

The support structures and the part were detached by wire cutting at KTS-mekano. The pieces after wire cutting are presented in Figure 159. A thin slice was cut to test the cutting accuracy for estimated the amount of cutting allowance needed. A one millimeter cutting allowance is fine for wire cutting of the bottom flange.

Removal of support structures by wire cutting

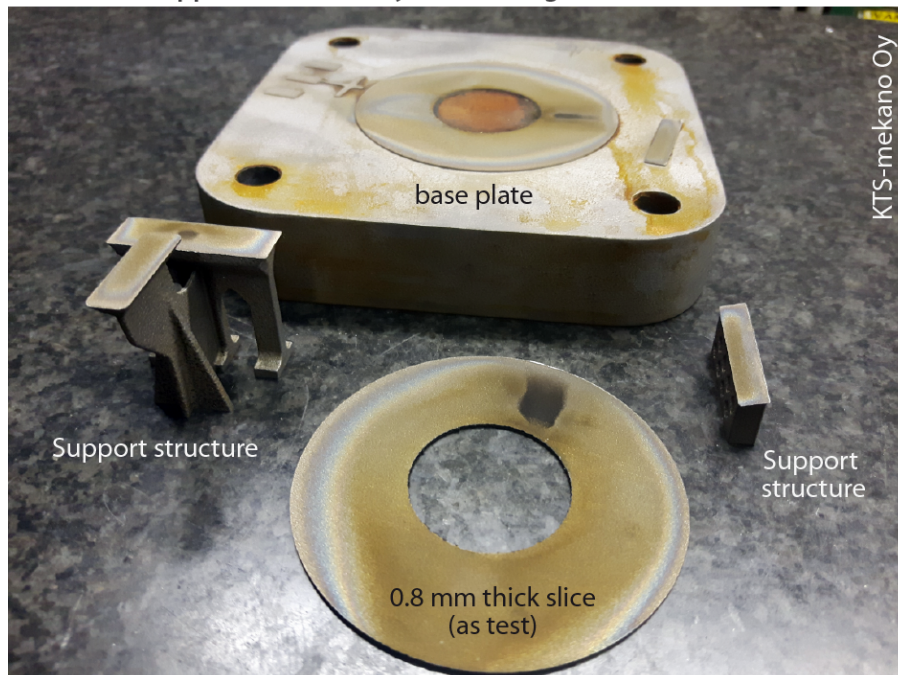


Figure 159. The support structures and the part were detached by wire cutting.

4.10 Machining

The test component was machined by KTS-mekano Oy. The tool steel H13 is typically very hard for machining in as-built condition and the component was heat treated to soft condition before machining. The machining operations were planned by Leevi Salonen, KTS-mekano. An example of fixing of the part, measuring the zero point of the part and milling the sides of the vertical flange are shown in Figure 160.

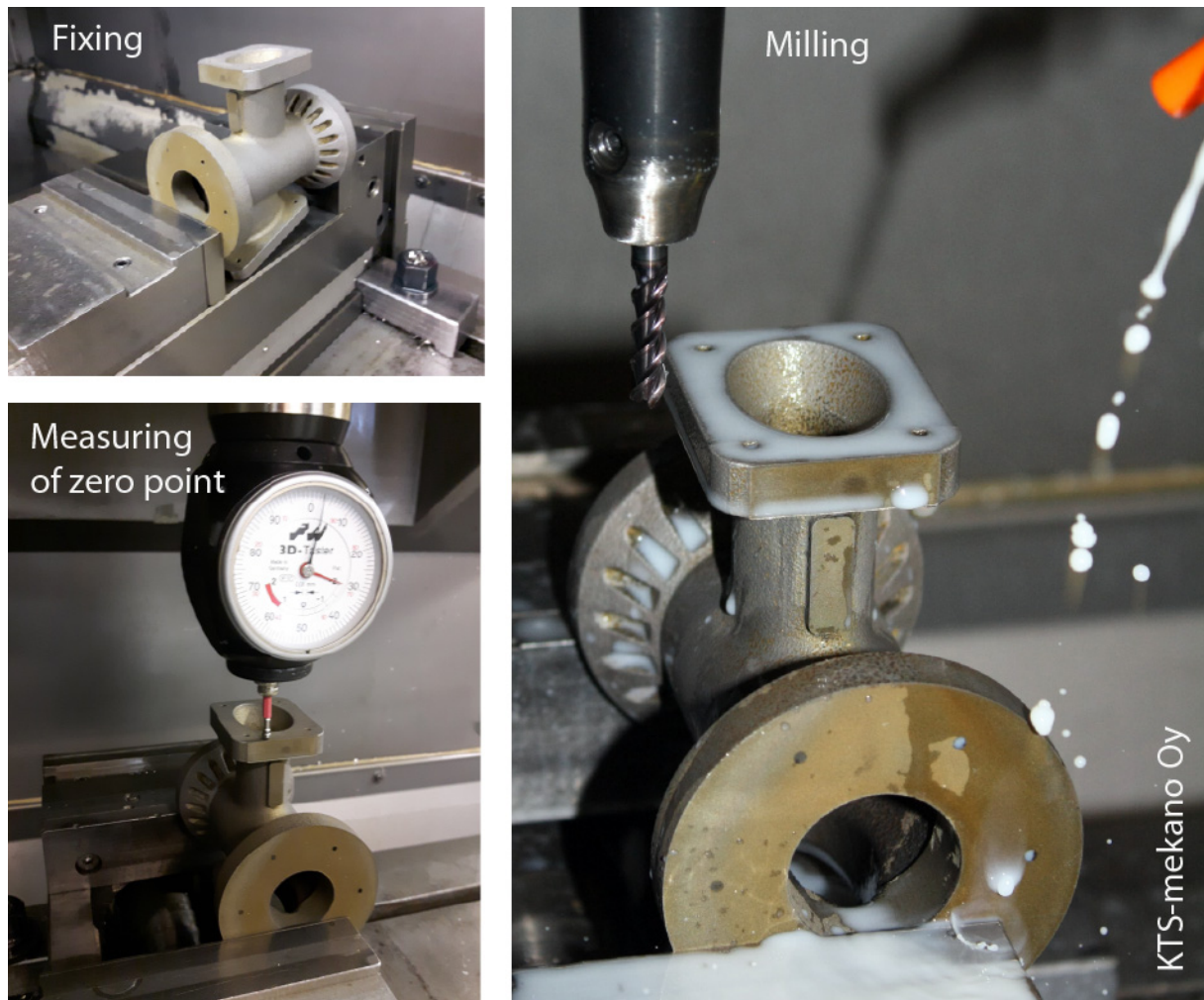


Figure 160. fixing of the part, measuring the zero point of the part and milling the sides of the vertical flange at KTS-mekano Oy workshop.

The borderline porosity typical to SLM process is revealed after the first pass of machining the sides of the vertical flange. After the second pass sound material is met. The steps in machining are presented in Figure 161.

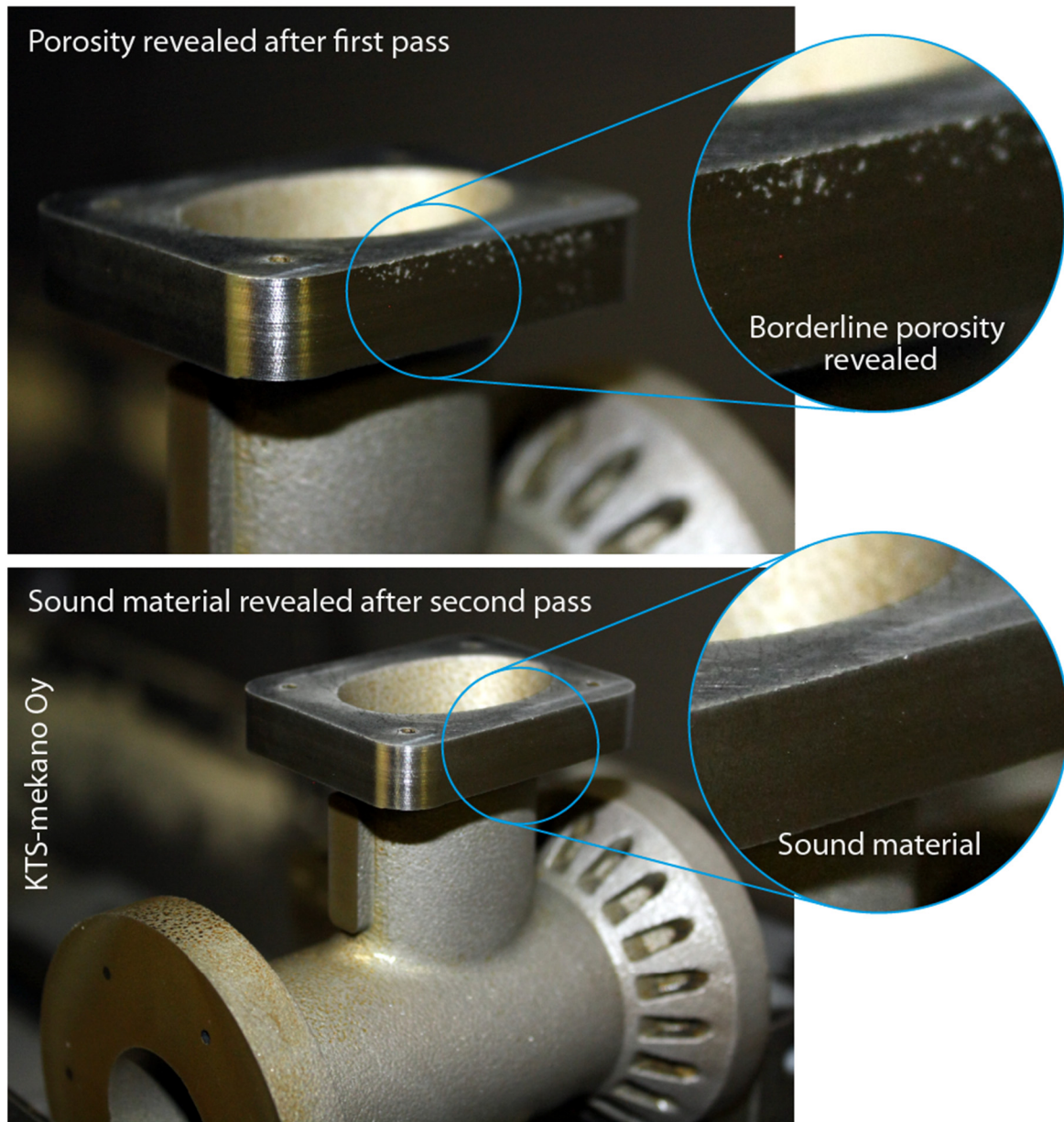


Figure 161. The borderline porosity typical to SLM process is revealed after the first pass of machining the sides of the vertical flange. After the second pass sound material is met.

The machined mock-up specimen is presented in the following two figures. The tool steel H13 is typically very hard for machining in as-built condition and the component was softened by heat treatment before machining. The surface of the component is rather rough after the heat treatment that was done in hurry in air (shield gas was not possible to arrange for the oven available for the work at VTT). The removal of the oxidation layer by etching and sand blasting has left the as-built surface pitted.

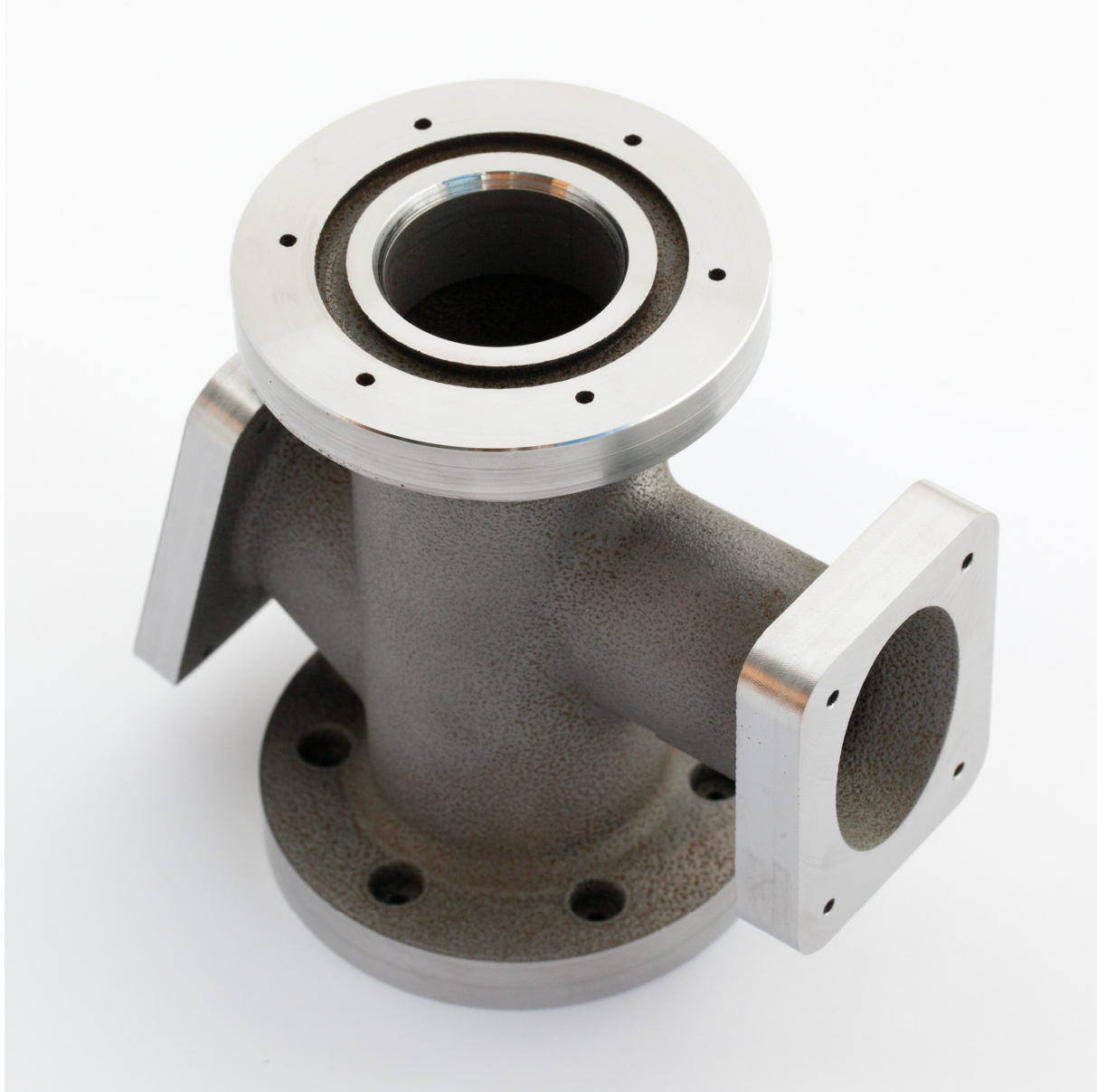


Figure 162. The machined mock-up component (tool steel H13). The removal of the oxidation layer by etching and sand blasting after the softening heat treatment has left the as-built surface pitted.

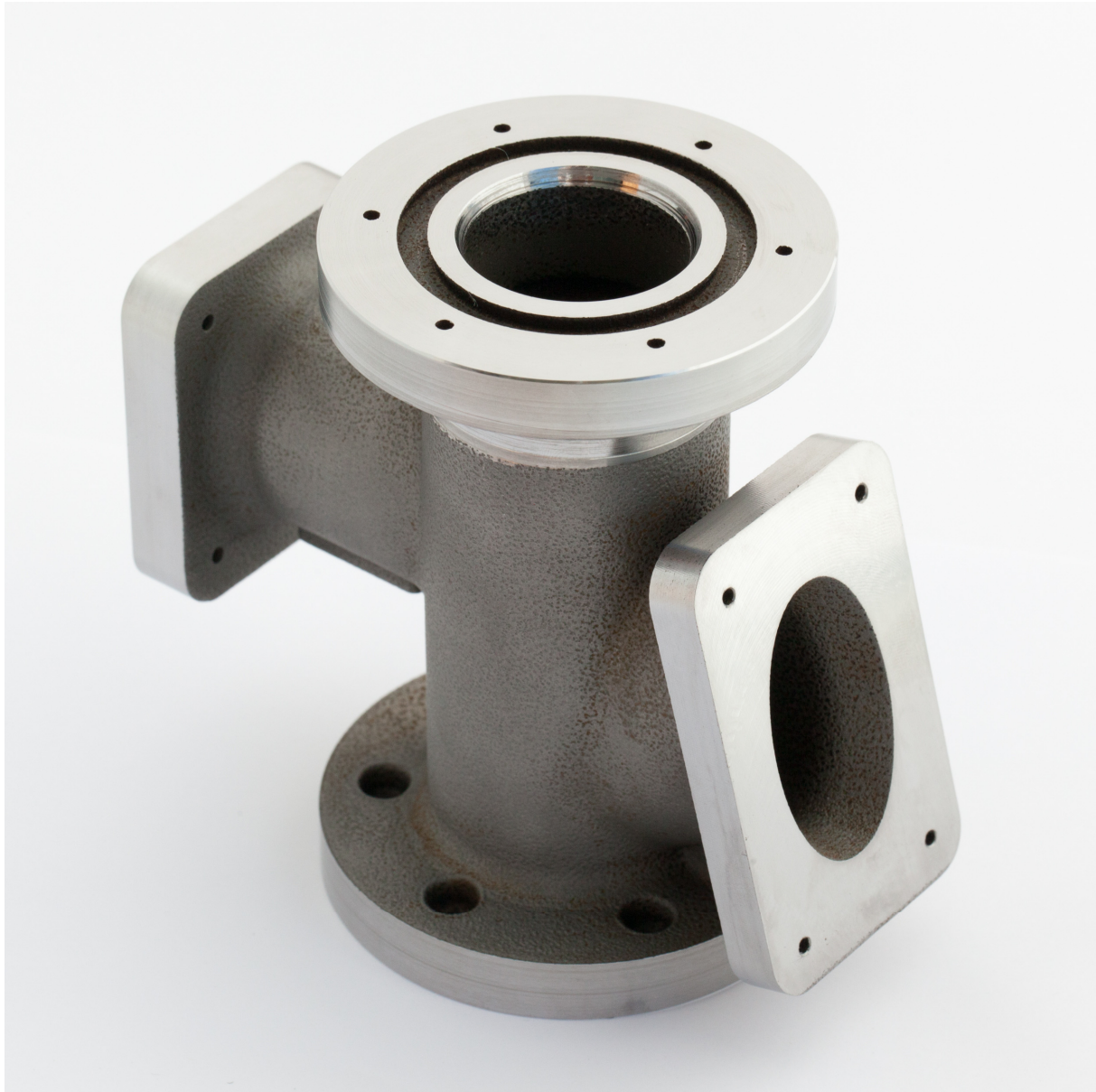


Figure 163. The machined mock-up component, view from the other direction.

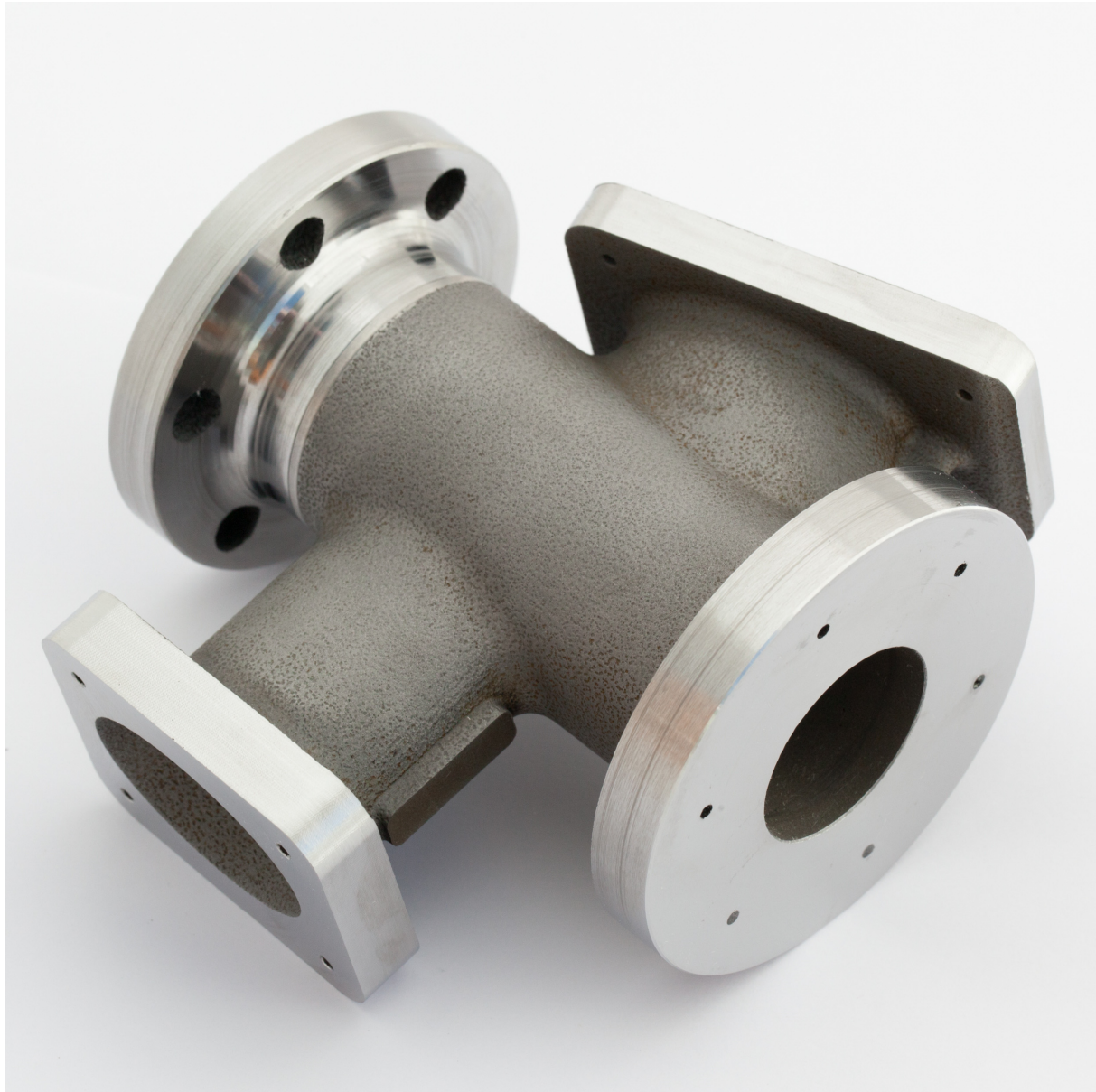


Figure 164. The machined mock-up component. The support structure of the top flange has been machined off (top left).

4.11 Alternative designs

Alternative designs studied during the design work are discussed in the following. These parts were not printed.

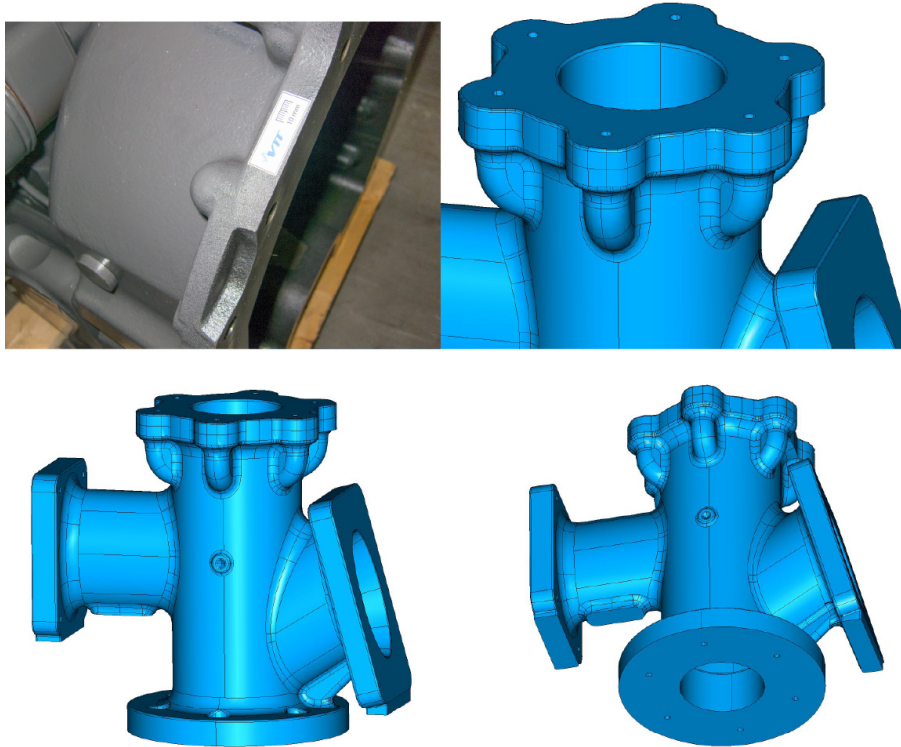


Figure 165. Alternative self-supporting design of the top flange. This is adapted for AM from the traditional casting designs. An example of such cast detail is shown on left.

An intermediate design step is presented in the following figures as an example of a trial modelling work flow. The idea was to model a support structure in CAD, mesh the volume describing the supports in for example 3-Matic, and join the lattice support to the component as .stl geometry. The intended work flow was however not easy to do with the current software and traditional CAD was used instead.

- Creating block supports in Magics for axisymmetric geometry is rather slow.
- Alternative, possibly faster work flow could be
 - prepare a volume for block supports in CAD
 - the collar volume is modelled with slight overlap for later joining to part
 - mesh the collar volume with *self supporting lattices* in 3-Matic
 - join the part and block supports in 3-Matic (or in Magics?)
- Supports are machined off after printing.
- Flange shown in pictures is part of a larger structure.

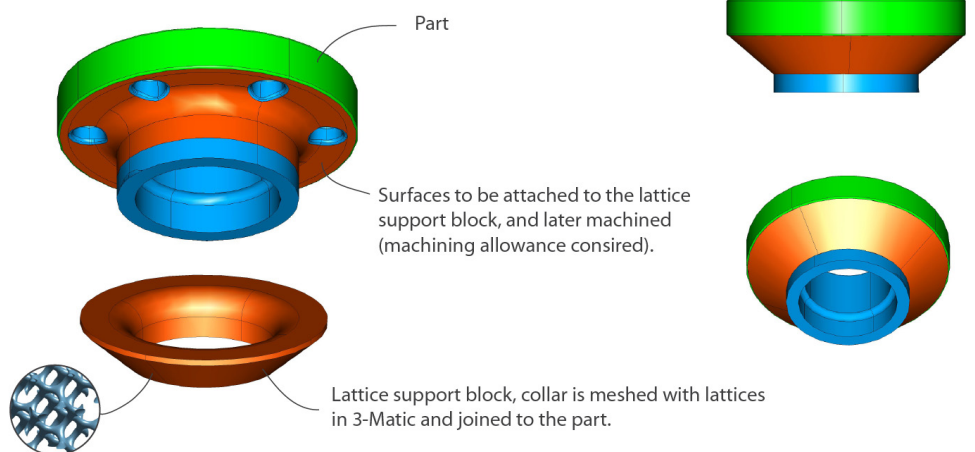


Figure 166. An alternative support design for the top flange overhang by combining CAD and polygon modelling.

4.12 Brief topology optimization study for the test component

The topology optimization was studied briefly with the dimensional accuracy test component. The design spaces and boundary conditions are shown in the following figure.

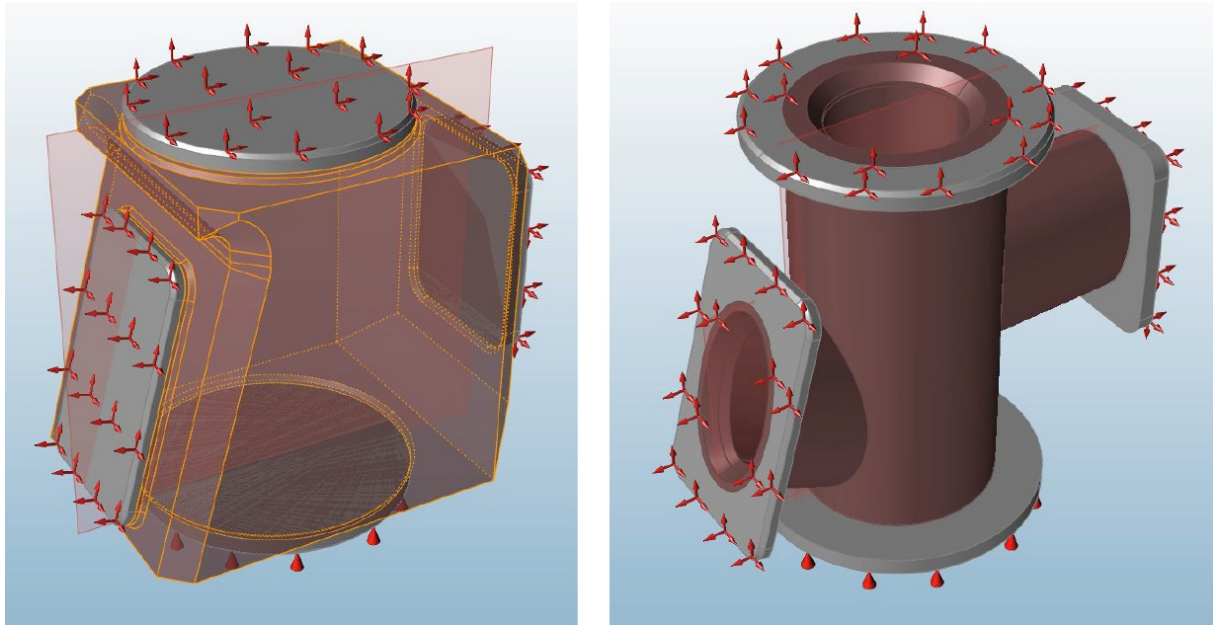


Figure 167. Larger design space on the left and the pipe like structure on the right. Both these and combinations of them were used in the brief topology optimization studies.

The material distributions resulting from the topology optimization studies at different design space and constraint settings are shown in the next figure.

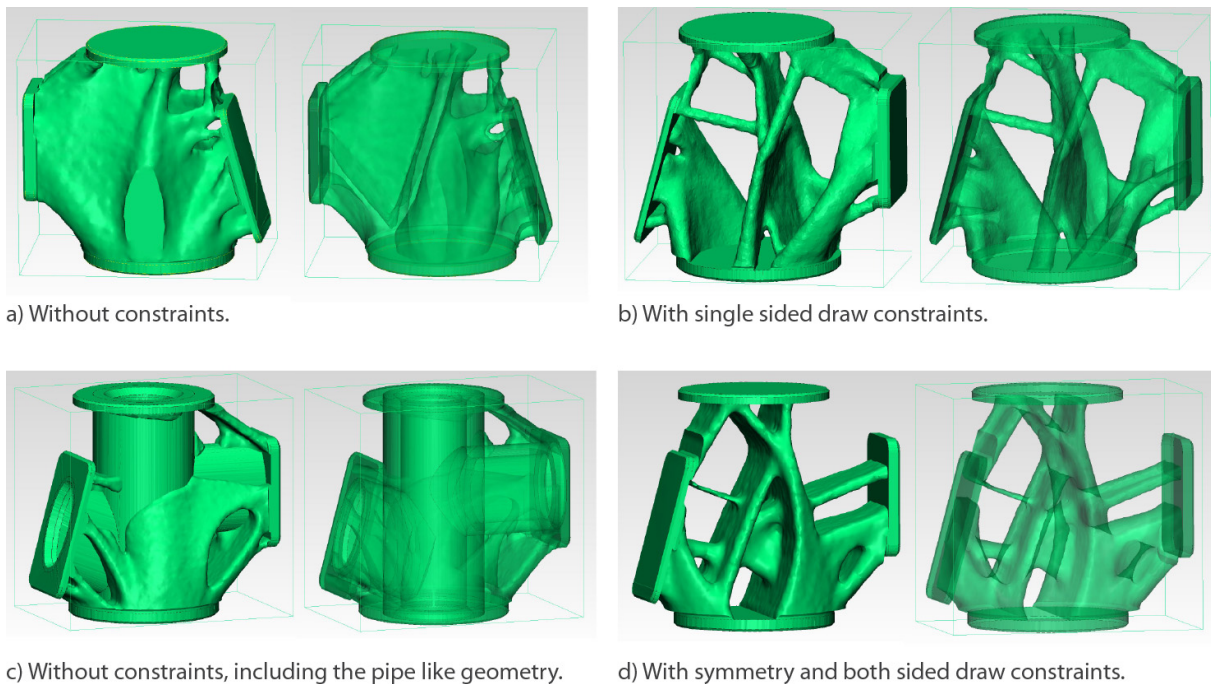


Figure 168. Material distributions resulting from the topology optimization studies at different design space and constraint settings. Transparent view on the right.

The topology optimization is in principle well suited for AM, but it is not possible to control the inclination angles of the resulting geometry in the current commercial software. The test

component was therefore designed traditionally by CAD for full control of the geometry in the design phase.

The topology optimization study shows, however, the potential of the method in concept studies. Variation in both the definition of the design space and the constraints, while boundary conditions (supports and loads) remain unchanged, leads to rather large variation in the resulting material distributions.

The topology optimization is studied in more detail by Erin Komi in VTT report [18].

5. Design studies

Several design studies were done to demonstrate the benefits of AM in component and product design. The main focus in the design studies was on the topology optimization, that was studied and reported by Erin Komi [18].

5.1 Topology optimized components

Finite element based topology optimization is a technique used to find the optimal distribution of material and voids in a given design space, dependent on loading and boundary conditions, such that the resulting structure meets prescribed performance targets [22]. The typical optimization process is described in Figure 169, starting with the definition of the design space limits and proceeding with FEM model creation, optimization definition and calculation, results interpretation, and finally smoothing and validation of a potential design.

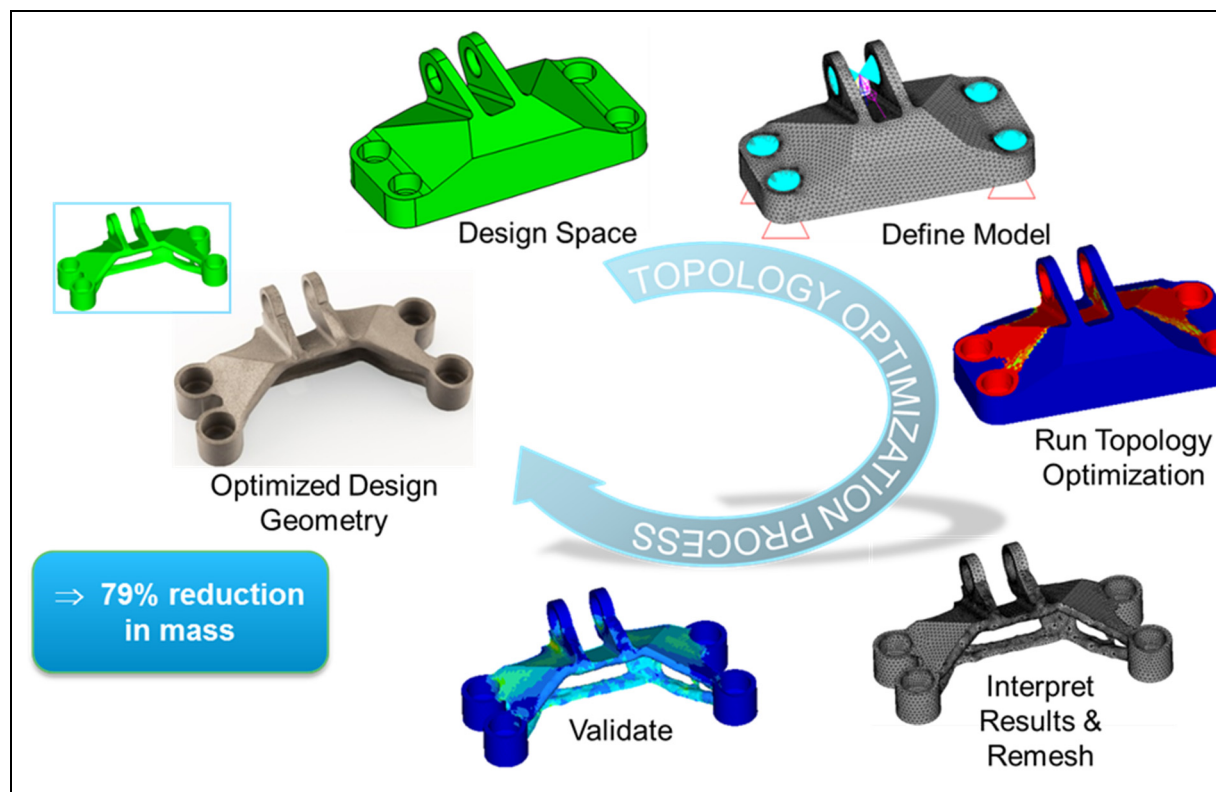


Figure 169. Description of the topology optimization process; redesign of a jet engine bracket shown as an example

Used in the early stages of the design process for concept generation, topology optimization can help reduce time and money spent by eliminating the need for typical trial and error methods and by reducing the number of necessary design iterations. Although this technique has been an available design tool for a few decades, restrictions imposed by traditional manufacturing techniques have severely limited its usefulness. This is changing now with the continuous development and increased use of AM in industry. With AM, it is possible to print almost any geometry – meaning that there are no longer harsh manufacturing restrictions limiting the potential for optimized design [23].

One example of utilizing topology optimization along with the developed SLM design guidelines is a topology optimized and additive manufactured hydraulic valve block that is described in Figure 170. Compared to the traditionally manufactured version that is made from circular drillings in a metal block and requires auxiliary drillings that must be plugged, this new design

features internal channels that improve fluid flow, minimizes the risk of leakage as there are no auxiliary drillings to be plugged, and reduces the size of the valve block by 76% [18].

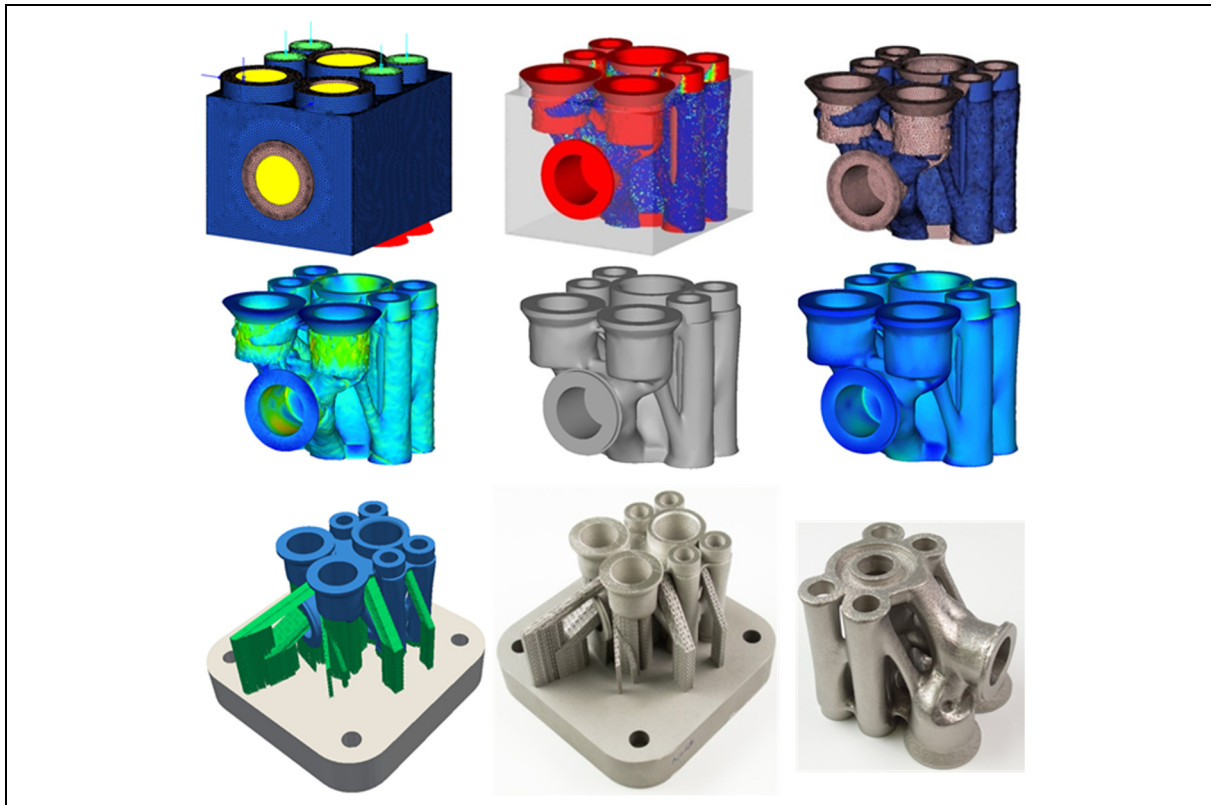


Figure 170. Process for designing a hydraulic valve block specifically for AM, including topology optimization, results interpretation, smoothing of design, design validation, and print preparation. The part was created for Nurmi Cylinders Oy.

While topology optimization can help determine the optimal placement of material in order to meet design requirements, there are additional factors to consider when designing for AM. Successfully printing a part necessitates knowledge of the specific requirements for a given AM technology, material being printed, build direction, build orientation, supporting structures and their removal, and post-processing procedures.

5.2 Light weight components utilising lattice structures

An illustration of a light weight component utilising lattice structure at the low stress areas is presented in the following figure. The lattices were modelled in MATLAB as examples. The 3D-printed lattice structures can be used in components in similar way to traditional honeycomb structures, but with the free form possibilities enabled by the SLM process. The lattice type should be self-supporting for best results in metal 3D-printing.

- Idea is to use *porous or lattice structure at low stress areas of structures*
 - shear forces between main load bearing structural elements can be transferred with porous material
 - traditionally honeycomb and foam type structures are used, but AM opens new possibilities
- *Load bearing areas* are needed to be build *as solid material* for high strength
- Areas with *functional surfaces* are needed to be build *as solid material*
- *High strength to mass -ratio is possible*
- Use of porous or lattice structures *reduces AM build time*
- New *possibilities for improved heat transfer, chemical reactions, etc.*
- Design principles, CAD modelling and stress analysis methods are in development phase

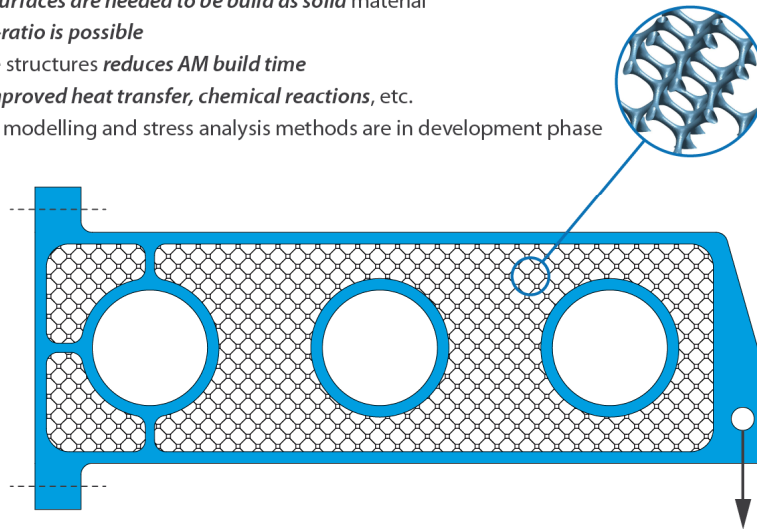
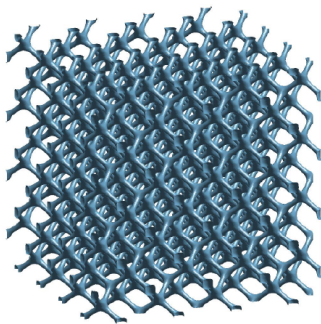
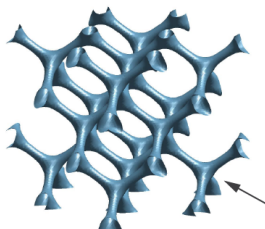


Figure 171. Illustration of a light weight component utilizing lattice structure at the low stress areas. The principles of traditional honeycomb structures can be used in SLM components utilizing the SLM design freedom and self-supporting lattices.

- Small repeating structures are possible with AM
- Very *small details* lead to decrease in *accuracy* and decrease for example in *fatigue strength*



A repeating structure (gyroid)



Transitions at junctions are in general good for fatigue strength with gyroid etc. mathematical, repeating geometries

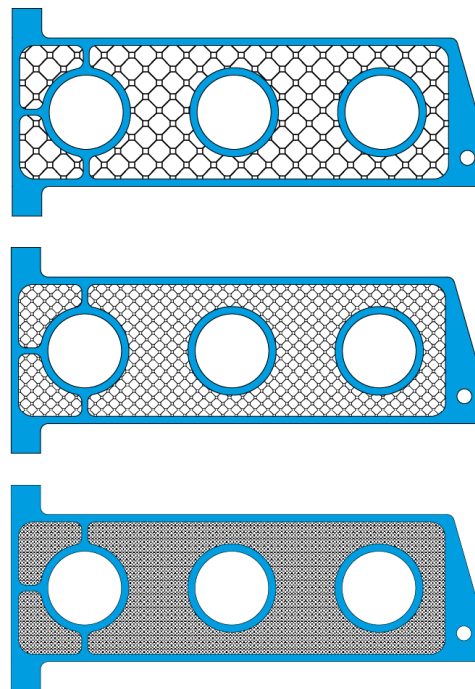


Figure 172. The basic thing to consider in using the 3D printed lattices is to choose a lattice unit cell geometry suited for metal printing and the size of the unit cell. The gyroid geometry is for example well suited for metal 3D-printing it is self-supporting. The surface roughness may limit the fatigue strength of a lattice structure. Care has therefore be taken in dimensioning such a structure for any real life structural use.

- Increase material towards the solid material regions or based on stress level
- Topology optimization can be used to guide material distribution
- Increase member thickness to carry more load locally
- For heat transfer
 - vary shape and member thickness to optimize heat conduction together with fluid flow through the net of cavities
- For vibration and noise
 - add damping material in cavities
- Approach is well suited for optimization

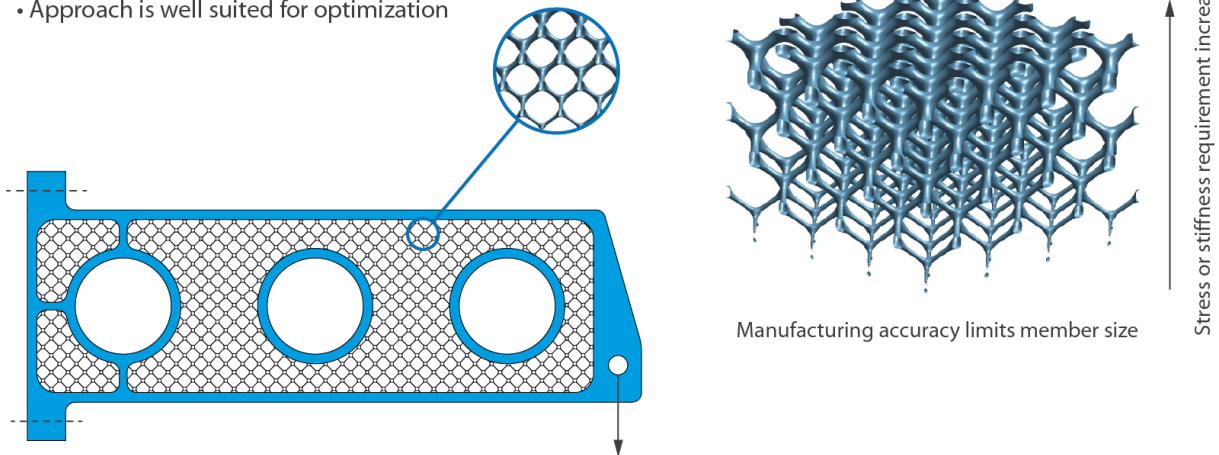


Figure 173. The thicknesses of the lattices can in principle be varied based on required stiffness and simulated stress.

The design study with lattices was decided to be left to later after the software support better design and analysis of such features.

5.3 Patterns and textures

Patterns and textures are straightforward to add on components by SLM. A design study was done to demonstrate a possible work flow for adding a pattern to a 3D-printed part. The example case is presented in the following two figures.

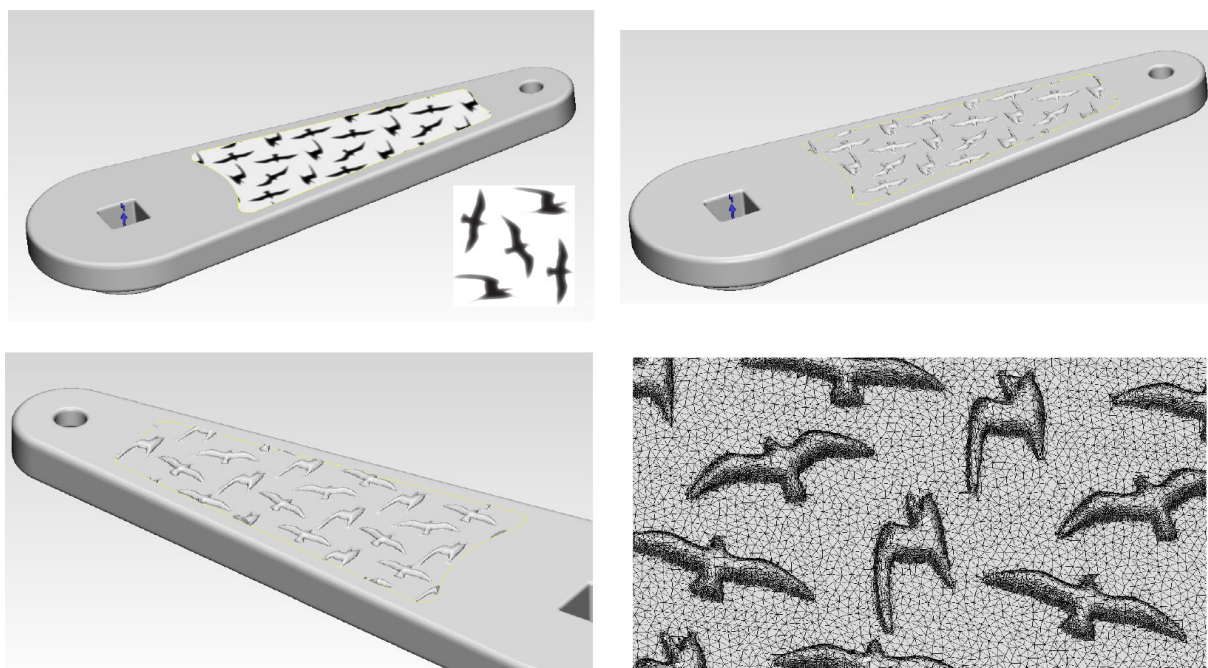


Figure 174. Example if emboss figures applied as pattern on an .stl model.

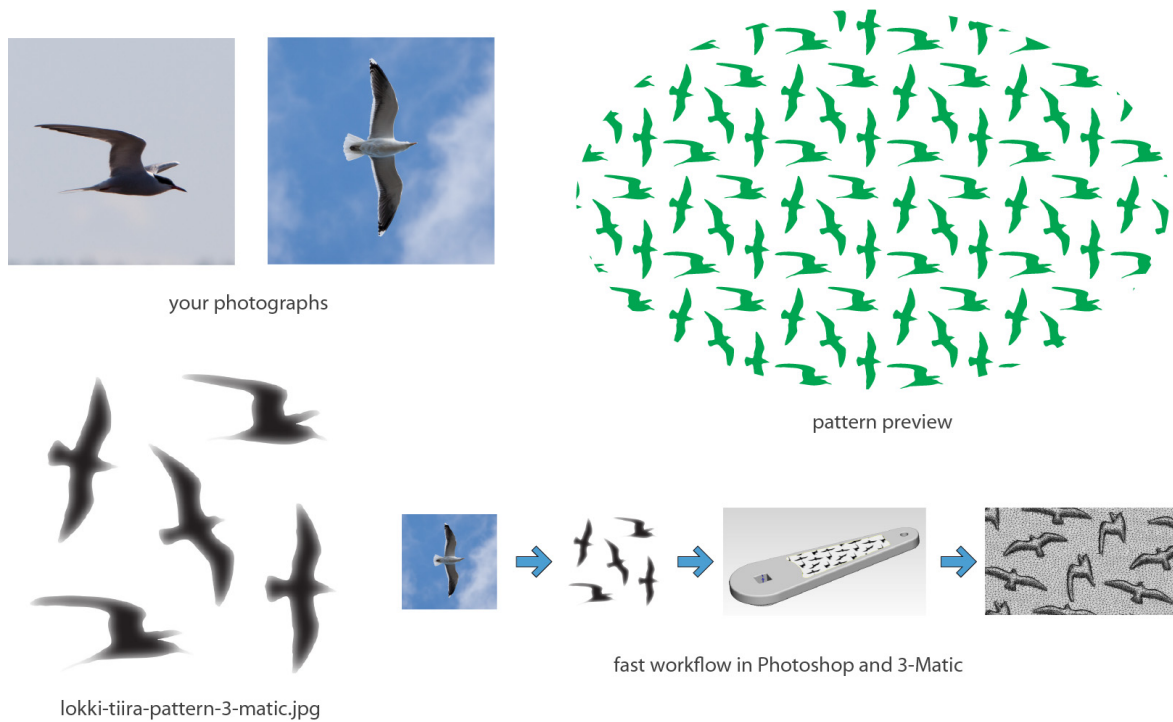


Figure 175. The work flow for creating a pattern from photographs in Photoshop and 3-Matic.

5.4 Design study of an ergonomic handle utilising re-engineering

An ergonomic joystick handle was studied as brief re-engineering study without traditional CAD-modelling based on laser scanning and editing the resulting polygon model. Laser scanning of the plastic clay model of the handle was done by Jukka Junttila, VTT, with FARO laser scanner. The scanned data was edited further in Materialise 3-Matic software.

- Case study of industrial joystick handle
- Traditional designs are based on CAD nurbs surface modelling
- Additive manufacturing (AM) allows organic free form design
- AM allows individual tailoring for improved ergonomics

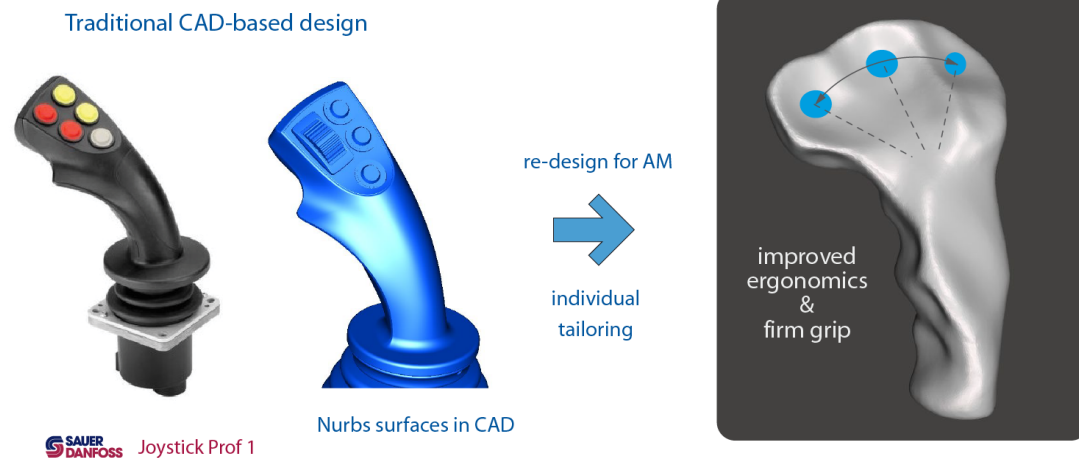


Figure 176. Example case follows the design of an existing commercial product.

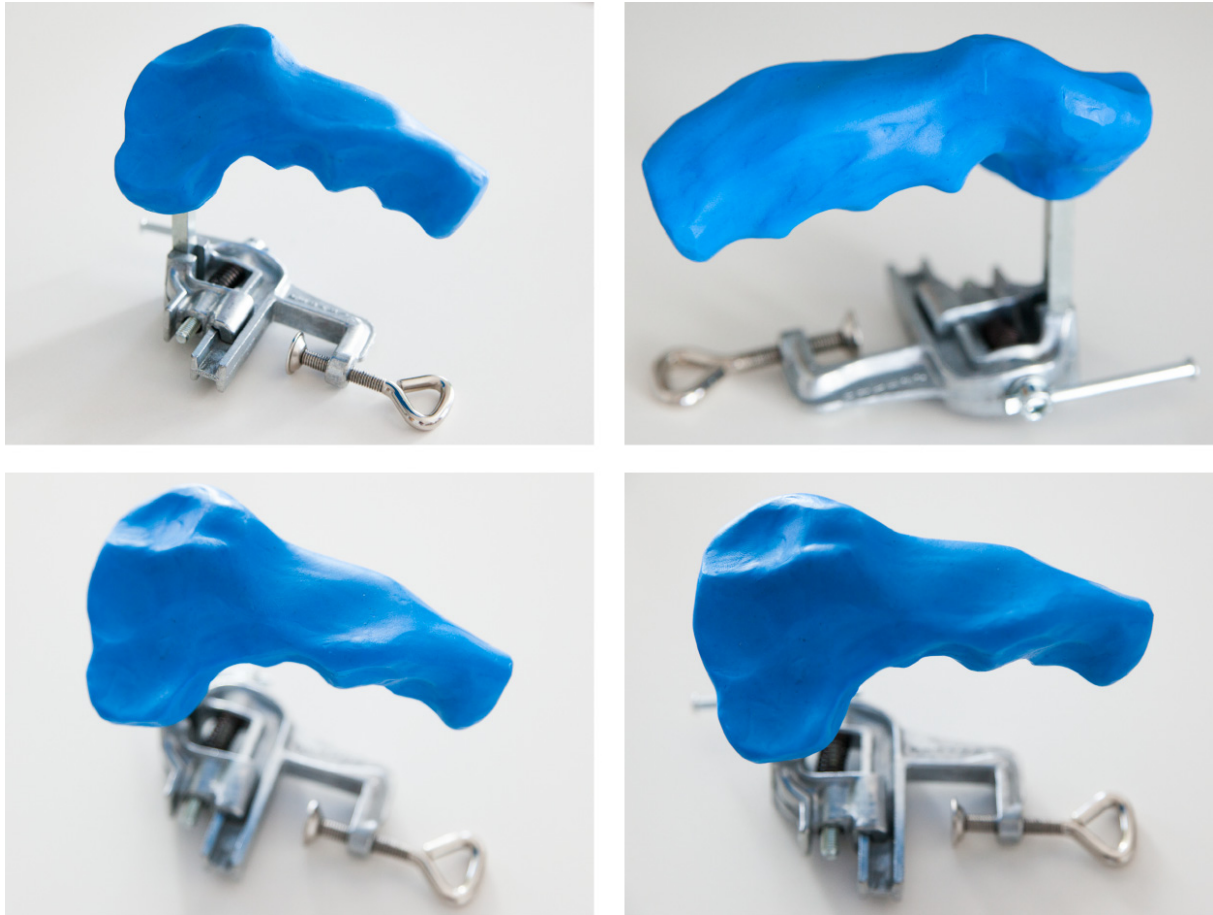


Figure 177. Plastic clay forming of the handle.

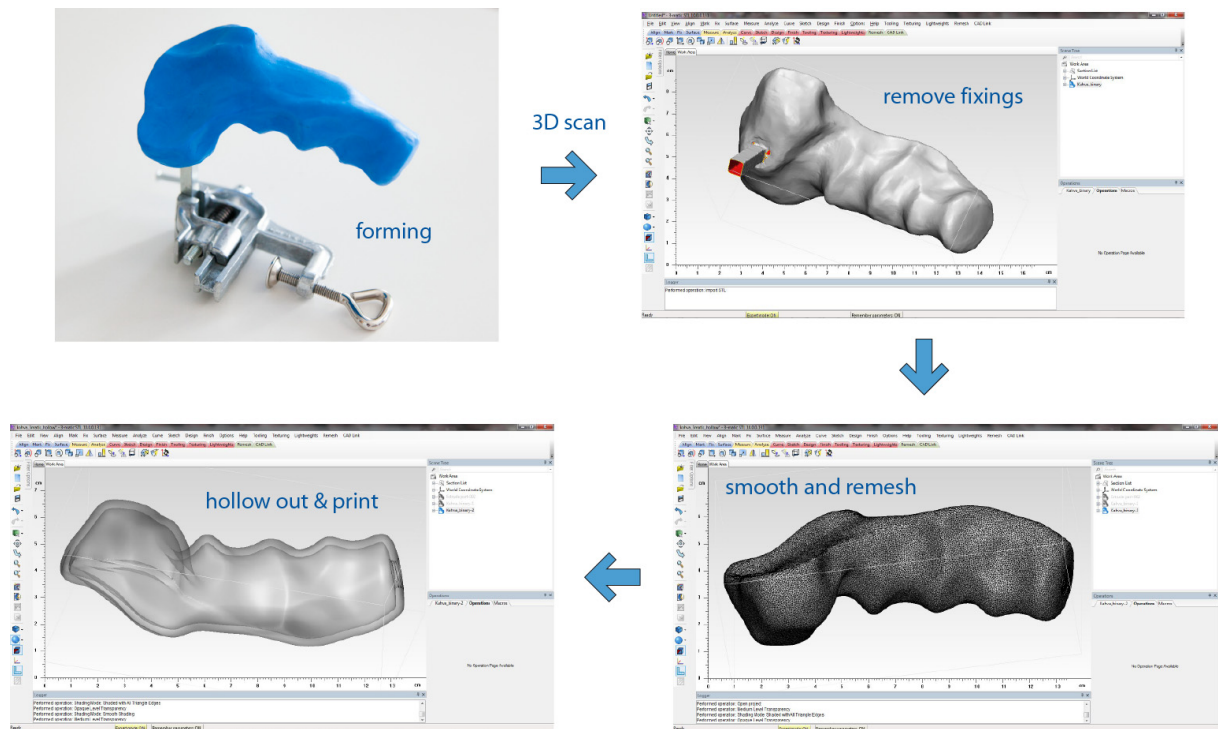


Figure 178. Editing, smoothing and hollowing out the model in 3-Matic –software.

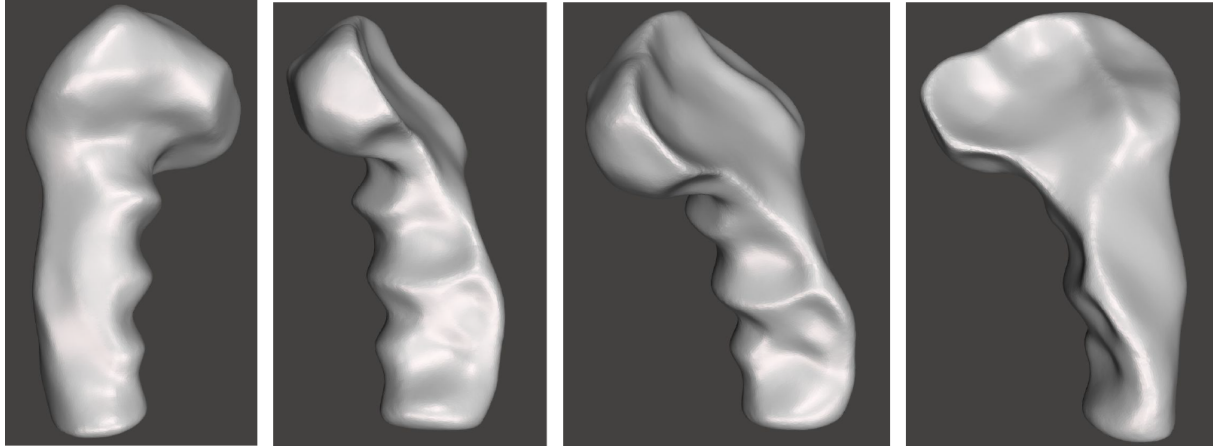


Figure 179. The completed shape as .stl file.

The handle was printed in plastic as a mock-up.

5.5 Concept study of consolidation of functions into single AM part

A fictional bioreactor concept utilising the AM design possibilities was drafted after examples in [6]. The sketch is illustrated in the following figure. The idea of combining the various functions to a single part is applied here in the example design. The various types of cellular and lattice structures can perhaps be used for mixing, heating (as heat exchanger), rotating and separation of fluids, etc. functions used in chemical processes.

The surface patterns and perforations may be used for cultivating bacteria or fungus for bioprocesses. From the design point of view, the lattice structures could be used as library elements and their sizes chosen based on fluid dynamic, thermal and chemical simulations to meet the process targets.

Bioreactor concept study utilising consolidation and AM lattice structures

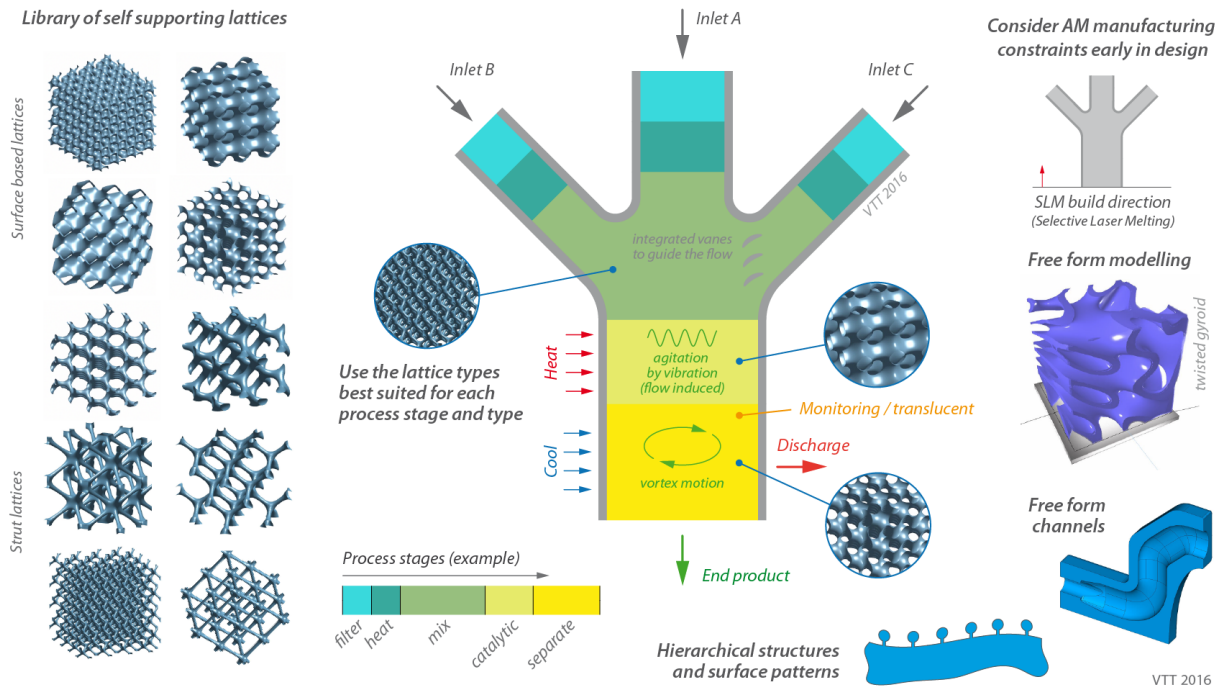


Figure 180. A highly fictional bioreactor concept utilising the AM design possibilities and various types of cellular and lattice structures. All the process functions are envisioned here to be consolidated into a single process component. The sketch is based on ideation and discussions between a larger group of people at VTT.

The smooth joining of the different types of lattices so that the part would be printable in metal is the main challenge from the design point of view with the current design software. For example the image based modelling software Monolith¹ that is being developed by Autodesk seems promising for this kind of modelling approach.

The design principles possible to be used in design of AM products were summarised from various sources during the work and are enclosed as Appendix B.

¹ <http://www.monolith.zone/#introduction>

6. Design and analysis workflows drafted for future research

Overviews of possible design and analysis workflows for SLM were discussed within the work group at VTT. The ideated workflows are presented as schematic illustrations in the following. The numerical simulation of the SLM process to get estimates of the thermal stresses, distortions and defect distributions early in the design phase was identified as a key component in the work flows. Including a numerical simulation of the SLM process in the workflow would increase the geometrical accuracy and durability of SLM components.

6.1 Geometrically accurate SLM components

A schematic workflow for obtaining geometrically accurate SLM components is presented in the following figure.

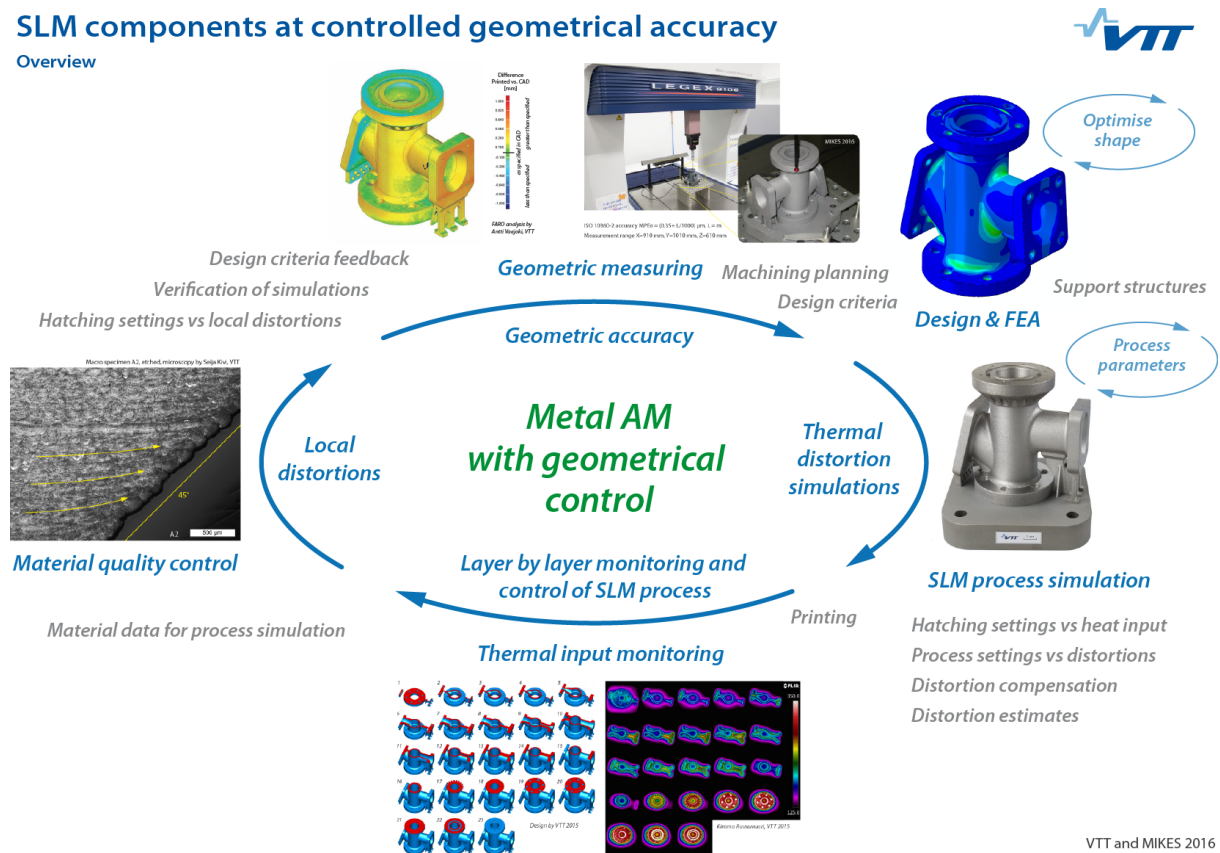


Figure 181. Distortion control workflow for obtaining geometrically accurate components.

6.2 Defect tolerant design of fatigue critical SLM components

The SLM process is prone to porosity, lack of fusion defects, thermal stresses and irregular surface quality. These factors have all significant effect on the fatigue strength of components. The thermal stresses acting as residual stresses during operation are known to have a significant effect on the fatigue strength of a component. The adjustments of the process parameters that improve the fatigue strength of SLM components tend also increase the build time and manufacturing cost. The situation is again similar to casting design, where assuming a defect free casting in fatigue dimensioning would lead to expensive manufacturing of such components. The standard practise in castings is to allow manufacturing and material defects for example at low stress areas of the components and revise the design based on casting simulation and structural optimization.

A similar design approach can be utilised in design of SLM components. An overview of such a defect tolerant fatigue design –concept for SLM process is illustrated in the following figure.

Defect tolerant fatigue design

Overview

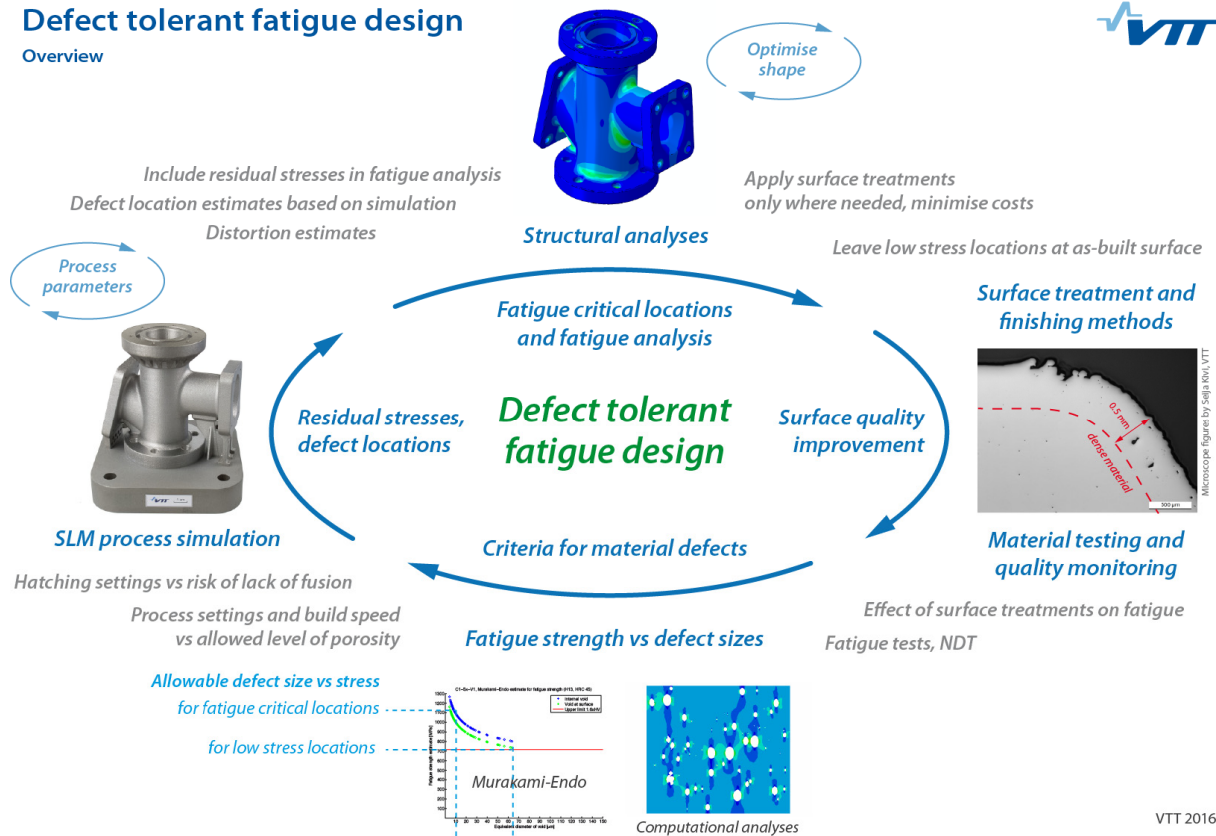


Figure 182. Overview of the defect tolerant fatigue design –concept.

The tools for assessing the effect of the defect sizes on the fatigue strength have been developed earlier at VTT for fatigue analysis of cast, welded and forged components. The tools were applied to SLM test print macro specimens as part of this work. Two approaches are used, a fast tool based on the Murakami-Endo method [11] and a numerical tool based on the finite element method (FEM). Both approaches utilise image analysis for detecting and classifying the defects (pores, graphite in cast iron, inclusions, etc.). Standard macro specimens and optical microscope images are used. The image analysis is done in the MATLAB environment. The meshing is done in MATLAB. The application writes the FEM input file with all the definitions needed to analyse the stresses in the main loading directions. The procedures are illustrated in the following figure.

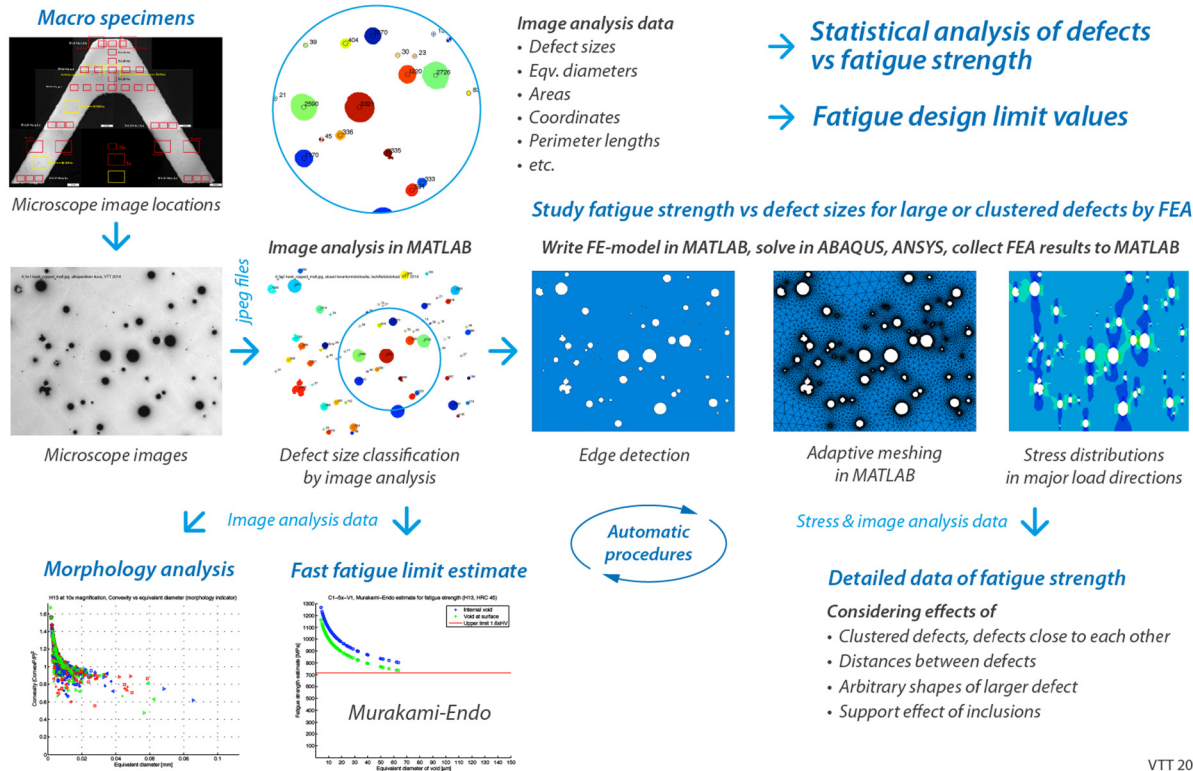


Figure 183. The tools for assessing the effect of the defect sizes on the fatigue strength.

The Murakami-Endo method [11] applied with image analysis of an SLM test print microscope image in MATLAB is explained in the following figure.

Murakami-Endo formula for fatigue strength

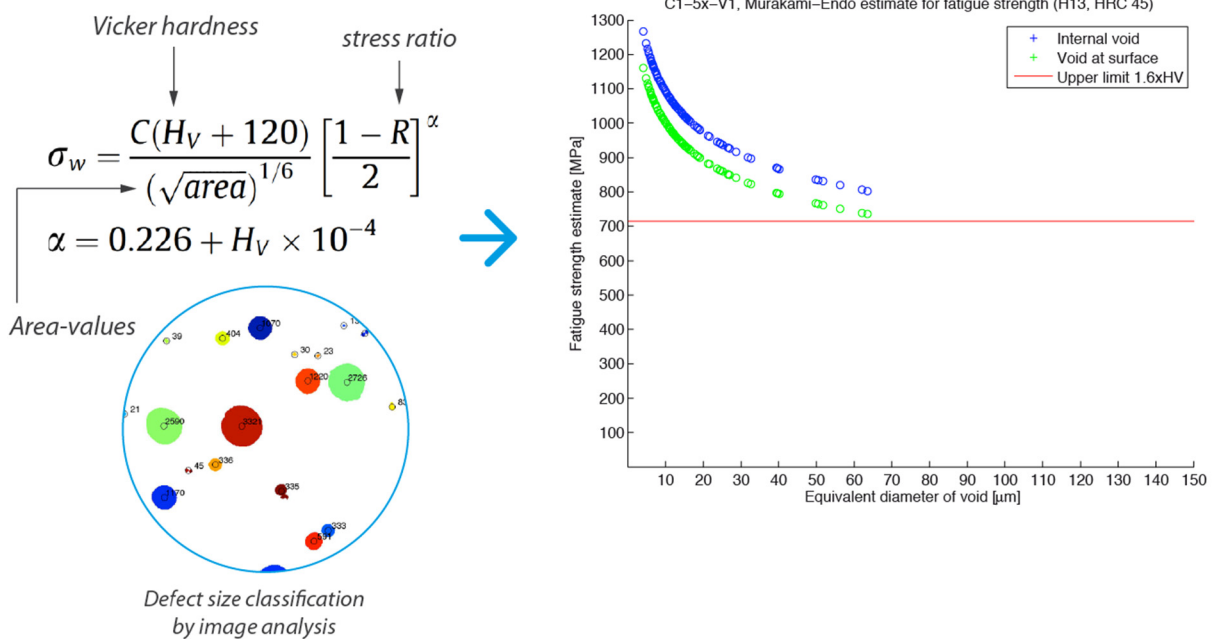


Figure 184. An example of the Murakami-Endo method applied with image analysis to SLM test print microscope image in MATLAB.

7. Discussion

7.1 Geometric accuracy of SLM components

The thermal distortions are the main cause of deviation of geometric accuracy in SLM manufactured parts. The extent of the distortions depends on the material, laser power, scanning strategy, process settings and process control, pre-heating, cooling between layers, and also on the geometry of the part, intended printing orientation and the support design.

Unsymmetry, open profiles, cut outs, holes, cavities, channels, undercuts, uniting branches, etc. features cause deviation of dimensional accuracy in SLM parts. The layers are built on top of the previous layers, and the dimensional inaccuracy at the bottom layers affects in principle the rest of the part.

The geometrical accuracy and the thermal distortions are considered more important than the dimensional deviations in the design of structural components. The geometric accuracy of the test component printed in H13 was assessed to fall between SFS-EN ISO 8062-3 linear dimension casting tolerance grades (DCTG) 4 and 5 at component level. Even DCTG 1 and DCTG 2 accuracies were met at individual features.

Sources of geometric inaccuracy in SLM due to thermal distortions are listed in Appendix D.

7.2 Machining allowances

SLM process is considered a near net shape manufacturing method in mechanical engineering point of view. The need for machining is at best minimal, when the thermal distortions are kept to minimum by careful design and controlled manufacturing, but some machining is required for the SLM components.

The machining allowances need to be defined to compensate the deviations of geometrical accuracy such as thermal distortions and local small ridges, surface irregularities and subsurface porosity.

Use of small machining allowances typically require detailed knowledge of the manufacturing process (SLM), close co-operation with manufacturing in the design phase, and use of process simulation to support the structural design.

The amounts of required machining allowances were noted to depend on the direction of the printed surfaces.

Accurate holes are needed to be drilled or reamed. A pre-hole helps in reaming. A suitable diameter of a pre-hole in small components is considered here as 0.8 x end diameter (for threaded holes). A rule of thumb machining allowance value of minimum of one millimeter is recommended for the SLM process.

The guide values for machining allowances for the SLM process defined in the VDI guideline [1] are consistent with the findings in this work. This work was limited to small test pieces and a rather small test component. Larger components are recommended to be studied in future research projects.

7.3 Surface quality of the SLM test prints

The surface roughness of SLM metal parts is generally too high in the as-built state to be used in actual end-products especially for functional and fatigue critical surfaces. The surface quality of SLM parts is affected e.g. by orientation of the parts, overhangs, layer thickness during printing and powder size.

When SLM parts are to be used in end-products, possible post-processing of the components is important already in the early stages of the process. The designer needs to take post-processing into account in the design phase similarly to designing machining allowances.

Different post-processing methods may vary substantially and there are multiple methods available. For example, depending on the material used when producing an SLM component, the part may need stress relieving or other heat treatments in elevated temperatures. This may also change the surface roughness of the part if the surface gets oxidised causing a need for subsequent removal of the oxidised layer. One needs to also be aware that post-processing may take substantial amount of time and resources. If the post-processing methods are not automated or automated processes cannot be used, this may mean many hours of manual labour. However, the requirements for the end-use should be deciding factors on which kind of post-processing to use.

Surface post treatment methods and the surface roughness of the test pieces are discussed more in detail in a research report by Antti Vaajoki and Sini Metsä-Kortelainen, VTT [20] (in Finnish), and in an article draft [21]. The corrosion resistance was not studied in this project.

7.4 Fatigue strength estimates of the SLM test prints

The brief study of the macro specimens by the Murakami-Endo method and image analysis indicate that the majority of the pores have rather little impact on the fatigue limit estimate. The majority the fatigue limit estimates are above the Murakami-Endo upper limit estimate $1.6 \times \text{Hv}$. Based on the brief study, only the larger pores indicate fatigue limit estimates below the Murakami-Endo upper limit estimate $1.6 \times \text{Hv}$.

Further studies in more detail with fatigue tests and including the effect of residual stresses in the assessment of fatigue strength need naturally to be done for forming understanding of fatigue behaviour of SLM materials.

8. Conclusions

Designing components manufactured by SLM requires knowledge of the SLM process, materials and machining in addition to just design practices. While the SLM process provides design freedom, it also sets many untraditional manufacturing constraints for design of metal components.

The manufacturing constraint limit values and findings of the test prints of the geometrical features are discussed in the report and are summarised as a slide enclosed as Appendix A.

After a reasonable learning period the SLM process could be applied to design and manufacturing of a rather complex component of main dimension of 104 mm x 110 mm x 70 mm with geometric accuracy comparable to traditional manufacturing. The printing time of the test component was 30 hours. The geometric accuracy of the test component printed in H13 was assessed to fall between SFS-EN ISO 8062-3 linear dimension casting tolerance grades (DCTG) 4 and 5 at component level.

As the SLM process is basically a welding process, it is prone to porosity and various manufacturing defects and thermal distortions and quality control and material testing are an important part of SLM manufacturing.

Based on the test series, the open grate type support structure with block support or direct build from base plate with cutting allowance are recommended as support types for SLM components for mechanical engineering applications.

The topology optimisation studied here by Erin Komi is an effective tool for minimising mass and build time of SLM components. The lack of automatic control of the SLM manufacturing constraints in the current topology optimisation software adds at the moment a bit the challenge in the use of topology optimisation in AM design.

The full benefit of AM is obtained by starting the design from a well defined design target and taking distance to the traditional design approaches and limits of the traditional manufacturing methods.

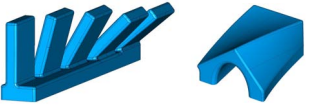
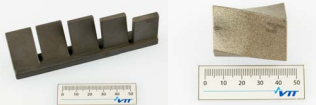



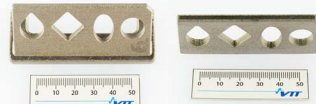

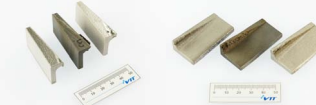
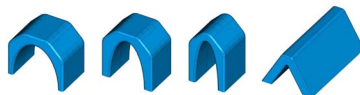


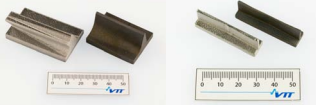
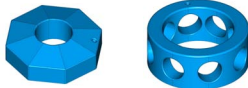

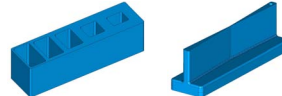

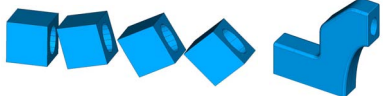
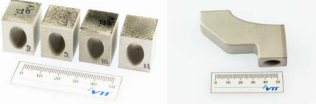


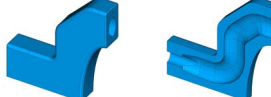

The fatigue strength and quality assurance topics, design work flows utilising the SLM process simulation and including systematic design methods, multiphysical simulation and optimisation in the design processes are seen as the recommended topics to study in future development projects.

References

- [1] VDI 3405 blatt 3, Additive Fertigungsverfahren. Konstruktionsempfehlungen für die Bauteilfertigung mit Laser-Sintern und Laser-Strahlschmelzen, VDI-Gesellschaft Produktion und Logistik, Düsseldorf 2015.
- [2] Ian Gibson, David Rosen, Brent Stucker, Additive Manufacturing Technologies 3D Printing, Rapid Prototyping, and Direct Digital Manufacturing, Second Edition, Springer 2015, ISBN 978-1-4939-2112-6.
- [3] Daniel Thomas, The Development of Design Rules for Selective Laser Melting, Ph.D. Thesis, University of Wales Institute, Cardiff, UK, 2009.
- [4] Guido A. O. Adam, Systematische Erarbeitung von Konstruktionsregeln für die additiven Fertigungsverfahren Lasersintern, Laserschmelzen und Fused Deposition Modeling, Dr thesis, Universität Paderborn 2015, ISBN 978-3-8440-3474-5.
- [5] Guido A.O. Adam, Detmar Zimmer, Design for Additive Manufacturing—Element transitions and aggregated structures, CIRP Journal of Manufacturing Science and Technology 7 (2014).
- [6] Olaf Rehme, Cellular Design for Laser Freeform Fabrication (Volume 4), Ph.D. Thesis, TU Hamburg 2010, ISBN 9783869552736.
- [7] Kai Zeng, Optimization of support structures for selective laser melting. University of Louisville, (2015). Electronic Theses and Dissertations. Paper 2221.
- [8] Fraunhofer Direct Digital Manufacturing Conference DDMC 2016, proceedings.
- [9] Jukka-Pekka Järvinen, Ville Matilainen, Xiaoyun Li, Heidi Piili, Antti Salminen, Ismo Mäkelä, Olli Nyrhilä, Characterization of effect of support structures in laser additive manufacturing of stainless steel, 8th International Conference on Photonic Technologies LANE 2014.
- [10] E. Yasa, T. Craeghs, M. Badrossamay, J.-P. Kruth, Catholic University of Leuven, Leuven, Belgium, RapidTech 2009.
- [11] Yukitaka Murakami, Metal Fatigue: Effects of Small Defects and Nonmetallic Inclusions, Elsevier 2002.
- [12] ISO/ASTM DIS 20195:2015-05, Standard Practice - Guide for Design for Additive Manufacturing, draft standard, ISO 2015.
- [13] ASTM F2792 Terminology for Additive Manufacturing--Coordinate Systems and Test Methodologies.
- [14] SFS-EN ISO 5817 en2006-11-06 Welding. Fusion-welded joints in steel nickel titanium and their alloys - beam welding excluded - Quality levels for imperfections.
- [15] SFS-EN ISO 6520-2en - 2002-03-04 - Welding and allied processes. Classification of geometric imperfections in metallic materials.
- [16] Paavo Asanti, Valukappaleen suunnittelu I - II, WSOY Porvoo 1962.
- [17] Reetta Riihiaho, Research Report No. VTT-S-08867-13, VTT Expert Services Ltd, 2013.

- [18] Erin Komi, Design for Additive Manufacturing, Research Report VTT-R-03159-16, VTT 2016.
- [19] Antero Jokinen, Tuomas Riipinen, AM:ään soveltuvien materiaalien ja materiaaliyhdistelmien ominaisuuksien tutkiminen ja kehittäminen, Tutkimusraportti, VTT 2016.
- [20] Antti Vaajoki, Sini Metsä-Kortelainen, AM-prosessin integrointi tuotantoon – metalliosien valmistuksen työvaiheet, Tutkimusraportti, VTT 2016.
- [21] Antti Vaajoki, Sini Metsä-Kortelainen, Pentti Eklund, Petri Laakso, The effect of micropeening on the surface roughness of SLM 316L specimens. Article draft 2016.
- [22] M.P. Bendsøe and O. Sigmund, "Topology Optimization: Theory, Methods, and Applications, 2nd ed., Berlin, Springer-Verlag Berlin Heidelberg, 2004.
- [23] K. Salonitis and S. Zarban, "Redesign optimization for manufacturing using additive layer techniques," Procedia CIRP, vol. 36, pp. 193-198, 2015.

Summary of SLM design recommendations

Feature	Test geometry design	SLM test pieces	Key remarks	Design limit values	Design recommendation
Inclined surface			Even 40° unsupported plate prints fine at small SLM layer thickness. Surface quality.	40° for materials with good temp. conductivity, small layer thickness and small parts.	40° is possible, but follow the 45° rule for large components. Mind proper heat conduction and machining allowances.
Round holes			Round holes print fine, but dross forms at inclined holes. Finishing/reaming is required.	Ø 1 mm is practical minimum for holes. Transversal holes print fine up to Ø 25 mm.	Supports are not needed at least up to 25 mm diameter based on VTT tests. Finishing is needed to remove dross.
Self supporting holes			Self supporting cross sections print fine. Sharper top shapes lead to less dross at top of hole.	Avoid small holes for long internal channels. Slight dross will result at top location.	Slight dross is formed at top of the cross section. Use diamond or tear drop sections for best surface quality.
Overhangs			Large overhang length leads to recoater wiper failure. Fillets support the overhang.	Use fillets to support overhangs and to avoid dross. Improve heat conduction for less dross.	Maximum unsupported overhang length is a few millimeters, as the rule of thumb. With fillets several millimeters are possible.
Island junctions			Island type parts print fine, but dross and transversal shrinkage take place.	Dross forms at top of arch. Transversal shrinkage increases as span length increases.	Use 45° inner angle and R0.5...1.0 fillet at top for minimum dross. Mind the effect of transversal shrinkage in design.
Fillets			Fillets print at rather rough surface quality and require finishing for structural parts.	The stair step -effect limits the min. radius. R0.2...0.5 possible. Mind the dross at downskins.	Stair step -effect leads to poor surface quality at near flat end of the fillet. Downskin fillets suffer from dross.
Effect of angular orientation			Slight spatter was the only variation along the angular orientation in the test prints.	Angular orientation does not affect the print quality to practical extent.	Angular orientation sets no limits due to printing quality. Consider the recoater direction in part orientation.
Wall thickness			All test pieces printed fine. Minimum thickness 0.15 mm possible, but slightly irregular.	Thick walls will collect heat. Minimum thickness 2...3 x laser focus diameter; 0.5 mm	Vertical walls print fine even at quite small wall thickness. Avoid excessive span length and height.
Elliptic channels			Elliptic channels printed fine at all inclination angles. Dross formation at top locations.	Avoid small holes for long channels. No supports needed. Dross removal may be needed.	Use self supporting cross sections for internal channels. 90° turns are possible and no supports are needed.
Small details			SLM resolution limits the quality of small details. Mind the burr at sharp edges.	Functional small grooves etc. are best done by machining.	Use overall fillet radius of min. (0.25 ...) 0.5 mm to avoid burr at sharp edges.
Dross at channel			Abrasive flow machining may be used for dross removal and finishing of the inner surfaces.	Avoid small holes for long channels. No supports needed. Dross removal may be needed.	Slight dross is formed at top of the cross section. Use diamond or tear drop sections for best surface quality.

Examples of solution principles that can be combined to meet the design target

Metal additive manufacturing

		Microstructure (localised, controlled)	Cellular & lattice structures Porosity	Free forming Solid structures	Internal channels and cavities	Surface patterns Perforation patterns		
Physical principles	Acoustics		sound absorbing structures		sound absorbing surfaces (patterns)			
	Vibration		consolidated design (combine functions to less parts)			embedded damping (cavities filled with granular material or elastomer)		
	Mechanics	hollow components low weight, low inertia		structural topology optimisation		chemical agitation by vibration		
	Heat transfer	weight, inertia, density, elastic modulus anisotropic properties		composites, multimaterial		integrated journal bearings (porous fluid pockets)		
	Fluid flow	mass transfer by vibration		modular and hierarchical structures			flow induced vibration	
	Electromagnetics	free form heat exchanger design		consolidated (integrated) design for continuous heat conduction			modify heat transfer coefficient by surface patterns	
	Energy	microfluidic systems		heat transfer topology optimisation		conformal cooling channels		
		buoyant components		various profile and non-circular channels			living bed and process conditions for bacteria or fungus	
		slow flow, filtration, diffusion		integrated vanes to guide flow				
		actuated membranes		flow straightening by vaned channels		channel flow topology optimisation		
	free form copper parts		directional flow (Tesla valve) (no moving parts)		injection of process chemicals via microchannels			
	free form magnetic parts		consolidated design (combine functions to less parts)		modify flow boundary layer by surface patterning		vortex generators	
			conformal functionality				vortex flow for separation	
			sintered coils		modify frequency dependent properties by surface patterning			
			composites, multimaterial					
			localised/optimised/conformal energy transfer					
			functional membranes hydrophilic/phobic surfaces		improved energy transfer/absorption		lotus leaf whale fin bumps gekko feet	

Material and surface science, advanced fabrication methods

Catalytic reactions
 Reactional surfaces
 Battery beds
 Filtering, separation, mixing
 Biomimics
 Chemical, process and bioengineering

AM terminology

The key terms related to metal additive manufacturing (AM) are listed in the following with brief descriptions. The AM process names and abbreviations are often trademarks, and similar processes may exist at various names by the various 3D-printer providers.

- 3DP, 3D-Printing, less formal name for additive manufacturing (AM)
- LAM, Laser Additive Manufacturing
- SLM, Selective Laser Melting
- SLS, Selective Laser Sintering
 - Also called as Direct Metal Laser Sintering (DMLS), which however may refer also to Selective Laser Melting –type process.
 - The difference between SLM and SLS is in practice that in SLM the material is heated above melting temperature, but in SLS it is not so the particles are only sintered together rather than fully melted. SLM has typically lower porosity and is therefore better suited for structural components.
 - and machines from 3D Systems Corporation.
- EBM, Electron Beam Melting
 - Electron Beam is used instead of laser in a powder bed process.
- LMD, Laser Metal Deposition
 - Also called as laser cladding (LC)
 - Powder feeding directly on the melt pool / laser focal point, therefore not needing a powder bed.
 - Can be used also for repair welding (coating) of a failed component.
 - For example LENS, Laser Engineered Net Shaping by Optomec Inc.
- SMD, Shaped Metal Deposition
 - SMD uses wire based welding as AM system. A near net shape part obtained by SMD is finished by machining.
- Hybrid methods in metal AM
 - Systems combining Laser Metal Deposition and CNC machining.
 - Systems are provided for example by DMG Mori and Matsuura.
- STL
 - The STL file format is currently widely used for representing the geometry for the 3D-printer. STL is based on linear (planar) triangular facets. Typically large amount of linear triangles are needed for curved components. More sophisticated file formats based on parabolic etc. higher order representations are being developed, for example the 3MF and AMF file formats.
 - STL does not support colors or other information than the geometry. Color, texture, support design and material information are being developed into the forthcoming file formats.
 - STL-files can be edited effectively by modelling software such as 3-Matic and Blender, but not by traditional NURBS based CAD software such as CATIA or I-DEAS. STL-based modelling software are good tools for smoothing topology optimization results, organic design, and adding patterns and textures, but not

for accurate engineering modelling. Both are needed for effective design of industrial AM components.

- NURBS, Non-uniform rational B-spline, mathematical representation of curves and shapes used in CAD/CAM software.
- NURBS based STEP file format is often used to transfer geometry data between CAD-software.
- Topology optimization, (no abbreviation)
 - A numerical method for estimating the best material distribution for various design intents. The target of optimization is called the *objective function* and the available space given for the optimization tool is called the *design space*.
 - Topology optimization can be used for example to
 - minimization of mass, maximization of stiffness, both with stress, frequency and displacement limits.
 - shaping cooling fins for heat transfer.
 - Optimization of internal channel flow with various inlets and outlets within complex and limited available space by computational fluid dynamics (CFD).
 - The AM manufacturing constraints are currently being developed into the commercial topology optimization software according to Altair etc. software vendors, but such features were not available at the time of AM-Liito project.
- Design freedom
 - The phrase often used in marketing. This is of course not entirely true as there are various manufacturing constraints related to AM and especially to metal AM such as SLM. But anyhow AM gives completely new ways to design products.
- Near net shape
 - Manufacturing parts close to final dimensions for less milling and finishing.
- Powder bed
 - In layer based AM methods the part is built layer by layer on a powder bed. The part is covered entirely in powder during printing.
- Recoater, wiper, blade
 - The blade spreading the new layer of powder after melting.
- Building platform
 - The base plate onto which the part is printed, providing rigid support for the built part.
 - The base plate is typically pre-heated before printing.
- Scanning
 - The laser path during the melting.
- Hatching
 - The sequence and shape of raster of the laser paths during the melting.
 - The scanning pattern is typically a chess board style grid. The direction of the pattern and the individual grid patterns are often varied from layer to layer.
- Lattice structures

- Hollow structures used for light weight structures. Often unit cube lattices are repeated and randomized for getting isotropic (uniform) properties.
- For example the traditional honey comb structures are often replaced by the lattice structures in AM.
- The current trend is to map stress analysis (FEA) results on the lattice structure and vary lattice thickness based on the stress. This is often called spatially varying stiffness and density.
- 45 degree limit angle
 - The often used rule of a thumb limit value for surface inclination for AM.
 - Limit value for inclination depends on material, process, layer thickness etc. but following the 45 degree limit value you are on safe side.
 - In practise there is no definite limit value, but quality decreases gradually.
- Supports
 - External support structures are added to the part before printing to support the down skin surfaces where needed. The support design is an important step in the production.
 - The melt metal needs support during solidification. The powder has insufficient stiffness, so additional support structures are built to provide support for the downward facing surfaces in powder bed processes.
 - The supports are important also for heat transfer and preventing warping due to thermal stresses.
 - The supports need to be removed manually or by power tools, so the use of supports is often kept to minimum. Planning the removal of supports needs to be considered during the design process.
 - Removal of supports require accessibility, may be time consuming, and has effect on the surface finish. In addition there is the risk that poorly planned removal of supports may damage the surfaces or distort the component.
 - Need of supports depends on the material, process, process parameters, layer thickness and accepted surface quality and distortions. You can compensate the rough manufacturing by bigger machining allowances and mill the part to required functional dimensions, if this leads to better over all cost effectivity and result.
- Fragmentation and perforation of supports
 - Adding break lines to the block supports for easier support removal.
 - The block supports can be also perforated for saving material and decreasing build time.
- Down skin and up skin surfaces
 - Downward and upward facing surfaces of the printed part.
 - Down-facing surface, up-facing surface.
 - In Finnish they are called yläpinta and alapinta.
- Self-supporting surfaces
 - Down skin surfaces with inclination angle above the 45 degree limit angle, therefore do not require external support structures.
- Overhangs

- Steps and undercuts that are not self-supporting, and therefore require external support structures during printing.
- Melt pool control
 - The quality of SLM can be improved especially at overhangs by image based evaluation of the melt pool and real time control of the laser melting.
- Nesting
 - Nesting means the placing of the individual parts on the base plate before printing.
 - The parts are typically tilted and rotated slightly, to avoid jamming of the recoater with the part edges and decrease the heat input per layer.
 - The orientation of the part for printing affects also the maximum dimensions of the part and the support design. The printing orientation needs to be considered already in the design phase for metal SLM parts.
- Slicing
 - Due the layer-by-layer approach of many AM processes, the part (.stl file) and supports are sliced in the printing software (e.g. Magics) and this sliced data is then sent to the 3D-printer for printing.
- Staircase effect
 - The layer based manufacturing leads to stepped surface in the 3D-printed part.
 - The staircase effect gets smaller and the surfaces smoother as the layer thickness is decreased.
- Dross formation
 - Partial melting and attachment of powder at the down skin surfaces due to local excessive heat input or insufficient heat transfer.
 - The metal powder does not conduct heat well. This causes the heat from laser to melt the powder under the down skin surfaces deeper than the desired layer thickness, leading to the attachment of powder called the dross formation.
 - The term dross is originally used in the casting industry.
- Warping, warpage, curving, curling
 - Thermal distortions.
- Electrical discharge machining (EDM)
 - https://en.wikipedia.org/wiki/Electrical_discharge_machining

Sources and minimising of geometric inaccuracy in SLM

The sources of geometric inaccuracy in SLM and the general recommendations how to minimize their effects are listed in the following.

Material related factors related to thermal distortions

- Thermal conductivity
- Thermal expansion coefficient

Process related factors related to thermal distortions

- Layer thickness
- Cooling time time between layers.
- Laser power, speed, etc. factors affecting the *heat input*

Design related factors related to distortions and deviations in geometric accuracy

- STL-file accuracy, using fine triangulation leads to best results.
- Unsymmetry, may cause curving of printed component.
- Open profiles
- Thick junctions, *ainekeskittymät*
 - Prefer thin sections and avoid heavy sections. Casting design guidelines provide good general design examples that are in principle applicable for SLM also. Use relief holes and cut outs to avoid thick sections that would result to excessive heat input during laser melting.
 - Use smooth transitions.
 - Avoid abrupt changes in material thickness.
 - Heat input per layer can be affected in design phase also by finding a favorable printing orientation.
- Cut outs, holes, cavities, channels, undercuts
- Junctions of uniting branches
 - Mind the transversal shrinkage.
 - The resulting ridges can often be included in machining allowances in small components.
- Wiper failure
 - Caused by dross locations (overhangs) with local heat concentrations.
 - Causes the sagging lines at all layers following the wiper break, as the wiper shape is copied on the spreaded powder.
 - Can be prevented or decreased by ensuring good heat transfer by proper support design for overhangs.

Other sources of geometric inaccuracy in SLM

The sources of geometric inaccuracy in SLM and the general recommendations how to minimize their effects are discussed in the following.

Material related factors

- Thermal expansion, thermal conductivity, melting temperature. The factors that affect the thermal distortions.
- Process simulation can be applied in the future as the software are available for SLM process, for finding appropriate process settings and design to minimise or compensate the thermal stresses and distortions.

Process related factors

- Location accuracy of the base plate in the SLM-machine.
 - (The operator of the SLM-machine should) eliminate clearances by tolerated self guiding surfaces and fitted screws.
- Layer thickness
 - Affects directly to the surface quality.
 - And indirectly to the distortions by the heat input per layer.
- Shrinkage (linear)
 - The extent of the thermal shrinkage may be different in different directions.
 - The operator of the SLM-machine compensates the thermal shrinkage by process settings based on test series for each material.
- Dross formation
 - Use appropriate settings for down skin surface to decrease heat input locally.

Manufacturing defects

Although additive manufacturing provides benefits and design freedom, there are also various possible manufacturing defects that the designer should consider at least for critical load bearing components produced by the SLM process.

The various defects possible to SLM components are listed below. The ISO 5817 [14]. weld quality terminology and the ISO 6520 [15]. classification are used for the defects where applicable. Typical actions to avoid or cope with the defects are listed after the defects.

- Thermal distortions
 - Avoid thick sections that gather heat in design to prevent distortions.
 - Consider simulating the component and revise the design to minimise distortions.
 - The concept of compensating the geometry based on simulated distortions is discussed in for example [8] at page 109, and may become a useful feature into future design and analysis software.
- Ruptures at supports
 - Lattice supports tend to break under stiffer components.
 - Stainless steel type alloys with low heat conductivity tend to require heavier supports for increased heat transfer from the component to the base plate.
 - Use lattice support types optimised for the material and laser power when available.
 - Consider using solid supports for large components, or for components with high geometrical accuracy requirements.
- Cracking in printing or in heat treatment
 - Possible causes are for example thick sections and high stiffness. Favor flexible shapes and avoid thick sections in design to prevent cracking.
 - Use preheating when printing materials that are prone to cracking. For example the tool steel H13 requires preheating of the base plate (increased base plate temperature).
 - Use proper ramps in heating and cooling during heat treatment.
- Porosity
 - Especially near surface porosity, called often *borderline porosity*. SLM process tends to produce lines of pores at certain depth below the surfaces. This depends on the hatching settings.
 - Often considered gas pores (due to humidity in powder) for AISi12 (2011 / ISO 6520-1:1998) or due to excessive laser power. Appropriate powder handling, vacuum and optimised process parameters decrease porosity.
 - Keyhole porosity, that is caused by the melt pool collapsing and forming a cavity.
 - Malfunctions in powder feed may cause larger pores.
 - Evenly distributed small diameter porosity does not necessarily affect too much the material properties. There are pores and carbides also in traditionally manufactured products.
 - Porosity decreases the ductility of materials.

- Weld like internal defects between beads
 - Lack of inter-run fusion (4012 / ISO 6520-1:1998)
 - These are due for example to insufficient overlap in hatching settings.
 - Large sharp defects may decrease the fatigue strength considerably.
- Microcracks
 - 1001 / ISO 6520-1:1998
 - Microcracks may occur at for example tool steels.
 - Apply preheat and slow ramps in heat treatments.
 - Microcracks may decrease the fatigue strength and lower the ductility.
- Inclusions
 - Solid inclusions (300 / ISO 6520-1:1998)
 - Slag inclusions (301 / ISO 6520-1:1998)
 - Oxide inclusions (303 / ISO 6520-1:1998)
 - Inclusions may occur due residual powder present in the printer after change of material type.
- Edge effect
 - Depending on the upskin lasering settings and hatching strategy, the edge beads may get rised and form a rim at the edges of flat surfaces.
 - Apply small fillets at edges to avoid the rim effect.
 - The edge effect was not considered a problem in the test prints in this project.
- Variation of surface roughness
 - Depends mainly on the print angle and layer thickness.
 - Depends also on setting if the upskin surfaces are laser (re)melted or not.
 - Consider surface treatments, grinding or machining for critical surfaces.
- Burr
 - Burr may be present at sharps edges.
 - This can be prevented or decreased by using small overall fillet (*yleispyöröstys*).
- Dross formation
 - Partial melting of powder at downskin surfaces at overhangs.
 - Often small amount of dross is accepted and ground off in the finishing phase.
- Color changes
 - Due to excessive heat and oxygen in powder.
 - Occurs typically together with dross formation.
 - 'burn marks'
 - Check local distortions at locations of color changes for critical components.
 - Use solid support structures to avoid burn marks.
- Sagging
 - Partial melting of powder at downskin surfaces at overhangs may cause sagging (vertical defect) if the melt pool lowers into the powder bed.

- The sagging was less of a problem than for example curving in the VTT test prints.
- Transversal shrinkage
 - Occurs at junctions of separately built branches (often called as islands).
 - Typically rather small linear defect (0.5 mm in small test pieces).
 - Defect size depends on the span length between the separately built branches, according to literature.
 - Transversal shrinkage defects can be avoided by connecting the separately built branches during build with removable supports.
 - Transversal shrinkage defects can be included in machining allowances, if the junction is located at machined surface.
- Sharp surface defects between partially melted particles
 - Note: good Ra value does not guarantee good fatigue strength in AM.
 - The traditional design data for fatigue reduction factors based on Ra values are not necessarily valid for SLM.
- Spatter
 - Spatter is typically higher at the wake side of shield gas, where the molten droplets are blown by the gas flow.
 - Higher quality is therefore in principle obtained for printed part regions on the incoming side of the shield gas than on the wake side where the spatter is blown.
 - Spatter was not a problem with the test prints studied in this work.
- Restart marks
 - If the printing is stopped and restarted, the part may have time to cool and the restart layer shows as horizontal shrinkage line at the edges.
 - Restarting is in principle not allowed for load bearing components, or the conditions and approval should be considered case by case.
 - Restart marks are avoided by refilling the powder container before it gets empty.

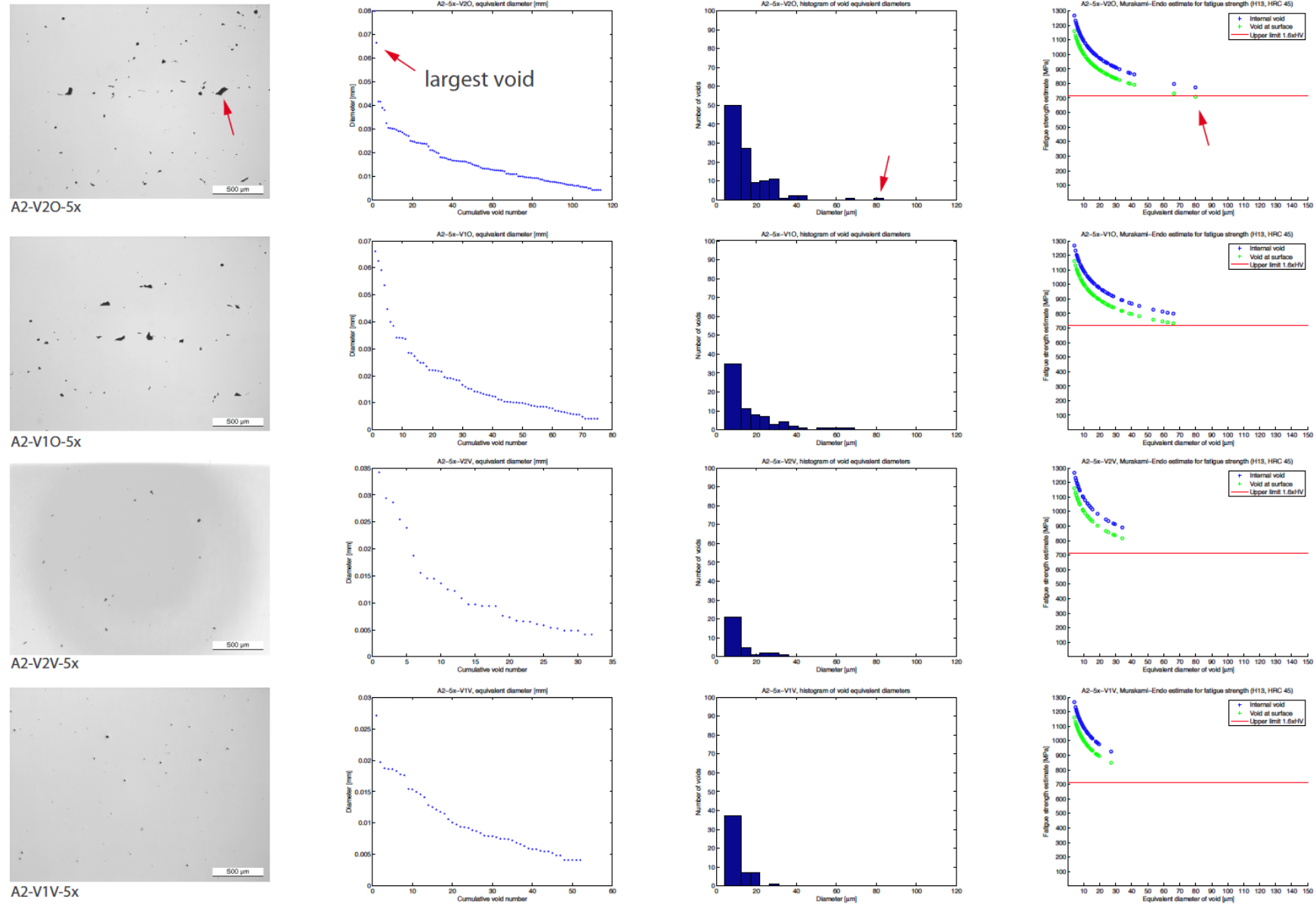
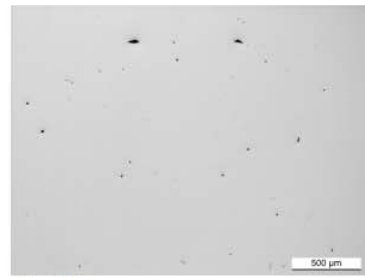
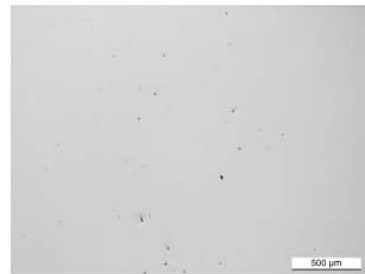


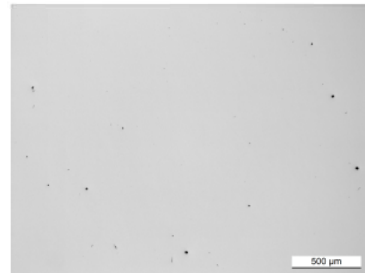
Figure 1. Optical microscope images at 5x magnification of H13 tool steel test piece, macro specimen A2, equivalent diameters of defects vs cumulative number of defects, histogram of defect sizes and resulting Murakami-Endo fatigue limit estimates (at stress ratio $R = -1$).



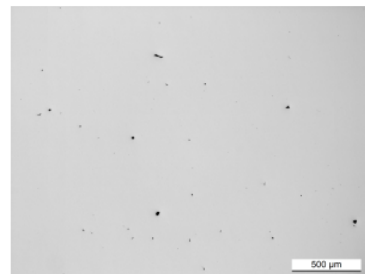
B1-V3-5x



B1-V4-5x



B1-V2V-5x



B1-V1V-5x

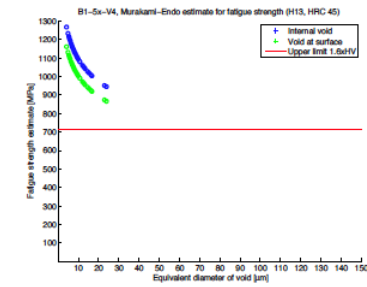
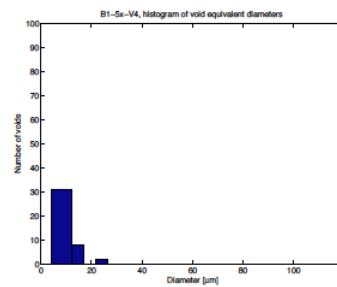
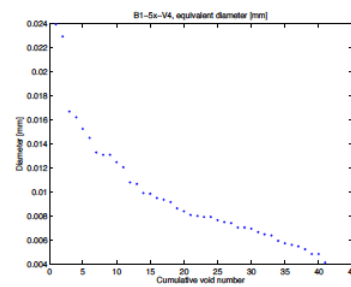
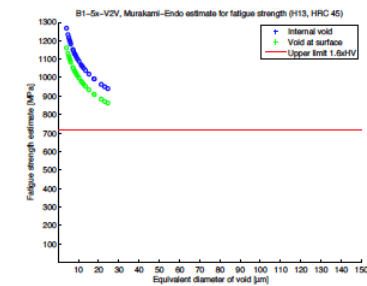
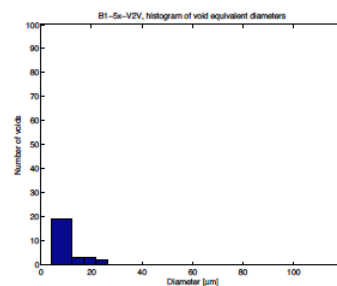
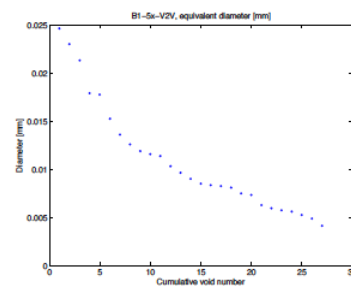
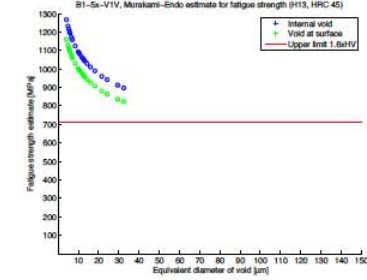
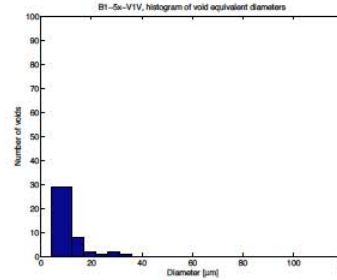
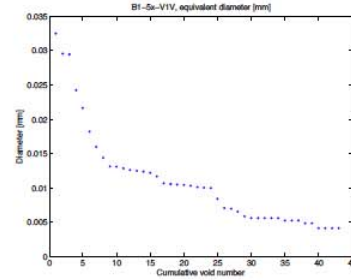
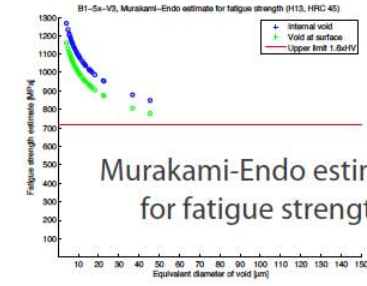
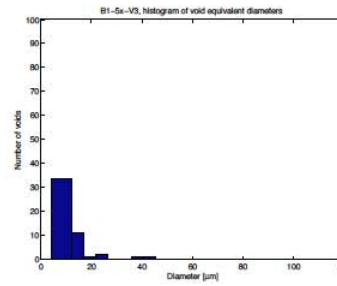
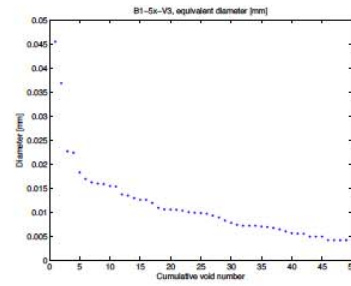
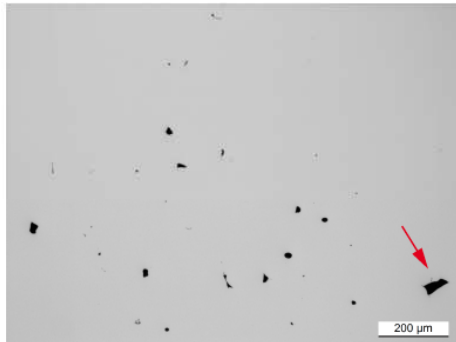
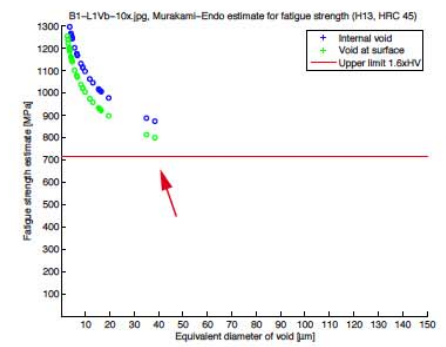
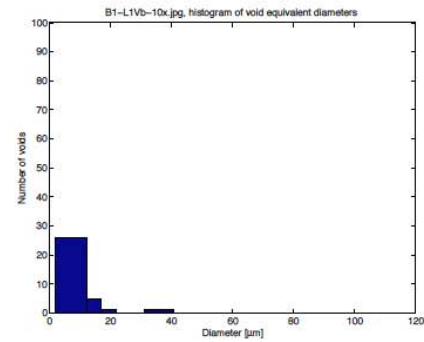
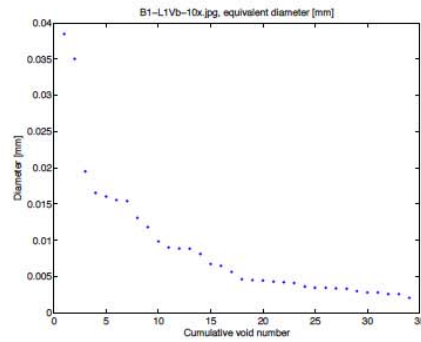


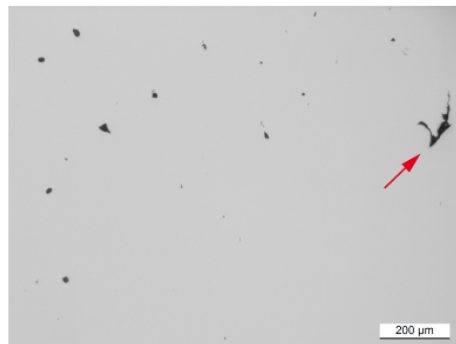
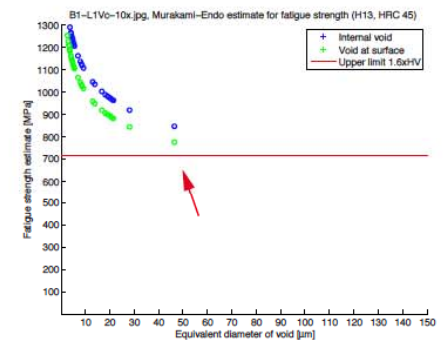
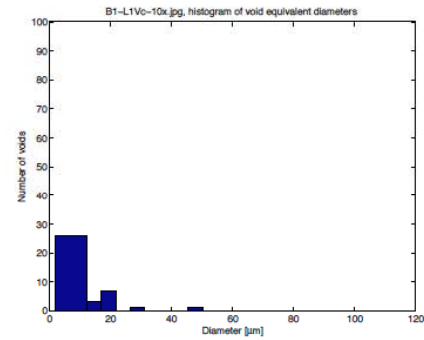
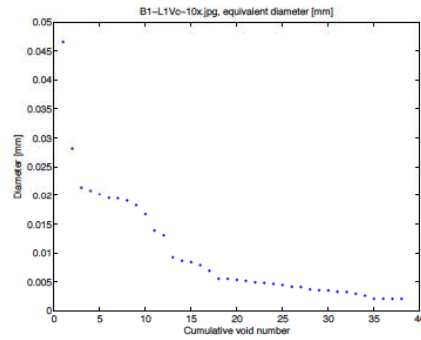
Figure 2. Optical microscope images at 5x magnification of H13 tool steel test piece, macro specimen B1, equivalent diameters of defects vs cumulative number of defects, histogram of defect sizes and resulting Murakami-Endo fatigue limit estimates (at stress ratio $R = -1$).



B1-L1V-10x b



B1-L1V-10x c



B1-L10-10x a

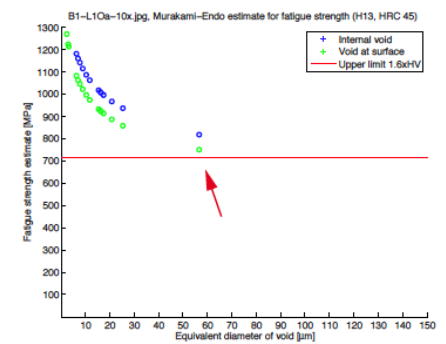
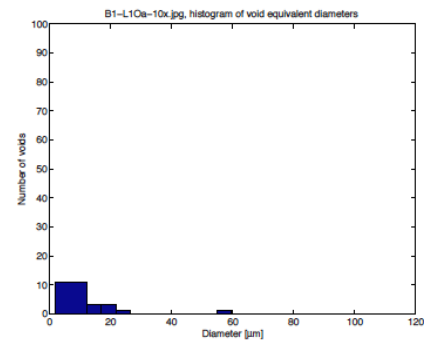
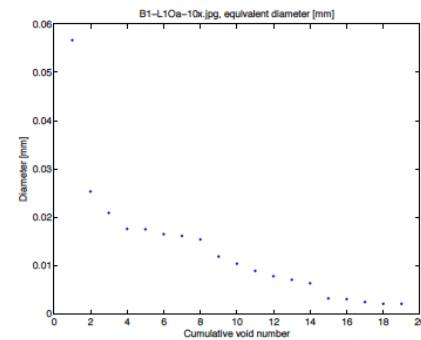


Figure 3. Optical microscope images at 10x magnification of H13 tool steel test piece, macro specimen B1, equivalent diameters of defects vs cumulative number of defects, histogram of defect sizes and resulting Murakami-Endo fatigue limit estimates (at stress ratio $R = -1$).

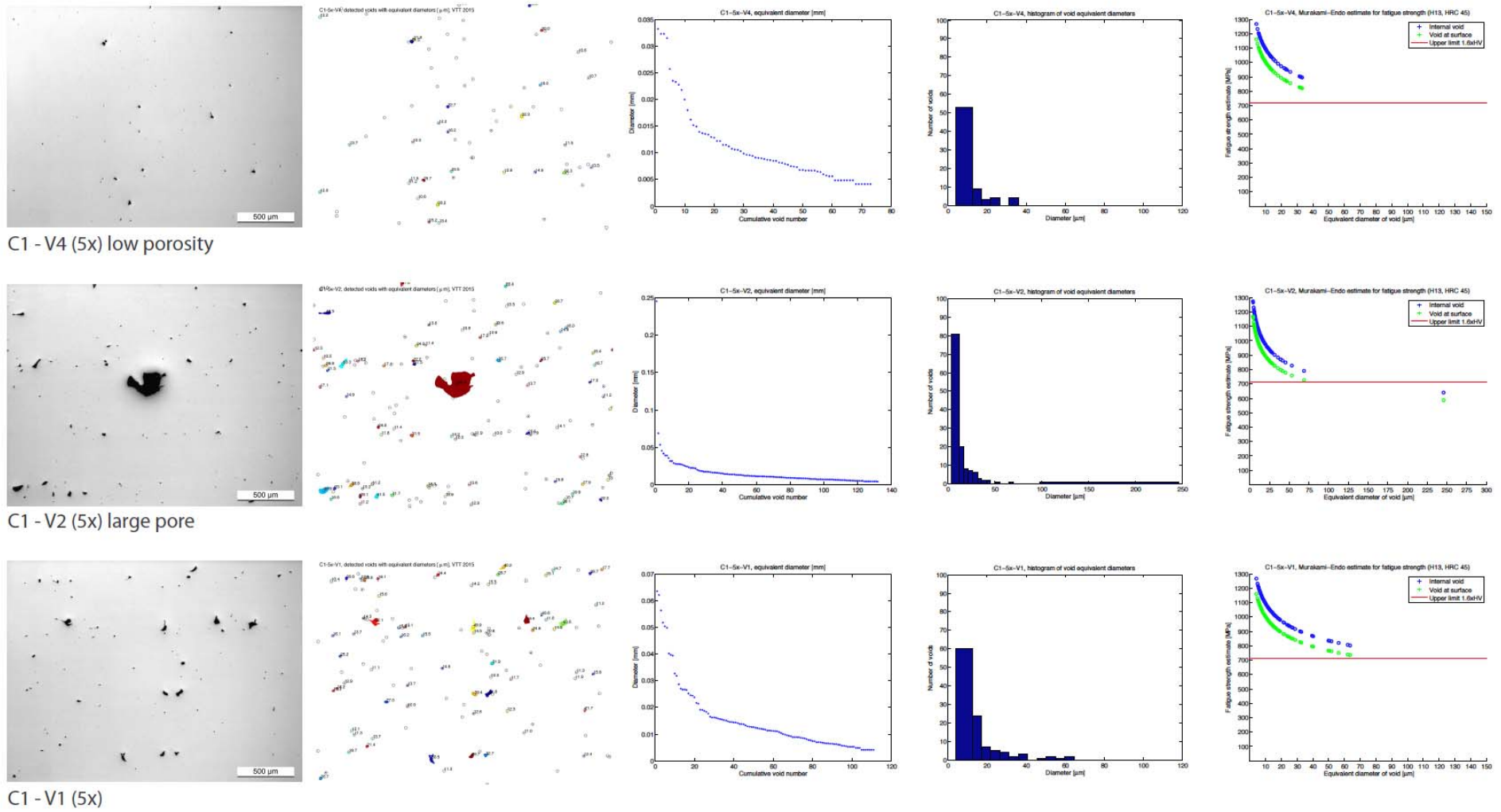
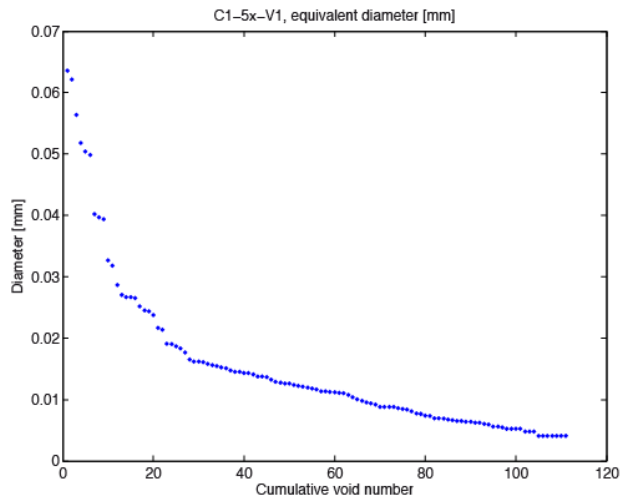
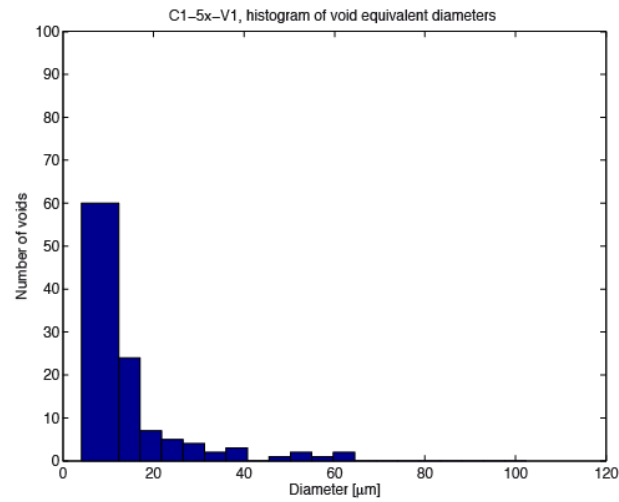


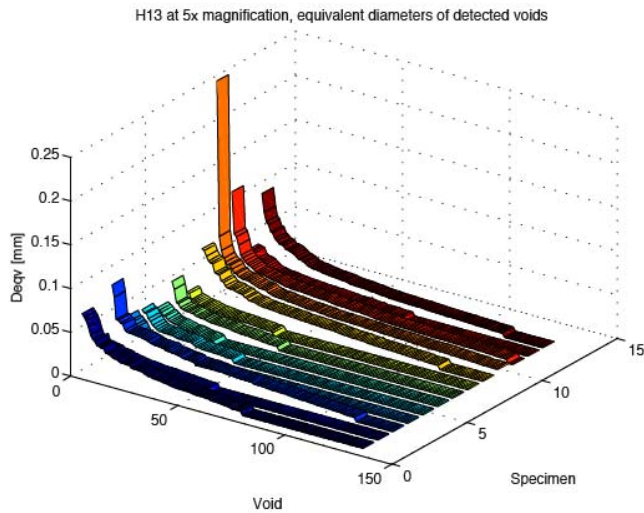
Figure 4. Optical microscope images at 5x magnification of H13 tool steel test piece, macro specimen C1, equivalent diameters of defects vs cumulative number of defects, histogram of defect sizes and resulting Murakami-Endo fatigue limit estimates (at stress ratio $R = -1$).



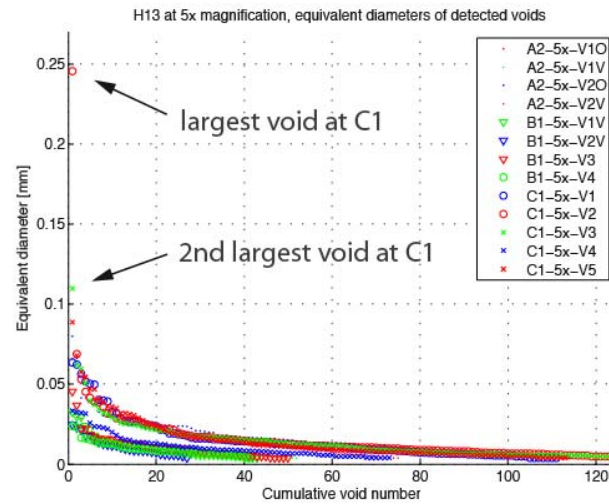
a) Equivalent diameters.



b) Equivalent diameters, histogram.



c) Equivalent diameters vs void number and 5x OM figures.



d) Equivalent diameters of all 5x OM figures.

Figure 5. Overviews of the detected and classified defects of the H13 tool steel test print specimens A2, B1 and C1. Defects of all microscope images at 5x magnification in (c) and (d).